Imperial College London

# CRISPR/Cas9 targeting of single genes in human blood cell progenitors to study Natural Killer cell development.

Nahide Koksal

Imperial College London

Department of Life sciences

PhD Supervisor: Prof. Hugh JM Brady

A thesis submitted for the degree of Doctor of Philosophy.

April 2021

## Declaration of originality

I, Nahide Koksal, confirm the work presented in this thesis is of my own. Where information or data has been derived from other sources is indicated in the thesis.

## Copyright declaration

The copyright of this thesis rests with the author. Unless otherwise indicated, its contents are licensed under a Creative Commons Attribution-Non Commercial 4.0 International Licence (CC BY-NC). Under this licence, you may copy and redistribute the material in any medium or format. You may also create and distribute modified versions of the work. This is on the condition that: you credit the author and do not use it, or any derivative works, for a commercial purpose. When reusing or sharing this work, ensure you make the licence terms clear to others by naming the licence and linking to the licence text. Where a work has been adapted, you should indicate that the work has been changed and describe those changes. Please seek permission from the copyright holder for uses of this work that are not included in this licence or permitted under UK Copyright Law.

## Acknowledgements

I would like to express my gratitude towards my supervisor Professor Hugh Brady for the opportunity to undertake research in his lab. Thank you for your unwavering support, guidance and mentorship to help me with my research, making me the scientist I am today. Thank you for always providing a joyous and encouraging work environment.

I would also like to express my gratitude and appreciation to my 2nd supervisor Dr Heather Ang, for without her help, I would not be where I am today. Thank you for your guidance, mentorship, friendship, and overall strength to deal with all my questions. Thanks for looking out for me, feeding me, motivating me and for all those hours going through my research and writing. And thank you, Heather, for finally letting me get there.

I am also very grateful to all the members of the Brady lab, past and present, for their support and assistance. I would like to specifically thank Ines Ullmo for helping me with my research while I was away, and for all the encouragement and friendship. I would like to acknowledge and thank our collaborators Mark Johnson and his group at Chelsea and Westminster hospital, as well as Dr Victoria Male, for providing us the resources and assistance needed to complete our work.

I would like to acknowledge all my colleagues and friends across Imperial who have made my PhD experience enjoyable, as well as save my experiments when I ran out of something. I am forever appreciative of Dr Myriam Haltalli, Dr Chiara Pirillo and Dr Ari Dwijayanti for their friendship and support. Thanks to the flow facility members including Jane Srivastava and Jessica Rowley for assisting me during those stressful FACS sorts. And thanks to Josh, Chris and Mo for providing constant encouragement and making me laugh.

Finally, I would like to express my deepest gratitude and appreciation to my family and friends outside of Imperial. Thank you for being my pillar and voice of reason in times of difficulty. Thank you for your love, support and encouragement needed to help me complete this thesis.

## Abstract

Natural killer (NK) cells provide a valuable resource for use in cellular immunotherapy, due to their ability to destroy cancerous cells without prior sensitisation or damage to healthy host cells. Here I show that I can generate biallelic knockout (KO) of genes known to be involved in mouse NK cell development in cord blood $CD34^+$ hematopoietic progenitor cells (HPCs) using a lentiviral CRISPR/Cas9 system. Biallelic KO of E4BP4, a transcription factor associated with NK cell commitment in mouse, resulted in the absence of human NK cell differentiation *in vitro*, indicating the importance of E4BP4 expression during early human NK cell development. Deletion of a single EOMES allele, a transcription factor associated with NK cell maturation, also resulted in a failure of NK cell differentiation, suggesting EOMES may impact early human NK cell development. Gene targeting of the inhibitory NKG2A receptor showed successful generation of a phenotypic NKG2A KO NK cell clone, allowing for investigation into the effect of NKG2A deficiency on human NK cell function. This methodology allows for the investigation of genes thought to be important in human NK cell development. Its further application will give insights into how such genes contribute to human NK cell production and function. By using cord blood $CD34^+$ progenitors to produce NK cells, we can generate large quantities of human NK cells. This provides the possibility of generating large amounts of “engineered” human NK cells with enhanced effector function(s) for NK cell immunotherapy.

Table of contents

**Declaration of originality** ..... **2**
**Copyright declaration** ..... **3**
**Acknowledgements** ..... **4**
**Abstract** ..... **5**
**Abbreviations** ..... **8**
**1. Introduction** ..... **10**
1.1. Natural Killer cells: an overview ..... 10
1.2. NK cell development. ..... 12
1.3. Transcriptional regulators for NK cell development. ..... 15
1.4. NK cell education and functional responses. ..... 21
1.5. NK cell receptors. ..... 26
1.6. Role of NKG2A in NK cell function and cancer therapy. ..... 29
1.7. NK cells and cancer immunotherapy. ..... 32
1.8. Differentiation of NK cells from UCB CD34$^+$ progenitors. ..... 37
1.9. CRISPR/Cas9 technology as a tool for NK cell gene modification. ..... 41
1.10. Aims and objectives. ..... 45
**2. Materials and methods** ..... **47**
2.1. Cell lines. ..... 47
2.1.1 293T and 293FT cells. ..... 47
2.1.2 MRC5 cells. ..... 47
2.1.3 EL08-1D2 cells. ..... 47
2.1.4 NK92 cells. ..... 48
2.1.5 K562 cells. ..... 49
2.1.6 PEO1 and PEO4 cells. ..... 49
2.2. Generation of CRISPR/Cas9 constructs. ..... 50
2.2.1 SgRNA design for CRISPR/Cas9 targeting. ..... 50
2.2.2 Cloning strategy for the final Cas9-eGFP vector. ..... 51
2.3. Targeting genes in CD34$^+$ HPCs and cell lines. ..... 54
2.3.1 UCB CD34$^+$ HPC depletion. ..... 54
2.3.2 Transfection. ..... 55
2.3.3 Virus concentration, transduction, and sorting of CD34$^+$ HPCs. ..... 55
2.3.4 Transduction of cell lines. ..... 57
2.3.5 Viral Titre and Multiplicity of infection (MOI) determination. ..... 57
2.4. CD34$^+$ derived NK cell differentiation. ..... 58
2.5. Functional assessment of NK cells ..... 59
2.6. Flow cytometry ..... 60

2.7. DNA extraction and genotyping. 61
**3. Development of human NK cells from UCB derived CD34⁺ HPCs. 63**
3.1. Background. 63
3.2. Differentiation of NK cells from untransduced CD34⁺ HPCs seeded at low cell densities. 66
3.3. CD34⁺ derived NK cells produce IFNγ and exhibit cytotoxic responses to cancer cell lines. 72
3.4. Effects of transduction on NK cell differentiation from CD34⁺ HPCs. 76
3.5. Discussion 78
**4. Effects of targeting E4BP4 and EOMES in CD34⁺ HPCs during NK cell differentiation 82**
4.1. Background. 82
4.2. Effects of deleting E4BP4 during human NK cell differentiation. 83
4.2.1 E4BP4 gene targeting strategy. 83
4.2.2 Validation of the E4BP4-Cas9-hCD2/eGFP vectors. 86
4.2.3 Biallelic E4BP4 gene deletion in CD34⁺ HPCs indicate detriment to NK cell differentiation. 88
4.3. Effects of deleting EOMES during human NK cell differentiation. 96
4.3.1 EOMES gene targeting strategy. 96
4.3.2 Validation of the EOMES-Cas9-eGFP vector. 98
4.3.3 Targeting EOMES within CD34⁺ HPCs reveals failure to expand during NK cell differentiation *in vitro*. 101
4.4. Discussion 107
**5. Optimisation and targeting of NKG2A within CD34⁺ HPC derived NK cells 112**
5.1. Background. 112
5.2. NKG2A expression on CD34⁺ derived NK cells. 113
5.3. Optimisation of the transduction procedure. 115
5.4. Designing the NKG2A-Cas9-eGFP vector. 123
5.5. Validation of the NKG2A-Cas9-eGFP vector 125
5.6. NKG2A gene deletion in CD34⁺ derived NK cells. 127
5.7. Killing assessment of NKG2A targeted CD34⁺ derived NK cells. 134
5.8. Discussion. 143
**6. Final discussion and future work 148**
6.1. Genes involved in early NK cell development. 148
6.2. Optimising CRISPR-Cas9 gene targeting with genes involved in late NK cell development. 151
6.3. Functional analysis of CD34⁺ derived NK cells 158

6.4. Applications of CRISPR/Cas9 gene editing in human NK cell development. .. ..... 161
**References ..... 164**

## Abbreviations

ADCC: Antibody dependent cellular cytotoxicity.

DSB: Double stranded breaks.

CAR: Chimeric antigen receptor.

CLP: Common lymphoid progenitor.

CRISPR: Clustered regularly interspaced short palindromic repeats.

E4BP4/NFIL3: E4 Promoter binding protein 4/ Nuclear factor regulated by IL-3.

EOMES: Eomesodermin.

E:T: Effector to target.

EV: Empty vector.

FACs: Fluorescence activated cell sorting.

GOI: Gene of interest.

Het: Heterozygous.

HLA: Human leukocyte antigen.

HPC: Hematopoietic progenitor cell.

HSC: Hematopoietic stem cell.

HSCT: Hematopoietic stem cell transfer.

ID2: Inhibitor of DNA binding 2.

iPSC: Induced pluripotent stem cell.

iNK: Immature NK.

ITAM: Immunoreceptor tyrosine-based activation motif.

ITIM: Immunoreceptor tyrosine-based inhibition motif.

KIR: Killer immunoglobulin-like receptor.

KO: Knock out.

MHC: Major histocompatibility complex.

mNK: Mature NK cell.

MOI: Multiplicity of infection.

NCR: Natural cytotoxicity receptors.

NHEJ: Non-homologous end joining.

NK: Natural killer.

NKG2A: Natural Killer group 2A.

NKP: Natural killer progenitor.

PAM: Protospacer adjacent motif.

PBMC: Peripheral blood mononuclear cell.

RNP: Ribonucleoprotein.

sgRNA: single guide RNA.

T-bet: T-box transcription factor TBX21.

UCB: Umbilical cord blood.

WT: Wild type.

# 1. Introduction

## 1.1. Natural Killer cells: an overview

First described in 1975, Natural Killer (NK) cells were initially identified as an unknown, non-B or non-T cell type that exhibits cytotoxic responses against malignant or transformed cells (Herberman et al., 1975a, Herberman et al., 1975b, Kiessling et al., 1975). These cells were later identified as large granular lymphocytes involved with innate immunity, mediating the removal of viral, bacterial or parasitic infected cells without prior sensitisation (Horowitz et al., 2011, Vivier et al., 2008). NK cells can also regulate responses within the adaptive immune system through the release of cytokines such as TNFα, IFNγ, TGF-β or IL-10. These cytokines can influence effector responses of T cells or dendritic cells to either act on a target cell or suppress its own activity (Vivier et al., 2008, Wu et al., 2017).

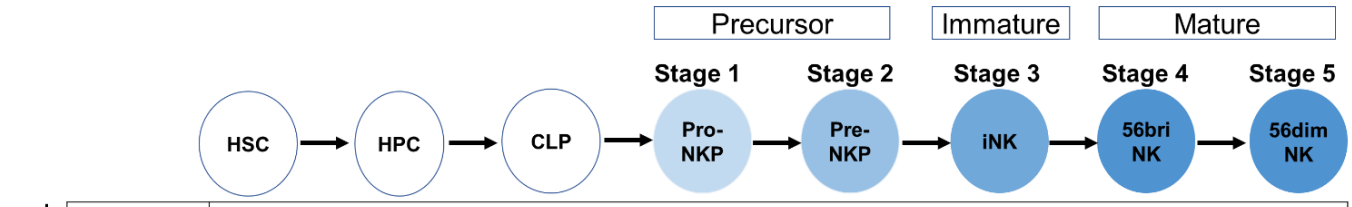
NK cells are characterised by cell surface expression of the adhesion molecule CD56, the type III Fcγ receptor CD16, the pan hemopoietic marker CD45 and the lack of T-cell receptor CD3 (Wu et al., 2017). Depending on the relative expression of CD56 and CD16, the NK cells can be divided into two main subsets that are commonly found within the body: $CD56^{bri}$ (bright) $CD16^{-}$ NK cells and $CD56^{dim}$ $CD16^{+}$ NK cells. Within the peripheral blood, where NK cells constitute 2-18% of total lymphocytes, $CD56^{dim}$ $CD16^{+}$ represent 90% of peripheral blood lymphocytes and are mainly associated with high levels of cytotoxicity. They are high in perforin and granzyme expression and can induce antibody dependent cellular cytotoxicity (ADCC) against a target cell. The $CD56^{bri}$ $CD16^{-}$ NK cells represent the other 10% and although these cells exhibit cytotoxic capacity in response to IL-2 (Nagler et al., 1990), these cells are mainly involved in secreting large amounts of cytokines such as IFNγ and TNFα (Wu et al., 2017). NK cells can also be found in circulation and in multiple different tissues, including the spleen, liver, mucosal tissues and the uterus during pregnancy. Cells that reside in these regions tend to be subset specific, originating from the bone marrow and expressing certain receptors that enable tissue homing and particular functional properties (Carrega and Ferlazzo, 2012). Tissue resident NK cells scan the surrounding environment for the removal of infected cells, play a role in regulating the pro-inflammatory response and in maintaining a homeostatic environment (Shi et al., 2011). Decidua NK cells, however, are involved in regulating developmental

processes between the fetal-maternal interface. These cells are associated with tissue remodelling and the formation of new blood vessels (Vacca et al., 2011).

With NK cells exhibiting functional roles across multiple organs, it is vital that how these cells are controlled and regulated is well described. Expanding our knowledge of NK cell biology has paved the way to using these cells as an alternative to T cells or hematopoietic stem cells in cancer immunotherapy. Further research to elucidate the undefined pathways involved in NK cell development and function can be harnessed to improve existing or develop new immunotherapies.

## 1.2. NK cell development.

### Human NK cell development.




Maturation

| | HSC | HPC | CLP | Pro-NKP | Pre-NKP | iNK | 56bri NK | 56dim NK |
|---|---|---|---|---|---|---|---|---|
| CD34 | + | + | + | Low | Low | - | - | - |
| CD38 | - | - | + | Low | Low | - | - | - |
| CD90 | + | - | - | - | - | - | - | - |
| CD45 | - | -/Low | + | + | + | + | + | + |
| CD117 | - | Low | Low | Low | + | Low | Low/- | - |
| CD127 | - | -/Low | + | + | + | Low | Low/- | - |
| CD122 | - | - | - | - | Low | Low/+ | + | + |
| CD25 | - | - | - | + | + | + | + | Low |
| CD56 | - | - | - | - | Low | Low | + (bri) | Dim |
| CD16 | - | - | - | - | - | - | - | + |
| CD94 | - | - | - | - | - | - | + | Low |
| NKG2A | - | - | - | - | - | - | + | Low |
| KIR | - | - | - | - | - | - | -/+ | +/Low |

Figure 1.1: Human NK cell development.

*Stages of mature NK cell development from HSCs are characterised based upon the surface receptor expression profile. Expression of a particular receptor is dynamic and changes over the course of NK cell differentiation, leading to many cells with intermediary expression profiles. The receptors indicated are an overview of development in relation to this thesis and does not include every identified NK cell receptor. HSC: hematopoietic stem cell, CLP: common lymphoid progenitor, NKP: natural killer progenitor, iNK: immature NK cell, mNK: mature NK cell (Freud and Caligiuri, 2006, Scoville et al., 2017, Seita and Weissman, 2010, Wang and Malarkannan, 2020).*

NK cells derive from hematopoietic stems cells (HSCs) that reside within the bone marrow (Figure 1.1). During human NK cell development, $CD34^{+}$ $CD38^{-}$ $CD90^{+}$ $CD45^{-}$ HSC's transition towards multipotent hematopoietic progenitor cells (HPCs) and common lymphoid progenitor cells (CLPs). This transition is marked by a decrease in CD90 expression and increase in CD45 and CD38 expression. Human CLPs are also

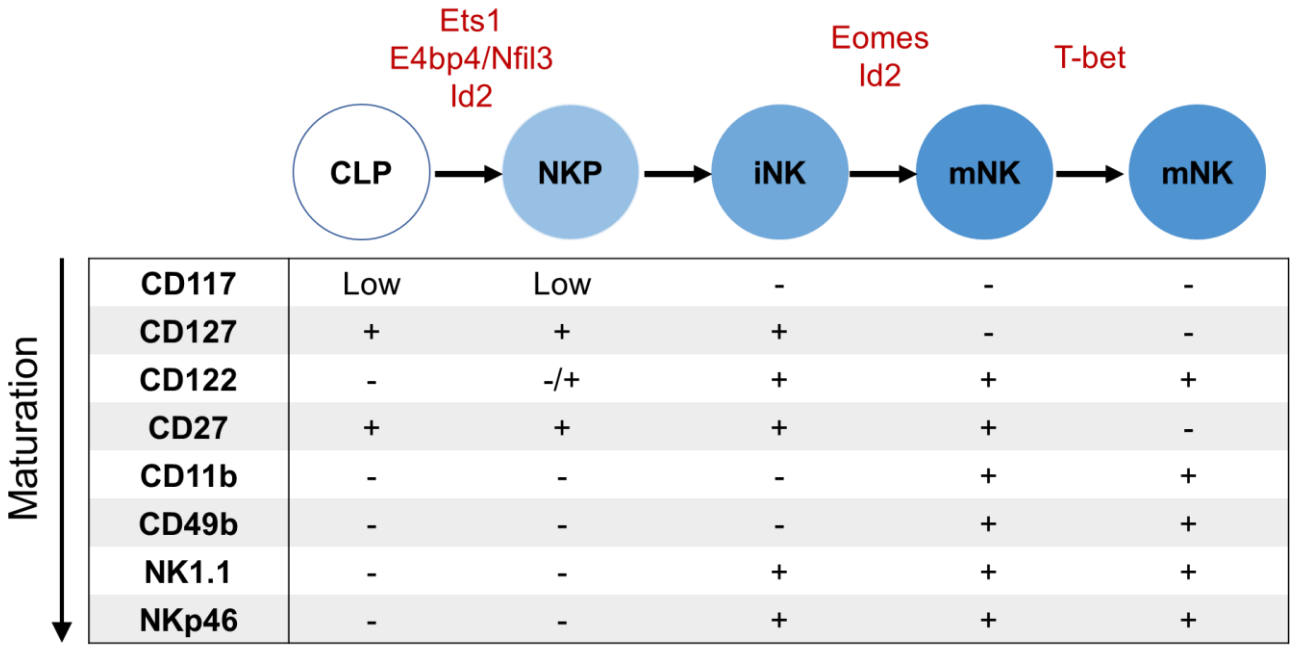
characterised as CD117$^{low}$ CD127$^{+}$, which when bound by cytokines SCF and IL-7 respectively, help commitment to lymphoid lineages. CLPs have the potential to give raise to T cells, B cells, NK cells and all the innate lymphoid cell (ILC) groups.

Human NK cell development downstream of CLPs encompasses five stages that can broadly be categorised as the NK cell precursor / progenitor stage (1 and 2), the immature NK cell stage (3) and the mature NK cell stage (4 and 5), (Figure 1.1). A defining point during the NK precursor stages 1 and 2 is the upregulation of CD117 and CD122, the latter being the IL-2 and IL-15 receptor β chain. With CD117 upregulation, the cells are now responsive to SCF, which in turn upregulates CD122 and permits signalling via the IL-15 cytokine to drive NK cell differentiation. In addition to this, expression of CD25 (IL-2 receptor α chain) also influences NK cell differentiation, proliferation, and activation (Freud and Caligiuri, 2006, Scoville et al., 2017).

In the immature NK cell (iNK) stage, the early HPC markers CD38 and CD34 are lost, and these cells begin to upregulate CD56 (also known as NCAM-1). CD56 mediated cell-to-cell adhesion influences NK cell maturation from the immature towards the mature stage during development (Montaldo et al., 2013). The cell receives signals in secondary tissues or within the BM to mature into CD56$^{bri}$ CD16$^{-}$ and CD56$^{dim}$ CD16$^{+}$ subsets previously described. These signals depend on presence of IL-15, IL-2 and in particular occasions, such as during an infection, the proinflammatory cytokines IL-12 and IL-18 (Shi et al., 2011).

Between the mature NK stages 4 and 5, the general consensus is that CD56$^{bri}$ CD16$^{-}$ NK cells are precursors of CD56$^{dim}$ CD16$^{+}$ population, although this has never been fully clarified *in vivo* (Allan et al., 2017, Freud and Caligiuri, 2006), (Figure 1.1). This notion is supported by studies that have found that CD56$^{bri}$ NK cells exhibit CD56$^{dim}$ CD16$^{+}$ NK cell characteristics upon activation *in vitro* and *in vivo* (Chan et al., 2007, Romagnani et al., 2007). In addition to this, CD56$^{bri}$ NK cells also express CD117, which is found on iNK cells but not the CD56$^{dim}$ subset. The transition between stages 4 and 5 can also be characterised as a loss of inhibitory receptor NKG2A/CD94 and the acquisition of a killer-immunoglobin like receptor (KIR) repertoire. KIRs can induce NK cell activation or suppression based upon the KIR subset expressed (Thielens et al., 2012).

Murine NK cell development




| | | | | | |
|---|---|---|---|---|---|
| **CD117** | Low | Low | - | - | - |
| **CD127** | + | + | + | - | - |
| **CD122** | - | -/+ | + | + | + |
| **CD27** | + | + | + | + | - |
| **CD11b** | - | - | - | + | + |
| **CD49b** | - | - | - | + | + |
| **NK1.1** | - | - | + | + | + |
| **NKp46** | - | - | + | + | + |

Figure 1.2: Murine NK cell development.

*The stages of murine NK cell development relevant for the scope of this thesis is summarised. The progenitor stages prior to CLPs are not presented and the different NKP populations (i.e. pre-NKP and refined NKP) are summarised as one. Two different mature NK cell populations exist, commonly characterised by CD27 and CD11b expression. CLP: common lymphoid progenitor, NKP: NK progenitor, iNK: immature NK cell, mNK: mature NK cell, (Goh and Huntington, 2017).*

Murine and human NK cell development is highly conserved, making it possible to use the mouse as a model to study the transcriptional regulation of NK cell development. The stages of murine and human NK cell development are also similar, beginning from early stem/progenitors to CLPs and transitioning into NKP, iNK and finally mNK cells (Figure 1.2). Further investigation into NK cell function however is limited in the mouse model due to species dependent target cell recognition, therefore the use of humanised mouse models in combination with human *in vitro* assays are required to investigate NK cell education and function (Cichocki et al., 2019).

Similar to human, mouse NK cells develop from bone marrow HSCs which generate murine CLPs. Murine CLPs are also marked by CD117$^{low}$ CD127$^{+}$ CD122$^{-}$ receptors (Figure 1.2), mirroring the human CLP populations. Unlike human, murine CLPs begin downregulating the CD117 receptor earlier at the NKP stage but the CD122 expression patterns is preserved between mouse and human.

In contrast to CD56 and CD16 defining human NK cells, mouse NK cells are defined by NK1.1$^{+}$ NKp46$^{+}$ and variable expression of CD27 and CD11b. In general, the transition of murine CD27$^{+}$ CD11b$^{+}$ mNK cells towards CD27$^{-}$ CD11b$^{+}$ mNK cells coincides with a loss of proliferative potential, cytokine production and a gain in cytotoxicity (Goh and Huntington, 2017). This resembles what is observed during the transition of human mNK cells from stage 4 to stage 5 (Chan et al., 2007).

The wide range of receptors expressed on the developing NK cell surface, for both human and mouse, is dependent upon the transcriptional profile of the cell before and during that stage of development. Much like the dynamic receptor expression profile, the regulation of transcription factor expression is also a continuously fluctuating process.

## 1.3. Transcriptional regulators for NK cell development.

There are several transcription factors associated with NK cell development. E4bp4/Nfil3, Ets1 and Id2 transcription factors were identified as important regulators for NK cell commitment at the CLP stage. Eomes and Tbet have also been identified to be important at the later stages of development, during NK cell maturation into functional effectors (Figure 1.2), (Kee et al., 2020). Much of the work investigating the roles of these transcription factors and how they impact each other during NK cell development has been identified using mouse knockout models (Figure 1.3).

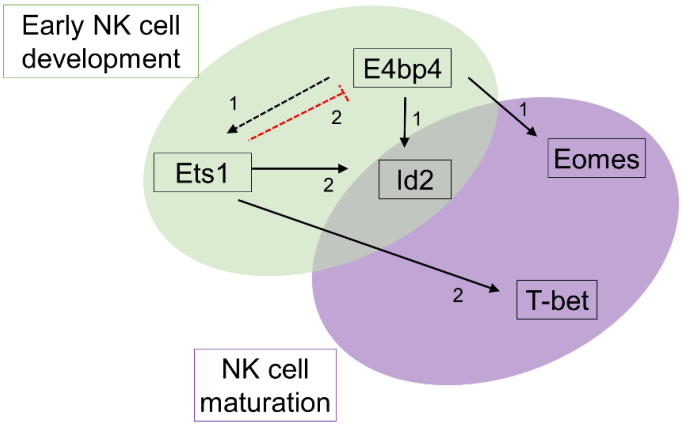



Figure 1.3: Transcriptional network involved in murine NK cell development.

*Summary of the transcriptional network during NK cell development and maturation as identified within mice. Solid lines represent direct interactions while dashed lines indicate associations. Black arrows represent upregulation, red blunted lines represent repression. Numbers reference the citations (1: Male et al. (2014), 2: Ramirez et al. (2012)). (1: solid lines) Id2 and Eomes are direct targets of E4bp4 in NK cells. Exogenous expression of these genes in E4bp4$^{-/-}$ mice rescued NK cell development. (1: dashed line) Ets1 is a direct target of E4bp4 in NK cells. Overexpression of Ets1 in E4bp4$^{-/-}$ mice rescued NK cell development. (2: solid lines) Id2 and T-bet are direct targets of Ets1. Ets1$^{-/-}$ NK cells in mice exhibited decreased levels of Id2 and T-bet expression. (2: dashed lines) Ets1 can negatively regulate E4bp4 expression. Ets1$^{-/-}$ mice exhibited elevated E4bp4 mRNA expression*.

## E4BP4/ NFIL3

E4BP4, also known as “nuclear factor regulated by IL-3” or NFIL3, is a basic leucine zipper (bZIP) transcription factor associated in a wide array of cellular processes. Referred to from here on as E4BP4, it was originally identified as a transcriptional repressor of the adenovirus E4 promotor (Cowell et al., 1992). In mice, expression of E4bp4 was found to be critical for the transition of CLPs towards the NK cell lineage (Gascoyne et al., 2009, Male et al., 2014). E4bp4$^{-/-}$ mice exhibit normal production of CLP but lacked NKP and downstream NK cell populations (Gascoyne et al., 2009, Kamizono et al., 2009). Exogenous expression of E4bp4 within these E4bp4$^{-/-}$ CLPs

managed to rescue the NK cell phenotype *in vitro*, indicating that this outcome was specific to E4bp4 expression alone (Male et al., 2014).

E4BP4 has also been found to act as a transcriptional activator of IL-3 expression in human T cells (Zhang et al., 1995) and a transcriptional repressor of the IL-12 promoter in LPS stimulated macrophages (Kobayashi et al., 2011). Other functions include transcriptional regulation of the circadian clock (Mitsui et al., 2001), IgE class switching in B cells (Kashiwada et al., 2010) and $CD8\alpha^{+}$ conventional dendritic cell development (Kashiwada et al., 2011), highlighting the diverse range of cells that require E4BP4 expression.

Transcriptional control of E4BP4 expression during NK cell development is not fully described in human. Of what is known within mouse NK cell development, within CLPs, IL-7 mediated STAT5 expression upregulated E4bp4 (Xu et al., 2015). Most other research investigating the regulation of E4BP4 expression is done so outside the context of NK cell development. For example, the nuclear receptor Rev-erbα, was found to directly repress E4bp4 expression in murine TH17 cells (Yu et al., 2013). Studies investigating whether these pathways are associated with E4bp4 mediated NK cell development is ongoing.

Downstream of E4bp4, chromatin immunoprecipitation and sequencing (ChIP-seq) data within mouse have identified that E4bp4 can bind to and regulate the genes encoding Eomes, Id2 (Male et al., 2014), (Figure 1.3), and Notch1 (Kostrzewski et al., 2018). Exogenous overexpression of Eomes and Id2 have been found to rescue the NK cell phenotype within $E4bp4^{-/-}$ murine CLPs. In addition to this, overexpression of the transcription factor Ets1 was shown to exhibit partial NK cell recovery (Male et al., 2014), however whether Ets1 is directly regulated by E4bp4 is unclear (Figure 1.3). NK cell development was also rescued in $E4bp4^{-/-}$ murine CLPs when these cells were exposed to Notch ligands such as Delta-like ligands 1 or 4 (DLL1/4), either as a plate bound recombinant protein or co-expressed by stromal cells (Kostrzewski et al., 2018).

Although E4bp4 expression first begins at the CLP stage in mice, its expression increases during NK cell maturation. In mNK cells, IL-15 can regulate E4bp4 expression via PDK1, a kinase that regulates mTOR signalling. Early deletion of PDK1 causes severe loss of NK cells (Yang et al., 2015), likely due to reduced CD122 expression and thus consequently E4bp4 induction. In addition to PDK1, it appears

that Ets1 also exhibits a repressive effect on E4bp4 expression in mNK cells (Figure 1.3), (Ramirez et al., 2012). In an $Ets1^{-/-}$ mouse model, mNK cells had high levels of E4bp4 mRNA, exhibited a chronically active phenotype and had impaired cytotoxicity responses. This suggests that E4bp4 performs different roles depending on the developmental stage of the NK cell.

A lot of work has been done in mouse to describe pathways associated with E4bp4 regulation and activity. However, the role of E4BP4 in human NK cell development is unknown. Due to the high conserved homology between the mouse and human E4BP4 protein, it would be important to know if E4BP4 plays as crucial a role in human NK cell development as it does in mouse.

Id2

Id2, or Inhibitor of DNA binding 2, is a protein that negatively regulates helix-loop-helix transcription factors by preventing them binding to the DNA. Studies using gene knockout mouse models indicate that Id2 acts downstream of E4bp4 and Ets1 expression during NK cell development (Figure 1.3). For example, $E4bp4^{-/-}$ mice showed a downregulation of Id2 expression within bone marrow derived CLPs and overexpression of Id2 within wild type CLPs increased NK cell production (Male et al., 2014). Deletion of the Ets1 gene also resulted in reduced Id2 expression within mNK cells (Ramirez et al., 2012). These studies indicate that Id2 expression is regulated at multiple stages of NK cell development (Figure 1.2).

In $Id2^{-/-}$ mouse models, a severe reduction of mature $CD27^{+}$ $CD11b^{+}$ and $CD27^{-}$ $CD11b^{+}$ NK cells were observed while the numbers of NKP remained the same (Boos et al., 2007, Zook et al., 2018). Id2 deficiency in NK cells also resulted in the suppression of genes associated with cytotoxicity, such as granzyme production, as well as a reduced ability to produce IFNγ upon IL-2 and IL-12 stimulation (Zook et al., 2018). This suggests that Id2 plays an important role during NK cell maturation and maintenance of effector responses.

Eomes

Eomesodermin, or Eomes, is a T-box transcription factor that has a wide range of functions, including vertebrate embryogenesis and $CD8^{+}$ T cell activation (Simonetta et al., 2016). First upregulated during the NKP stage in mice, its expression increases

until the early stages of maturation ($CD27^+$ $CD11b^+$), after which it begins to decrease during terminal NK maturation ($CD27^-$ $CD11b^+$), (Male et al., 2014, Simonetta et al., 2016). When Eomes gene expression was ablated in murine mNK cells, these cells appeared to revert to an immature phenotype (Gordon et al., 2012).

Study of Eomes gene expression earlier during NK cell development is limited as complete Eomes gene ablation results in an embryonic lethal phenotype. Because of this, much research has been conducted using a heterozygous Eomes model, usually within a $Tbx21^{-/-}$ (encoding T-bet) mouse background (Intlekofer et al., 2005). Both T-bet and Eomes are closely associated with NK cell cytotoxicity, playing a synergistic yet separate role regarding the production of IFNγ, perforin and granzyme by NK cells (Intlekofer et al., 2005, Simonetta et al., 2016). Mice with a $Eomes^{+/-}$ $T\text{-}bet^{-/-}$ genotype exhibited a severe reduction of NK cell production compared to the $Eomes^{+/+}$ $T\text{-}bet^{-/-}$ control, likely due to Eomes regulation of CD122 and consequently decrease in IL-15 signalling (Intlekofer et al., 2005). This suggested that the loss of a single Eomes allele was enough to impede NK cell development in $T\text{-}bet^{-/-}$ mice.

Another interesting finding was that in $E4bp4^{-/-}$ mice, the bone marrow derived NK cell population ($Eomes^+CD49b^+$) is reduced, but not hepatic $Eomes^-$ $CD49b^-$ NK cells. T-bet expression was not affected by E4bp4 deficiency (Crotta et al., 2014). The observation of a population of NK cells developing independently from E4bp4 expression was unusual, given the importance of E4bp4 in NK cell commitment. These $Eomes^{-/low}$ NK cells exhibited an immature phenotype and were only identified in a few peripheral organs such as the thymus and liver (Crotta et al., 2014, Gordon et al., 2012). Whether this population of cells are a distinct, fully differentiated NK cell subset or are E4bp4-independent medullary precursors to the more mature $Eomes^+$ $CD49b^+$ NK cell subset is still inconclusive. Gordon et al. (2012) found these $Eomes^-$ NK cells gave rise to an $Eomes^+$ NK cell population after adoptive transfer into an immunocompromised $IL\text{-}2R\gamma^{-/-}$ $Rag2^{-/-}$ mice recipient. Conversely, Daussy et al. (2014) suggests $Eomes^-$ NK cells are a distinct NK cell subset found mainly in the bone marrow and the liver and not precursors to the $Eomes^+$ conventional NK cells. Further research is required to clarify this relationship between Eomes expression and the development of NK cell subsets within the periphery.

In human, EOMES appears to be expressed at higher levels in $CD56^{bri}$ $CD16^{-}$ NK cells than $CD56^{dim}$ $CD16^{+}$ NK cells (Knox et al., 2014). This is parallel to what is seen in mice, where early mature NK cells express more Eomes than terminally differentiated NK cells. Also like mouse, $EOMES^{low}$ NK cells have been found in the human liver. Similar to the findings by Gorden et al., 2012, it has been shown that these human $EOMES^{low}$ NK cells are likely precursors to the $EOMES^{hi}$ NK cell subsets within the liver (Cuff et al., 2016). Upon entry into the liver from the circulation, exposure to IL-15 and TGF-β induced EOMES upregulation within $EOMES^{low}$ cells, producing an $EOMES^{hi}$ conventional NK cell phenotype. Conversely, other studies have found that these intra-hepatic tissue resident $EOMES^{-}$ $T\text{-}bet^{+}$ NK cells produce high proinflammatory cytokines (IFNγ, TNFα, GM-CSF) and are phenotypically like the murine $Eomes^{-}$ NK cells discussed in Daussy et al. (2014), (Marquardt et al., 2015). These cells did not appear to be able to differentiate into a fully mature $EOMES^{+}$ subset *in vitro*. It appears that, just like the mouse, more research is required to clarify what role EOMES plays during NK cell development and maturation in human.

Further clarification of EOMES function could also provide a clinical benefit. In a tumour infiltrating mouse model which underwent adoptive NK cell transfer, there was rapid loss of Eomes and T-bet expression within transferred NK cells. This correlated with poor cytotoxic function and an exhaustive NK cell phenotype (Gill et al., 2012). Exogenous overexpression of Eomes improved NK cell function and suggested a possible role in regulating NK cell exhaustion. Therefore, it is of interest to clarify what EOMES effects during the different stages of human NK cell development. This would identify, on a mechanistic level, what EOMES directly interacts with so that current cellular immunotherapies might be adapted or modified to improve their efficacy for patients.

T-bet

T-bet, a T-box transcription factor, works with Eomes as a critical regulator of NK cell development and maturation (Figure 1.3). Its expression can be found in NK cells and ILC1 groups, however T-bet independent NK cell development can still occur if Eomes expression is maintained. Loss of both genes causes a severe reduction in NK cell development in mice (Daussy et al., 2014). In $T\text{-}bet^{-/-}$ mice, there was a reduction in mNK cells within the periphery such as the blood, spleen and liver, however the

numbers remained high within the bone marrow. In addition to this, most of the NK cells retained their immature phenotype (Simonetta et al., 2016, Townsend et al., 2004). The retention within the bone marrow could be due to the decrease in sphingosine-1-phosphate receptor (S1pr5) and transcription factor Zeb2 within T-bet$^{-/-}$ mice, both of which are involved in NK cells egressing from the bone marrow into the periphery (Jenne et al., 2009, van Helden et al., 2015). In addition to Zeb2, T-bet$^{-/-}$ also resulted in a reduction of Blimp1, both of which are associated with NK cell maturation, survival and activation (Kallies et al., 2011, van Helden et al., 2015).

## 1.4. NK cell education and functional responses.

NK cells can specifically target an infected or cancerous cell without inflicting damage to healthy host cells and without the need for prior sensitisation. This is a consequence of NK cells undergoing education.

Much like T cell education within the thymus, NK cell education is the process where a NK cell becomes a functional, self-tolerant, mature cell through signalling of their activating and inhibitory receptors. Many receptors are associated with NK education, such as the classical MHC Class I dependant HLA A/B/C interaction with KIRs, the non-classical MHC Class I dependant HLA-E interaction with NKG2A and the MHC independent CD155 interaction with NK surface receptor TIGIT. These discoveries led to the development of several models which suggest how NK cells are educated (Figure 1.4).

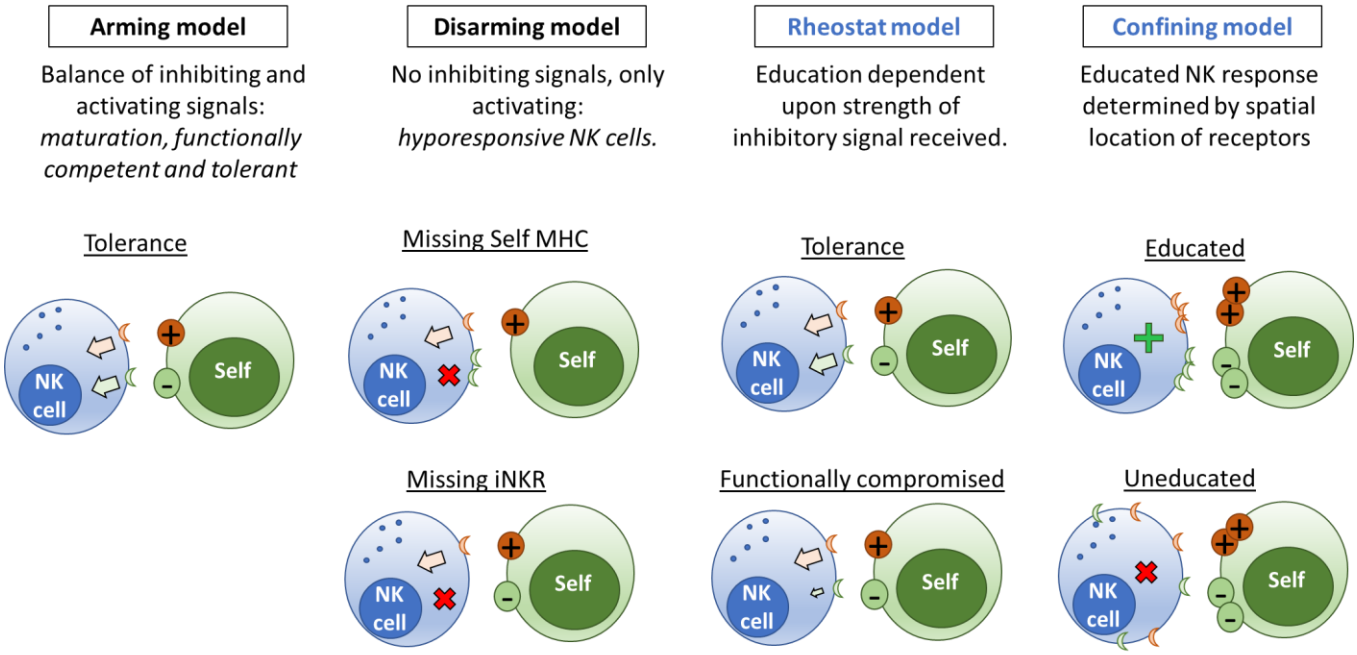



Figure 1.4: Models of NK cell education

*Schematic diagram describing four different models of NK cell education. The arming and disarming models are previously established models for NK cell education, while the rheostat and confining models provide further explanation in situations that do not quite fit in with the first two. Signalling through a receptor is shown as an arrow, with the size representing the intensity. Lack of signalling is represented by a red cross.*

The arming model describes the events where there is equal signalling from both activating and inhibiting receptors on an NK cell, enabling completion of NK cell maturation and functional competency. The inhibitory NK receptors (iNKR) also become highly sensitive to detect low levels of its ligands, ensuring no inappropriate autoreactive response occurs (Nash et al., 2014).

NK cells are “disarmed”, or in other words rendered hyporesponsive, when they receive continuous, low levels of activating signals but no inhibiting signal. This could be due to the lack of MHC on the target cell surface (missing self) or lack of iNKR expression on NK cell (Long et al., 2013). Goodridge et al., (2019) identified that in the absence of self-specific inhibitory signalling, for example through NKG2A/HLA-E interactions, basal level activation of NK cells resulted in calcium release from secretory lysosomes that sequester cytolytic proteins granzyme B and perforin,

leading to a reduction in degranulation and IFNγ production upon target cell exposure. The depletion of stores which contain cytolytic proteins acts as a safety mechanism that ensure that no hyper-responsive NK cell that cannot regulate its activation goes left unchecked within the body.

The rheostat and confining models are not as well defined as the other two but do provide explanations in circumstances that do not fit into the arming or disarming category. The rheostat model presents the notion that NK cell education is not a static process, determined only by the presence or absence of signals, but is dynamic and incorporates the strength of the signal or cumulative signals from multiple inhibitory receptors to educate NK cells. Even if all the necessary receptors are present, it does not mean the NK cells will be educated if there is a net shift towards positive stimulation resulting in overall hypo-responsiveness and functional compromise (He and Tian, 2017, Joncker et al., 2009). In the confining model, educated NK cells have been shown to organise its activating, inhibiting and even adhesion molecules in confined regions on the cell surface, not seen in uneducated NK cells. It is thought that as the balance between the activating or inhibiting signals has to be shifted in order to get an NK cell response, concentrating the receptors to a specified location would amplify the overall signal above the threshold requirement (He and Tian, 2017).

Once educated, NK cells generally remain hyporesponsive and inactive when in circulation or residing within the tissue as it interacts with normal host cells (Figure 1.5, top panel). This is mainly due to the high expression of self-MHC and low expression of any activating ligands on the host surface. When a host cell becomes infected, malignant or encounters other forms of stress, it results in a disruption of its surface ligand expression that can proceed to influence the NK cell response.

Malignant or infected cells can downregulate its host MHC molecules in order to evade immune detection by T cells but can still be recognised by NK cells. This is called the missing self-hypothesis, as a lack of inhibitory signalling results in a net shift towards NK cell activation and effector responses (Figure 1.5, middle panel). Infected or transformed cells can also upregulate other activating ligands, such as stress related proteins MIC-A and MIC-B ligands recognised by the NK cells activating NKG2D receptor. With increased signalling through the activating receptors, the shift in signal balance pushes NK cell activation and cytotoxicity (Figure 1.5, bottom panel).

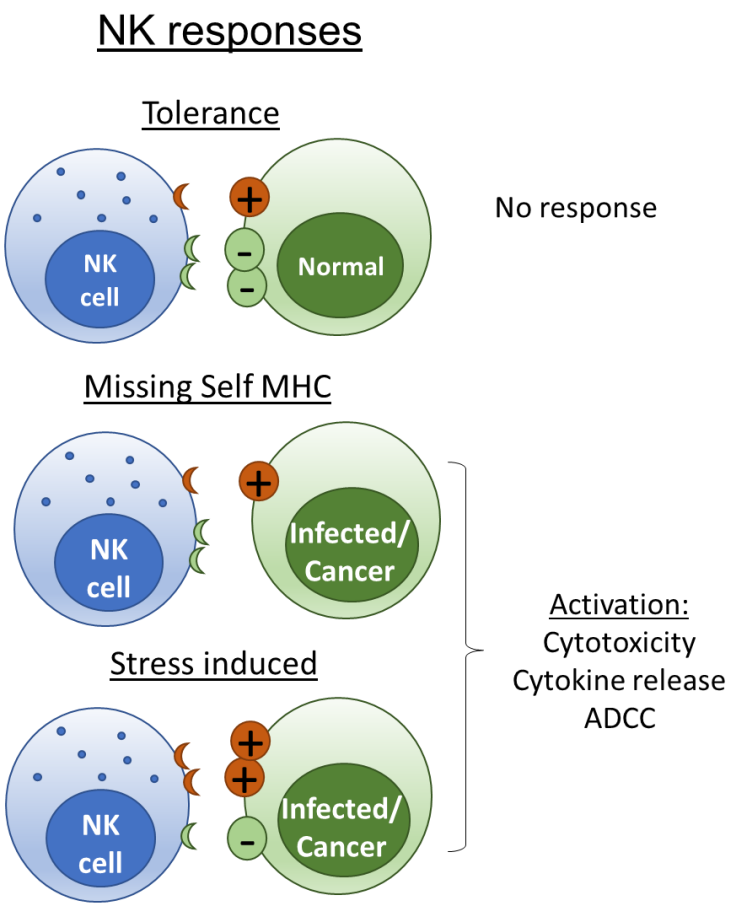



Figure 1.5: Different NK cell responses

*When an NK cell encounters a host cell, different responses can occur depending on the state of the cell and the receptor types expressed on the surface of the NK cell. A balance of signals with a majority being inhibitory results in no response and NK cell tolerance. This usually is the case for normal healthy host cells. Infected or cancerous cells can downregulate NK inhibitory ligands (missing self) or upregulate activating ligands (stress induced), causing a net shift towards NK cell activation and a functional response.*

NK cell cytotoxicity induces lysis of the target cell in various ways. NK cell receptor-ligand interaction by means of activating receptors, such as NKG2D, can trigger the release of cytotoxic proteins, perforin and granzyme, from their acidic secretory lysosome stores (Goodridge et al., 2019, Sordo-Bahamonde et al., 2020).The expression of perforin and granzyme B are regulated by cytokines such as IL-2

(Salcedo et al., 1993), IL15 and SCF (Meade et al., 2009) during NK cell maturation, with the highest amounts of these proteins found within the mature $CD56^{dim}$ NK cell subset (Jacobs et al., 2001). Upon NK cell activation and degranulation, perforin likely functions to introduce granzymes, apoptosis inducing proteins, into the target cell by either creating a pore within the cell membrane or within granzyme-containing endocytosed vesicles. Antibody dependent cellular cytotoxicity (ADCC) can also induce release of cytotoxic granules however this response is mediated by the Fcγ receptor CD16 binding to antibodies on the target cell surface (Lanier et al., 1988, Sordo-Bahamonde et al., 2020). Ligand binding to TRAIL or FasL receptors on the NK cell surface can induce target cell apoptosis through caspase mediated pathways (Sordo-Bahamonde et al., 2020, Zamai et al., 1998). Cytokines released by NK cells, such as IFNγ and TNFα, can activate any surrounding $CD8^{+}$ cytotoxic T cells or encourage dendritic cell (DC) maturation, respectively. Mature DC cells can present antigens on the surface of their cells to regulate T cell immune responses (Spits and Di Santo, 2011).

What is intriguing about NK cell education and their subsequent functional capacity is that, unlike T cell education where a single event determines the T cell fate, NK cells can “reset” their response depending on their environment (Joncker et al., 2010). With education presenting itself to be a continuous process, the fine line between whether an NK cell becomes “re-educated” in a new environment versus becoming activated or suppressed depending on the change in ligand expression remains unclear. Further research into the receptors associated with NK cell education and its effector functions is needed to better predict how to optimise NK cell responses during adoptive cellular therapy.

## 1.5. NK cell receptors.

Once educated, NK cell responses vary depending on what receptor was stimulated (Figure 1.6).

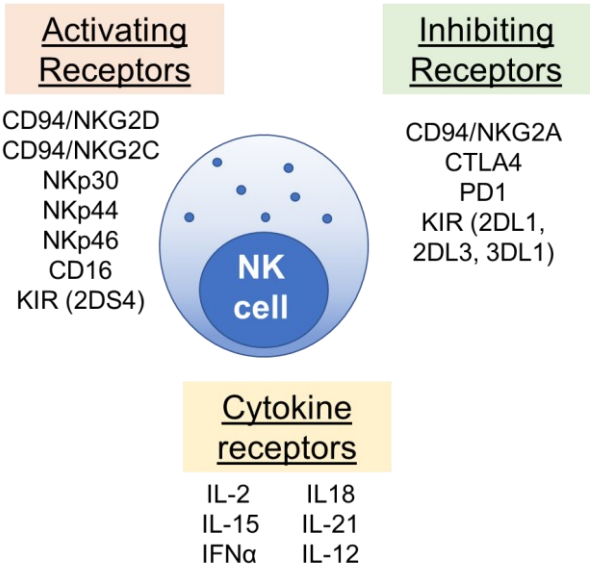



Figure 1.6: Classification of a range of NK cell surface receptors.

*Several different receptors are expressed on a mature NK cell surface at a given time. Receptors commonly associated with activating or inhibiting the NK cell effector responses are shown, as well as common cytokine receptors that are associated with regulating NK responses.*

Activating receptors:

Natural cytotoxicity receptors (NCR), such as NKp46, NKp30 and NKp44, interact with a vast array of non-HLA ligands. For example, NKp46 (Mandelboim et al., 2001) and NKp44 (Ho et al., 2008) both recognise influenza viral hemagglutinin to activate NK cells. NKp30 can recognise B7-H6, a transmembrane protein upregulated in several tumours (Schlecker et al., 2014). Activating KIR2DS4, on the other hand, interacts with the host cells HLA-A and HLA-C surface molecules presenting foreign or stressed peptides, for example conserved peptide sequences derived from bacterial recombinase A (Sim et al., 2019). Similarly, activating KIR2DS2 receptor also recognises HLA-C bound conserved peptides, such as those derived from flavivirus helicases belonging to hepatitis C, Ebola and Zika viruses (Naiyer et al., 2017). Upon receptor-ligand binding, both activating NCRs and KIRs transmit intracellular signals

using adaptor proteins that recognise the cytoplasmic tails of these receptors. Some common adaptor proteins are DAP12, FcεR1γ or CD3ζ. These adaptor proteins are small polypeptides consisting of short extracellular domains and a cytoplasmic tail that contain immune-receptor tyrosine-based activating motifs (ITAMs). It is the tyrosine residues within the ITAMs that are phosphorylated, interacting with intracellular signalling proteins and induce NK cell activating responses (Moretta et al., 2001).

The NKG2C/CD94 heterodimer interacts with the non-classical HLA-E present on the surface of host cells. Foreign peptides, such as those derived from human cytomegalovirus, presented by HLA-E will stimulate a response through the NKG2C receptor and initiate NK cell effector function (Pupuleku et al., 2017).

NKG2D on the other hand does not need to couple with CD94 and is expressed on the surface as a homodimer. It recognises the stress-induced MIC-A, MIC-B and ULBP ligands. These ligands are upregulated in many cancers, such as kidney, breast, lung and ovarian (Moretta et al., 2001). When stimulated, NKG2D signals through DAP10 to activate the NK cell and overcome any inhibitory signals received. NKG2D stimulation induces strong lytic responses and IFNγ production from NK cells (Moretta et al., 2001).

CD16 recognises antibody coated cells and induces NK cell antibody dependent cell cytotoxicity (ADCC) and cytokine production. CD16 also interacts with ITAM containing adaptor proteins in order to induce NK cell effector responses (Vivier et al., 2011). ADCC responses are limited by shedding of the CD16 receptor post activation as well as NK cell exhaustion (Muntasell et al., 2017).

Inhibiting receptors:

Several inhibiting NK cell receptors signal through immune-receptor tyrosine-based inhibitory motifs (ITIMs) located on their cytoplasmic tail. When phosphorylated, ITIMs recruit phosphatases SHP1 and SHP2 which in turn lead to an inhibition of NK cell effector functions (Montaldo et al., 2013). Examples of inhibitory receptors that mediate NK cell responses via ITIMs are inhibitory KIRs, such as the KIR2DL1 / 2DL3 / 3DL1 variants and the NKG2A/CD94 heterodimer. Ligands for these receptors are HLA molecules expressing self-peptides on the surface of host cells. KIR2DL1 and 2LD3 recognise the HLA-C haplotype, KIR3DL1 recognises the HLA-Bw4 haplotype and NKG2A/CD94 recognises the HLA-E haplotype.

The inhibitory receptor Programmed death-1 (PD-1) has previously been identified on a subset of mature, terminally differentiated $CD56^{dim}$ NK cells lacking NKG2A and expressing KIR receptors. PD-1 expression is not well characterised and its detection is mainly associated in cytomegalovirus (CMV) positive patients (Lanuza et al., 2019). NK cells from patients with ovarian carcinoma also exhibited high PD-1 expression, low proliferative responses and impaired anti-tumour activity. Antibody mediated blockage of PD-1 signalling did partially restore some activity (Pesce et al., 2017), indicating that for some cancers, targeting PD-1 expression on NK cells could provide beneficial effects.

The expression of CTLA-4 on the NK cell is less defined than other receptors. CTLA-4, or cytotoxic T lymphocyte-associated antigen 4, is largely associated with decreasing T cell effector function and competes with the activating co-stimulation receptor, CD28, for the same antigen presenting cell ligands: B7-1 and B7-2. Activated murine NK cells show upregulated CTLA-4 expression, however in human, CTLA-4 was reported to be found at low levels intracellularly (Beldi-Ferchiou and Caillat-Zucman, 2017).

With the success of blocking PD-1 and CTLA-4 receptor signalling to enhance T cells cytotoxicity against various malignancies during immunotherapy, investigations as to whether a similar approach can enhance NK mediated cellular immunotherapy is ongoing (Muntasell et al., 2017).

Cytokine receptors:

The expression of cytokine receptors is highly dependent upon the stage of NK cell maturation and whether the cell is circulating or tissue resident. Most of these cytokines signal via different family members associated with the Janus Kinase (JAK) / signal transducer and activator of transcription (STAT) pathway to upregulate the expression of NK cell related genes. JAK kinases associate with the tyrosine residues on the intracellular region of the cytokine receptor, leading to STAT phosphorylation. Once phosphorylated, STAT proteins dimerise and can bind onto the promoter regions of various genes (Gotthardt et al., 2019).

In general, IL-2 and IL-15 receptor signal via the JAK1/3 STAT5 pathway to mediate cell survival (Bcl-2), proliferation (Ccnd2), maturation (T-bet) and production of perforin and IFNγ. IL-21 signals through the JAK1/3 STAT1/3 pathway and upregulates genes

encoding IFNγ, perforin and NKG2D, promoting NK cell cytotoxicity. IL-12 signals through JAK2/TYK2 family member and the STAT4 protein, while IFNα signals via the JAK1/TYK2 and STAT1/2 pathway. Both IL-12 and IFNα leads to the upregulation of IFNγ and T-bet while IL-12 also upregulates perforin expression. These genes induce NK cell cytotoxicity and maturation (Gotthardt et al., 2019).

IL-18 on the other hand was shown to prime NK cells to produce IFNy when IL-12 is provided, and signals through MyD88 and STAT3 in order to achieve this (Chaix et al., 2008).

Several *in vitro* protocols include these cytokines in order to drive NK development, expansion and activation for experimental purposes. This is also done within a clinical setting, in particular, during the preparation of peripheral NK cells *ex vivo* for adoptive cell transfer (Gotthardt et al., 2019).

### 1.6. Role of NKG2A in NK cell function and cancer therapy.

NKG2A is a calcium dependent C-type lectin belonging to the NKG2 family, which comprises 7 distinct subsets (A-F and H). NKG2A functions as an inhibitory receptor on the surface of mature NK cells by forming a heterodimer with CD94 to recognise self-peptides presented on HLA-E molecules on the hosts cell surface (Beziat et al., 2010). These self-peptides are derived from the leader peptides of MHC Class I molecules HLA-A, -B and -C (Lee et al., 1998, Leibson, 1998) and HLA-G (Rolle et al., 2018) indicating to the NK cell that the opposing cell is a healthy host cell with normal MHC expression (Joyce and Sun, 2011). In addition to NK cells, γδ T and $CD8^+$ T cells also express the NK2GA/CD94 heterodimer (Khan et al., 2020).

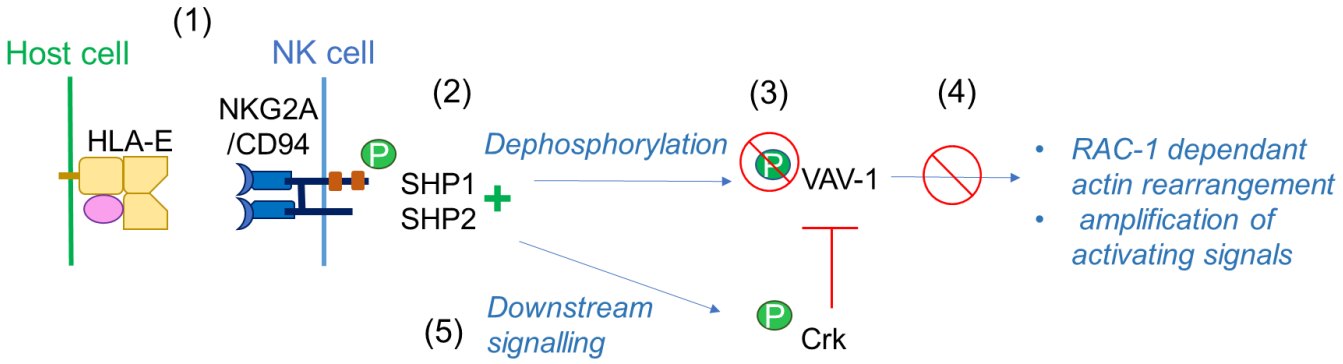



Figure 1.7: NKG2A signalling pathway associated with NK cell response inhibition.

*(1) Interactions of the HLA-E and NKG2A/CD94 complex induces phosphorylation (green Ⓟ symbol) of the tyrosine residues within the ITIM domain (orange box).*

*(2) Phosphorylated Tyrosine residues recruits and activates (green + symbol) SHP-1 and SHP-2 phosphatases.*

*(3) SHP1 dephosphorylates activating signalling molecules such as VAV-1 (symbolised by a red sign).*

*(4) Dephosphorylated VAV-1 cannot continue downstream signalling initiated by activating signals.*

*(5) ITIM signalling also results in phosphorylation of adaptor protein Crk, which inhibits VAV-1.*

Upon ligand binding of the NKG2A/CD94 heterodimer, intracellular ITIM phosphorylation recruits SH2-domain containing protein tyrosine phosphatases (SHP) 1 and 2 (Figure 1.7). Upon binding, these phosphatases undergo structural changes that permit interactions with downstream signalling proteins, such as VAV-1 or adaptor protein CD3ζ (Kabat et al., 2002, Nash et al., 2014). VAV-1 mediates the amplification of signals received from activating receptors as well as encourages actin rearrangement through GTPase RAC-1, enabling release of cytotoxic granules. As SH2-domain proteins dephosphorylate VAV-1, it now becomes inactive, suppressing the activation signals and shifting the balance towards NK cell inhibition (Billadeau et al., 1998, Nash et al., 2014). VAV-1 can also be inhibited by ITIM mediated Crk protein activation (Figure 1.7).

Certain cancers evade NK cell immune recognition by upregulating receptors for its inhibitory ligands, therefore understanding NKG2A signalling within a clinical setting is important. For example, high levels of HLA-E corresponding to poor prognosis has been identified in kidney renal carcinoma, head and neck squamous cell carcinoma, ovarian cancers and chronic lymphocytic leukaemia to name a few (Kamiya et al., 2019, Khan et al., 2020). Targeting NKG2A expression as a way to enhance NK cytotoxicity for immunotherapy is currently being tested. Antibodies like Monalizumab, which are designed to block NKG2A signalling, has shown improve NK cell dysfunction in chronic lymphocytic leukaemia *in vitro* and is being tested in combination with anti-PD-1 antibody Cetuximab for the treatment of patients with recurrent or metastatic squamous cell carcinoma of the Head and Neck (NCT02643350), (Andre et al., 2018, Rezvani, 2019).

An issue with blocking NKG2A with antibody immunotherapy, however, is that the effect can be overcome in a couple of different ways. Tumour cells can upregulate HLA-E in response to IFNγ release from anti-tumour cells in the surrounding environment. This increase can induce resistance towards NK cells with inefficient anti-NKG2A antibody binding (Kamiya et al., 2019). Another limitation with antibody therapy is due to the recycling of NKG2A/CD94 heterodimer between the surface and cytoplasm of the cell. The continual supply of new and existing NKG2A receptors to the cell surface reduces the ability of the antibody to consistently inhibit NKG2A signalling (Kamiya et al., 2019).

An alternative approach that produced better cytotoxicity when compared to the anti-NKG2A antibody is the downregulation of NKG2A expression by retaining it in the endoplasmic reticulum/golgi apparatus (Kamiya et al., 2019). Using retroviral mediated knockdown of NKG2A surface expression, $NKG2A^-$ peripheral blood NK cells and NK92 cells (an NK cell line) exhibited a greater cytotoxic response to HLA-E overexpressing tumours. No change in proliferation or marker expression was observed except for a slight decrease in CD25 (IL-2Rα) expression, although this did not appear to effect IL-2 mediated expansion.

Given the potential NKG2A targeting has in improving cancer therapy, much work is required in order to understand the full effect of deleting NKG2A gene expression within NK cells. A permanent deletion of NKG2A expression on mature NK cells would

present itself as a solution to the current issues caused by receptor recycling. However, one key observation is that NKG2A$^{+}$ NK cells respond better to stimulation with HLA Class I negative target cells (i.e. the 721.221 or K562 cancer cell lines) than do NKG2A$^{-}$ NK cells (Ivarsson et al., 2013). This is due to NKG2A-mediated education of NK cells at some point during the cell's development or maturation, leading the NK cell to respond appropriately to the target cell it encounters. Further elucidation on how NKG2A regulates NK cell education, function and overall responses towards the target cells is required for the benefit of enhancing NK cell-mediated therapy for NKG2A ligand related cancers.

### 1.7. NK cells and cancer immunotherapy.

There are several different types of immunotherapy strategies. These can be broadly summarised into two main categories: antibody-based enhancement of immune responses or adoptive cell transfer. The latter can also be subdivided further regarding the transfer of activated, endogenous immune cells or genetically engineered immune cells with enhanced effector or cancer recognition functions (Figure 1.8), (Shin et al., 2020).

The majority of antibody-mediated NK cell therapy involves the combined use of antibodies against multiple inhibitory NK cell receptors. As previously described, anti-NKG2A Monalizumab and anti-PD-1 Cetuximab showed enhanced NK cell cytotoxicity towards head and neck cancer (Andre et al., 2018). Other treatments against solid tumours include combinations of anti-KIR (Lirilumab) with anti-PD-1 (Nivolumab) (NCT01714739) or with anti-CTLA-4 (Ipilimumab) (NCT01750580). In addition, the combination of antibody and cellular therapy is also in use, for example anti-PD-1 antibody Sintilimab injected together with autologous peripheral blood NK cells to treat advanced non-small cell lung cancer (NCT03958097).

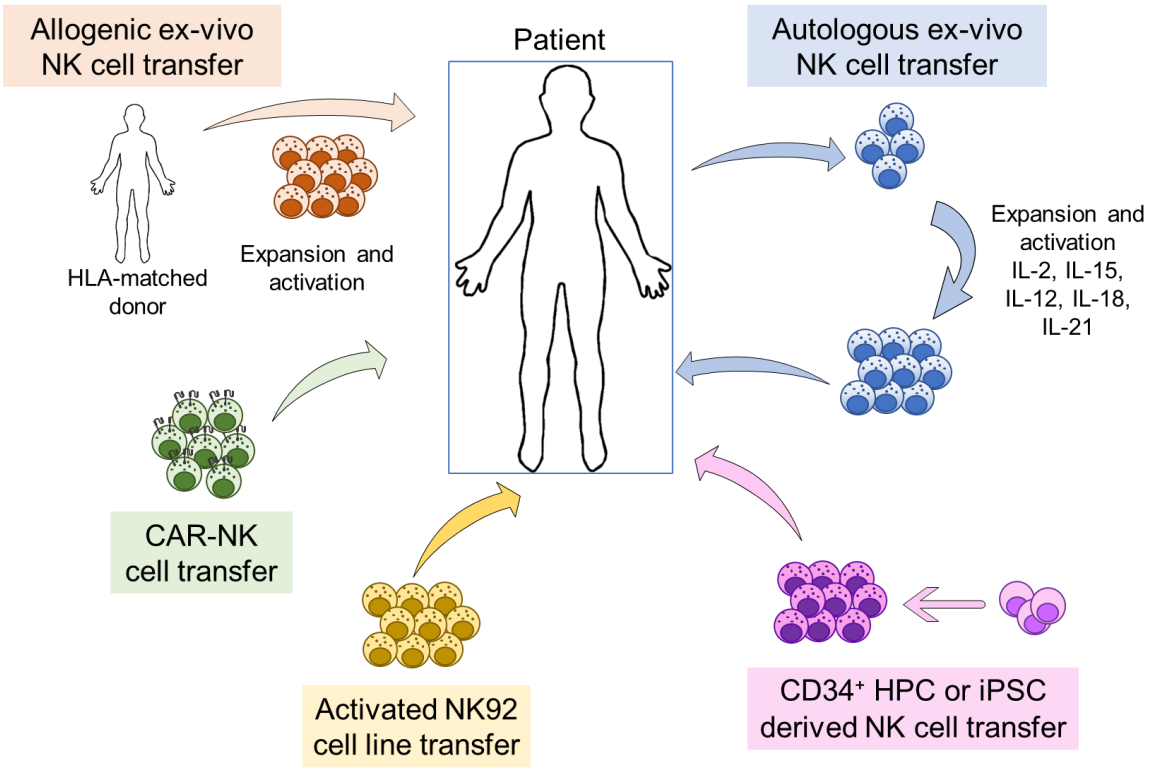



Figure 1.8: Summary of cell sources for adoptive cell transfer.

*Summary of the different NK cell sources for adoptive cell transfer for cancer treatment. Ex-vivo expansion and activation from patient or donor derived NK cells can be achieved using a range of cytokines as outlined above. NK cells for adoptive transfer can also be genetically modified to improve specificity against the cancer type or enhance effector functions.*

Autologous (patient derived) adoptive NK cell transfer was one of the earliest established methods for cancer treatment (Figure 1.8), providing anti-tumour responses to a range of different cancers. Peripheral blood NK cells from the patient can be a source of autologous NK cells, expanded and activated *ex vivo* using cytokines such as IL-2 to treat melanoma and renal cell carcinomas (Parkhurst et al., 2011). A well-tolerated and safe anti-tumour response has also been shown in patients with advanced chronic lymphocytic leukaemia or metastatic tumours with infusion of $1x10^8$ NK cells/Kg (Lundqvist et al., 2011). One major drawback, however, in using autologous NK cells is the consequence of a reduced cytotoxic response due to self-HLA recognition and NK cell inhibition (Cheng et al., 2013, Lundqvist et al., 2011).

An approach to overcome the issue of reduced NK cell cytotoxicity is the of use allogenic (donor derived) haploidentical NK cells (Figure 1.8). HLA-matched allogenic NK cells have shown to improve remission in high-risk myelodysplastic syndrome patients (Bjorklund et al., 2018), as well as allogenic HLA-matched KIR mismatched donors, seen to improve remission in acute myeloid leukaemia patients (Curti et al., 2016, Miller et al., 2005, Pfefferle and Huntington, 2020). Unlike autologous NK cells, HLA-matched KIR mismatched allogenic NK cells are unable to receive inhibitory signals through their KIR receptors, allowing for enhanced cytotoxic responses. Nevertheless, identical HLA-matching is difficult and the slight differences in HLA haplotype may lead to the gradual rejection of adoptively transferred NK cells. Several alternative sources of allogenic NK cells exist, ranging widely from mature *ex vivo* expanded NK cells, NK cell lines, CAR-NK cells and iPSC or progenitor derived NK cells (Figure 1.8), which provide more options for cancer treatment (Cheng et al., 2013, Shin et al., 2020).

The expansion of allogenic NK cells with the presence of IL-2 has showed potential in the treatment of metastatic tumours (NCT00855452) and malignant melanomas (NCT00846833). However, with the inclusion of other cytokines such as IL-15, IL-12, IL-18 and IL-21 to expand these cell populations, it has been noted that telomere length post expansion can be reduced, indicating senescence and NK cell exhaustion (Chabannon et al., 2016, Denman et al., 2012, Guillerey et al., 2016). Loss of telomere length is likely the result of extensive proliferation and activation of already mature NK cells prior to NK cell transfer (Bi and Tian, 2017, Gill et al., 2012). Exhaustion of NK cells are also a common feature for both allogenic and autologous adoptive transfer as, soon after transfer, NK cells expressed significantly lower activating receptors and exhibited poor tumour killing responses (Cheng et al., 2013).

NK-92 cells, an NK cell line, was established from a patient with non-Hodgkin's lymphoma and have been phenotypically characterised as $CD56^+$ $CD45^+$ $CD3^-$ $CD16^-$ $HLA\text{-}DR^-$ (Yan et al., 1998, Zhang et al., 2019). This cell line consists of 100% activated NK cells that can be easily maintained *in vitro* and expanded into large numbers for immunotherapy. Although these cells lack the ability to induce ADCC, they have already shown encouraging responses after irradiation and infusion into patients with advanced treatment-resistant malignancies and renal cell carcinoma (Arai et al., 2008, Cheng et al., 2013, Guillerey et al., 2016). In spite of this, the

requirement for IL-2 restricts its efficacy during immunotherapy with the *in vivo* application of recombinant IL-2 posing a significant risk of unwanted side effects (Zhang et al., 2019). However, NK-92 cells can be engineered to be more useful for immunotherapy using CRISPR/Cas9 gene editing (Huang et al., 2020).

CRISPR/Cas9 modification of NK cell lines can be used to generate Chimeric Antigen Receptor (CAR) NK cells. CARs consist of an extracellular, tumour specific single-chain variable fragment and an intracellular signalling domain that induces cell activation upon antigen interaction. This can be integrated using the Cas9 endonuclease via homology directed repair using a donor template (Afolabi et al., 2019). Compared to CAR-T cell therapy, CAR-NK cells provide an alternative, safer approach as they exhibit reduced responses upon self-recognition, release far less proinflammatory cytokines that can result in cytokine-release syndrome (e.g. IL-2, IL-6, IL-8) and were found to have reduced risk for graft versus host disease (Liu et al., 2020, Xie et al., 2020). In addition to CAR-NK92 cells, other the NK cell sources that can be genetically modified include, iPSC derived NK cells (Li et al., 2018), peripheral blood NK or $CD34^+$ HPC derived NK cells (Xie et al., 2020).

Human iPSCs are generated from human somatic cells, commonly from fibroblasts, providing a source of easily obtainable progenitors to produce NK cells for therapy (Cichocki et al., 2020, Takahashi et al., 2007). Generation of iPSCs involve viral mediated overexpression of transcription factors Oct3/4, Sox2, Klf4 and c-Myc in the somatic cells to induce a pluripotent like state (Takahashi et al., 2007). When iPSCs were used to produce NK cells, these NK cells exhibited high proliferative potential and functional responses against multiple hematopoietic and solid cell cancers *in vitro* as well as ovarian cancer *in vivo* (Cichocki et al., 2020). While these advantages make iPSC derived NK cells a suitable alternative NK cell source for cancer therapy, the generation of iPSCs is inefficient and carry a risk of producing oncogenic progenitors due to overexpression of c-Myc and Klf4. IPSC differentiation potential is variable based on what cell is used to generate the iPSC (Cichocki et al., 2020), making the use of iPSCs as a progenitor challenging when investigating the role genes play during human NK cell development.

$CD34^+$ HPC progenitor cells that can give raise to NK cells *in vitro* are obtainable from a few different sources, such as the bone marrow, immobilised peripheral blood or

umbilical cord blood (UCB) (Cheng et al., 2013). Some well-established benefits of using UCB as a source of HPCs are that they have a reduced risk of viral transmission from donor to recipient, is relatively available through UCB collection and these cells require less stringent HLA matching during HSC transplant, reducing the risk of graft versus host disease (GvHD), (Chabannon et al., 2016, Sarvaria et al., 2017). UCB $CD34^+$ $CD38^-$ cells also exhibit greater proliferative potential to cytokines and are less dependent on a stromal cell layer in order to expand compared to bone marrow or peripheral blood progenitors. This high proliferative potential is thought to be because UCB cells have long telomeric DNA and therefore are capable of multiple rounds of replication (Domogala et al., 2017, Hordyjewska et al., 2015). NK cells produced *in vitro* from UCB $CD34^+$ HPCs has shown to be safe and is currently being tested in the oNKord clinical trial, testing the effectivity of these cells in patients with acute myeloid leukaemia (EudraCT number 2010-018988-41), (Sarvaria et al., 2017).

One slight drawback is that UCB contains 10-100 fold less nucleated cells compared to other sources of HSC's, which in turn limits how many cells can be obtained from one UCB unit (Sarvaria et al., 2017). The percentage of $CD34^+$ cells within the cord blood is approximately 0.02-1.43%, while in adult bone marrow this value increases to 0.5-5% (Hordyjewska et al., 2015). Cryopreservation of $CD34^+$ HPCs is one way to overcome the low yield, as multiple UCB units can be preserved with no implications to its ability to differentiate into functional NK cells (Luevano et al., 2014).

UCB $CD34^+$ HPCs are therefore a valuable resource for the development of clinical grade NK cells suitable for the use of immunotherapy. These $CD34^+$ derived NK cells are also able to be cryopreserved without detriment to its effector capabilities (Domogala et al., 2016). This permits the use of these cells as an "off the shelf" product for multiple treatments from the same batch, reducing variability across treatments. In addition to this, the ability to develop fully functional human NK cells *in vitro* allow for targeting genes associated with NK cell development and maturation early during the developmental process, in order to study their function.

## 1.8. Differentiation of NK cells from UCB CD34$^+$ progenitors.

Several methodologies have been tested to differentiate UCB CD34$^+$ progenitors into NK cells *in vitro*. These can be divided into two main groups, feeder free or feeder inclusive (Table 1).

| Method | NK cell production / fold expansion at end | Culture length | NK cell purity at end of culture | NK phenotype | Cytotoxicity: Lysis, E:T ratio, co-culture time | Cytokines / additives | Citation |
|---|---|---|---|---|---|---|---|
| **Feeder free** | 1435-2657 fold expansion.<br>Begin: 0.89-6.34x$10^6$<br>End: 1.6-3.7x$10^9$ | 35-42 days | >90% | CD56+ CD3- NKG2D+ NCR+ | • 40-60% lysis of K562<br>• 10:1<br>• 18hr | SCF, Flt3-L, TPO, G-CSF, IL-2, IL-6, IL-7, IL-15. Low molecular weight heparin. | Spanhotlz et al., 2011. |
| | Begin: 5x$10^4$ – 5x$10^5$<br>End: 9.1x$10^8$ | 30 days | N/A | CD56+, CD16 int, CD94 int, NKG2D+, NKp46+, Perforin+, KIR low | • 78% lysis of K562<br>• 5:1<br>• 4hr | Flt3-L, IL-15, IL-21. Hydrocortisone. | Perez et al., 2006. |
| | >1000 fold<br>Begin: 1x$10^6$<br>End: 1.09x$10^6$ | 35 days | >80% | CD56+, CD45+, NKG2A+, Perforin+, NCR+, NKG2D+, Eomes+, CD16low, KIRlow | • >80% lysis of K562.<br>• >60% lysis of ovarian cancer cell lines<br>• 3:1 and 10:1<br>• 24hr | SCF, Flt3L, TPO, IL-7, IL-12, IL-15. StemRegenin1. | Hoogstad-Van Evert et al., 2017. |
| **With Feeder** | | | | | | | |
| EL08-1D2 | 2852 fold (by 14 days) | 28 days | 99% | CD56+, NKp30/44+, NKG2Aint, NKG2Dint, CD16low, KIRlow | • >50% lysis of K562<br>• 5:1<br>• 4hr | SCF, Flt3-L, IL-3, IL-7, IL-15. Hydrocortisone. | Grzywacz et al., 2006. |
| ATF024 or EL08-1D2 | Begin: single cell<br>End: 2.3x$10^4$ (ATF024)<br>End: 1.2x$10^5$ (EL08-1D2) | 28 days | Not described | CD56+ CD45+ CD3- NKG2A int, KIR int | Not described | Flt3-L, IL-3, IL-15 (ATF024). SCF, Flt3-L, IL-3, IL-7, IL-15, IL-21 (EL08-1D2). | McCullar et al., 2008. |
| MS-5 | 112-130 fold | 21 days | 95% | CD56+, otherwise not described | Not described | SCF, Flt3-L, IL-2, IL-7, IL-15. | Haddad et al., 2004. |
| OP9 | 700-1000 fold | 28 days | 90% | CD56+, CD16+, CD94+, Perforin+ | • >50% lysis K562<br>• 12.5:1<br>• 4hr | SCF, Flt3-L, IL-3, IL-7, IL-15. | Herrera et al., 2017. |
| Human BM stromal cells | 2 fold<br>Begin: 1.28x$10^6$<br>Day 3: 2.84x$10^6$ | 3-9 days | 25.8% | CD56 int, CD16 int | • 12-20% lysis of K562<br>• 5:1 – 10:1<br>• 4hr | SCF, Flt3-L, IL-2, IL7, IL-15. | Frias et al., 2009. |

Table 1: Summary of NK cells differentiated from UCB CD34$^+$ HPCs.

*E:T, Effector: Target ratio; Int, Intermediate.*

When differentiating NK cells without a feeder layer, it is quite common to include additives such as low molecular weight heparin, hydrocortisone or StemRegenin1 (Table 1). Heparin can bind to and activate different cytokines and NCR's, enhancing HPC expansion and inducing IFNγ secretion respectively (Tanaka et al., 2012). The glucocorticoid hydrocortisone induced CD122 expression, enhancing IL-15 mediated $CD56^+$ NK cell expansion, as well as inducing IFNγ, IL-10 and TNFα release (Perez et al., 2005). StemRegenin1 induced not only HPC expansion but when combined with NK differentiating cytokines, it induced $CD56^+$ NK cell proliferation and expression of ID2 and EOMES (Roeven et al., 2015). These additives generally led to increased expansion and enhanced cytotoxicity of $CD34^+$ derived NK cells (Perez et al., 2006, Roeven et al., 2015, Tanaka et al., 2012).

With the use of bioreactor culture bags, feeder free conditions also enable large quantities of relatively pure NK cells to be generated, within the $10^9$ cell range from 0.9-1.7x$10^6$ $CD34^+$ HPCs (Spanholtz et al., 2011). These methods provide a readily accessible source of good manufacturing practice (GMP) grade NK cells suitable for use in the clinic. These NK cells also appeared to have good cytotoxicity when co-cultured with the MHC-deficient erythroleukemic cell line K562 (Table 1). Nevertheless, the requirement to produce such a high number of NK cells is dependent on the seeding number of $CD34^+$ HPCs at the beginning of culture, ranging from 1x$10^4$ – 1x$10^6$ UCB $CD34^+$ HPCs (Perez et al., 2006).

The inclusion of a feeder layer provides two advantages for NK cell differentiation, lower progenitor cell requirement for NK cell development and earlier emergence of $CD56^+$ NK cells (McCullar et al., 2009). Feeder inclusion allows for differentiation from as low as a single $CD34^+$ HPC (Table 1), however the number of NK cells produced is still dependant on the initial seeding density. Additionally, feeder-included conditions show detection of $CD56^+$ NK cell expression earlier, around 3-4 weeks of culture, while non-feeder methods show NK cell detection around 4-5 weeks (Table 1). Therefore, feeder co-culture reduces the culture time required to generate NK cells for adoptive cell therapy. For example, $CD34^+$ HPCs differentiating into NK cells using a EL08-1D2 feeder cell co-culture underwent a 2852-fold expansion within 14 days (Grzywacz et al., 2006), while HPCs differentiating in feeder-free conditions exhibited a 500-fold expansion by day 21 of NK cell differentiation (Hoogstad-van Evert et al., 2017). Henceforth, these advantages make inclusion of a feeder layer the better option when

investigating NK cell differentiation from single, or few, $CD34^+$ HPCs for the purpose of clonal NK cell development.

The type of feeder used also influences the development of $CD34^+$ derived NK cells, with both human and mouse derived feeder layers encouraging development of human NK cells. Of the various feeder layers that are compared, the mouse fetal liver EL08-1D2 cell line appears to produce the greatest number of human NK cells with good cytotoxicity towards K562 targets (Table 1). EL08-1D2 feeder cells resulted in 4 to 8-fold increase in NK cell numbers compared to the fetal liver fibroblast cell line AFT024, even when seeded at a low starting density of 10 cells per well (McCullar et al., 2009). The bone marrow derived fibroblast MS-5 cell line encouraged 112 to 130-fold expansion from cells seeded between 1 to 300 cells/well, however these cultures are also found to support the production of B and T cell lineages (Haddad et al., 2004). This not only reduces the efficiency in generating NK cells, but these contaminating cells would need to be removed as it could result in unwanted side effects during adoptive cell transfer. The OP9 feeder cell line, bone marrow fibroblast in origin, exhibited lower expansion rates when compared with EL08-1D2. In addition to this, OP9-derived NK cells require a higher effector: target (E:T) ratio in order to lyse K562 cells (Herrera et al., 2017). Human bone marrow stroma gave the lowest yield, with only 2-fold expansion and a population of $CD56^+$ NK cells that had intermediate expression of both CD56 and CD16 receptors (Frias et al., 2008). As human bone marrow stromal cells need to be processed prior to co-culture with $CD34^+$ HPCs, in addition to the lower NK yields they produce, mouse-derived feeder cells such as EL08-1D2 provide a cost effective and simpler alternative when generating NK cells from low HPC populations.

In summary, UCB $CD34^+$ HPCs can be differentiated into functional NK cells in the presence of additives or a feeder cell layer. NK cell production is dependent on the number of HPCs seeded at the beginning of differentiation, with feeder cell inclusion providing the additional support to differentiate from lower starting populations. This feature also allows for enough NK cells to be generated to meet the high demand requirement for NK cell therapy. The only prerequisite is that feeder derived NK cells must be purified from their feeder layer in order to establish safe GMP grade NK cell populations. In addition to the clinical advantages, the ability to differentiate a single

HPC into NK cells in the presence of feeder cells enables clonal differentiation of gene targeted progenitors.

## 1.9. CRISPR/Cas9 technology as a tool for NK cell gene modification.

Developed from the Streptococcus pyogenes (Sp) type II system, the Clustered Regularly Interspaced Short Palindromic Repeats (CRISPR) genome editing technique allows for the manipulation, mutation or deletion of genes (Figure 1.9). This system requires two components for gene targeting: Cas9 endonuclease to induce double stranded DNA breaks (DSB's) and a short single guide RNA (sgRNA) complex that guides the Cas9 to a specific gene location (Jinek et al., 2012). CRISPR/Cas9 is now the editing method of choice for gene deletion in contrast to other genome modification systems, such as the zinc finger proteins (ZFP) or transcription-activator like effectors (TALEs). Because ZFP's and TALEs require the generation of novel proteins to target the DNA region, CRISPR/Cas9 systems provide an easily customisable alternative as DNA specificity is mediated by sgRNA (Cong et al., 2013, Kabadi et al., 2014).

The sgRNA complex is composed of a short 20 nucleotide sequence or spacer (known as CRISPR RNA or crRNA) complementary to the genomic region of interest and a pre-determined scaffold sequence (known as trans-activating CRISPR RNA or tracrRNA) necessary for Cas9 binding (WareJoncas et al., 2018). Each sgRNA sequence must be upstream and adjacent to a protospacer-associated motif (PAM). In the case of an SpCas9, the recognised PAM motif is N(GG), where N represents any nucleotide (Sander and Joung, 2014). Cas9 mediated DSB's occur 3bp upstream of the PAM sequence, cutting directly within the sgRNA sequence (Figure 1.9). The PAM requirement restricts Cas9 cleavage to the guide sequences found within the host cell DNA and not the CRISPR DNA, ensuring specificity to the host cell only.

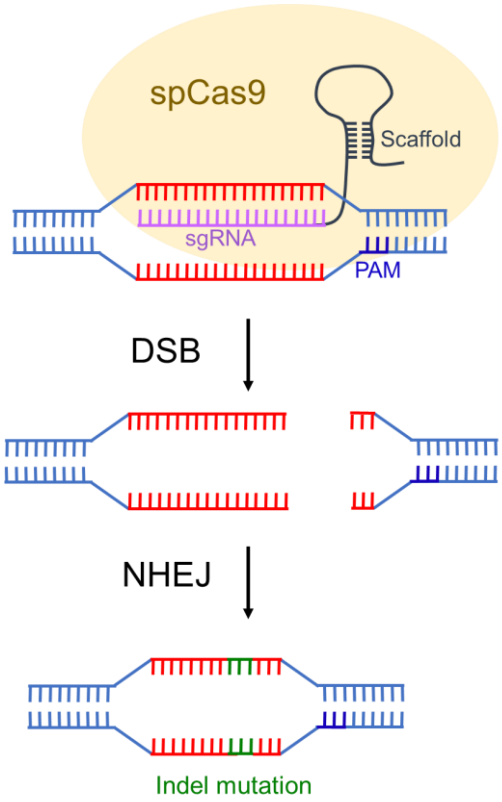



Figure 1.9: CRISPR/Cas9 genome editing procedure.

*When the sgRNA and SpCas9 are expressed, they form a complex that is stabilised by the scaffold (yellow circle). The SpCas9 then undergoes a conformational change allowing it to bind to DNA. The sgRNA region localises the Cas9 complex to the target gene of interest where the SpCas9 will induce a DSB 3 nucleotides upstream of the PAM sequence. The DSB is then repaired by non-homologous end joining, resulting in random insertions or deletions (Indels), (Sander and Joung, 2014).*

Within the host cell, the DSB is then repaired by two methods, non-homologous end joining (NHEJ) or homology directed repair (HDR). NHEJ is the dominant repair mechanism observed in targeted eukaryotic cells, creating a small region consisting of base insertions or deletions (Indels) between the DSB (Figure 1.9). This method is most common when generating a gene knockout cell population. The expression of at least two sgRNA on either side of the gene of interest would result in the Cas9 mediated excision of that region and repair by NHEJ mechanisms. Efficiency can be improved by multiplexing the CRISPR/Cas9 gene system. This involves co-expressing

the Cas9 with more than two sgRNA, so that there are more chances of inducing a DSB as well as expanding the DNA target region (Kabadi et al., 2014). HDR, on the other hand, requires the presence of a donor DNA segment that is incorporated into the region of the DSB. This is the method of choice is particularly useful when trying to generate a gene or reporter knock-in cell population. This process can utilise a modified Cas9 endonuclease or single strand DNA templates with partial host DNA homology in order to boost knock-in efficiency (Ryu et al., 2019, WareJoncas et al., 2018).

During the sgRNA design, two important factors are taken into consideration, specificity and activity. The specificity of a sgRNA towards its genomic target of interest is most important, as recognition of a few base pairs to different sites on the genome can result in Cas9 mediated off-target cleavage. The activity of a sgRNA is measured by its efficiency to induce a Cas9 mediated DSB. For example, sgRNA sequences rich in guanine bases and few in adenosine bases provides better guide stability and hence efficiency (Labun et al., 2016). The specificity of sgRNA towards on and off-target sequences can be measured using an MIT specificity score, while the activity of guides best suited for *in vitro* or *in vivo* cell targeting can be scored as the Doench score and Moreno score respectively (Doench et al., 2014, Hsu et al., 2013, Moreno-Mateos et al., 2015). Online algorithms quantify these factors so guides can be compared to one another during the design process. Nevertheless, target specificity of the Cas9 is never perfect and checking for off-target effects post CRISPR/Cas9 targeting can be achieved through sequencing these predicted off-target sites. Off-target effects can also be calculated through methods such as the Surveyor nuclease assay to detect mutations from nuclease-induced DNA repair (Kabadi et al., 2014).

One final aspect to consider with CRISPR/Cas9 mediated genome modification is the choice of method used to express the system within the target host cell. Overcoming the cell membrane barrier can be achieved by electroporation, or more recently, nucleofection, creating pores within the membrane or nucleus and permitting entry of a pre-formed Cas9-sgRNA protein complex. However, while methods like these provide high gene targeting efficiency, they also result in high rates of cell death post electroporation (Morgan et al., 2017). An alternative is to clone the Cas9, sgRNA and scaffold sequences in an expression vector under the control of ubiquitous mammalian

promoters. Target cells can be transfected with these vectors where the expression of the Cas9 and guides is achieved by the hosts translational machinery (Ryu et al., 2019). For cells difficult to transfect, such as $CD34^+$ HPCs, viral expression vectors can be used. Immortalised cell lines used for virus production, such as the human embryonic kidney cell line 293T, can be transfected with the Cas9 viral expression vector and the virus produced can be used to transduce the target cell of choice (Kabadi et al., 2014; Morgan et al., 2017). Combined with protocols that have previously been established to successfully transduce $CD34^+$ HPCs using a lentiviral expression vector (Adair et al., 2016, Liu et al., 2008, Naldini et al., 1996, Zielske and Gerson, 2002), it is possible to achieve a CRISPR/Cas9 mediated gene knockout in $CD34^+$ HPCs to investigate cell biology and for future clinical applications.

NK cells are a valuable resource for the treatment of various types of cancers during immunotherapy. Their versatility in target cell recognition, activation and cytotoxic responses give them unique advantages compared to T cells during adoptive cell therapy. Nevertheless, there are still some limitations associated with NK cell therapy that needs to be addressed in order to utilise these cells to their full potential. To meet the demand for an efficient treatment, a large number of functional NK cells are required. Current strategies to expand and activate NK cells *ex vivo*, such as autologous or allogenic peripheral blood NK cells, exhibit limited proliferation and early exhaustive phenotype soon after transplant (Gill et al., 2012). Targeting different genes associated with NK cell development and function could be the answer to drive NK cell production and enhancement of effector responses. E4bp4 and Eomes are known to be crucial for NK cell development and maturation in mice, and thus good potential targets to investigate during human NK cell development. NKG2A has already shown success as a therapeutic target to enhance NK cell cytotoxicity when blocked, however current therapies involve transient action and are not long lasting. Combining the use of CRISPR/Cas9 mediated gene targeting and the ability to differentiate NK cells from human cord blood $CD34^+$ HPCs *in vitro*, it is possible to study the effect of these genes during NK cell development. Further characterisation of these cells would identify the mechanisms these genes utilise to influence NK cell development and function. This provides us with potential therapeutic targets that could overcome the limitations of restricted NK cell proliferation and premature NK exhaustion observed in current NK cell immunotherapy.

## 1.10. Aims and objectives.

The efficiency of NK cell therapies can be affected by several factors including the maturation of NK cells and the ability of these cells to exhibit an appropriate effector response. One major hurdle that clinicians face during NK cell therapy is the limited proliferative capacity of mature NK cells, making it difficult to produce the number of fully functional cells required to treat a patient. Another issue is the onset of premature exhaustion and dysfunction caused by extensive expansion and activation prior to patient transplantation. This limits the efficacy of human NK cells for effective cellular therapy.

To expand cells without harming downstream functional responses, a reasonable solution is to target known pathways associated in NK cell development. To enhance cytotoxic ability, targeting pathways associated with inhibition so as to reduce the threshold level necessary for cell activation may lead to more effective NK cells. To achieve these aims, I have attempted to study the role of three genes believed to be critical to human NK cell development and function:

1. E4bp4 is a transcription factor whose expression within lymphoid progenitors is crucial for commitment towards the NK cell lineage. Research on E4bp4 and its signalling has largely been conducted in mouse models, including a great deal investigating the functions of E4bp4 outside of NK cell development. The importance of E4BP4 during human NK cell development has yet to be established and whether its roles match what is observed in mouse. By identifying potential targets downstream of E4BP4 signalling, it could be possible to develop strategies that enhance NK cell production.
2. Eomes is another transcription factor whose expression is required for the maturation of NK cells and, with T-bet, the development of a fully functional NK cell. Again, much of this research has been established in mice and information regarding human NK cell development is limited. Identifying the pathways that EOMES utilise to push NK cell maturation could be exploited in order to accelerate mature NK cell production from progenitor cells, either for cell therapy or for the study of NK cells in general.
3. NKG2A is an inhibitory receptor that has been shown to enhance NK cell cytotoxicity when its signalling is compromised. However, clinical trials targeting

NKG2A use antibody-based therapy. This only provides a transient blockade of signalling, and as NKG2A is continuously recycled between the cell membrane and the cytoplasm, this reduces the efficacy of this type of therapy. Developing an NKG2A knockout (KO) NK cell that is completely deficient in NKG2A expression could provide an alternative strategy that overcomes this problem.

To investigate the roles of these genes in NK cell development, I plan to generate a lentivirus mediated CRISPR/Cas9 gene knockout in UCB $CD34^+$ derived NK cells. The lentiviral CRISPR/Cas9 expression system will allow me to target either E4BP4, EOMES or NKG2A within progenitors, prior to any expression of the genes and therefore any influence they may exhibit during NK cell development. The progenitor cells will then be differentiated into NK cells as a single or low cell starting numbers, so that the generated population of cells will be clonal.

Upon production of a transduced cell population, the genotype of these cells will be identified using PCR and the NK cell phenotype characterised using flow cytometry. Identification of a NK cell population with wild type, heterozygous or homozygous gene deletion will then be tested for its functional capacity. This will entail co-culture of these cells with various cancer cell lines and determination of target cell lysis by flow cytometry. Comparisons between the gene targeted $CD34^+$ derived NK cells and the NK cell line, NK92 will also be conducted. The efficacy of NK92 is also being investigated in clinical trials, therefore, these functional comparisons will allow me to translate the information gained from these experiments into a clinical setting.

With the information gained from these experiments, I hope to provide a better insight into the biology of NK cell development, maturation and function and contribute to improved production of highly functional NK cells for use in adoptive therapy.

# 2. Materials and methods.

## 2.1. Cell lines.

### 2.1.1 293T and 293FT cells.

The 293T and 293FT (Francis Crick Institute) human embryonic kidney (HEK) cell lines were cultured at 37°C, 5% $CO_2$ in media that comprised: Dulbecco's modified eagles' medium (DMEM, high glucose; SIGMA) and 10% Fetal bovine serum (FBS; both from SIGMA). Cells were split for maintenance upon reaching 80-90% cell confluency in 10cm tissue culture plates. To harvest 293T cells, the old media was aspirated from the plate and the cells were harvested using mechanical force with fresh media from a stripette. 293FT cells were harvested by first washing the plate with Dulbucco's PBS (dPBS; SIGMA), followed by addition of trypsin-EDTA solution (diluted to 1x in dPBS; SIGMA) to detach the cells. After a 5-minute (min) incubation at 37°C, detached 293FT cells were quenched at a 1:1 ratio using DMEM 10% FBS, collected and centrifuged at 500 *xg* for 5 min. Once both 293T and 293FT cells were resuspended in fresh media, they were maintained at a split ratio between 1:6 to 1:8 with a full media change every 2 days.

### 2.1.2 MRC5 cells.

The MRC5 lung fibroblast cell line (Francis Crick Institute) was cultured at 37°C, 10% $CO_2$ in media that comprised: DMEM and 10% FBS. Upon reaching 80-90% cell confluency in 10cm plates, the cells were harvested using trypsin for 5-10 min as described previously and quenched 1:1 in DMEM 10% FBS. Cells were centrifuged at 500 *xg* for 5 min and maintained at split ratio between 1:2 to 1:5, with a media change every 2 days.

### 2.1.3 EL08-1D2 cells.

The EL08-1D2 mouse embryonic fetal liver cell line was cultured at 32°C, 5% $CO_2$ in EL08-1D2 media that comprised: Minimum essential Medium Eagle AQ media (αMEM; SIGMA), 50% Myelocult (StemCell Tech), 20% conditioning EL08-1D2 media, 7.5% embryonic stem cell FBS (ES-FBS; Merck), 1% L-glutamine (Gibco), 1% Penicillin and streptomycin (P/S; Gibco), 50μM β-Mercaptoethanol (β-Me; Gibco) and

1μM hydrocortisone (added fresh; SIGMA). Conditioning media was composed of filter sterilised supernatant from a confluent EL08-1D2 cell culture. For maintenance, 3-4x$10^5$ EL08-1D2 cells were seeded in a 75$cm^2$ (T75) flask, which was gelatinised by adding 0.1% porcine skin gelatine water solution (SIGMA) to the flask for 15 min at 37°C and washed with dPBS prior to cell addition. Upon reaching 80-90% cell confluency, the cells were harvested using trypsin as described previously, quenched 1:1 with DMEM 10% FBS and centrifuged at 300 *xg* for 7-10 min for resuspension in fresh EL08-1D2 media for plating.

To irradiate EL08-1D2 cells, freshly harvested cells were irradiated in 50ml falcons at 25 Gy using a Nordion Gamma irradiator. Post irradiation, the tubes were centrifuged at 300 *xg* for 7-10 min, resuspended in fresh EL08-1D2 media and seeded in gelatinised 96 well flat bottom plates at a range of 1-1.5x$10^4$ cells/ well for NK cell differentiation experiments. Plates containing irradiated EL08-1D2 were cultured at 37°C, 5% $CO_2$. Irradiated EL08-1D2 cells could also be cryopreserved by resuspending the recently irradiated, pelleted cells in freezing media which comprised 45% DMEM, 45% FBS, 10% DMSO (SIGMA). These cells were placed in Mr Frosty (Nalgene, USA) at -80°C overnight prior to long term storage in liquid nitrogen. Cryopreserved cells were thawed halfway using a 37°C water bath and combined with DMEM 10% FBS (pre-warmed to 37°C) to melt the rest of the ice pellet. Cells were centrifuged at 300 *xg* for 7-10 min, resuspended in fresh EL08-1D2 media and seeded as described before for NK cell differentiation.

### 2.1.4 NK92 cells.

The NK92 NK cell line was a kind gift from Dr. Nadia Guerra (Imperial College London) and was maintained at 37°C, 5% $CO_2$ in NK92 media that comprised: αMEM, 12.5% horse serum (Gibco), 12.5% FBS, 1x glutamax (Gibco), 0.1mM β-Me, 1x non-essential amino acids (NEAA; SIGMA), 0.02mM Folic acid (SIGMA), 0.2mM myo-inositol (SIGMA) and 100U/ml recombinant human IL-2. NK92 cells were maintained in 25$cm^2$ flasks (T25), seeded at 3x$10^5$ cells/ml and split every 3 days upon reaching 0.8-1x$10^6$ cells/ml. To split these suspension cells, the cells were collected in a falcon, counted, and centrifuged at 300 *xg* for 5-7 min. NK92 cells were resuspended in fresh NK92 media at the desired concentration and replated.

### 2.1.5 K562 cells.

The K562 chronic myelogenous leukaemia cell line was cultured at 37°C, 5% $CO_2$ in media that comprised: RPMI 1640 and 10% FBS. These cells were maintained in T75 flasks, seeded at $3x10^5$ cells/ml and split every 2-3 days upon reaching $0.8\text{-}1x10^6$ cells/ml. These suspension cells were split as described previously, however were centrifuged at 500 *xg* for 5 min.

### 2.1.6 PEO1 and PEO4 cells.

The PEO1 and PEO4 ovarian cancer cell lines (Francis Crick Institute) were maintained at 37°C, 5% $CO_2$ in media that comprised: RPMI 1640, 10% FBS and 1% glutamax. Upon reaching 80-90% cell confluency in T75 flasks, the cells were harvested using trypsin for 5-10 min as described previously and quenched 1:1 in RPMI 10% FBS. Cells were centrifuged at 300 *xg* for 5-7 min. PEO1 cells were maintained at a split ratio between 1:5 to 1:10 every 3 to 4 days. PEO4 cells were maintained at a split ratio between 1:4 to 1:5 every 5-6 days. Media was changed every 2 days.

## 2.2. Generation of CRISPR/Cas9 constructs.

### 2.2.1 SgRNA design for CRISPR/Cas9 targeting.

SgRNA sequences were designed using online tools CHOPCHOP and USCS genome browser, selected upstream of a NGG PAM sequence. For the human E4BP4 gene, the guides were designed in collaboration with Tiago Brazao (Francis Crick Institute) while the EOMES and NK2GA gene guides were designed by Sangwoo Kim and Dr Heather Ang (Hugh Brady group, Imperial College London), (Table 2.1). SgRNA sequence selection was dependent on criteria of an MIT specificity score above 70 and the highest obtainable Doench and Moreno-Mateos scores, with precedence towards the Donech score.

**A.** E4BP4

| Location | sgRNA | Cleavage site | Mismatch | Guide sequence | PAM |
|---|---|---|---|---|---|
| exon 2 | 1 | 91410581 | 2(5) 3(34) 4(243) | GCTTCTCAGTGAAGGAAGTG | TGG |
| | 2 | 91410555 | 3(18) 4(205) | AGAACAAATCTTCTGCATGT | CGG |
| exon 2 | 3 | 91409430 | 2(6) 3(27) 4(217) | AGAACTTGTATTTGAAGCAG | GGG |
| | 4 | 91409408 | 2(1) 3(9) 4(98) | GATAGCAAACTTATCTGCAG | AGG |

**B.** EOMES

| Location | sgRNA | Cleavage site | Mismatch | Guide sequence | PAM |
|---|---|---|---|---|---|
| exon 1 | 1 | 27721580 | 3(1) 4(26) | CCAGGGTACGGCCCGTAGAG | CGG |
| | 2 | 27721550 | 3(4) 4(82) | GTACCCTGGAGCCGCAGCGG | CGG |
| exon 2 | 3 | 27720272 | 3(4) 4(25) | CTCTACGAACACATTGTAGT | GGG |
| | 4 | 27720252 | 3(2) 4(46) | CTACAATGTGTTCGTAGAGG | TGG |

**C.** NKG2A

| Location | sgRNA | Cleavage site | Mismatch | Guide sequence | PAM |
|---|---|---|---|---|---|
| intron 2-3 | 1 and 2 | 10451275 | 3(8) 4(48) | GTGAGGTGGAGAACGAGTAT | TGG |
| exon 4 | 4 | 10450510 | 3(4) 4(46) | AACAACTATCGTTACCACAG | AGG |
| intron 4-5 | 3 | 10450458 | 3(11) 4(68) | CTATTTTCGAAGATTACAAG | GGG |

Table 2.1: SgRNA sequences for human E4BP4, EOMES and NKG2A

*Details of the sgRNA sequences are described. Cleavage site indicates the chromosomal location of the dsDNA break. Mismatches are annotated as the number of mismatched bases in the off-target sequence followed by the number of off-target sequences identified by the online tools in parentheses.*

### 2.2.2 Cloning strategy for the final Cas9-eGFP vector.

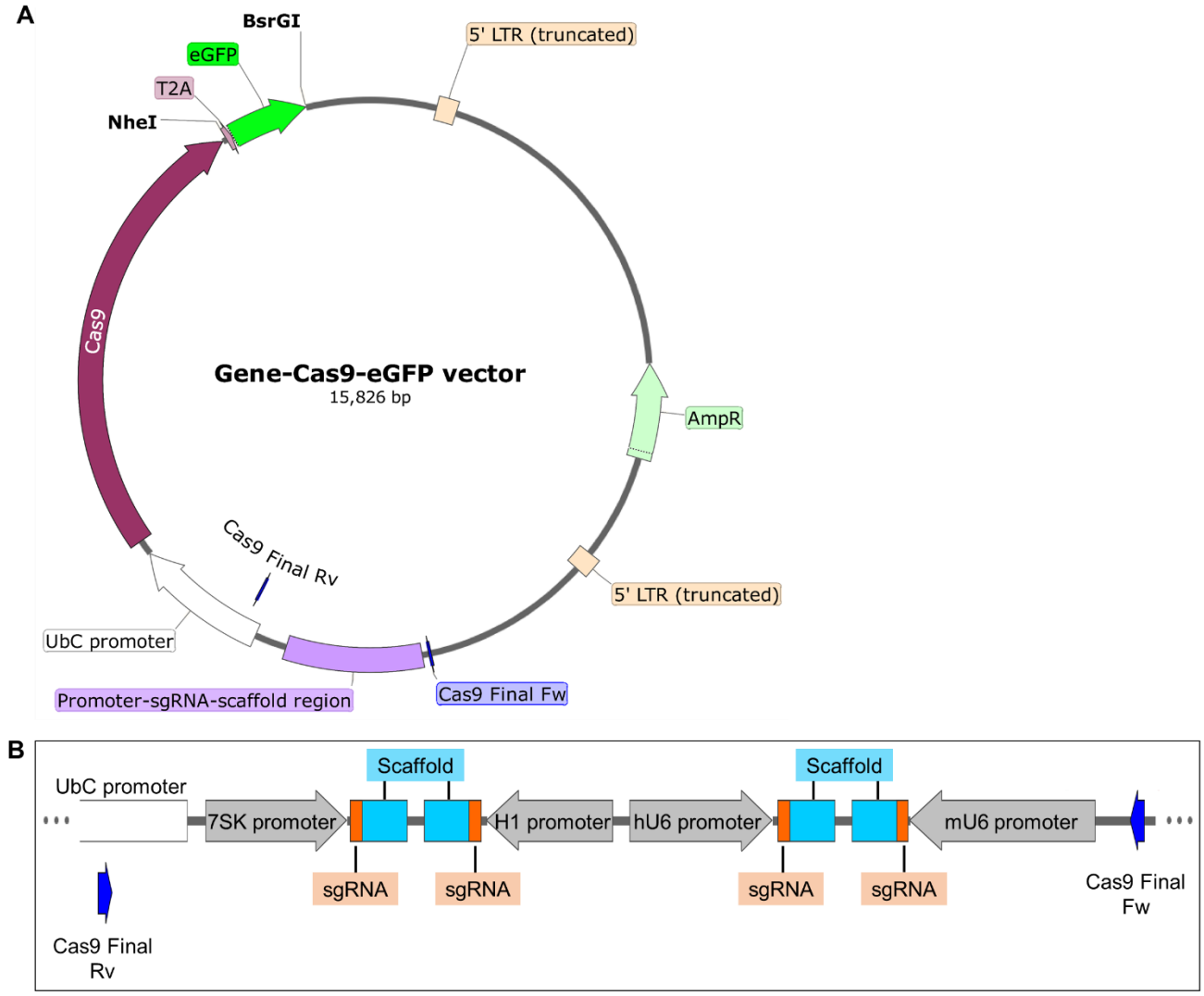



Figure 2.1: Final Gene-Cas9-eGFP vector map.

*(A) Vector map showing the final Cas9-eGFP vector with sgRNA designed to target specified genes of interest. The entire promoter-sgRNA-scaffold region is represented by a purple box. The SpCas9 and eGFP were under the expression of the human UbC promoter. (B) Enlarged view of the promoter-sgRNA-scaffold region from (A). The four individual promoters that expressed separate sgRNA and scaffolds were 7SK, H1, human U6 (hU6) and mouse U6 (mU6). Cas9 final forward (Fw) and reverse (Rv) primers (dark blue) are located outside of the entire promoter-sgRNA-scaffold region (Kabadi et al., 2014).*

The methodology used to produce and verify the final gene targeting Cas9-eGFP vector (Figure 2.1), was obtained from Kabadi et al., (2014), with all the vector plasmids purchased from Addgene. In brief, the lentiviral pLV-hUbC-SpCas9-T2A-eGFP vector (Addgene plasmid #53190) was used as the backbone for the insertion of four individual promoter-sgRNA-scaffold cassettes (Figure 2.1B). These cassettes were generated by cloning one of the four gene specific sgRNA oligonucleotides into the phH1-gRNA (Addgene plasmid #53186), the pmU6-gRNA (Addgene plasmid #53187), the phU6-gRNA (Addgene plasmid #53188) or the ph7SK-gRNA (Addgene plasmid #53189) vector using PCR. Each of these vectors were sequence verified and the promoter-sgRNA-scaffold region was isolated using restriction enzyme digest and agarose gel purification (QIAquick gel extraction kit; QIAGEN). After ligation into the pLV-hUbC-SpCas9-T2A-eGFP vector, the final gene targeting vector (now referred to as the gene-Cas9-eGFP vector) was verified using PCR and sequencing (Table 2.2). For confirmation by PCR, primers located outside the promoter-sgRNA-scaffold clone site (termed Cas9 final primers) generated a 1.8kb band representing the entire region and an additional 1.2kb and 0.5kb band due to the repetitive sequences within this region (Kabadi et al., 2014). The original pLV-hUbC-T2A-SpCas9-eGFP vector was also used as the empty vector control, now referred to as EV-Cas9-eGFP.

| Target/ Primer ID | Primer sequence (5' → 3') | Use |
|---|---|---|
| UbC promoter | GAAGGATCAGGACGCTCGCT | Sequencing for sgRNA insertion (via the 7SK promoter) |
| H1 promoter | CAGTGTCACTAGGCGGGAACA | Sequencing for sgRNA insertion |
| hU6 promoter | TTTCTTGGGTAGTTTGCAGTTT | Sequencing for sgRNA insertion |
| mU6 promoter | GGAAACTCACCCTAACTGTAAAGTAA | Sequencing for sgRNA insertion |
| Cas9 Final Fw | TCGGGTTTATTACAGGGACAGCAG | PCR for Promoter-sgRNA-scaffold insertion[1] |
| Cas9 Final Rv | TCTAAGGCCGAGTCTTATGAGCAG | PCR for Promoter-sgRNA-scaffold insertion[1] |

Table 2.2: Primer sequences for the gene-Cas9-eGFP vector.

*Sequencing primers were used to confirm insertion and orientation of sgRNA. The Cas9 final Fw (forward) and Rv (reverse) primers were used to screen and confirm successful cloning of the promoter-sgRNA-scaffold site described in Figure 2.1B. [1]Primer sequences and PCR cycle protocol for the Cas9 final Fw and Rv primers were obtained from Kabadi et al., (2014).*

The Cas9 vector used to target E4BP4 was initially produced with a truncated human CD2 reporter in place of the eGFP reporter. To produce the E4BP4-Cas9-eGFP vector, both the E4BP4-Cas9-hCD2 vector and the EV-Cas9-eGFP vector was digested with BsrGI and NheI (NEB; Figure 2.1A) for 3 hours (h) at 37°C in NEB buffer 2.1. The digests were run on a 0.8% agarose gel stained with ethidium bromide (SIGMA) and the 15kb E4BP4-Cas9 backbone and the 800bp eGFP reporter fragment was excised and gel purified. The E4BP4-Cas9 vector and the eGFP fragment was ligated at molar ratio of 1:3, respectively, using T4 ligase (NEB) and 5µl of this mixture was used to transform 25µl of One Shot Stbl3 competent bacteria (Invitrogen), all following manufactures instructions. Transformations were plated onto LB agar (VWR) plates containing 100µg/ml Ampicillin for an overnight incubation at 37°C, and the selected colonies were grown in Ampicillin containing LB broth (VWR). DNA was isolated using the QIAquick Spin miniprep kit (QIAGEN) and successful insertion of the 800bp eGFP insert was verified using BsrGI and NheI digestion and gel electrophoresis.

## 2.3. Targeting genes in CD34$^+$ HPCs and cell lines.

### 2.3.1 UCB CD34$^+$ HPC depletion.

UCB from healthy neonates was collected in collaboration with Mark Johnson (department of Obstetrics and Gynaecology, Chelsea and Westminister hospital) with informed consent under the study "The *in vitro* investigation of the maternal immune system" (REC reference: 11/LO/0971 from REC: London-Chelsea ethics committee).

Whole blood was diluted 1:1 in transport buffer (PBS, 0.05uM β-Me, 0.63% w/v trisodium citrate (SIGMA)) and layered on top of Ficoll Paque Plus (GE Healthcare) at a respective 3:1 ratio for PBMC separation in falcon tubes. The tubes were centrifuged at 400 *xg*, 30 min, 20-21°C with the brake off and the PBMC buffy coat layer was isolated. The buffy coat was washed with 2.5x the volume of room temperature RPMI 1640 and centrifuged at 225 *xg* for 10 min. Pellets were resuspended in 1ml of ACK lysing buffer per 2 falcon tubes (ThermoFisher scientific), combined, and incubated at 37°C for 1 minute. Cells were washed with 40ml of RPMI 1640 media and centrifuged at 145 *xg* for 10 min. Pellets were resuspended in 300µl of ice-cold AB labelling buffer comprising 20% human AB serum (SIGMA) in MACS buffer (PBS, 1% BSA (Fisher Scientific), 2mM EDTA (SIGMA)). Cells were then stained using the Human CD34 microbead depletion kit (Miltenyi) following manufacturer's instructions. Stained samples were washed with 10ml of ice-cold MACS buffer, centrifuged at 225 *xg*, 10 min, 4°C and resuspended in 500µl of MACS buffer per $10^8$ PBMCs. Using the quadroMACS magnetic separator and LS columns (Miltenyi), the columns were equilibrated with MACS buffer and the cell sample was added to the column following manufacturer's instructions, with the exception of washing the column with 3ml of cold MACS buffer four times. The CD34$^+$ HPC fraction was collected, centrifuged at 225 *xg* for 7-10 min, 4°C, and resuspended in 300µl of ice-cold AB labelling buffer for a second round of depletion using the LS column. This time, the 25µl of the FcR blocking reagent and 25µl of the microbeads from the CD34 microbead depletion kit was used to stain the cells, irrespective of the total number.

Samples were taken from the freshly depleted CD34$^+$ HPCs for purity analysis and the rest of the cells were cryopreserved in 90% human AB serum and 10% DMSO (SIGMA), using a Mr Frosty as previously described. Purity analysis involved staining the cells with anti-CD34 and anti-CD45 (details in Section 2.6) and analysing the

double positive population using flow cytometry. Depleted $CD34^+$ HPCs were generally above 90% $CD34^+$ $CD45^+$ marker expression, with the single positive $CD34^+$ HSC population comprising 0.2-1% of the total live, single cell population.

### 2.3.2 Transfection.

293T and 293FT cells were seeded at 3.5-4x$10^5$ cells/10cm plate one day prior to transfection, with 2 plates seeded for transduction of 0.5-1x$10^5$ $CD34^+$ HPCs. 9µg of the lentiviral Cas9-reporter vector was combined with 2$^{nd}$ generation packaging vectors psPAX2 (Addgene plasmid #12260) and pMD2.G (Addgene plasmid #12259) at a ratio of 1:1:0.3, respectively, for every 10cm plate transfected. Using lipofectamine 2000 reagent (Invitrogen), the vector DNA mix was incubated with 30µl of lipofectamine and 3ml of Opti-MEM (Gibco) following manufacturer's instructions. Transfected plates were maintained at 37°C, 5% $CO_2$ for 5-6h and underwent a full media change with fresh DMEM 10% FBS. Plates were incubated for another 2 days until viral supernatant was harvested for transduction. Transfected 293T or 293FT cells were harvested as previously described and cells were analysed for eGFP expression using flow cytometry. A live and dead non-fixable dye (TO-PRO-3 or DAPI) was included to identify live $eGFP^+$ percentages.

### 2.3.3 Virus concentration, transduction, and sorting of $CD34^+$ HPCs.

One day prior to transduction, cryopreserved $CD34^+$ HPCs were thawed as previously described in αMEM, 10% AB serum and centrifuged at 300 *xg* for 7-10 min. Pellets were resuspended in $CD34^+$ undifferentiation media at a final concentration of 5x$10^5$ cells/ml and plated in 48w or 24w tissue culture plates for an overnight recovery. $CD34^+$ undifferentiation media comprised StemSpan serum free media (StemCell technology) 1% L-glutamine and P/S (Gibco), 10ng/ml GM-SCF, 100ng/ml SCF, 100ng/ml TPO, 100ng/ml Flt3L, 10ng/ml IL-3 and 10ng/ml IL-6 (all purchased from Peprotech). When specified, UM171 (StemCell Technologies) was added to the wells at a final concentration of 35nM, 16-18h prior to transduction.

2 days after transfection, viral supernatant (S/N) was harvested from transfected plates, centrifuged for 5 min at 500 *xg* and filtered using a 0.45uM filter (Pall

corporation). For benchtop centrifugation, the harvested S/N was aliquoted into 1.5ml Eppendorf's and were centrifuged for 45 min – 1h at 28,000 *xg*, 4°C. The S/N was discarded and the viral pellets were resuspended in 500-900µl of $CD34^+$ undifferentiation media. E4BP4-Cas9-hCD2, E4BP4-Cas9-eGFP and EOMES-Cas9-eGFP lentivirus was concentrated using this approach.

For low-speed ultracentrifugation, filtered viral S/N from transfected plates were layered on top of a 10% sucrose cushion (sucrose in 50mM Tris-HCL, pH 7.4, 100mM NaCl, 0.5mM EDTA) at a 4:1 ratio within ultracentrifuge tubes (Beckman Coulter). These tubes were centrifuged under vacuum pressure for 4h at 10,000 *xg*, 4°C using a Beckman Coulter Optima L-100 XP ultracentrifuge. The viral pellets were resuspended in 200µl of StemSpan serum free media for an overnight incubation at 4°C. The rest of the components of the $CD34^+$ undifferentiation media was added to the concentrated virus at the transduction step. NKG2A-Cas9-eGFP lentivirus was concentrated using this approach.

To transduce using spinfection, $CD34^+$ HPCs were counted and resuspended in the $CD34^+$ undifferentiation media containing concentrated virus to a final concentration of $1x10^5$ cells/ml. Polybrene (Merck Millipore) was added at a final concentration of 8µg/ml and 100µl of the cell/virus mix was added into 96 well V bottom tissue culture plates. These plates were centrifuged at 700 *xg* for 45 min, 20°C and the wells were topped up with 50µl of fresh $CD34^+$ undifferentiation media prior to incubation at 37°C, 5% $CO_2$ for 2 days.

To transduce using Retronectin, 96 or 48 well flat bottom non-tissue culture plates were coated with 4µg/ml of Retronectin/$cm^2$ (TaKaRa) and left to incubate at 4°C overnight. The next morning, these coated wells were blocked with PBS, 2% BSA for 30 min at room temperature and washed twice with PBS. Concentrated virus was added to these wells and the plates were centrifuged at 2000 *xg* for 1h, 37°C, followed by a 3-4h incubation at 37°C, 5% $CO_2$. $CD34^+$ HPCs resuspended in $CD34^+$ undifferentiation media was added to these cells to make a final 1x concentration containing $0.5x10^5$ cells/ 96well or $0.7\text{-}1x10^5$ cells/48well. If the cells were treated with UM171, this was included again at this step. When specified, Cyclosporin H (SIGMA) was also added to the virus/cell mix at a final concentration of 8µM. These plates were incubated for 2-3 days at 37°C, 5% $CO_2$.

Transduced CD34$^+$ HPCs were collected into FACs tubes and stained with anti-CD34 and, for E4BP4-Cas9-hCD2 transduced cells, anti-hCD2 (details in section 2.6). As the cells were generally all CD34$^+$, transduced cells were sorted for reporter expression using a BD FACS Aria III. E4BP4-Cas9-hCD2/eGFP transduced cells were sorted directly into 96 well plates containing CD34$^+$ undifferentiation media for 5 days, while EOMES-Cas9-eGFP and NK2GA-Cas9-eGFP transduced cells were sorted as a pulled population in CD34$^+$ undifferentiation media and plated in 48 well or 24 well plates for recovery overnight. Transduced HPCs were then transferred into NK cell differentiation conditions (Section 2.4).

### 2.3.4 Transduction of cell lines.

2.5x10$^4$ MRC5 cells or 6.5x10$^5$ 293T cells were seeded in 6 well plates one day prior to transduction. The media in these wells was discarded and filtered, neat viral S/N from transfected 293T or 293FT was added to the wells. Polybrene was added at a final concentration of 8µg/ml. Cells were incubated at 37°C, 5% $CO_2$ for 2 days prior to harvesting for flow cytometry analysis, with a media change after the first day. Transduced cells were analysed for live cells using a non-fixable live and dead dye and eGFP$^+$ or hCD2$^+$ reporter expression.

### 2.3.5 Viral Titre and Multiplicity of infection (MOI) determination.

Viral S/N from EV-Cas9-eGFP or a representative gene of interest GOI-Cas9-eGFP transfected plates was concentrated using ultracentrifugation. The same batch was serially diluted to determine viral titre as well as MOI for CD34$^+$ HPCs and 293T cells.

To determine viral titre, 1x10$^5$ 293T cells were transduced with 2-fold dilutions of virus, ranging from 1/8 to 1/512, in 12 well plates. Wells were seeded in triplicate and dilutions were made in DMEM 10% FBS. After 2 days, the cells were harvested for flow cytometry analysis and the percentage of live, eGFP$^+$ cells were determined. These percentages were used to calculate viral titre as described in Section 6.3.

To determine MOI, 5x10$^4$ 293T cells were transduced with 2-fold dilutions of virus, ranging from 1/64 to 1/2048, in 24 well plates in triplicate. Simultaneously, 5x10$^4$ CD34$^+$ HPCs were transduced in virus/retronectin coated 96 well plates. Both

transduced 293T cells and CD34$^+$ HPCs were analysed for live, eGFP$^+$ expression after 3 days using flow cytometry. With the calculated viral titre, MOI for 293T at various dilutions was determined (amount of virus added /number of cells transduced), plotted against the percentage of eGFP$^+$ cells and the line of best fit equation was used to determine the CD34$^+$ HPC MOI when the 293T MOI was 1 (Section 6.3).

## 2.4. CD34$^+$ derived NK cell differentiation.

Transduced or untransduced CD34$^+$ HPCs were resuspended in NK cell differentiation media and were seeded at the specified densities in 96 well plates containing irradiated EL08-1D2 cells. When testing the effects of UM171 on seeding density, CD34$^+$ HPCs were seeded in 24 well plates for differentiation (Section 6.3). NK cell differentiation media comprised: αMEM, 20% human AB serum, 50μM β-Me, 5ng/ml sodium selenite (SIGMA), 50μM ethanolamine (SIGMA), 20μg/ml ascorbic acid (SIGMA), 5ng/ml IL-3 for the first week), 20ng/ml IL-7, 20ng/ml SCF, 10ng/ml Flt3L, 10ng/ml IL-15. Wells containing single cell sorted E4BP4-Cas9-hCD2 or E4BP4-Cas9-eGFP transduced HPCs were cultured for 5 days prior to transfer into NK cell differentiation conditions. These wells were transferred by removing half of the media, resuspending the cells with a pipette, and adding it to a new 96 well containing irradiated EL08-1D2. The previous wells were washed with the same volume of 2x NK cell differentiation media and was combined to the new wells. EOMES-Cas9-eGFP or NKG2A-Cas9-eGFP transduced HPCs were serially diluted in αMEM prior to transfer onto irradiated EL08-1D2. The wells were topped up with concentrated NK cell differentiation media to make a final 1x concentration. Plates were incubated at 37°C, 5% $CO_2$.

From the first week of differentiation, half of the media was exchanged for fresh NK cell differentiation media without IL-3 every 3-4 days. During this time, cell confluency was measured using a light microscope. Wells above 40% CD34$^+$ derived cell confluency, determined by their circular, reflective appearance, were split 1:2 into new 96 wells for genotyping or were transferred into 48 wells for expansion. Wells above 40% confluent in a 48 well were split 1:2 for flow cytometry analysis or were transferred into larger wells for further expansion and functional assessment. After 24-28 days

from the start of differentiation, cells were maintained without EL08-1D2 cells unless specified.

## 2.5. Functional assessment of NK cells

To measure IFNγ production, wells containing differentiating $CD34^+$ derived NK cells were counted using a haematocytometer, centrifuged at 500 *xg* for 5 min and resuspended in fresh NK cell differentiation media. $1x10^5$ cells were transferred into 96 well U bottom plates with or without 20ng/ml IL-12 (Peprotech) for 24h at 37°C, 5% $CO_2$. NK92 cells were treated the same way but were resuspended in RPMI, 10% FBS and $5x10^4$ cells were plated in 96 well plates. After incubation, the cells were washed using 1ml of αMEM 10% human AB ($CD34^+$ derived NK cells) or RPMI 10% FBS (NK92), centrifuged and resuspended in their corresponding media for replating into 96 well plates. 100ng/ml of PMA (Phorbol 12-myristate 13-acetate) and 1µg/ml of Ionomycin (together, PMA/I) was added to wells without IL-12 stimulation and the plates were incubated for an hour at 37°C. 10µg/ml of Brefeldin A (SIGMA) and 7µg/ml of GolgiSTOP (BD) was added to all the wells and the plates were cultured for a further 4h. The cells were then harvested and stained for NK cell surface markers CD3, CD45, CD56 as well as intracellular IFNγ (details in Section 2.6). Results were normalised by extracting the baseline percentage of $IFN\gamma^+$ cells obtained from the unstimulated control.

For cytotoxicity assessment, a sample from wells containing $CD34^+$ derived NK cells were stained for CD3, CD45 and CD56 to measure NK cell percentages. BD calibrate beads were added during acquisition to calculate the number of NK cells present within the well (details in section 2.6). On the same day, adherent PEO1 and PEO4 target cells were stained with a CFSE cell division tracker kit (Biolegend) following manufacturer's instructions. The target cells were resuspended in RPMI, 10% FBS and $1.5\text{-}2x10^4$ cells were seeded into 24 well tissue culture plates. The next day, K562 cells were treated the same way and were plated into 24 well plates. The appropriate number of NK92 cells and $CD34^+$ derived NK cells for the specified effector to target (E:T) ratio was harvested, centrifuged and resuspended in RPMI 10% FBS to seed on top of the target cell containing wells. Plates were incubated at 37°C, 5% $CO_2$ for the length of time specified. Wells with adherent target cells were harvested using trypsin

without discarding any S/N or wash media. During acquisition, 3-5x$10^3$ $CFSE^+$ cells were recorded and the percentage of dead $CFSE^+$ cells was determined using a live and dead non-fixable dye. Results were normalised by extracting the baseline percentage of dead $CFSE^+$ cells obtained from the target only control.

## 2.6. Flow cytometry

Cells were stained in 5ml FACS tubes or 96 well V or U bottom plates using antibodies detailed in Table 2.3. After harvesting the cells, FACS buffer (PBS, 2% FBS) was added to the sample and the tubes/plates were centrifuged at 500 *xg* for 5 min. S/N was discarded and the cells were resuspended in an antibody cocktail diluted in FACS buffer for surface marker staining. These cells were incubated for 15-20 min, 4°C, in the dark. 200µl (for plates) or 1ml (for FACS tubes) of FACS buffer was added to the sample, the cells were centrifuged and resuspended in 200-300µl FACs buffer for analysis using a BD LSR Fortessa. Live and dead non-fixable dye and Calibrite beads were added just before acquisition. NK cell numbers were calculated with the calibrate beads using this formula: [(number of beads added x NK cell count within the gate) / bead count] x dilution factor of the sample.

For intracellular IFNγ staining, Zombie aqua was used to determine live and dead populations instead of non-fixable dyes. The harvested cells were first stained with Zombie Aqua (diluted in PBS) for 15 min at room temperature in the dark. These cells were then washed with FACs buffer followed with the surface stain as described previously. The stained cells were then resuspended in permeabilisation buffer using the BD Cytofix/cytoperm Plus with BD GolgiStop kit (BD science). Following manufacturer's instructions, these cells were then stained with anti-IFNγ antibody for 30 min, 4°C, in the dark. After washing, the cells were resuspended in permeabilisation buffer for acquisition.

| Marker | Clone | Company |
|---|---|---|
| CD2 | RPA-2.10 | Biolegend |
| CD3 | UCHT1 | Biolegend and eBioscience |
| CD34 | 4H11 | eBioscience |
| CD45 | H130 | Biolegend |
| CD56 | CMSSB | eBioscience |
| CD94 | REA-113 | Miltenyi |
| CD159a (NKG2A) | REA-110 | Miltenyi |
| IFNγ | 4S.B3 | Biolegend |
| TO-PRO-3 iodide | - | Biolegend |
| DAPI | - | Miltenyi |
| Zombie Aqua fixable dye | - | Biolegend |

Table 2.3: List of antibodies and dyes

*Live and dead dyes are highlighted in grey. TO-PRO-3 iodide and DAPI are non-fixable.*

## 2.7. DNA extraction and genotyping.

Cells to be genotyped were transferred into 0.5ml or 1.5ml Eppendorf's and diluted in PBS prior to centrifugation at 500 *xg* for 5-7 min. DNA was isolated from pellets consisting of less than $1x10^3$ cells to $0.5x10^5$ cells. The centrifuged pellets were resuspended using 30-50µl of Quick extract DNA extraction solution 1.0 (Epicenter) following manufacturer's instructions, and 5-10µl of lysed samples were used directly to set up PCR. Cell pellets were also resuspended with 50-200µl lysis buffer that comprised: 50mM Tris, pH 8.0, 100mM NaCl, 10mM EDTA, 0.5% SDS, 1mg/ml proteinase K. Cells resuspended in lysis buffer was incubated at 50°C for 3h or overnight, shaking at 700 rpm. NaCl was added to the solution at a final concentration of 1.5M and the lysate was centrifuged at 28,000 *xg* for 20-30 min, 4°C. The DNA containing S/N was transferred into clean Eppendorf's for isopropanol precipitation, where 0.7-1x of isopropanol was added and the tubes were centrifuged for a further 20 min. S/N was discarded and the pellets were washed with ice cold 100% ethanol. After another 15 min centrifugation, this step was repeated with 70% ice cold ethanol (in nuclease free water) and centrifuged for another 10-15 min. Finally, the pellets were air-dried for 1-5 min and resuspended in 10-50µl of nuclease free water.

The isolated DNA was used to set up genotyping PCR using Phusion polymerase (Invitrogen) in HF buffer following manufacturer's instructions. For EOMES, 2.5M betaine was included into the mixture for the external PCR. The cycle steps and primers for each gene are outlined in Figure 2.3.

| Gene | Primers 5' → 3' | Cycle protocol |
|---|---|---|
| E4BP4 | Fw:<br>AAGCACCACGGTATGCATGT<br>Rv:<br>GCCTTCGCATGGACTATCTGA | 98°C – 30"<br>x35 98°C – 10"<br>68°C – 20"<br>72°C – 1'<br>72°C – 10' |
| EOMES | External Fw:<br>GAAGTTGGACTTAGACAAAGCGTCC<br>External Rv:<br>TCCGATGGAAGACAGTTGGATATTT<br>Internal Rv:<br>GAGATGCGGTGTCTACGGAGATTTA | For External and internal<br>98°C – 3'<br>x35 98°C – 10"<br>63°C – 30"<br>72°C – 1' 30" external<br>30" internal<br>72°C – 10' |
| NK2GA | Fw:<br>TGCAGACCACATAGTCTTAACCATTA<br>Rv:<br>TGCATCAGAAGCGAATACTTTCAAC | 98°C – 30"<br>x35 98°C – 10"<br>67°C – 20"<br>72°C – 1'<br>72°C – 10' |

Table 2.4: Genotyping primers and PCR protocol

*Cycle protocol shown as minutes (') and seconds ("), with the annealing step repeated 35 times for each gene.*

# 3. Development of human NK cells from UCB derived CD34$^+$ HPCs.

## 3.1. Background.

To study the effects of targeting gene expression on human NK cell development, a protocol was designed that incorporated lentiviral mediated CRISPR/Cas9 gene targeting in CD34$^+$ HPCs and their subsequent clonal differentiation into NK cells. To ensure NK cell differentiation was not affected by clonal expansion as well as the transduction process itself, both untransduced and transduced CD34$^+$ HPCs were seeded at a range of low densities and differentiated into NK cells. I show that it is possible to develop a clonal population of NK cells from transduced CD34$^+$ HPCs using the protocol set out below.

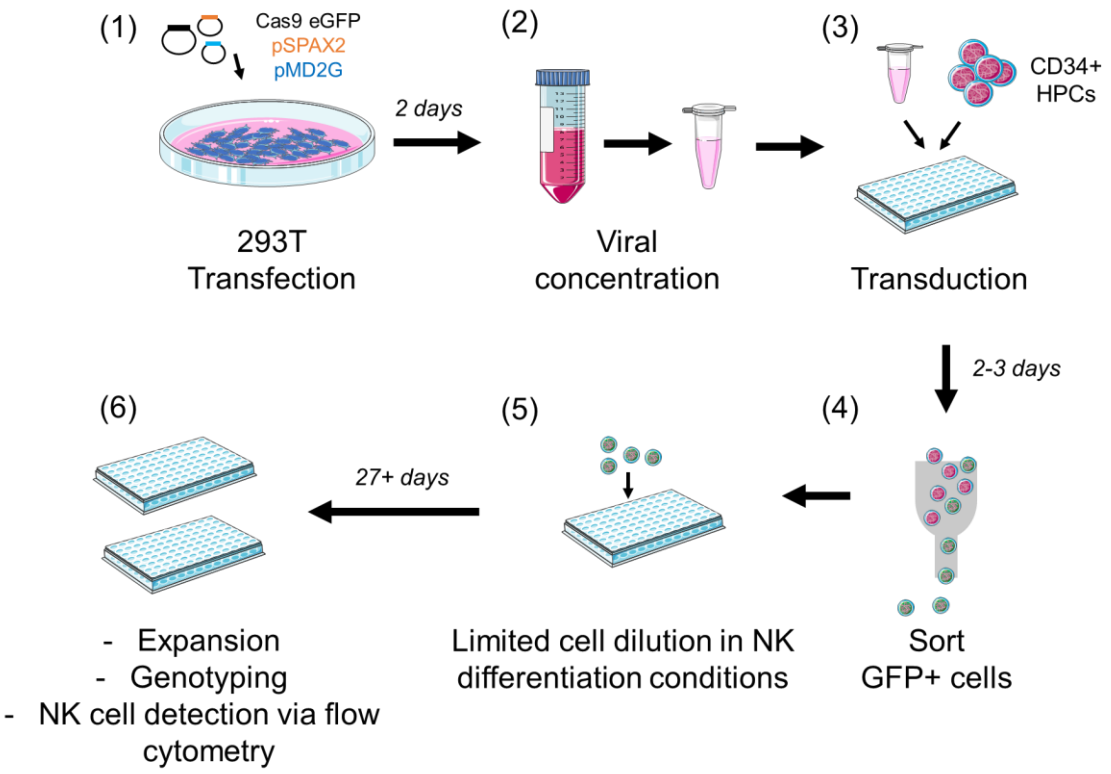



*Figure 3.1: Outline for lentiviral CRISPR/Cas9 mediated gene deletion in human CD34⁺ HPCs followed by in vitro NK cell differentiation.*

*(1) 293T cells were transfected with the Cas9-eGFP vector and lentiviral packaging vectors pSPAX2 and pMD2G. (2) Viral supernatant was harvested and concentrated by standard benchtop centrifugation or ultracentrifugation. (3) CD34⁺ HPC transduction was achieved through the use of polybrene or retronectin as transduction reagents (4) Transduced cells were sorted via reporter expression, i.e. eGFP, using FACS. (5) Sorted cells, either as a pooled population or as a low/single cell population, were cultured in undifferentiation media for a 1 or 5 days, respectively. Pooled populations were serially diluted prior to transfer into NK cell differentiation conditions for clonal expansion. The differentiation procedure comprised NK differentiation cytokines and co-culture with an irradiated EL08-1D2 feeder layer in a 96 well plate. (6) During the 27+ days of NK cell culture, expansion of the clonal populations was monitored and the cell confluency of the well was estimated. When confluency was above 40% of the well, the population could be sampled for genotyping and/or NK cell detection by flow cytometry.*

Successfully transduced CD34⁺ HPCs with the concentrated Cas9 lentivirus were sorted based on reporter expression and differentiated into clonal populations of NK cells (Figure 3.1). Differentiation included the co-culture with irradiated EL08-1D2 cells and a cytokine cocktail for at least 24 days, after which the differentiated NK cells were maintained without EL08-1D2 and with IL-15 only. Growth of these populations was monitored over time and expanding populations were sampled for genotyping and detection of NK cell markers by flow cytometry (Figure 3.2).

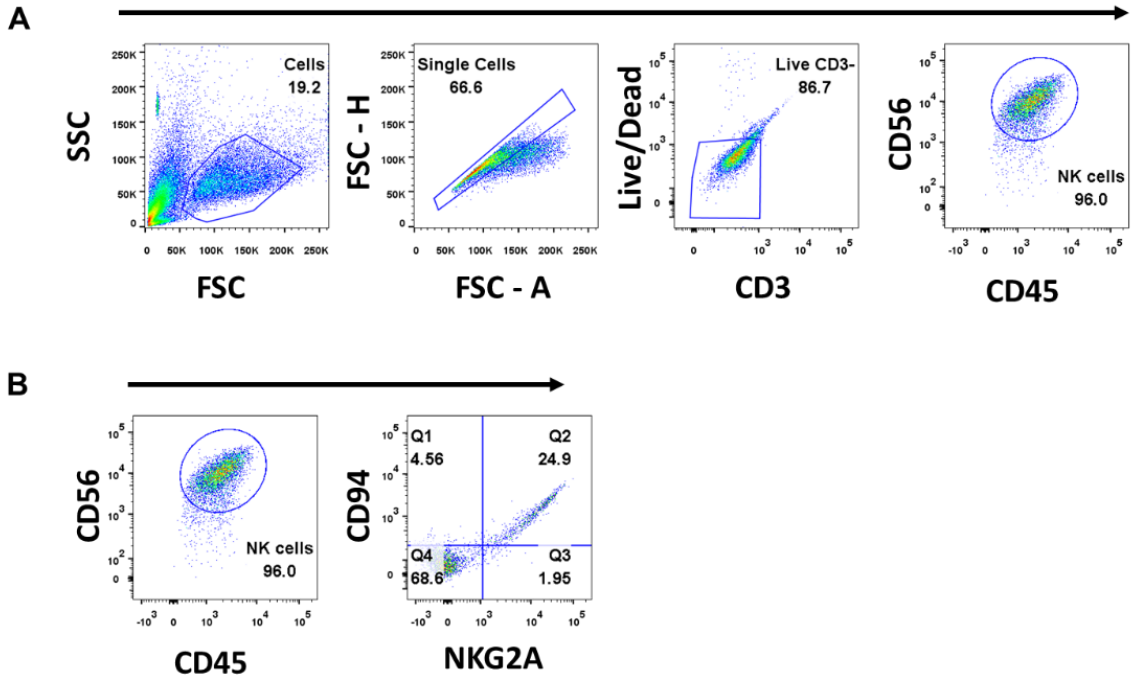



*Figure 3.2: Gating strategy to determine NK cell populations using flow cytometry.*

*Flow cytometry plots indicating the gating strategy used to determine NK cells. (A) Post selection for live, single cells, NK cells were characterised as CD3⁻ CD45⁺ CD56⁺ cell populations. (B) When investigating the role of NKG2A gene deletion on NK cell development, NK cells from (A) were further characterised for expression of NKG2A and its co-receptor CD94. The sample presented was collected from untransduced CD34⁺ derived NK cells after differentiation for 36 days.*

Using flow cytometry, NK cells were identified as $CD3^-$ $CD45^+$ $CD56^+$ (Figure 3.2A). When investigating the effects of NKG2A gene targeting on NK cell development, detection for NKG2A and its co-receptor CD94 was included in the panel to validate successful gene knockout (Figure 3.2B).

Applying the methods described in Figure 3.1 and 3.2, the effects of clonal NK cell development was assessed when progenitors, both untransduced and transduced, were seeded at low starting numbers. This assessment is crucial in establishing expectations for NK cell development prior to the influence of targeting gene expression.

## 3.2. Differentiation of NK cells from untransduced $CD34^+$ HPCs seeded at low cell densities.

Validation of the clonal differentiation process involved analysing the development of NK cells from sorted, untransduced $CD34^+$ HPCs seeded at 100, 50, 20 and 3-cells/well. NK cell percentage (Figure 3.3) and NK cell number (Figure 3.4) were measured at different time points to track the development of NK cells over time. As differentiating NK cells appear bright, round and reflective within the *in vitro* cultures, these characteristics were utilised to monitor cell confluency within the well at each time point. Wells with over 40% confluency was sampled for NK cell characterisation using flow cytometry.

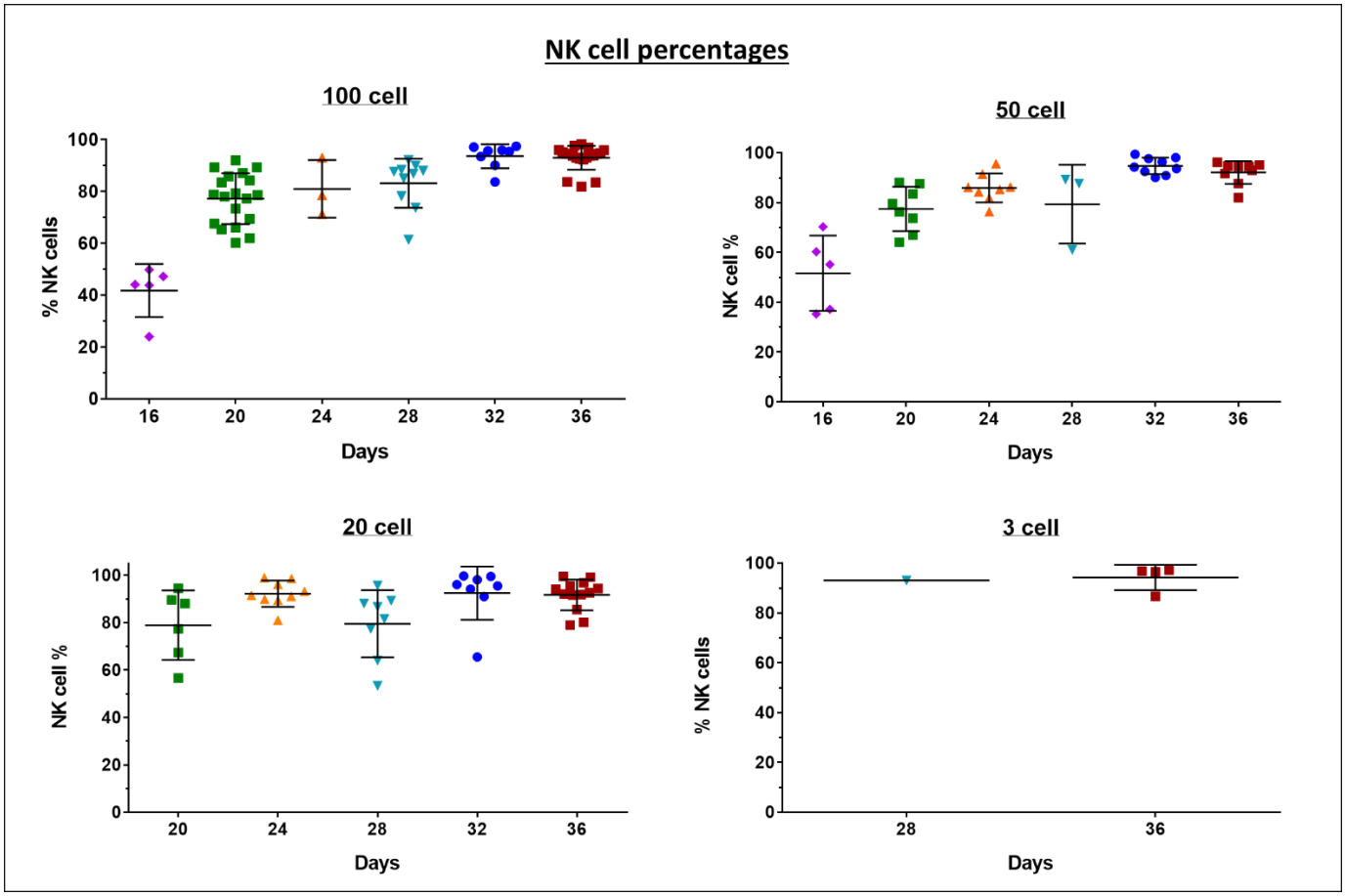



Figure 3.3: Timepoint analysis of CD34⁺ derived NK cell percentages per well, seeded at different starting densities.

*The percentage of NK cells determined by flow cytometry are shown at different time points from wells seeded with 100, 50, 20 or 3-cell untransduced, sorted CD34⁺ HPCs at the start of differentiation. In total, 60 wells were seeded for the 3 and 20-cell densities and 30 wells were seeded for the 50 and 100-cell densities. Wells above 40% CD34⁺ derived cell confluency were selected for analysis. NK cell populations were co-cultured with irradiated EL08-ID2 cells throughout the entirety of the culture. Results were from a single experiment; bars represent average values plus standard deviation.*

The percentage of untransduced $CD34^+$ derived NK cells/well, seeded at different starting densities for differentiation, was measured at various time points during the NK differentiation culture (Figure 3.3). The 100 and 50-cell densities reached 40% cell confluency and were sampled as early as day 16 while the 20-cell density reached 40% confluency from day 20 and 3-cell density reached 40% confluency from day 28. While there was a delay in the onset of assessment for the lower seeded densities, the NK cell percentage by day 28 was 80% or above for all the seeded densities. This percentage was maintained above 80% at both day 32 and day 36 of culture.

The total number of wells that produced NK cells by the end of culture (day 36) was lower for the 20-cell and 3-cell densities. 100% of the wells seeded at the 100 and 50-cell density (30/30 wells) showed growth. Meanwhile 36.7% of the wells seeded at the 20-cell density (22/60 wells) and 6.7% of the wells seeded at the 3-cell density (4/60) showed growth.

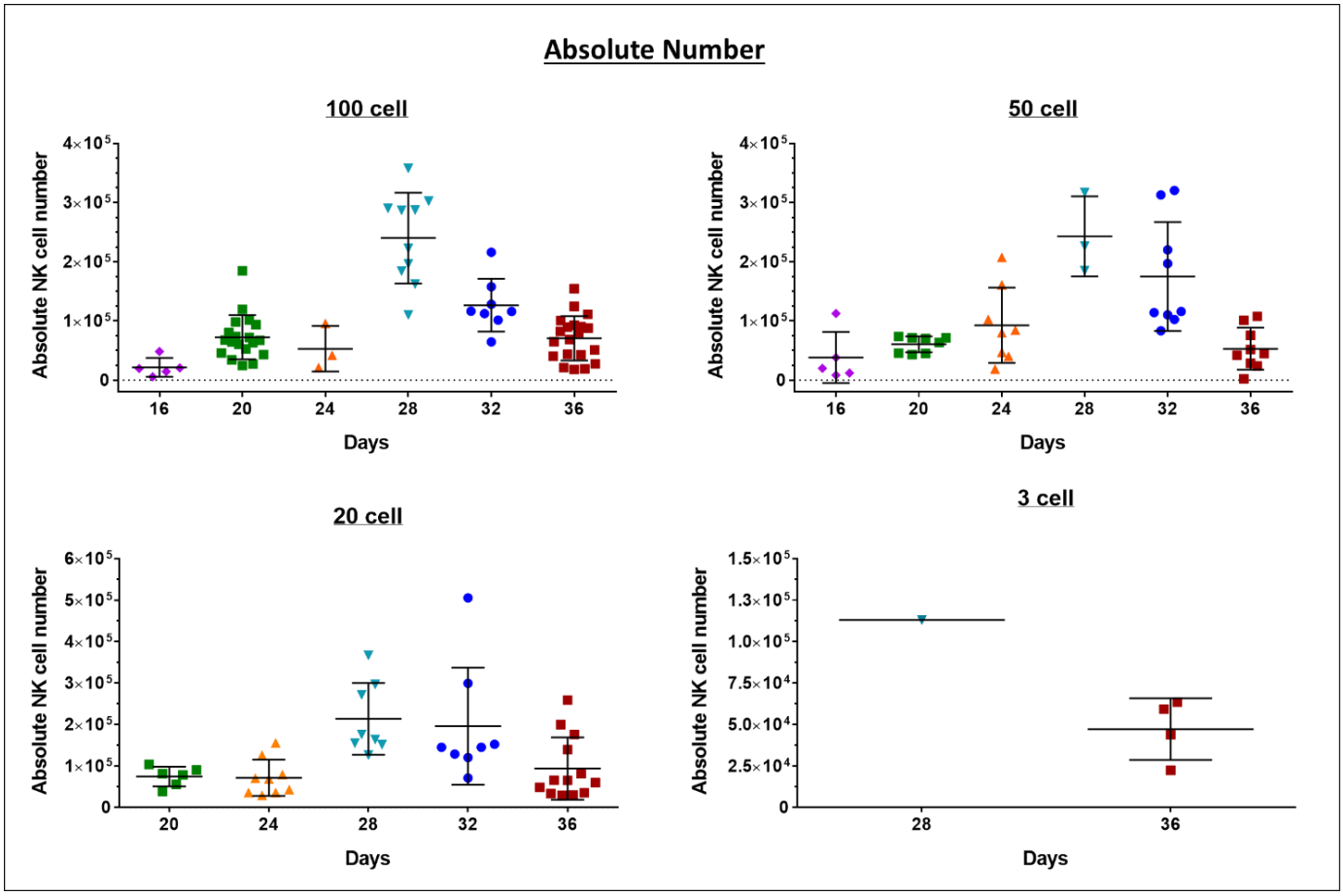



Figure 3.4: Timepoint analysis of the absolute number of CD34⁺ derived NK cells per well, seeded at different starting densities.

*The number of NK cells, determined by flow cytometry and calibrite beads, are shown at different time points from wells seeded with 100, 50, 20 or 3 untransduced, sorted CD34⁺ HPCs at the start of differentiation. In total, 60 wells were seeded for the 3 and 20-cell densities and 30 wells were seeded for the 50 and 100-cell densities. Wells above 40% CD34⁺ derived cell confluency were selected for analysis. NK cell populations were co-cultured with irradiated EL08-ID2 cells throughout the entirety of the culture. Results were from a single experiment; bars represent average values plus standard deviation.*

Absolute $CD34^+$ derived NK cell numbers were measured per well at different time points (Figure 3.4). For the 100, 50 and 20-cell seeding densities, there is an observable increase in NK cell number by day 28, with the largest expansion occurring between day 24 to day 28 (Figure 3.4). After this time point, the number of NK cells steadily decreased by day 36. For example, the 100-cell density showed an increase in NK cell number from an average of $5.3x10^4$ NK cells/well on day 24 to $2.6x10^5$ NK cells/well on day 28, which then decreased to $7x10^4$ NK cells/well by day 36. Both the 50 and 20-cell densities also measured above $2x10^5$ NK cells/well at day 28, the peak of NK cell production, and decreased to below $1x10^5$ NK cells/well by day 36.

For the 3-cell density, however, only two timepoints were analysed. The NK number from a single well analysed on day 28 produced $1.2x10^5$ NK cells/well, approximately 1.7-fold lower than the second lowest seeding density at 20 cell/well, which produced $2.13x10^5$ NK cells/well on the same day. By day 36, the number of NK cells from the 3-cell density decreased, producing an average of $4.7x10^4$ NK cells/well and matching the pattern that is seen with the 100, 50 and 20-cell seeded densities.

Until this point, differentiating NK cells were maintained with an irradiated EL08-1D2 feeder layer for the entirety of the 36-day culture. To assess if exclusion of the EL08-1D2 layer affected NK cell development, some of the day 28 NK cell populations were split and half was transferred into empty wells for up to 8 days (Figure 3.5).

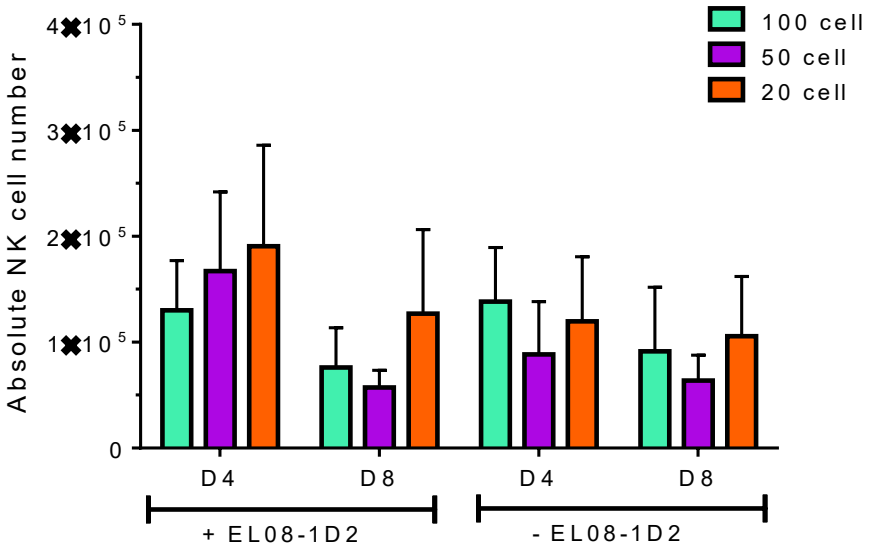



*Figure 3.5: Absolute number of NK cells cultured with and without EL08-1D2 after 28 days of differentiation.*

*$CD34^+$ derived NK cell populations from 100, 50 and 20-cell seeded densities were split after 28 days into cultures with and without irradiated EL08-1D2 cells. These populations were selected based upon a cell confluency above 40% within the well. In the absence of EL08-1D2, only 50ng/ml of IL-15 was included. After 4 and 8 days (D4 and D8 respectively), the wells above 40% were analysed by flow cytometry and NK cell number was determined using counting beads. Results were from a single experiment; bars represent average values plus standard deviation. No significant difference was observed using a two-way ANOVA. Day 4 +EL08-1D2 100 cell N=7, 50 cell N=2, 20 cell N=3; Day 8 +EL08-1D2 100 cell N=11, 50 cell N=3, 20 cell N=8; Day 4 -EL08-1D2 100 cell N=6, 50 cell N=9, 20 cell N=9; Day 8 -EL08-1D2 100 cell N=11, 50 cell N=3, 20 cell N=8.*

The NK cell numbers across all seeded densities decreased from day 4 to day 8 of culture (Figure 3.5), corresponding with the decrease observed from day 32 to day 36 (Figure 3.4). When the NK cell number was compared using a 2-way ANOVA test, no significant difference was found on day 4 with and without EL08-1D2 and on day 8 with or without EL08-1D2, irrespective of seeding number. There was also no significant difference in NK cell number between the 100, 50 or 20-cell densities on either day 4 or 8, with or without EL08-1D2.

### 3.3. CD34⁺ derived NK cells produce IFNγ and exhibit cytotoxic responses to cancer cell lines.

CD34⁺ derived NK cells were assessed on their ability to exhibit a functional response to various stimuli, as well as how this compared to the activated NK92 cell line. CD34⁺ HPCs were first seeded at 500-1000 cells/96 well for NK cell differentiation and harvested between days 28 and 35 of culture. These cells were examined on their production of intracellular IFNγ cytokine using flow cytometry (Figure 3.6) as well as the cytotoxic response towards cancer target cell lines PEO1 and K562 (Figure 3.7).

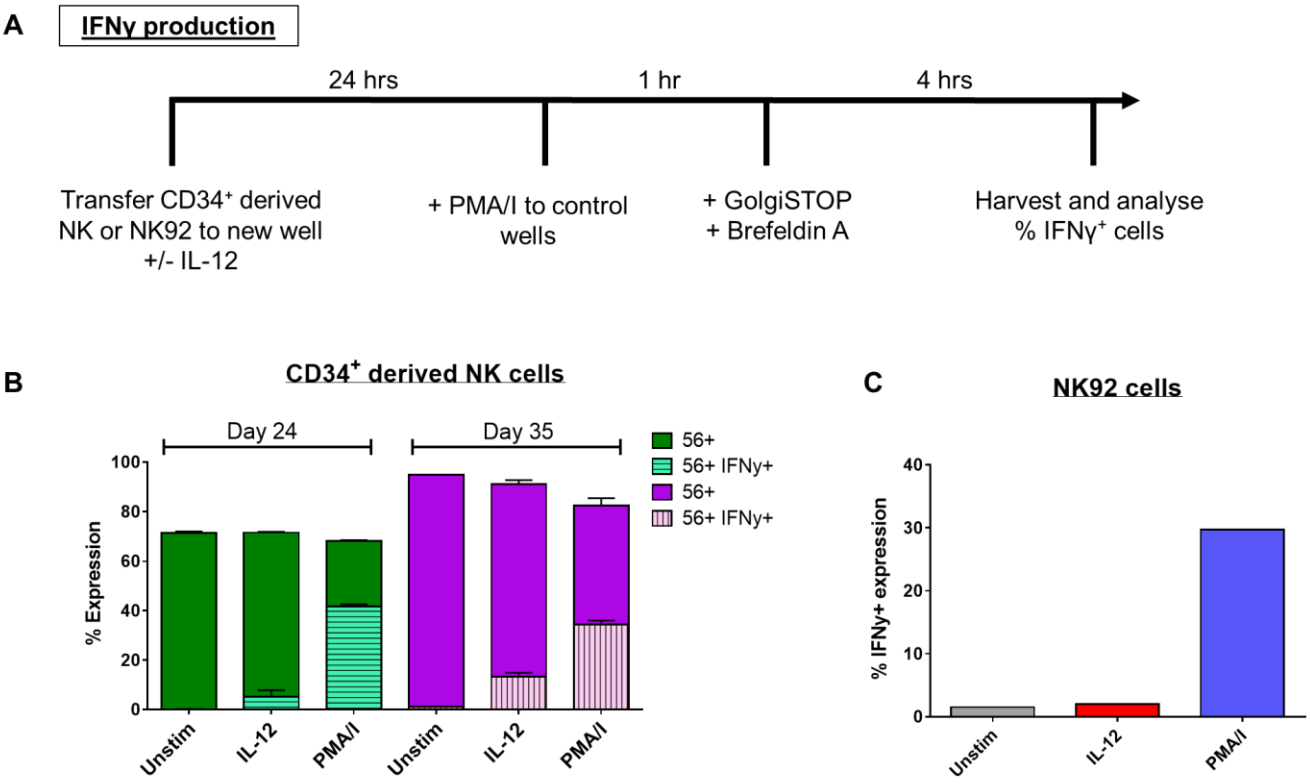



Figure 3.6: IFNγ production from CD34⁺ derived NK cells and NK92 cells.

*(A) Experimental outline to investigate intracellular IFNγ from NK cells. Cells were stimulated with and without IL-12 for a total of 29h (hours). PMA/I was added to non-IL-12 stimulated wells for the last 5h of culture. Golgi-STOP and Brefeldin A was added for the last 4h of culture. (B) The percentage of Day 24 and Day 35 CD34⁺ derived CD56⁺ NK cells (56⁺, solid bar) and its relative IFNγ production after stimulation with IL-12 or PMA/I (56⁺IFNγ⁺, lined bar) is shown. Results from a single experiment; bars represent average values plus standard deviation. N=2 except for D35 unstimulated control, where N=1. (C) The percentage of IFNγ⁺ NK92 cells is shown after stimulation with IL-12 or PMA/I. NK92 cells were gated using the same strategy as CD34⁺ derived NK cells. Results were obtained from a single experiment, N=1. Unstim: Unstimulated cells.*

$CD34^+$ derived NK cells and NK92 cells were stimulated with IL-12 for 29h (hours) or PMA/I for 5h prior to analysis of intracellular IFNγ production by flow cytometry (Figure 3.6A). When stimulated with IL-12, the percentage of $CD56^+$ $IFN\gamma^+$ NK cells derived from $CD34^+$ HPCs increased from 5% on day 24 of differentiation to 13% on day 35 of differentiation (Figure 3.6B). Both days were higher than NK92 cells stimulated with IL-12, which had only 2% $IFN\gamma^+$ expression (Figure 3.6C). While PMA/I stimulation resulted in day 35 $CD34^+$ HPC derived NK cells exhibiting lower $CD56^+$ $IFN\gamma^+$ NK cell percentages than day 24 (34% versus 41.5%, respectively), both days had higher percentages of $IFN\gamma^+$ NK cells than NK92 cells, which revealed 30% $IFN\gamma^+$ NK cells after PMA/I stimulation.

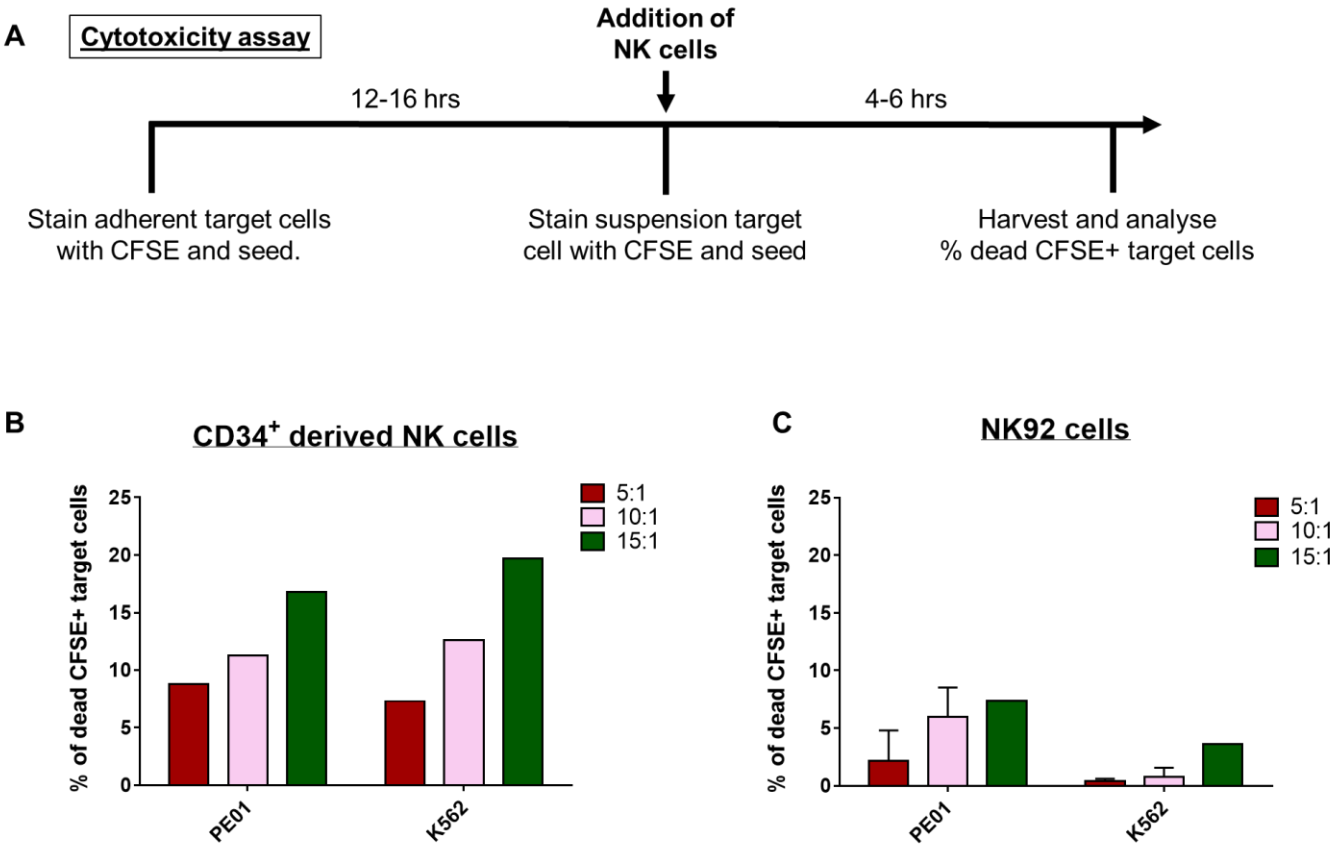



Figure 3.7: Cancer cell line cytotoxicity assay with CD34⁺ derived NK cells and NK92 cells.

*(A) Experimental outline to investigate cytotoxic responses of NK cells after a 4-6h co-culture with target cancer cell lines PEO1 and K562. NK cell effector: target (E:T) ratios were set up at 5:1, 10:1, 15:1. Cells were analysed for percentage of dead CFSE⁺ cells using flow cytometry (B) The percentage of dead CFSE⁺ target cells after co-culture with day 28 CD34⁺ derived NK cells. Results were from a single experiment, N=1. (C) The percentage of dead CFSE⁺ target cells after co-culture with NK92 cells. Results were from a single experiment; bars represent average values plus standard deviation. Replicates for each ratio was 5:1 N=2, 10:1 N=3, 15:1 N=1. Percentages from both (B) and (C) were normalised to the target cell alone control: 1.33% for PEO1 and 0.79% for K562 cells.*

Cytotoxic responses of the CD34$^+$ derived NK cells and NK92 cells were calculated from the percentage of dead, CFSE$^+$ target cells after a 4-6h co-culture at different effector:target (E:T) ratios (Figure 3.7A). CD34$^+$ derived NK cells were able to kill more PEO1 and K562 cells than the NK92 cell line, even at the lowest E:T ratio of 5:1 (Figure 3.7B and C). For instance, the percentage of dead PEO1 cells from CD34$^+$ derived NK cells went from 9% at the 5:1 ratio to 17% at the 15:1 ratio, while NK92 cell-mediated killing went from 2% at the 5:1 ratio to 7% at the 15:1 ratio. The percentage of dead K562 when co-cultured with CD34$^+$ derived NK cells increased from 7% at the 5:1 ratio to 20% at the 15:1 ratio, whereas NK92 co-culture resulted in only 3.6% dead K562 with the highest E:T ratio (15:1).

## 3.4. Effects of transduction on NK cell differentiation from CD34$^+$ HPCs.

The effects of transduction on NK cell differentiation from CD34$^+$ HPCs was investigated. Lentivirus produced from the empty Cas9 vector (EV-Cas9-eGFP), lacking the sgRNA and promoter components for gene targeting, was used to transduce CD34$^+$ HPCs prior to NK cell differentiation. Transduced cells were sorted and cultured in NK differentiation conditions starting from 100 cells, 50 cells or as a single cell per well (Figure 3.8).

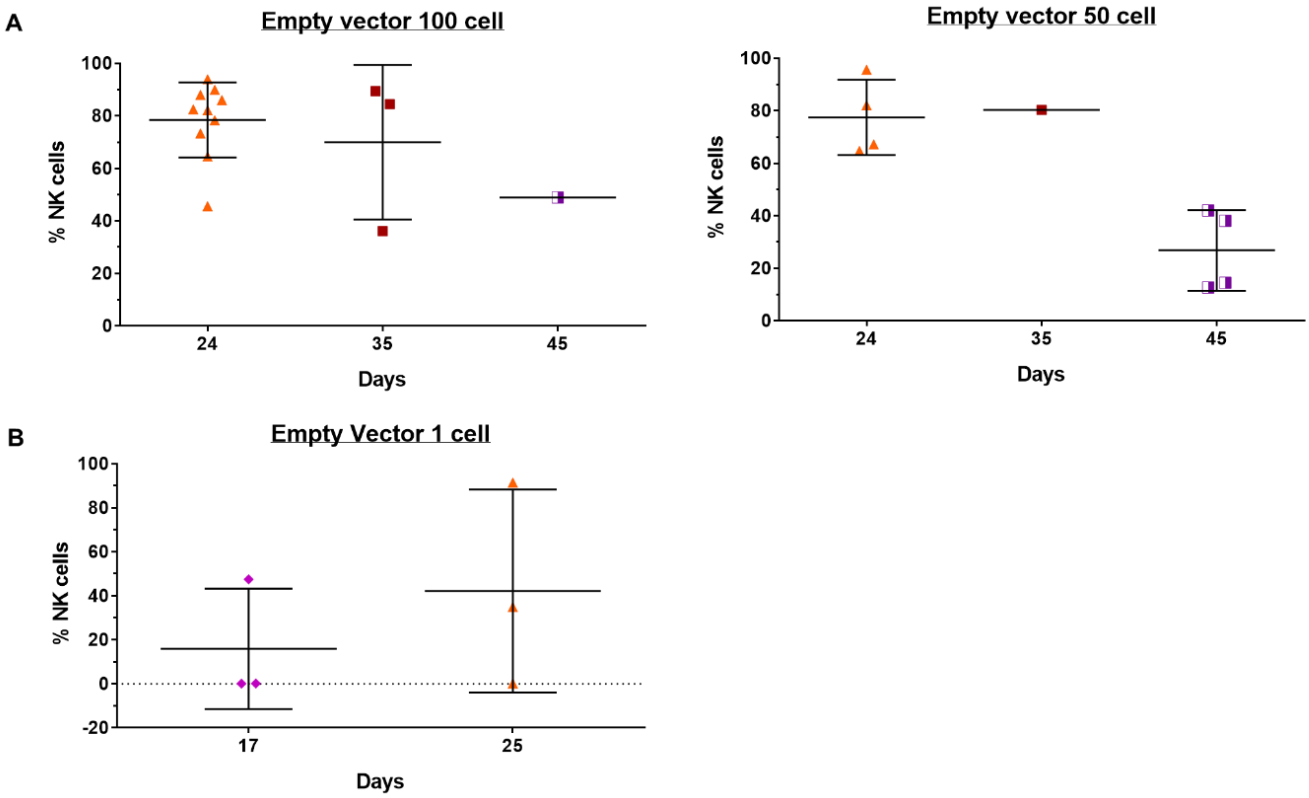



*Figure 3.8: Percentage of empty vector transduced NK cells on different days of differentiation.*

*The percentage of NK cells differentiated from CD34⁺ HPCs transduced with EV-Cas9-eGFP is shown for various time points during culture. (A) HPCs were transduced using retronectin as a transfection reagent and were seeded as 100 or 50-cells/96 well after a day recovery post sort. A total of 60 wells were seeded per condition and NK cell production was analysed using flow cytometry on day 24, 35 and 45 from differentiation. (B) HPCs were transduced using polybrene as a transfection reagent and were sorted as single cells using FACS. After 5 days recovery, cells were transferred to NK differentiation conditions in 96well plates. A total of 30 wells were seeded and NK production was analysed using flow cytometry on day 17 and 25. NK cell populations in both (A) and (B) were transferred off the irradiated EL08-1D2 feeder after day 24 of differentiation. Results for (A) and (B) are from 2 separate experiments; bars represent average values plus standard deviation.*

The 100 and 50-cell seeded densities were analysed at three time points, from day 24 until day 45 (Figure 3.8A). On day 24, both the 100 and 50-cell densities had NK cell percentages above 75%. This percentage was maintained between 70-80% until day 45, where the percentage of NK cells had decreased to 49% for the 100-cell density and an average of 27% for the 50-cell density. In addition to this, transduced cells seeded at the 100-cell density yielded only 16% (10/60) of wells with an NK cell population by the end of culture, while the 50-cell density yielded less, at 8.3% (5/60).

Of the single cell seeded conditions, only two timepoints were analysed, day 17 and day 25 (Figure 3.8B). Upon seeding at this lower density, it is evident that the range of NK cell percentages is far greater than the 100 and 50 cell densities. The percentage of NK cells increased from an average of 16% on day 17 to 42% on day 25, however of the three wells analysed on day 25, the percentages ranged from 91%, 35% and 0% NK cells. At this single cell density, only 6% (2/30) of seeded wells contained an NK cell population by the end of the assay.

## 3.5. Discussion

As the investigation of targeting gene expression on human NK cell development relies on clonal expansion of $CD34^+$ HPCs transduced by the CRISPR/Cas9 lentivirus (Figure 3.1), it was important to establish if these progenitors could differentiate into NK cells at low cell numbers, whether the generated NK cells were functionally responsive and whether transduction affected the differentiation process.

To assess clonal expansion of NK cell development, untransduced progenitors were seeded at various low densities and encouraged to differentiate into NK cells. These cells were also sorted so as to control for any effects of the sorting process on HPC viability and thus NK cell differentiation. Results show that seeding wells at the lower 20 or 3-cell densities did require more time to reach 40% cell confluency for analysis by flow cytometry (Figure 3.3). However, this did not affect the ability of these progenitors to produce the same NK cell percentages as the higher 100 or 50-cell densities from day 28 of differentiation. In fact, the NK cell percentages from day 24 onwards were similar to what was shown by Luevano et al. (2014), where 500 $CD34^+$ HPCs were seeded for NK cell differentiation. Although seeding at a lower density did exhibit a lower frequency of wells containing an NK cell population, the percentage

results indicate that differentiation of CD34$^+$ HPCs at low cell numbers does not affect the ability of the HPC to differentiate into an NK cell.

Analysis of the absolute number of NK cells within these wells reveal NK cell proliferation is highest between days 24 to day 28 for the 100, 50 and 20-cell seeded densities (Figure 3.4). This increase in proliferation is evident as the number of NK cells/well increases during this timepoint while the percentages remain constant (Figure 3.3). After day 28, all seeded densities exhibited a decrease in NK cell proliferation by day 36. This decline in NK cell number after 28 days of differentiation has been previously reported (Domogala et al., 2017, Luevano et al., 2014), suggesting this is a limitation with the culture process. While the 3-cell density exhibited a 1.7-fold decrease in NK cell number when compared to the 20-cell density, a high enough number of NK cells can still be generated suitable for downstream applications such as flow cytometry.

One important factor that characterises successful NK cell development is their ability to show a functional response upon stimulation. Therefore, to perform a wide array of functional tests, a higher number of CD34$^+$ HPCs were seeded at the start of differentiation to generate enough NK cells for experimental set up. Stimulation with IL-12, a cytokine that activates peripheral blood NK cells cytokine response (Fehniger et al., 1999, Lehmann et al., 2014), as well as the general lymphocyte activation reagent PMA/I, induced IFNγ production within our CD34$^+$ derived NK cells (Figure 3.6B). Cytotoxicity assessments of the CD34$^+$ derived NK cells also revealed that these cells were capable of killing the ovarian cancer PEO1 cell line as well as the myelogenous leukaemia K562 cell line (Figure 3.7B). While Domogala et al., (2016) show similar the percentages of PMA/I stimulated IFNγ$^+$ (CD34$^+$ derived) NK cells using the same NK cell differentiation and activation method, supporting my findings in Figure 3.6B, cytotoxicity towards the K562 cell line was lower than what was previously seen (Grzywacz et al., 2006, Luevano et al., 2014). For example, our CD34$^+$ derived NK cells at the 10:1 E:T ratio exhibited a 2-fold (Luevano et al., 2014, Domogala et al., 2016) to 4-fold (Grzywacz et al., 2006) lower K562 lysis than what was previously shown with other CD34$^+$ derived NK cells. As NK cell cytotoxic responses towards cancer cells were found to be greater with longer co-culture periods (Chan et al., 2019), it is possible that a longer time period is required to see higher cytotoxicity levels with our CD34$^+$ derived NK cells. Therefore, later

experiments testing the cytotoxic responses from transduced CD34$^+$ derived NK cells will involve extending the co-culture period to 18-24h, as this was found to be the maximum time period that can be tested with low percentages of spontaneous lysis in fluorescently labelled tumour cells (Chan et al., 2019).

Interestingly, even with the lower-than-expected K562 lysis seen with our CD34$^+$ derived NK cells, both the killing efficiency and IFNγ production efficiency was higher in these cells when compared to the activated NK92 cell line (Figure 3.6C and 3.7C, respectively). NK92 cells are currently being used in immunotherapy, with some improvements in survival reported in patients with renal cell cancer or melanoma (Arai et al., 2008, Klingemann et al., 2016). However, the radiation requirement for NK92 cells can restrict the period of the therapeutic efficacy (Tonn et al., 2013). Therefore, with the higher levels of functional responses seen by our CD34$^+$ derived NK cells, it gives us confidence that these NK cells provide a suitable alternative for cancer immunotherapy.

An additional consideration for downstream functional analysis is the removal of the contaminating irradiated EL08-1D2 feeder layer. Therefore, it was important to test whether the removal of the feeder cells affected NK cell development (Figure 3.5). Similar to previously described studies (Luevano et al., 2014; Domogala et al., 2017), the removal of EL08-1D2 cells at day 28 does not show a significant difference in NK cell number, even at 100, 50 or 20-cell seeded densities. This indicates gradual transfer off the EL08-1D2 layer upon NK cell differentiation is a suitable approach if purification of NK cells using other methods is not feasible.

It has been shown in several papers that viral transduction does not affect the differentiation of CD34$^+$ HPCs towards various cell lineages (Banerjea et al., 2004, DiGiusto et al., 2010, Yam et al., 2006). To confirm that our approach of lentiviral transduction to introduce the CRISPR/Cas9 system also exhibits no effect, CD34 HPCs$^+$ were transduced with an empty Cas9 vector and differentiated into NK cells at 100, 50 and single cell densities (Figure 3.8). Like the untransduced cells, transduced CD34$^+$ HPCs are capable of generating NK cell populations when seeded at either 100, 50 or as a single cell/well. The percentages of the NK cells from the transduced 100 and 50-cell densities were also similar to the untransduced conditions around days 24 and 35. In addition to this, transduced cells seeded at the higher 100 and 50-

cell densities had more frequent production of NK cells/well than the lower seeding density, matching what was observed with the untransduced conditions.

Even though the percentages of NK cells were similar, the earliest timepoint to measure wells with transduced cells for the 100 and 50-cell densities was day 24 compared to the untransduced cells, which was day 16. Also, the frequency of wells containing NK cells decreased upon transduction, going from 100% for the untransduced 100 and 50-cell densities to 16% for the 100-cell and 8.3% for the 50-cell density. These results suggest transduction can affect the expansion of $CD34^+$ HPCs during *in vitro* culture, explaining the delay in measurements as well as the reduced frequency of wells with NK cells populations. An interesting observation, however, was that upon seeding cells at a very low density (below 5 cell/well), the frequency of wells containing NK cells were similar for both transduced and untransduced populations (~6%). Although the range of NK cell percentages is large for the EV transduced single cell populations, altogether these results do not negate the fact that the generation of an NK cell population from transduced $CD34^+$ HPCs is possible, even when seeded as a single cell.

In summary, the results presented in this section provide evidence that transduced $CD34^+$ HPCs can be differentiated into clonal populations of NK cells. Although transduction can affect the expansion of progenitor cells, reducing the frequency of wells that contain NK cells, we believe it does not affect the ability of these cells to differentiate into an NK cell population. Therefore, it remains possible to investigate the effects of gene deletion on NK cell differentiation from transduced $CD34^+$ HPCs.

# 4. Effects of targeting E4BP4 and EOMES in CD34$^+$ HPCs during NK cell differentiation.

## 4.1. Background.

To improve NK cell development from CD34$^+$ HPCs, two transcription factors thought to be involved in human NK cell differentiation and maturation were studied. In mice, expression of the transcription factor E4bp4 within HPCs has been shown to be crucial for NK cell development. Additionally, expression of the transcription factor Eomes has been shown to be important for functional maturation of mouse NK cells. The exact role of these genes within human NK cell development is unknown. By investigating the consequence of the loss of E4BP4 or EOMES during human NK cell development, it may facilitate the enhancement of NK cell production or function for use in cancer immunotherapy.

CRISPR/Cas9 lentiviral vector constructs were cloned to target E4BP4 or EOMES in human UCB CD34$^+$ HPCs. Utilising the method described in Figure 3.1, transduced HPC's were sorted and seeded at low cell densities for clonal NK cell differentiation. Growth across the wells seeded was observed and monitored. Of the growing clones, gene deletion was assessed using PCR and NK cell development was assessed using flow cytometry.

I observed that biallelic gene deletion of E4BP4 or EOMES was possible, and that these knockout (KO) CD34$^+$ derived cell clones failed to generate NK cells. This suggests that within our NK cell differentiation system, loss of E4BP4 or EOMES expression within CD34$^+$ HPCs compromises human NK cell differentiation.

## 4.2. Effects of deleting E4BP4 during human NK cell differentiation.

### 4.2.1 E4BP4 gene targeting strategy.

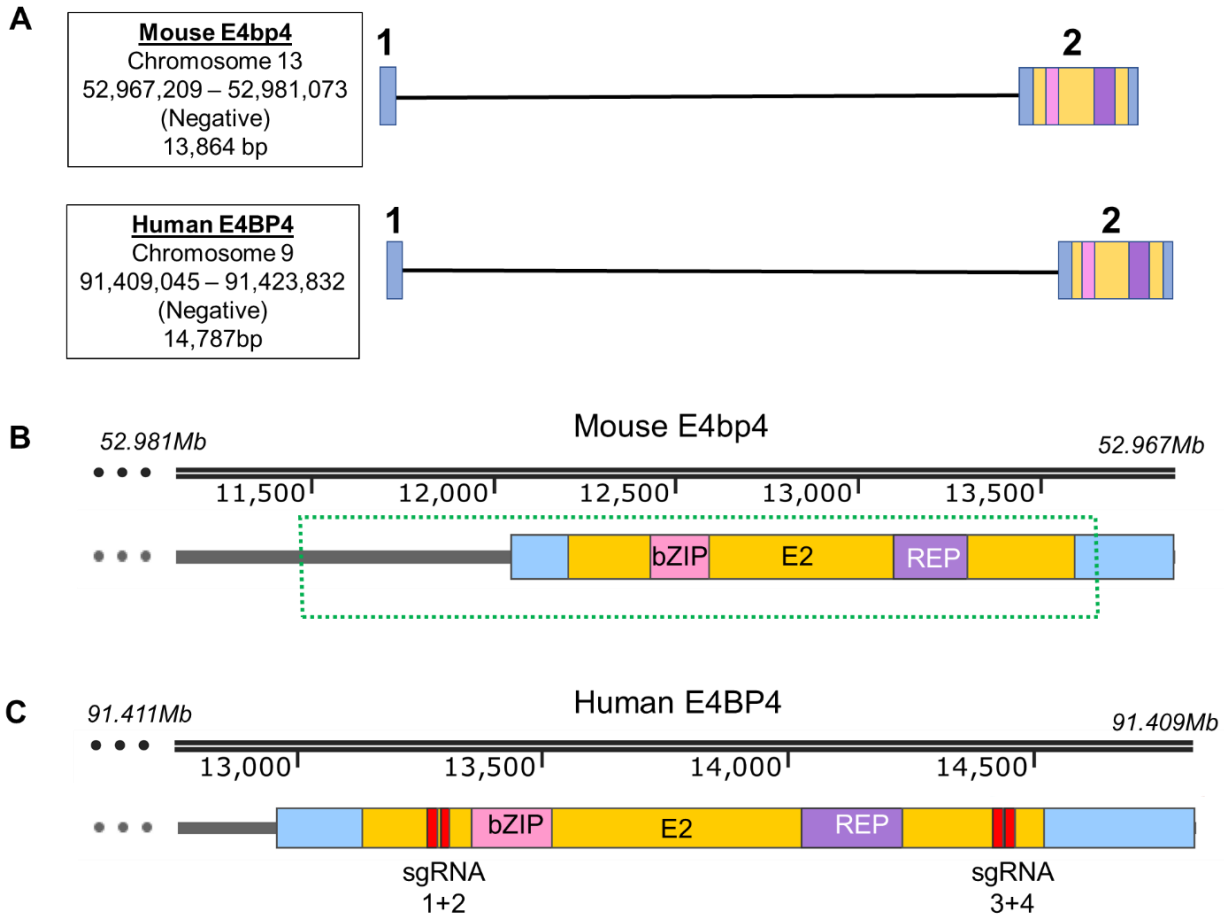



Figure 4.1: Schematic of the E4bp4 gene in mouse and human.

*(A) Chromosomal location, size and coding regions are shown for both the mouse and human E4bp4 gene. Exons are numbered and shown as boxes, yellow representing the coding and blue the non-coding regions. Pink and purple boxes represent the bZIP and repression (REP) domain, respectively. (B) Enlarged view of the mouse E4bp4 coding region on Exon 2, with the bZIP and REP domain. The dotted green box highlights the region that was targeted to produce E4bp4$^{-/-}$ mice in Kamizono et al., 2009. (C) Enlarged view of the human E4BP4 coding region on Exon 2, with the bZIP and REP domain. A pair of sgRNA was designed on either side of the coding region (red boxes). E: Exon.*

Human and mouse E4bp4 genes were compared when designing sgRNA to target human E4BP4 (Figure 4.1). For both species, the entire coding region of E4BP4, encompassing the functional DNA binding bZIP domain and the repression (REP) domain, are located on a single exon (exon 2) approximately 1.3kb long (Figure 4.1A). Four sgRNA were designed to target this entire region for the human E4BP4 gene (Figure 4.1C), similar to what was targeted in established E4bp4$^{-/-}$ mouse models (green dotted box, Figure 4.1B), (Gascoyne et al., 2009, Kamizono et al., 2009).

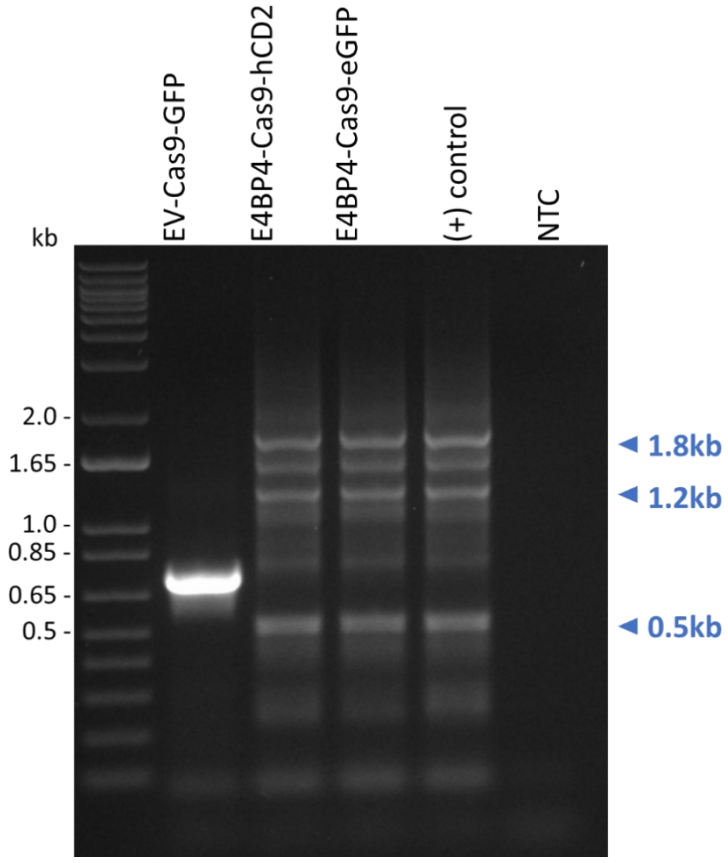



*Figure (4.2): PCR gel of the E4BP4-Cas9-hCD2/eGFP vectors.*

*PCR was performed on the E4BP4-Cas9-hCD2 and E4BP4-Cas9-eGFP vectors with primers to amplify the clone site. Presence of the original template produced a 0.7kb band while presence of all four promoters-sgRNA-scaffold regions produced a distinct band pattern of 1.8kb, 1.2kb and 0.5kb (Kabadi et al., 2014). EV: Empty vector, (+) control: positive final Cas9-eGFP vector control, NTC: Non template control.*

The four sgRNA oligonucleotides were cloned into the CRISPR/Cas9 lentiviral vector along with their own Cas9 scaffold and individual promoters. The initial E4BP4 targeting Cas9 vector that was generated had a truncated hCD2 reporter (E4BP4-Cas9-hCD2) which was later exchanged for an eGFP reporter (E4BP4-Cas9-eGFP). This change was necessary as the CD2 receptor is upregulated during NK cell differentiation, therefore, future measurements of endogenous CD2 expression could be made without interference from the E4BP4-Cas9-hCD2 vector. However, both vectors, now referred to as E4BP4-Cas9-hCD2/eGFP when discussed together, still contain the same sgRNA sequences and hence target the same E4BP4 gene region, so both were still used to generate E4BP4 KO HPC clones. PCR using previously established primers (Kabadi et al., 2014) was used to amplify the insertion site of these vectors, producing a band pattern that comprised 1.8kb, 1.2kb and 0.5kb bands if all four sgRNA domains were present (Figure 4.2). In addition to this, the E4BP4-Cas9-hCD2/eGFP vectors also lost the 0.7kb band that corresponds to the original, unedited Cas9 vector backbone, as seen by the EV-Cas9-eGFP vector. Sequencing confirmed correct insertion of the sgRNA oligonucleotides.

### 4.2.2 Validation of the E4BP4-Cas9-hCD2/eGFP vectors.

To validate the E4BP4-Cas9-hCD2/eGFP vectors, they were tested for their ability to transfect and transduce cell lines and mediate Cas9 deletion at the specified E4BP4 target region. The results from the E4BP4-Cas9-eGFP vector are shown (Figure 4.3).

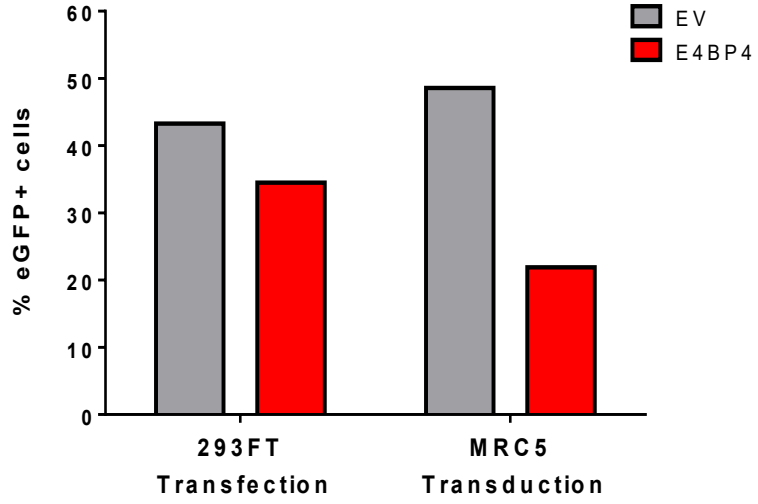



*Figure 4.3: Transfection and transduction efficiency of the E4BP4-Cas9-eGFP vector on 293FT and MRC5.*

*Percentage of eGFP⁺ cells is shown for transfected 293FT cells and transduced MRC5 cells using the EV-Cas9-eGFP vector (grey) or the E4BP4-Cas9-eGFP vector (red). Transfected or transduced cells were analysed for eGFP expression after 48h using flow cytometry. Results were from a single experiment, N=1.*

293FT cells transfected with the EV-Cas9-eGFP vector resulted in 43% eGFP⁺ expression, while cells transfected with E4BP4-Cas9-eGFP vector was slightly lower, at 34% eGFP⁺ expression. Viral supernatant was used to transduce MRC5 cells, a human primary lung cell line. EV-Cas9-eGFP transduced MRC5 cells had 48% eGFP⁺ expression, still higher than E4BP4-Cas9-eGFP transduced MRC5 cells, at 22% eGFP⁺ expression.

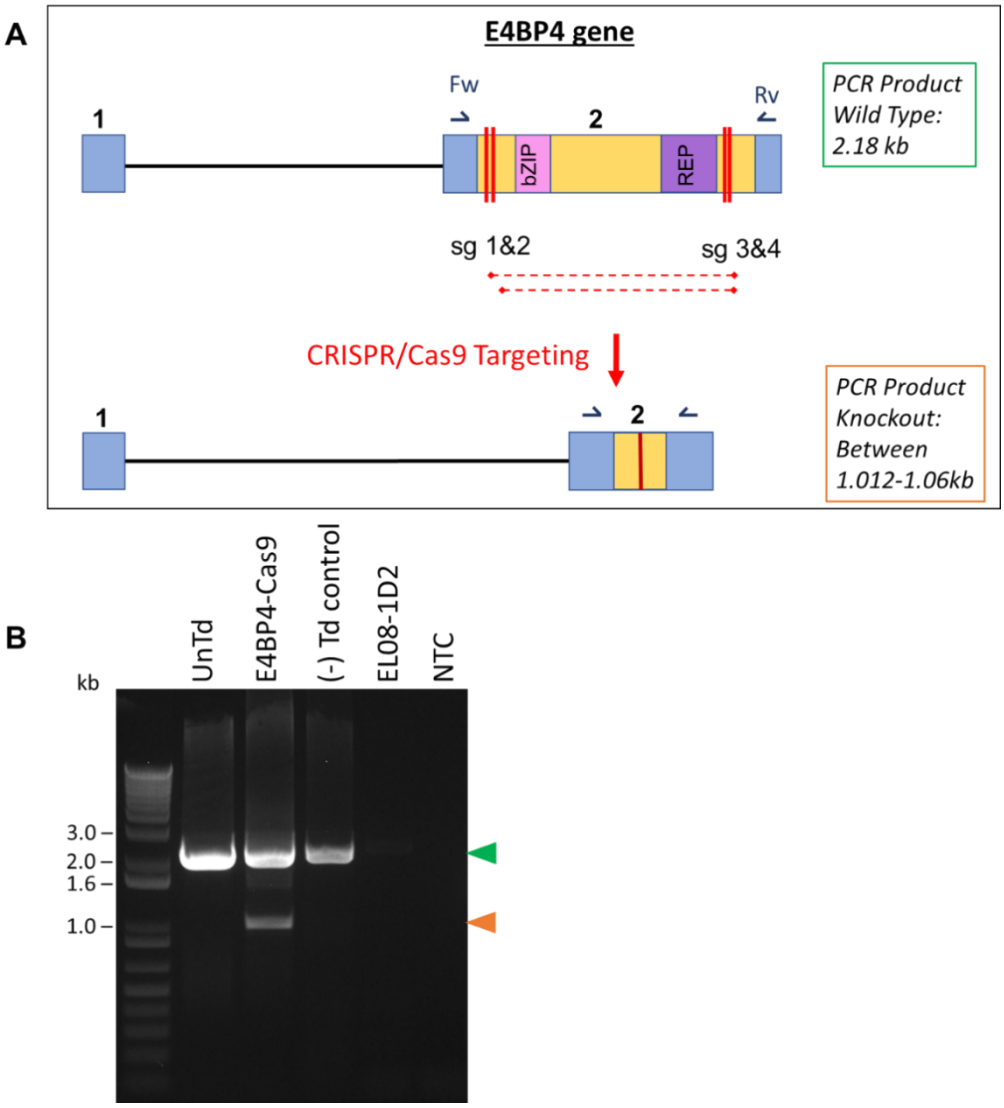



*Figure 4.4: Genotyping strategy for E4BP4.*

*(A) Schematic of the E4BP4 gene shown in Figure 4.1 indicates the location of the forward (Fw) and reverse (Rv) primers, just outside the targeting region. A 2.18kb band is produced prior Cas9 targeting while a range of bands between 1.012-1.06kb is produced after Cas9 targeting. SgRNA's (sg1-4) are represented by red lines on the top image while the indel site after NHEJ is represented by the maroon line on the bottom image. (B) Gel image showing the PCR genotyping results of MRC5 cells, untransduced (UnTd) or transduced with either the E4BP4-Cas9-eGFP vector or a Cas9-eGFP vector targeting a different gene (transduced negative control, (-) Td control). EL08-1D2 feeder cell line was also tested. Green arrowhead indicates the 2.18kb wild type (WT) band and the orange arrowhead indicates the 1kb knockout (KO) band. NTC: non template control.*

Transduced MRC5 cells were genotyped using a PCR based approach to amplify just outside the targeted region of E4BP4 (Figure 4.4A). If the E4BP4 gene remains intact, these primers produce a 2.18kb wild type (WT) band. After Cas9 mediated gene deletion at one of the upstream and downstream sgRNA sites, a range of bands from 1.012kb to 1.06kb would be produced. Therefore, any band around the 1kb mark was considered as a knockout (KO) band. Transduced MRC5 cells reveals the presence of the 2.18kb WT band and a 1kb KO band, while the untransduced and transduced negative control reveals only the 2.18kb WT band (Figure 4.4B). Since downstream applications involve irradiated EL08-1D2 co-culture, EL08-1D2 DNA was also tested and reveal no amplification.

After the E4BP4 Cas9 reporter vectors have been checked for correct sgRNA insertion and tested for their ability to produce a lentivirus capable of effecting E4BP4 gene deletion in transduced cells, the next step was to target $CD34^+$ HPCs then investigate the effects of gene loss during human NK cell differentiation.

### 4.2.3 Biallelic E4BP4 gene deletion in $CD34^+$ HPCs indicate detriment to NK cell differentiation.

Based upon efficiencies from MRC5 transductions, we suspected the E4BP4-Cas9-hCD2/eGFP lentivirus would have lower efficiencies upon transduction of $CD34^+$ HPCs. To mitigate any loss of efficiency when transducing $CD34^+$ HPCs, we increased the Cas9 DNA concentration during transfection to 12µg/10cm plate instead of 9µg/10cm plate. The Cas9 vector ratio to pSPAX and pMD2G was maintained at 1:1:0.3 respectively. $CD34^+$ HPCs were then transduced with E4BP4-Cas9-eGFP and EV-Cas9-eGFP lentivirus using the polybrene transfection reagent. After 48h, transduced cells were analysed for eGFP expression by flow cytometry (Figure 4.5).

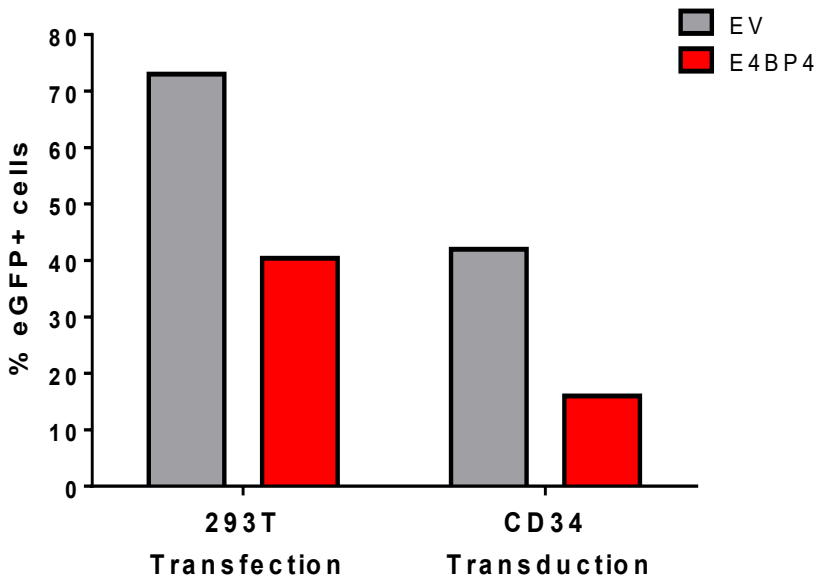



*Figure 4.5: Transfection and transduction efficiency of the E4BP4-Cas9-eGFP vector on 293T and CD34⁺ HPCs.*

*Percentage of eGFP⁺ cells is shown for transfected 293T cells and transduced CD34⁺ HPC's using the EV-Cas9-eGFP vector (grey) or the E4BP4-Cas9-eGFP vector (red). 12µg/10cm plate of Cas9 vector was used, at a 1:1:0.3 ratio of Cas9-eGFP: pSPAX: pMD2G. Virus harvested from 293T was concentrated using benchtop centrifugation and polybrene as a transduction reagent. Transfected or transduced cells were analysed for eGFP expression after 48h using flow cytometry. Results were from a single experiment, N=1.*

Results show that transfection with the EV-Cas9-eGFP vector produced 73% eGFP⁺ 293T cells, while the following transduction of CD34⁺ HPCs revealed 42% eGFP⁺ cells (Figure 4.5). The efficiency was lower using the E4BP4-Cas9-eGFP vector, with a transfection percentage of 40% eGFP⁺ 293T cells followed by a transduction percentage of 16% eGFP⁺ CD34⁺ HPCs. Nevertheless, this percentage was sufficient to continue with the sort of E4BP4-Cas9 transduced CD34⁺ HPCs.

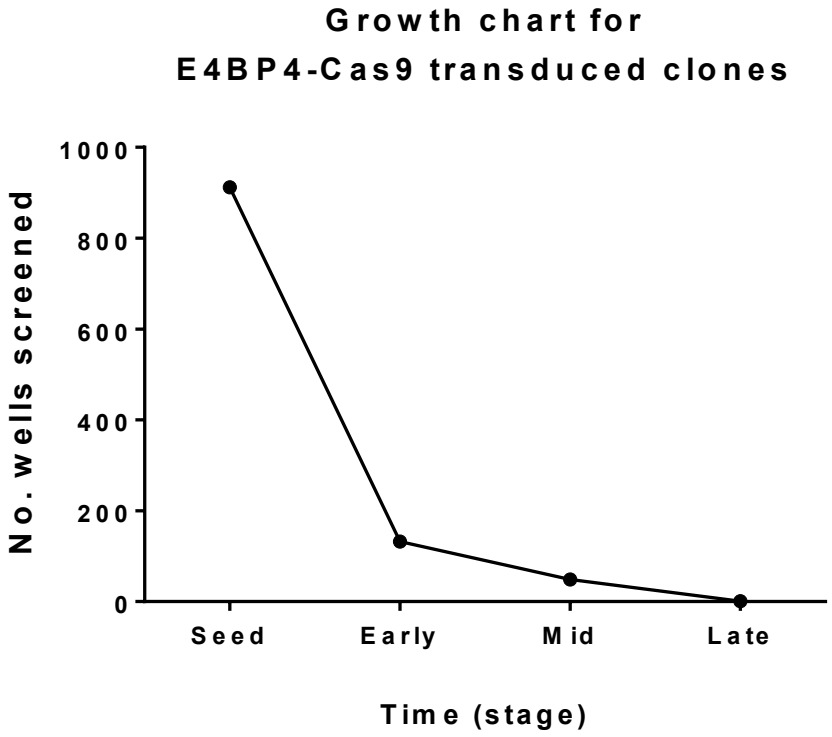



*Figure 4.6: Summary of the number of wells containing CD34⁺ derived cell populations after E4BP4 gene targeting.*

*Line chart of the number of wells that contained an E4BP4-Cas9 transduced CD34⁺ derived cell population during NK cell differentiation. 912 wells were seeded as single cells prior to NK cell differentiation. The NK differentiation culture was divided into three stages, the early stage (days 6-15), the mid-stage (days 16-27) and the late stage (days >27). Results were from four separate experiments, total N=912 wells.*

Following the protocol outlined in Figure 3.1, transduced $CD34^+$ HPCs with either E4BP4-Cas9-hCD2/eGFP vectors were sorted as single cells in undifferentiation media and transferred into NK differentiation conditions after 5 days. Any well containing differentiating HPCs cells was monitored during the early stage (days 6-15), mid-stage (days 16-27) and late stage (days >27) of culture (Figure 4.6). Of the 912 wells that were seeded with a single, transduced $CD34^+$ HPC for NK cell differentiation, 14.5% (132/912) of the wells contained a $CD34^+$ cell derived population during the early stage. By the mid-stage, this percentage decreased to 5% (49/921) of wells and by the late stage, less than 1% (1/912) of wells.

Any well above 40% cell confluency was maintained in culture and sampled for genotyping (Figure 4.7) and NK cell characterisation by flow cytometry (Figure 4.8).

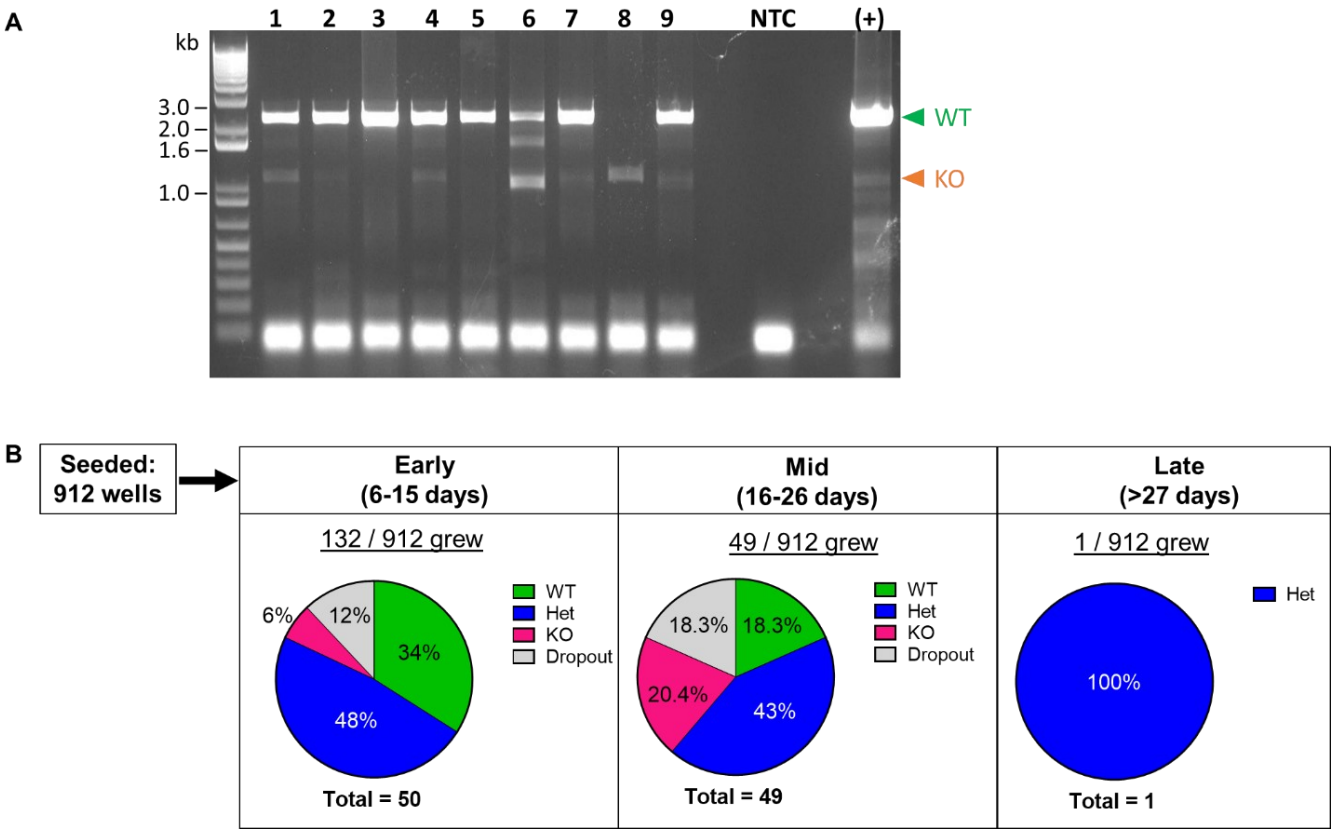



*Figure 4.7: Summary of the genotyping results from growing CD34⁺ derived cell populations after E4BP4 gene targeting.*

*(A) Representative genotyping gel of 9 CD34⁺ HPC targeted clones 16 days post sort and differentiation into NK cells (numbers 1-9). WT (2.18kb) and KO (1kb) bands are highlighted by the green and orange arrowheads, respectively. NTC: non template control, (+): positive control of DNA from a pooled population of transfected 293T cells with the E4BP4-Cas9 vector. (B) Summary of the genotypes from the well populations (clones) over the course of NK cell differentiation. Within each stage, the numbers of wells that had clonal populations are indicated above the pie chart (e.g. 132/912 grew) while the total number of wells within that group that was genotyped is indicated at the bottom. Dropout clones had no visible band when genotyped. WT: wild type, Het: heterozygous, KO: knockout. Results were from four separate experiments, total N=912 wells.*

A representative gel image indicates how clonal cell populations (now referred to as clones) were genotyped (Figure 4.7A). Clones with only the 2.18kb WT band were classified as WT for E4BP4, such as clones 3 and 5. Clones with only the 1kb KO band were classified as a biallelic E4BP4 KO, like clone 8. Clones that contained both WT and KO bands, irrespective of band intensities, were classified as heterozygous (Het), like clones 1, 2, 4, 6, 7 and 9. Sequence confirmation of the 1kb KO band to confirm it corresponds with the expected target region is ongoing.

The genotypes from clones that were above 40% confluent within the well is summarised across the early, mid and late stages of differentiation (Figure 4.7B). Almost all the clones had stopped expanding by the late stage, with only a single clone remaining until day 27. At the early stage, between days 6-15, 38% (50/132) of the 132 clones were able to be genotyped. The largest proportion of clones were Het, at 48%, followed by WT, at 34%, and finally KO, at 6%. 12% of these clones did not produce bands during genotyping, even if the same clone was checked at a later stage. At the mid-stage, all 49 clones that expanded could be genotyped. Although most of the clones were still of the Het genotype (43%), the percentage of WT decreased slightly to 18.3% and KO increased to 20.4%. The percentage of dropout clones also increased, up to 18.3%. The single clone that stopped growing on day 27 was identified to be a Het population.

Clones that were 40% confluent in a 48 well or larger were able to be analysed for NK cell surface markers by flow cytometry. Only at the mid-stage did some of the clones expand to a point that could be analysed (Figure 4.8).

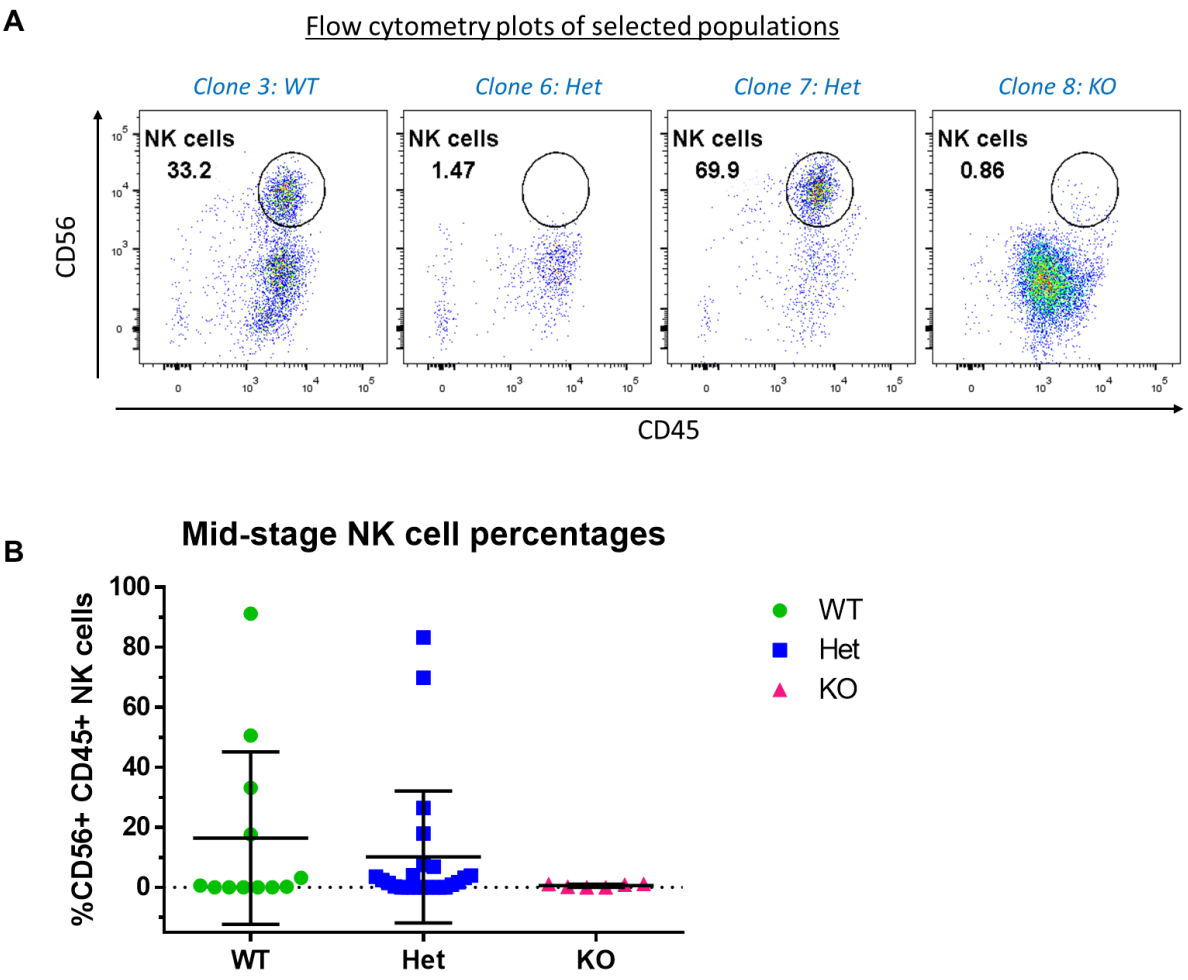



*Figure 4.8: NK cell percentages of E4BP4-Cas9 transduced CD34⁺ derived cell populations during mid-stage of NK cell development.*

*(A) Representative flow cytometry plots showing NK cell percentages of 4 selected clones. Genotypes of these clones were shown in Figure 4.7A. (B) NK cell percentages of all the clones able to be screened for flow cytometry during the mid-stage of NK cell development. Results were from four separate experiments; bars represent average values plus standard deviation. No significant comparisons were observed using a one-way ANOVA. Replicates for WT: N=12, Het: N= 23, KO: N=6.*

Representative flow cytometry plots shown in Figure 4.8A indicate a distinct $CD56^+$ $CD45^+$ NK cell population for WT clone 3 and Het clone 7, previously genotyped in Figure 4.7A. The Het clone 6 and KO clone 8 do not contain any NK cells, however, do reveal presence of a $CD45^+$ $CD56^-$ cell population.

The summary of all the clones analysed during the mid-stage reveal that of the WT clones, 42% (5/12) where able to produce NK cells, with an average 16% $CD45^+$ $CD56^+$ NK cell population (Figure 4.8B). For the Het clones screened, 57% (13/23) produced NK cells with an average of 10% $CD45^+$ $CD56^+$ NK cell population. Only 6 KO clones were able to be analysed, of which none produced an NK cell population above 1%.

## 4.3. Effects of deleting EOMES during human NK cell differentiation.

### 4.3.1 EOMES gene targeting strategy.

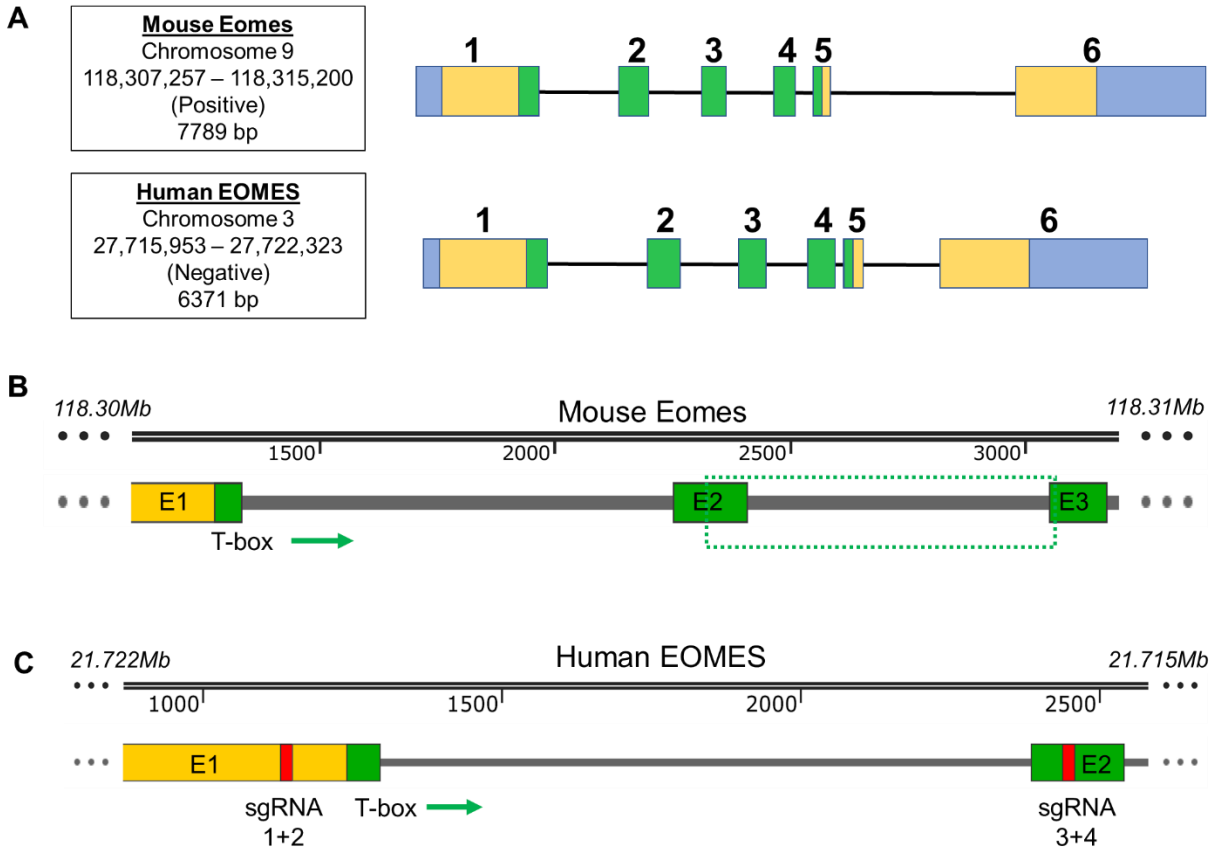



Figure 4.9: Schematic of the Eomes gene in mouse and human.

*(A) Chromosomal location, size and regions coding for functional domains are shown for both the mouse and human Eomes gene. Exons are numbered and shown as boxes; yellow representing the coding region, blue the non-coding region and green the T-box domain. (B) Enlarged view of the mouse Eomes gene, highlighting the T-box domain (green boxes and arrow). The region between Exon 2 and Exon 3 was targeted to generate Eomes$^{-/-}$ mice (dotted green box), (Russ et al., 2000). (C) Enlarged view of the human EOMES gene, highlighting the T-box domain (green boxes and arrow). SgRNA 1 and 2 on Exon 1 and sgRNA 3 and 4 on Exon 2 is highlighted in red. E: Exon.*

The Human and mouse Eomes genes are comprised of 6 exons, with the coding region spanning across all exons (Figure 4.9A). The T-box DNA binding domain encompasses most of this coding region and is conserved in both species. The deletion of Eomes gene expression within mice involved the replacement of parts of Exon 2 and intron 2 with an antibiotic resistance cassette (Figure 4.9B), (Russ et al., 2000). When this region was considered for deletion of the human EOMES gene, sgRNA were selected at the end of Exon 1 (sgRNA 1 and 2) and within Exon 2 (sgRNA 3 and 4), (Figure 4.9C).

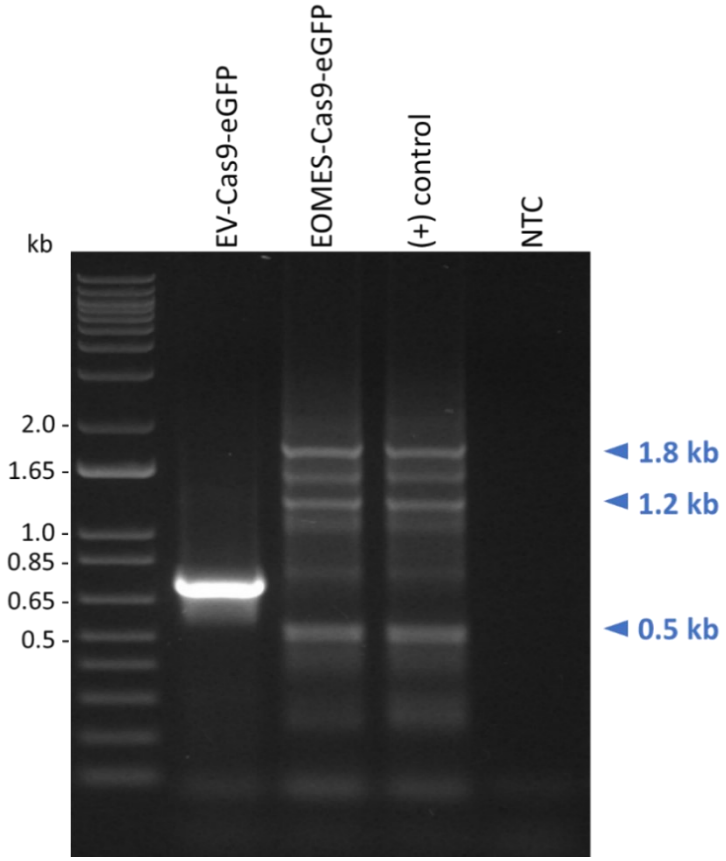



Figure 4.10: PCR gel of the EOMES-Cas9-eGFP vector.

*PCR was performed on the final EOMES-Cas9-eGFP lentiviral vector with primers to amplify the clone site. Presence of the original template produced a 0.7kb band while presence of all four promoter-sgRNA-scaffold regions produced a distinct band pattern of 1.8kb, 1.2kb and 0.5kb (Kabadi et al., 2014). EV: Empty vector, (+) control: positive final Cas9-eGFP vector control, NTC: Non template control*.

PCR was used to determine successful insertion of all four promoter-sgRNA-scaffold regions within the final EOMES-Cas9-eGFP vector, revealing the expected band pattern of 1.8kb, 1.2kb and 0.5kb (Figure 4.10). Sequencing confirmed insertion and correct orientation of the sgRNA.

### 4.3.2 Validation of the EOMES-Cas9-eGFP vector.

The EOMES-Cas9-eGFP vector was assessed on its ability to transduce 293T cells and result in EOMES gene deletion at the specified target site. 293T cells transfected or transduced with either EV-Cas9-eGFP or EOMES-Cas9-eGFP was measured for eGFP reporter expression using flow cytometry after 48h (Figure 4.11).

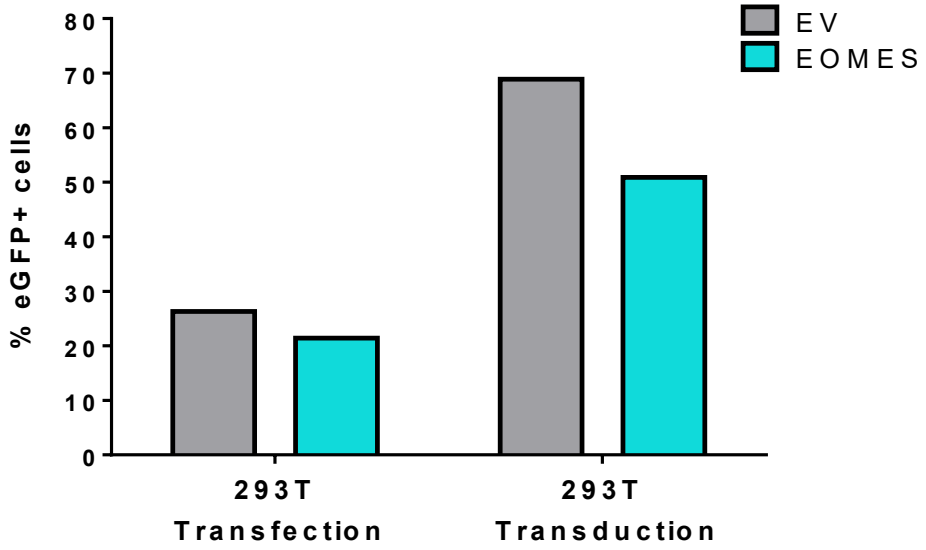



Figure 4.11: Transfection and transduction efficiency of the EOMES-Cas9-eGFP vector on 293T cells.

*Percentage of eGFP⁺ cells is shown for transfected and transduced 293T cells with the EV-Cas9-eGFP vector (grey) and the EOMES-Cas9-eGFP vector (blue). Transfected or transduced cells were analysed for eGFP expression after 48h using flow cytometry. Results were from a single experiment, N=1.*

Transfected 293T cells with the EV-Cas9-eGFP vector produced 26% eGFP⁺ cells, slightly higher than the 21% of EOMES-Cas9-eGFP transfected eGFP⁺ cells. (Figure 4.11). After transduction, the percentage of eGFP⁺ cells was still higher for EV transduced cells, at 69%, compared to EOMES transduced cells, at 51%.

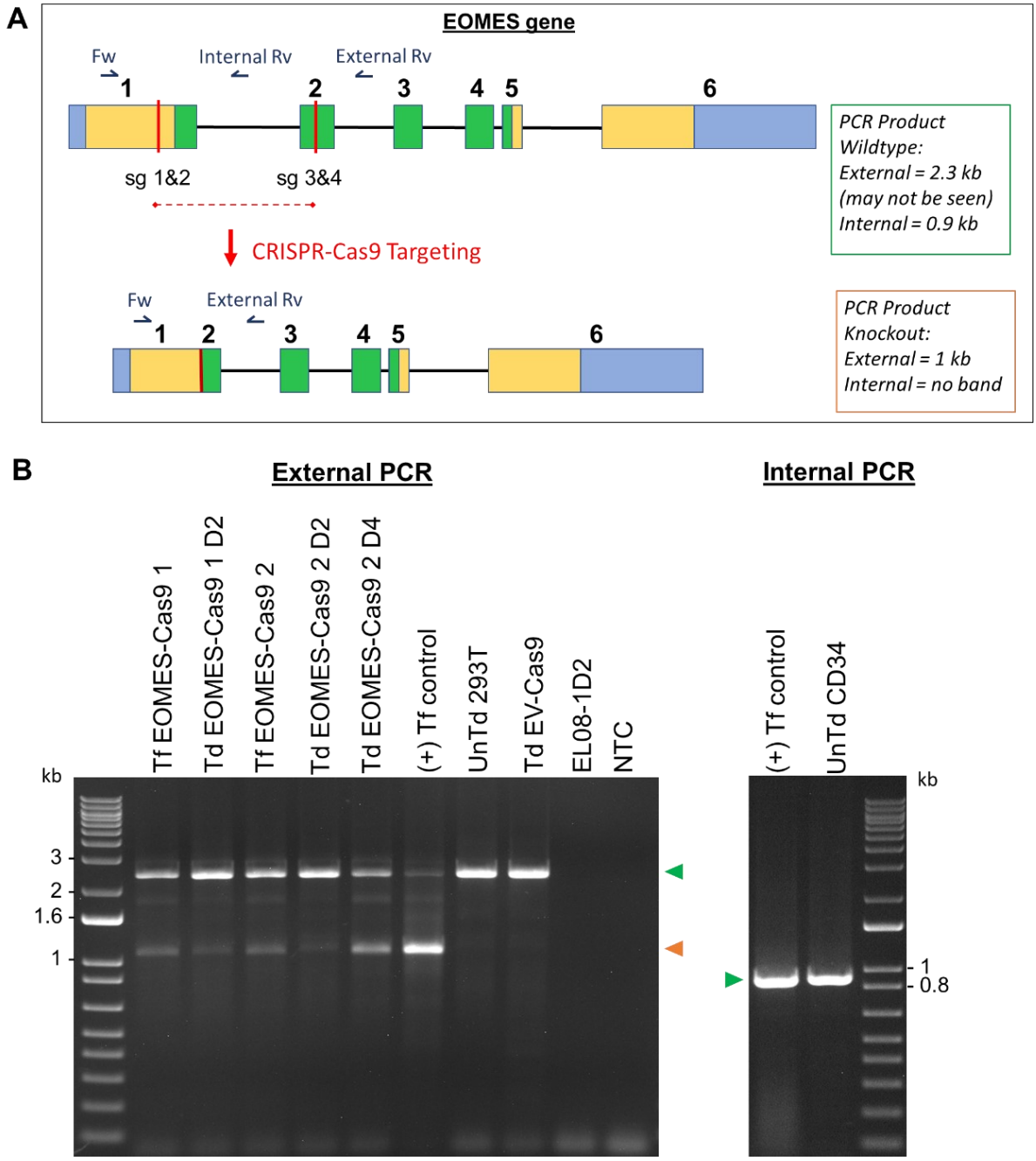



Figure 4.12: Genotyping strategy for EOMES.

*(Legend on next page).*

Figure 4.12: Genotyping strategy for EOMES.

*(A) Schematic of the EOMES gene shown in Figure 4.9 indicating the location of the forward (Fw), the external reverse (eRv) and the internal reverse primers (iRv). Prior to Cas9 targeting, the external PCR (using Fw and eRv primers) occasionally amplified a 2.3kb WT band while the subsequent internal PCR (using the same Fw but iRv primers) amplified a 0.9kb WT band. After Cas9 mediated gene deletion, the external PCR produce a 1kb external KO band. (B) Gel showing the external PCR genotyping results of 293T cells transfected (Tf) or transduced (Td) with EOMES-Cas9-eGFP, replicates labelled with 1 and 2. Transduced cells were analysed for genotyping after 2 days (D2) or 4 days (D4) post transduction, in the case of replicate 2. Arrowheads mark the 2.3kb WT bands (green) and 1kb KO bands (orange). For the internal PCR, the positive EOMES-Cas9-eGFP control and untransduced CD34$^+$ HPC were tested. 0.9kb WT band is indicated by a green arrowhead. (+) Tf control: positive control consisting of 293FT transfected with EOMES-Cas9-eGFP, UnTd 293T: Untransduced 293T, Td EV-Cas9: 293T transduced with EV-Cas9-eGFP virus. NTC: Non-template control.*

EOMES genotyping consisted of primers amplifying outside the sgRNA target region (external PCR), followed by a PCR that used the same forward but an internal reverse primer from within the target site (internal PCR), (Figure 4.12A). The internal PCR confirmed the presence of any intact target region if the 2.3kb external WT band was absent, producing a 0.9kb internal WT band. If Cas9 mediated EOMES targeting was successful, the external PCR would reveal a 1kb external KO band and the internal PCR would show no band amplification.

In the external PCR, the 2.3kb WT band and the 1kb KO band was seen for 293T cells transfected or transduced with EOMES-Cas9-eGFP (Figure 4.12B). This was present for both replicates (1 and 2). External PCR also showed amplification of only the 2.3kb WT band for the untransduced 293T and the EV-Cas9-eGFP transduced 293T controls, in addition to no presence of a band from EL08-1D2 DNA. The internal PCR was run on the positive EOMES-Cas9-eGFP transfected control and the untransduced CD34$^+$ HPC control, which showed amplification of the 0.9kb WT band.

After confirming that the EOMES-Cas9-eGFP vector could transduce cells based upon reporter expression and a gene KO was identifiable using PCR, CD34$^+$ HPCs were then targeted to observe the effects of EOMES deletion prior to NK cell differentiation.

### 4.3.3 Targeting EOMES within CD34$^+$ HPCs reveals failure to expand during NK cell differentiation *in vitro*.

CD34$^+$ HPCs were transduced with EOMES-Cas9-eGFP and EV-Cas9-eGFP lentivirus using a retronectin based approach. After 48h, transduced cells were analysed for eGFP expression by flow cytometry.

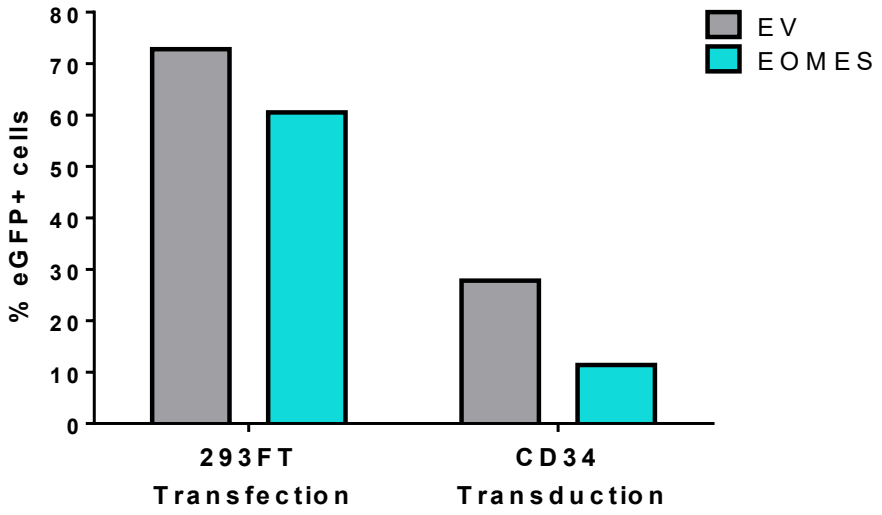



Figure 4.13: Transfection and transduction efficiency of the EOMES-Cas9-eGFP vector on 293FT and CD34$^+$ HPCs cells.

*Percentage of eGFP$^+$ cells is shown for transfected 293FT cells and transduced CD34$^+$ HPCs using the EV-Cas9-eGFP vector (grey) and EOMES-Cas9-eGFP vector (blue). Virus harvested from the 293FT supernatant was concentrated using benchtop centrifugation and bound to retronectin coated plates to transduce the CD34$^+$ HPCs. Cells were analysed for eGFP expression 48h post transfection and transduction. Results were from a single experiment, N=1.*

CD34$^+$ HPCs were transduced with EV-Cas9-eGFP or EOMES-Cas9-eGFP lentivirus produced and concentrated from transfected 293FT cells (Figure 4.13). EV-Cas9-eGFP transfected 293FT were 72.8% eGFP$^+$, while EOMES-Cas9-eGFP transfected cells had a lower eGFP$^+$ cell percentage, at 60.5%. After viral concentration and transduction of CD34$^+$ HPCs, EV-Cas9 transduced HPCs still had a higher eGFP$^+$ percentage, at 28%, compared to the 11.4% of EOMES-Cas9 transduced HPCs.

Transduced CD34$^+$ HPCs with EOMES-Cas9-eGFP were sorted as a pooled population of eGFP$^+$ cells, recovered in undifferentiation media overnight and serially diluted into NK cell differentiation conditions at low cell numbers (below 5 cell/well). Growth of these cells within each well (clones) was monitored over three culture stages, the early stage (days 6-15), the mid-stage (days 16-27) and the late stage (days >27) (Figure 4.14).

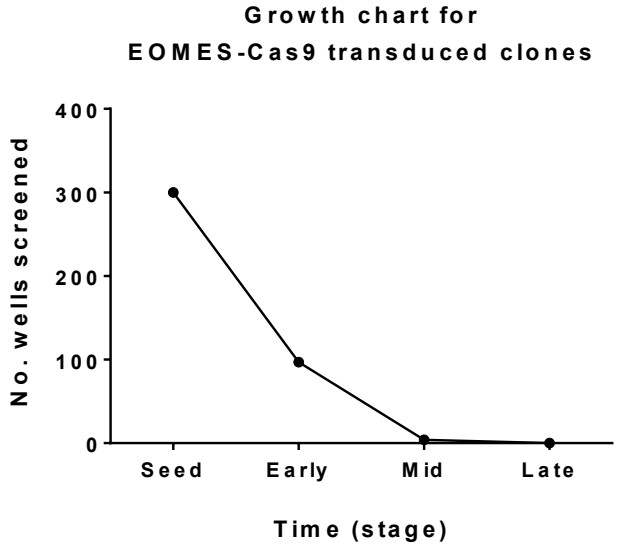



Figure 4.14: Summary of the number of wells containing CD34$^+$ derived cell populations after EOMES gene targeting.

*Line chart of the number of wells that contained an EOMES-Cas9-eGFP transduced CD34$^+$ derived cell population during NK cell differentiation. 300 wells were seeded with less than 5 cells/well for NK differentiation. The NK differentiation culture was divided into three stages, the early stage (days 6-15), the mid-stage (days 16-27) and the late stage (days >27). Results were from a single experiment, N=300 wells.*

After seeding, the number of wells that contained $CD34^+$ derived cell clones decreased to 32.3% (97/300) by the early stage (Figure 4.14). By the mid-stage, this value continued to decrease to 1.7% (5/300) until no visible growth was observed at the late stage.

Over the course of culture, wells above 40% confluency were sampled for genotyping. By the late stage, some wells still had observable $CD34^+$ derived cells which failed to show proliferation past 40% confluency during the early and mid-stage. These cells were labelled as “failed growths” and on day 27/28 of culture, the entire well was harvested for genotyping, irrespective of cell confluency (Figure 4.15 and 4.16). Clones above 40% cell confluency but had showed arrest in cell growth after the mid-stage were also categorised as “failed growths” and were analysed for NK cell determination by flow cytometry (Figure 4.17).

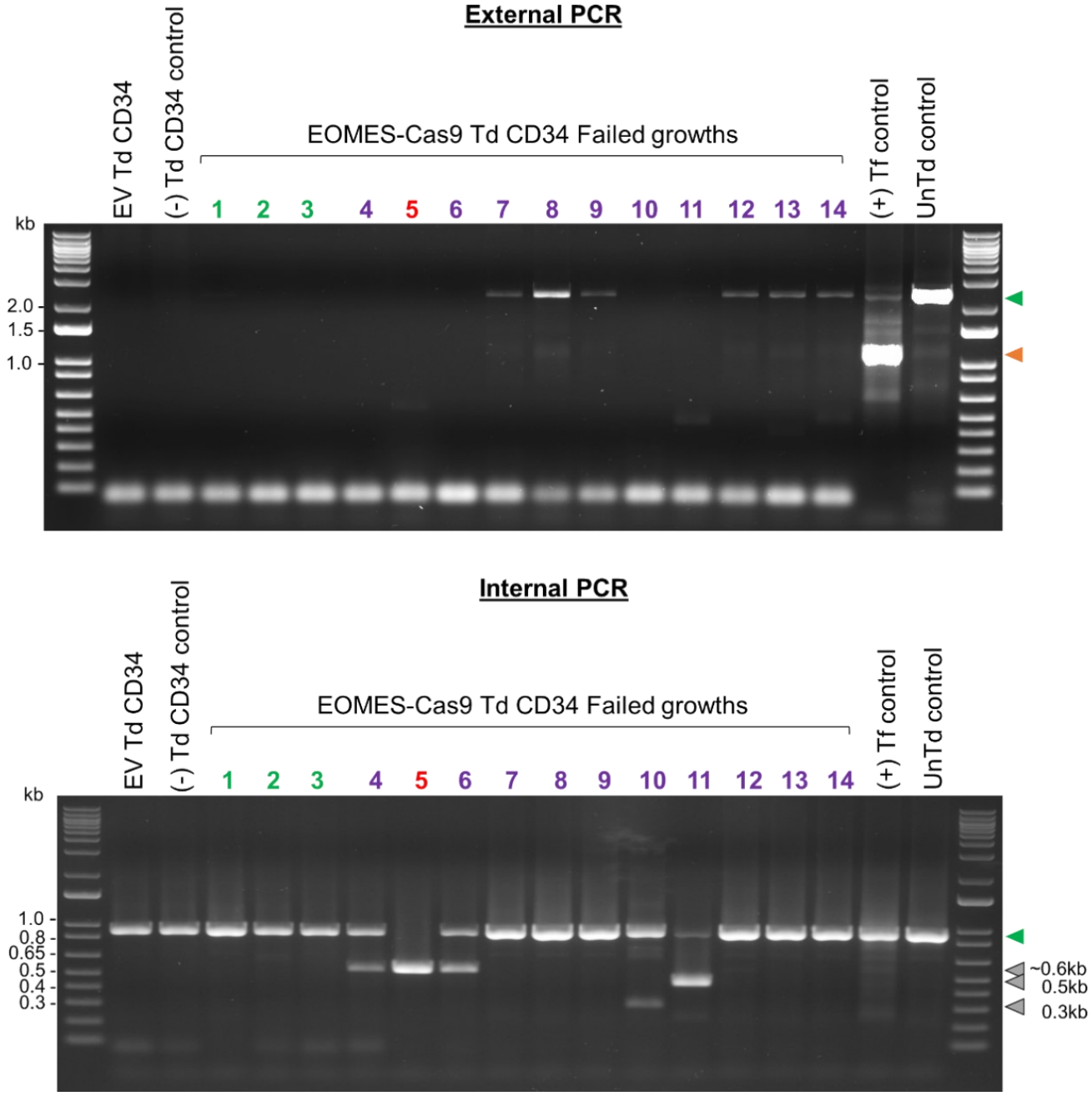



Figure 4.15: Genotyping gel of failed growth EOMES-Cas9-eGFP transduced populations at the late stage of NK cell culture.

*(Legend on next page).*

Figure 4.15: Genotyping gel of failed growth EOMES-Cas9-eGFP transduced populations at the late stage of NK cell culture.

*Gel image showing genotyping results of EOMES-Cas9-eGFP transduced CD34⁺ derived cell clones that stopped growing by day 27/28. Above each lane, EOMES WT clones are labelled in green, Het clones are labelled purple and biallelic KO clones are labelled red. Top: external PCR of clones and controls producing a 2.3kb WT band (green arrowhead) if there is presence of an intact EOMES allele and a 1kb KO band (orange arrowhead) if there is presence of a targeted EOMES allele. Bottom: internal PCR of clones and controls producing a 0.9kb WT band (green arrowhead) if there is presence of an intact EOMES allele. Grey arrowheads mark unexpected band sizes found across some clones (~0.6kb, 0.5kb, 0.3kb). EV Td CD34: EV transduced CD34⁺ cells, (-) Td CD34 control: negative control of CD34⁺ cells transduced with a Cas9 vector targeting a different gene, (+) Tf control: positive EOMES-Cas9-eGFP transfected control of 293FT cells, UnTd control: Untransduced CD34⁺ cell control. Gel images were edited with a +20% contrast using the Microsoft PowerPoint correction tool.*

The genotyping gel of the failed growth clones reveal the 2.3kb external WT band was not always present, therefore a WT clone was determined by presence of at least the 0.9kb internal WT band and absence of the 1kb external KO band (Figure 4.15). This was the case for clones 1-3, labelled in green. Het clones, labelled purple, were determined by possible presence of the 2.3kb external WT band, a 1kb external KO band and a 0.9kb internal WT band (clones 4 and 6-14). However, for some Het clones, the external PCR did now show the presence of a 1kb KO band but the internal PCR did show presence of a band below it, around 0.6kb (clone 4 and 6), 0.5kb (clone 11) or 0.3kb (clone 10), in addition to the 0.9kb internal WT band. These clones were still considered as Het populations, with the sequence of these smaller bands currently being investigated. For Clone 5, labelled in red, the only band amplified was in the internal PCR at ~0.6kb. It was decided this clone was still a biallelic KO due to the absence of the 0.9kb internal WT band.

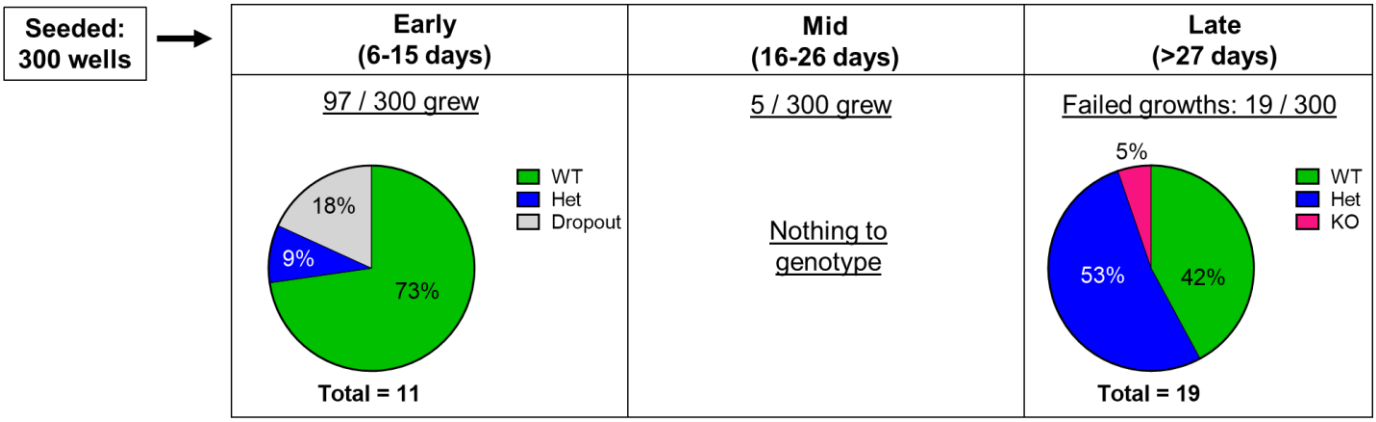



Figure 4.16: Summary of genotyping results from EOMES-Cas9-eGFP transduced CD34$^+$ derived cell clones.

*Summary of the genotypes from EOMES-Cas9-eGFP transduced clones during the early (days 6-15), mid (days 16-26) and late (days >27) stages of culture. Within each stage, the number of clones that were growing are indicated above the pie chart, with the total number of clones that could be genotyped indicated below (total). Results were from a single experiment, N=300 wells.*

At the early stage, the number of clones that could be genotyped from the growing population was 11% (11/97), (Figure 4.16). 73% of the clones at this stage were WT while only 9% was Het. At the mid-stage, although there were some clones growing, they were all below 40% confluent within the well and were not sampled for genotyping. By the late stage, all growth had halted and any well that had a visible presence of CD34$^+$ derived cells, based on their circular, reflective appearance, was genotyped. 5% of clones within this “failed growth” group was KO for EOMES, while the majority, 53%, was identified as Het. This was followed closely by WT clones, representing 42% of this failed growth population.

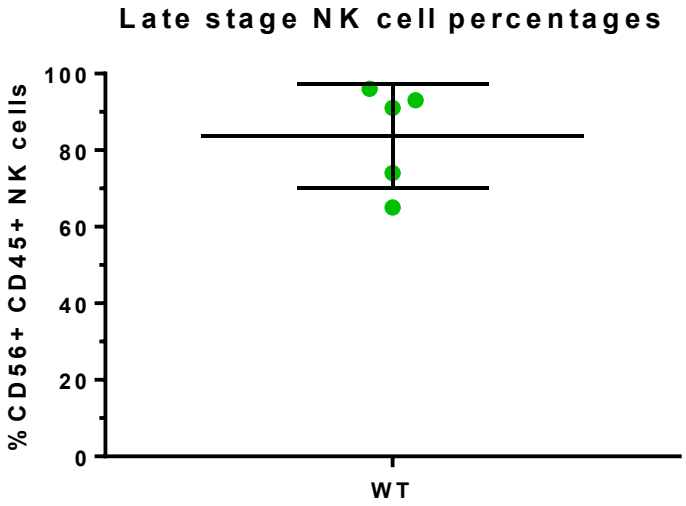



Figure 4.17: NK cell percentages of the failed growth EOMES-Cas9-eGFP transduced clones at the late stage of NK cell culture.

*NK cell percentages from clones that stopped growing by the late stage are shown. These clones were still above 40% confluent when they were harvested and genotyped on day 28. Results were from a single experiment; bars represent average values plus standard deviation. Replicates for WT: N=5.*

When harvesting the failed growth clones, only 5 of the clones had above 40% well confluency and were analysed for NK cell surface marker expression using flow cytometry (Figure 4.17). All these clones were identified as WT after genotyping and had an average of 84% $CD3^-$ $CD45^+$ $CD56^+$ NK cells within the well.

## 4.4. Discussion

The effect of two genes thought to be involved in human NK cell differentiation and maturation, E4BP4 and EOMES, was investigated to try to gain more information about their role in human NK cell development for future application to enhance NK cell immunotherapy. E4bp4 expression was shown to be crucial for NK cell development in mouse HPCs (Gascoyne et al., 2009, Male et al., 2014) while Eomes expression was shown to regulate murine NK cell maturation into functionally

competent effector cells (Gordon et al., 2012, Intlekofer et al., 2005). Using a lentiviral CRISPR/Cas9 system to target these genes in human CD34$^+$ HPCs, my results show it is possible to generate biallelic E4BP4 or EOMES KO clones. These KO clones failed to generate CD56$^+$ NK cells, indicating that the loss of these genes at the progenitor stage compromised NK cell differentiation.

The biallelic deletion of E4BP4 resulted in a lack of growth and differentiation into CD56$^+$ NK cells. Knockout of E4BP4 gene expression in CD34$^+$ HPCs was achieved by deleting the entire coding region comprising the functional DNA binding bZIP domain and the repression domain, mirroring the targeting approach used in mouse (Gascoyne et al., 2009, Kamizono et al., 2009), (Figure 4.1). The E4BP4-Cas9 lentiviral construct was effective at generating gene deletion of E4BP4 alleles at the target site, as determined by genotyping PCR on transduced MRC5 cells and CD34$^+$ HPCs (Figure 4.4B and 4.7A, respectively). Of the transduced CD34$^+$ HPCs differentiating into NK cells, results show that biallelic E4BP4 KO clones were detected as early as days 6-15 (early stage), (Figure 4.7B) and that these clones failed to produce CD56$^+$ NK cells at the mid-stage of culture (Figure 4.8). Additionally, while E4BP4 Het clones were the most prevalent across all the stages analysed, they averaged a lower percentage of CD56$^+$ NK cells than E4BP4 WT clones (Figure 4.8B). The 1kb E4BP4 KO band seen during genotyping PCR corresponds to the expected target region (Figure 4.4), and sequencing of this band to confirm is ongoing. Collectively, the data suggests that the loss of E4BP4 expression in CD34$^+$ HPCs negatively impacts human NK cell differentiation *in vitro*, supporting similar findings within *in vivo* E4bp4$^{-/-}$ mouse models.

Deletion of a single EOMES allele in CD34$^+$ HPCs was sufficient to compromise growth and differentiation into CD56$^+$ NK cells. The N-terminal portion of the T-box domain, commonly associated with DNA binding (Papaioannou, 2014), was targeted to delete EOMES expression in human, similar to established Eomes$^{+/-}$ mouse models (Russ et al., 2000), (Figure 4.9). By removing this region, we believe it should prevent the ability for EOMES, if expressed, to induce gene transcription. The EOMES-Cas9-eGFP lentiviral construct was effective at generating gene deletion of EOMES alleles within transduced 293T cells and CD34$^+$ HPCs (Figure 4.12B and 4.15, respectively). Results indicate that deletion of EOMES negatively impacted growth of transduced CD34$^+$ HPC derived clones in our NK cell differentiation culture, as the detection of

EOMES KO clones, as well as most Het clones, were found only within the “failed growth” population (Figure 4.16). Further supporting the importance of EOMES expression for NK cell differentiation is the result that, of the clones that differentiated into $CD56^+$ NK cells, they were all WT for EOMES (Figure 4.17). Interestingly, genotyping results from the internal PCR also revealed clones that had bands below the expected 0.9kb internal KO band (Figure 4.15). As CRISPR/Cas9 mediated dsDNA breaks are repaired by non-homologous end joining (NHEJ) in $CD34^+$ HPCs (Lieber et al., 2003), the creation of an indel mutation would explain the differences in band sizes during genotyping PCR. While sequence validation of these bands is ongoing, we believe that the smaller band sizes than expected correspond to a bigger deletion of the target site and were therefore still considered a KO band when determining genotype. In total, these results indicate that loss of EOMES expression at the progenitor stage shows a detriment to NK cell development.

Overall, a reduction in cell growth was observed in E4BP4 and EOMES WT clones during NK cell differentiation over time (Figure 4.7B and 4.16, respectively), an effect believed to be a result of seeding low cell numbers of transduced $CD34^+$ HPCs for clonal NK cell differentiation. As WT clones should retain the ability to express E4BP4 and EOMES, the reduction of WT clone numbers past the mid-stage of culture is not thought to be due to gene targeting but an arrest in cell growth. Further supporting this idea, a similar reduction in clone growth was observed when untransduced and EV-Cas9-eGFP transduced clones were seeded at lower cell densities at the start of differentiation (Figure 3.3 and 3.8, respectively). Increasing the seeding density of EOMES-Cas9-eGFP transduced $CD34^+$ HPCs to no more than 5 cells/well at the start of differentiation did not appear to improve WT clone growth during the course of differentiation (Figure 4.16), indicating that this density was still too low to make a significant improvement. Increasing the seeding cell density above 5 cells/well should facilitate a corresponding increase in growth of clones overall, as seen in EV transduced cells (Figure 3.8A). However, in order to seed at a higher density, the $CD34^+$ HPC transduction efficiency must be considered to ensure biallelic KO clones can still be obtained.

A lower transfection and transduction efficiency was observed with either gene targeting Cas9 vector compared to the EV-Cas9-eGFP control, which compromises the frequency of successful biallelic KO in targeted $CD34^+$ HPCs. Using reporter

expression as a measurement of efficiency, the transfection efficiencies seen with the E4BP4-Cas9-eGFP (Figure 4.3 and 4.5) or the EOMES-Cas9-eGFP (Figure 4.11 and 4.13) were consistently lower than EV-Cas9-eGFP. With fewer cells transfected, less viral particles would be produced, resulting in a reduced transduction efficiency. This is seen when $CD34^+$ HPCs were transduced, where both gene targeting vectors exhibited a 2.5-fold lower efficiency than the EV-Cas9-eGFP (E4BP4, Figure 4.5 and EOMES, Figure 4.13). This decrease in efficiency can be explained by the vector size, as previous reports reveal the larger the vector is, the fewer viral particles are generated (Cante-Barrett et al., 2016). Since the gene targeting Cas9 vectors were 15.8kb and the EV-Cas9-eGFP vector was 14.7kb, the difference in size could explain the gap in transfection and transduction efficiency. Lentiviral transduction of $CD34^+$ HPCs using vectors between 5-10kb was reported to have transduction efficiencies below 20%, like what was seen with the E4BP4 and EOMES Cas9 vectors, even with a reasonably high multiplicity of infection (MOI) ranging from 50-1000 (Case et al., 1999, Guenechea et al., 2000). This highlights the difficulty in transducing $CD34^+$ HPCs, especially with a lentiviral vector above 10kb in size. Since our “all-in-one” CRISPR/Cas9 lentiviral vector is designed to express both the Cas9 and the sgRNA together, eliminating the possibility of transduced cells expressing one of the components, it is difficult to further reduce the vector size to improve transfection and transduction efficiencies. Therefore, while the transduction efficiency using the E4BP4 or EOMES Cas9 vectors were sufficient to achieve biallelic KO clones, optimisation of the transduction process to increase the number of transduced $CD34^+$ HPCs is necessary to be able to seed these cells at higher densities and generate more possible KO NK cell clones.

The next steps taken to optimise the transduction process for our gene targeting vectors was directed at improving viral entry and infection of $CD34^+$ HPCs, as well as the survival of transduced cells during NK cell differentiation. Since the deletion of E4BP4 and EOMES compromise the generation of $CD56^+$ NK cells, these genes cannot be used to assess whether optimisation improved transduced cell differentiation into NK cells. NKG2A, an inhibitory receptor, is expressed after $CD56^+$ NK cell differentiation and therefore its loss at the progenitor stage should not affect NK cell development to this point. The effects of targeting NKG2A prior to $CD34^+$ derived NK cell differentiation was used to evaluate the final optimised protocol.

In summary, we see that biallelic E4BP4 gene deletion in human $CD34^+$ HPCs resulted in a failure of these cells to generate NK cells *in vitro*. Additionally, loss of at least a single EOMES allele in $CD34^+$ HPCs effected the ability of these cells to grow past the early stages of our NK cell differentiation culture. These findings reveal the importance of E4BP4 and EOMES gene expression at the progenitor stage for human NK cell development. These findings also highlight the inefficiency of our current Cas9 targeting protocol, and therefore warrant further optimisation to improve the generation of KO NK cell clones. Future work investigating the mechanisms of E4BP4 and EOMES involvement during NK cell differentiation would provide potential avenues that can be explored for the enhancement of human NK cell production for immunotherapy.

# 5. Optimisation and targeting of NKG2A within CD34$^+$ HPC derived NK cells.

## 5.1. Background.

The NKG2A/CD94 receptor suppresses NK cell effector function when bound to self-peptide presenting HLA-E ligands on host cells. Clinical trials using antibody therapy to inhibit NKG2A signalling within NK cells show improved cytotoxicity against various cancers but are believed to be limited due to receptor recycling (Borrego et al., 2002, Kamiya et al., 2019). While NKG2A knockdown strategies demonstrate greater cytotoxic effects than antibody therapy (Kamiya et al., 2019), much of this work has been done on mature NK cells with limited capacity to expand to meet the therapeutic demand. To investigate the role of NK2GA during human NK cell development from the progenitor stage, we used the CRISPR/Cas9 system to target NKG2A in CD34$^+$ HPCs for the generation of biallelic NKG2A KO NK cells.

Up until this point, two common issues that I encountered were firstly, seeding at low cell densities (below 5 cells/well) led to low frequency in the number of CD34$^+$ derived cell clones, and, secondly, that these clones had insufficient proliferation to conduct downstream assays. In order to increase seeding density and overcome these limitations, we sought methods known to improve transduction efficiency so as to ensure a greater proportion of the well had homogenous gene targeting. To increase viral titre, larger quantities of viral supernatant was concentrated and the MOI of CD34$^+$ HPCs was calculated based on the titres that could be obtained. Further enhancement of transduction efficiency and cell survival was explored using Retronectin, known to encourage cell to virus interaction (Pay et al., 2018), and the small molecules Cyclosporin H (CsH) and UM171, shown to downregulate HPC immunogenicity responses upon virus entry (Petrillo et al., 2018) or enhance progenitor proliferation and NK development (Ngom et al., 2018), respectively.

Utilising the optimised changes, CD34$^+$ HPCs transduced with NKG2A-Cas9-eGFP resulted in the identification of a NKG2A KO CD3$^-$ CD45$^+$ CD56$^+$ NK cell clone. By increasing the seeding density, it was also possible to analyse killing capacity of NKG2A Het and WT cell clones against various cancer cell lines. Further optimisation is required, however, to clarify the relationships between NKG2A surface expression and target cell lysis.

Overall, optimisation of the transduction procedure improved the efficiency of successful biallelic gene targeting and cell survival during NK cell differentiation. With this new protocol, we can also assess the effector responses of gene targeted NK cells. Therefore, the generation of NKG2A KO NK cells from targeted CD34$^+$ HPCs is reproducible and will facilitate future investigation of NKG2A on NK function.

## 5.2. NKG2A expression on CD34$^+$ derived NK cells.

To determine the expression pattern of the NKG2A receptor during NK cell differentiation from CD34$^+$ HPCs, sorted untransduced HPC's were seeded at 100, 50, 20 and 3-cell densities for NK differentiation. Upon reaching 40% cell confluency within the well, these wells were sampled and analysed for presence of NKG2A$^+$ NK cells using flow cytometry (Figure 5.1).

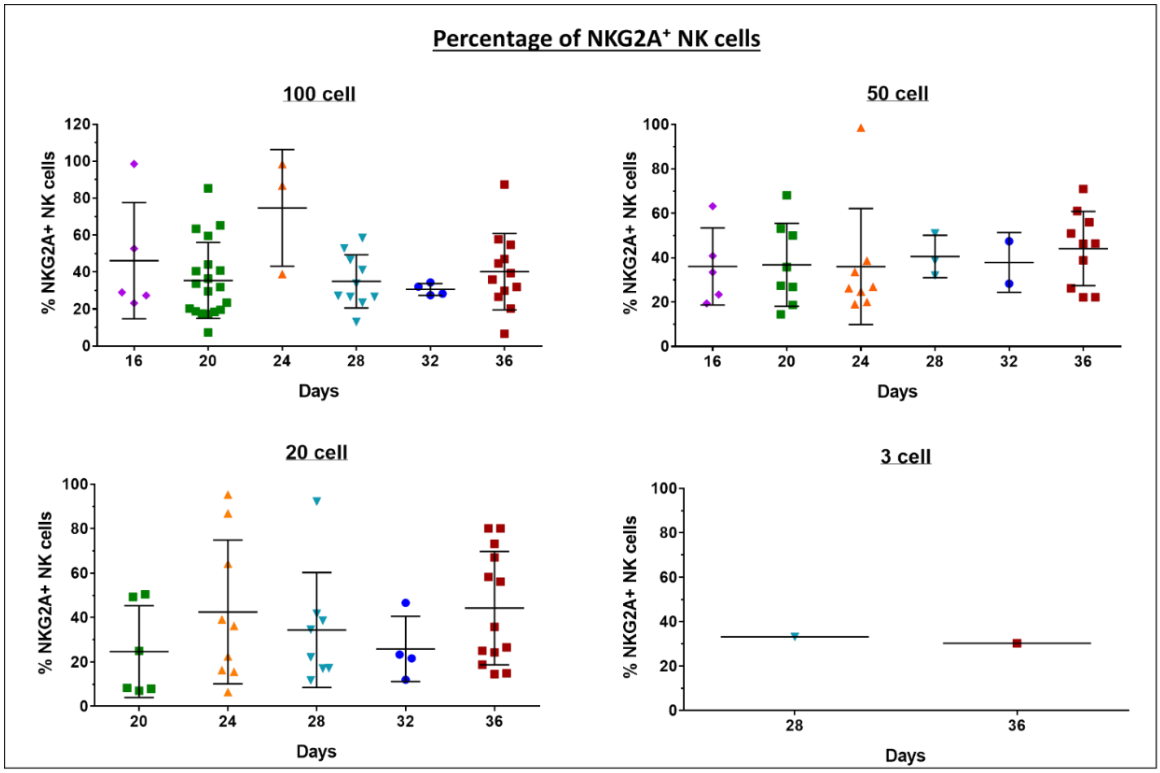



Figure 5.1: NKG2A expression on CD34⁺ derived NK cells.

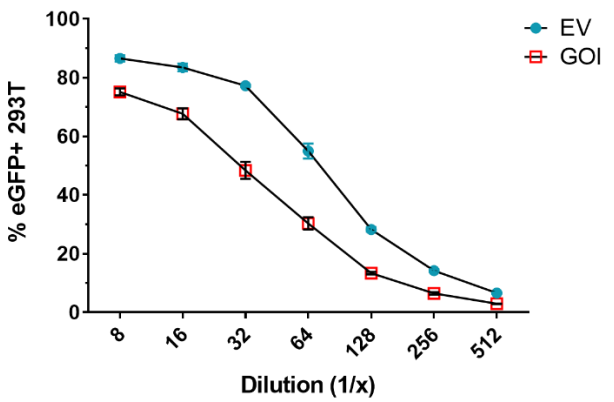
*CD34⁺ HPCs were sorted for CD34⁺ expression and seeded at 100, 50, 20 and 3 cell densities for NK differentiation. 30 x 96 wells were seeded at the 100-cell and 50-cell density while 60 x 96 wells were seeded at the 20-cell and 3-cell density. Wells above 40% cell confluency, based on their circular, reflective appearance, were sampled for flow cytometry over the course of culture. NKG2A⁺ NK cells were initially gated on CD3⁻ CD45⁺ CD56⁺ expression. Results were from a single experiment; bars represent average values plus standard deviation.*

Wells seeded with the 100-cell or 50-cell seeded densities were analysed at day 16, revealing 46% and 36% NKG2A⁺ NK cell populations, respectively. Over the course of differentiation, the percentage of NKG2A⁺ NK cells fluctuated slightly but were generally within the 20%-45% range, except for day 24 for the 100-cell seeded density which averaged to 74%. Wells seeded at the 20-cell and 3-cell densities were analysed at later time points (day 20 and 28, respectively) and only a single well was analysed for the 3-cell condition. Percentages of NKG2A⁺ NK cells were still within the same 20-45% range as the 100-cell and 50-cell densities.

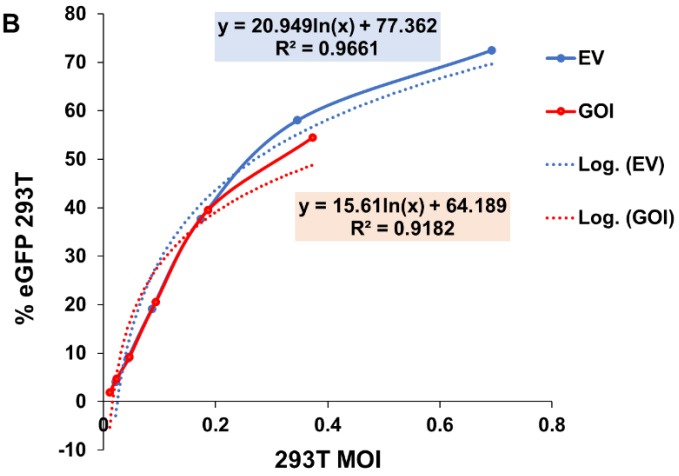
## 5.3. Optimisation of the transduction procedure.

Prior to NKG2A targeting, the transduction procedure was optimised to increase transduction efficiency and cell survival of gene targeted clones. To increase viral titre, viral supernatant was concentrated from three 10cm plates of 293T transfected with EV-Cas9-eGFP or a representative gene of interest (GOI)-Cas9-eGFP vector. In contrast to the protocols used in chapters 3 and 4, concentration was achieved using low speed ultracentrifugation and a 10% sucrose cushion (adapted from Jiang et al., 2015). The titre of both vectors was determined and the MOI of $CD34^+$ HPCs was calculated using the same viral stock (Figure 5.2).

A




B




C

| | Titre (TU/ml) | % eGFP+ CD34 | Calculated MOI of CD34 (if 293T MOI =1) |
|---|---|---|---|
| EV-Cas9-eGFP | 6647009 | 1.91 | 37 |
| GOI-Cas9-eGFP | 3577410 | 0.94 | 54 |

Figure 5.2: Viral titre and CD34⁺ HPC MOI using the Cas9-eGFP vectors.

*EV-Cas9-eGFP or GOI-Cas9-eGFP lentivirus was concentrated and the same viral stock was used to transduce 293T cells with polybrene or CD34⁺ HPCs with Retronectin. (A) The percentage of eGFP⁺ cells from transduced 293T's with the EV-Cas9-eGFP (blue filled circle) or GOI-Cas9-eGFP (red open square) is shown for a range of viral stock dilutions. EGFP expression was analysed 48h after transduction. (B) The percentage of eGFP⁺ transduced 293T is shown for EV-Cas9-eGFP (blue) and GOI-Cas9-eGFP (red) at different MOI. R-values and the equation for the logarithmic line of best fit (dotted line) is shown for both the EV (blue box) and GOI (orange box) plots. EGFP expression was analysed 48h after transduction. (C) Table listing the viral stock titre (transduction units, TU/ml) after concentration, the percentage of eGFP⁺ transduced CD34⁺ HPCs and the CD34⁺ HPC MOI for the EV-Cas9-eGFP and the GOI-Cas9-eGFP vector. Transduced CD34⁺ HPCs was analysed for eGFP expression after 72h. Results from (A), (B), (C) were from a single experiment; bars represent average values plus standard deviation. Replicates for 293T cells N=3, CD34⁺ HPCs N=1.*

Concentrated EV-Cas9-eGFP and GOI-Cas9-eGFP viral stock was serially diluted and used to transduce 293T cells. At each viral dilution tested, 293T cells transduced with EV-Cas9-eGFP had higher eGFP expression than the GOI-Cas9-eGFP transduced 293T (Figure 5.2A).

The viral titre was calculated for each dilution using the formula described below (Kutner et al., 2009). These titres were then averaged to determine the stock viral titre (Figure 5.2C).

$$\text{Titre (TU/ml)} = (E \times N/V) \times D$$

*Where:*

*E = Transduction efficiency (%)*

*N = number of transduced cells*

*V = volume in transduced well (ml)*

*D = dilution of virus.*

The stock titre for the EV-Cas9-eGFP was calculated at $6.66 \times 10^6$ TU/ml, 1.85-fold higher than the GOI-Cas9-eGFP, at $3.58 \times 10^6$ TU/ml (Figure 5.2C).

This viral stock was used to transduce $CD34^+$ HPCs resulting in 1.91% $eGFP^+$ HPCs with the EV-Cas9-eGFP and 0.94% $eGFP^+$ HPCs with the GOI-Cas9-eGFP (Figure 5.2C). To determine the corresponding $CD34^+$ HPC MOI, these percentages were then applied to the line of best fit equation produced when 293T cells were transduced at a range of MOI's using the same viral stock (Figure 5.2B). Therefore, with the EV-Cas9-eGFP, when 293T MOI was 1, $CD34^+$ HPC MOI was 37 whereas using the GOI-Cas9-eGFP was higher, with a calculated MOI of 54.

Determination of a higher $CD34^+$ HPC MOI for the GOI-Cas9-eGFP led us to seek strategies to improve transduction efficiency, such as encouraging virus to cell interactions with the use of Retronectin. $CD34^+$ HPCs were transduced with the GOI-Cas9-eGFP using Retronectin or polybrene and spinfection, while EV-Cas9-eGFP transduction was achieved only with polybrene and spinfection. The percentage of live cells as well as live $eGFP^+$ cells were compared after 48h (Figure 5.3).

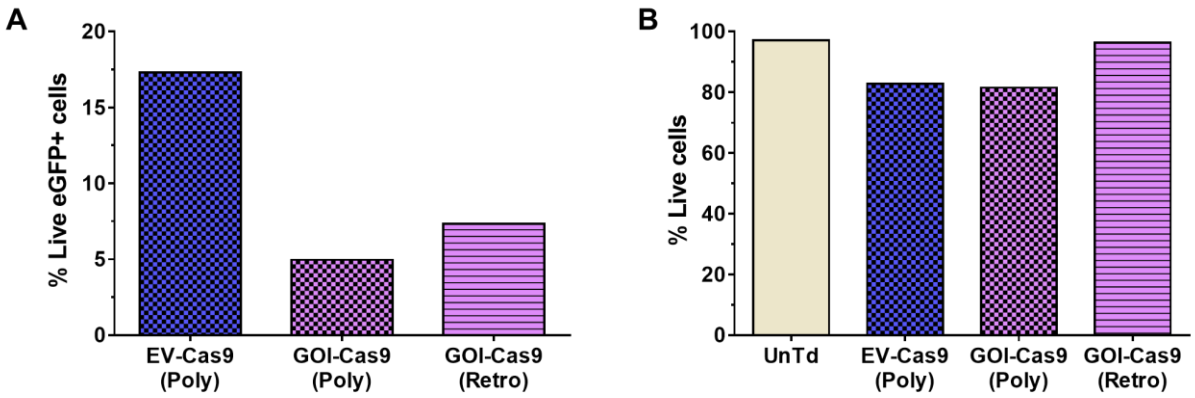



Figure 5.3: Transduction of CD34⁺ HPCs with EV or GOI-Cas9-eGFP using Retronectin or polybrene and spinfection.

*CD34⁺ HPCs were transduced with EV-Cas9-eGFP (blue) or GOI-Cas9-eGFP (pink) using either polybrene and a spinfection (Poly, squared bars) or, in the case of the GOI-Cas9-eGFP, Retronectin (Retro, lined bars). Untransduced cells (cream, solid bar) were also spinfected. (A) The percentage of live, eGFP⁺ HPCs determined by flow cytometry after 48h from transduction. (B) The percentage of live, single cells as determined by exclusion dye using flow cytometry. UnTd: untransduced. Results were from a single experiment, N=1.*

The percentage of live eGFP⁺ cells transduced with GOI-Cas9-eGFP was higher when Retronectin was used (7.3%) than polybrene (5%), (Figure 5.3A). Although these values were still below the EV-Cas9-eGFP control using polybrene, at 17%, the use of polybrene led to lower percentages of live cells (Figure 5.3B), irrespective of the EV or GOI vectors. The percentages of live cells transduced with EV-Cas9-eGFP or GOI-Cas9-eGFP using polybrene was 83% and 82%, respectively, while GOI-Cas9-eGFP transduced with Retronectin had 96% live cells, closer to the untransduced control at 97%.

An additional approach previously found to increase transduction efficiency was to include Cyclosporin H (CsH) during the transduction step (Petrillo et al., 2018). CD34⁺ HPCs were transduced with and without CsH, using Retronectin and the GOI-Cas9-

eGFP vector. Transduced HPCs were sorted for eGFP expression and seeded at low numbers (below 5 cells/well) for clonal NK cell differentiation. By day 31 of differentiation (end-point), the number of clones that had proliferated above 40% cell confluency and their genotypes relative to the GOI being targeted was assessed (Figure 5.4).

**A**

| Condition | % eGFP+ CD34⁺ HPCs post transduction | Total no. cells seeded | Total no. clones that expanded by end-point |
|---|---|---|---|
| With CsH | 1.2% | 120 | 39 |
| Without CsH | 0.8% | 120 | 15 |

**B**

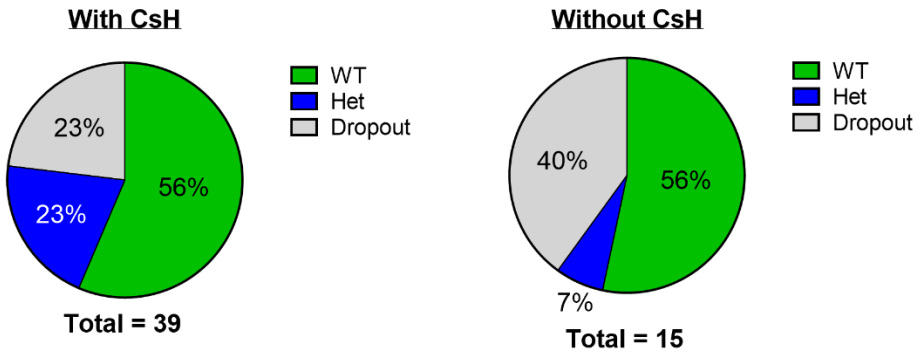



Figure 5.4: Summary of GOI-Cas9-eGFP transduced CD34⁺ derived cell expansion and genotyping with or without CsH.

*Shown are the number of CD34⁺ derived clones that grew during NK differentiation after transduction with a GOI-Cas9-eGFP vector, in the presence and absence of CsH. Sorted cells were seeded at a low cell seeding density (below 5 cells/well) to mimic previous experiments. (A) The percentage of eGFP⁺ CD34⁺ transduced cells after 48h, the total number of clones seeded and the total number of clones that expanded by day 31 of NK cell differentiation (end point) is shown. (B) The genotype ratio, relative to the GOI being targeted, of the expanded clones from (A). Results were from a single experiment, N=120 wells.*

32% (39/120) of the clones treated with CsH had wells above 40% cell confluency, more than double the 12.5% (15/120) of non-CsH treated clones (Figure 5.4A). Genotypes of the CsH treated clones at the end-point of culture show 3.2-fold higher proportion of Het (23%) than non-CsH clones (7%), while the WT proportions are equal (56%), (Figure 5.4B). Furthermore, the proportion of dropout clones was 1.7-fold lower with CsH treatment (40% non-CsH versus 23% CsH treated).

Finally, to improve survival of transduced cells and their differentiation into NK cells, we examined the effects of treating $CD34^+$ HPCs with small molecule UM171 prior to NK cell differentiation. The percentage and absolute number of NK cells was measured after 16 and 28 days from UM171 treatment and seeding of untransduced $CD34^+$ HPCs at a low (1200 cells/24 well) or high (12,000 cells/24 well) cell density (Figure 5.5).

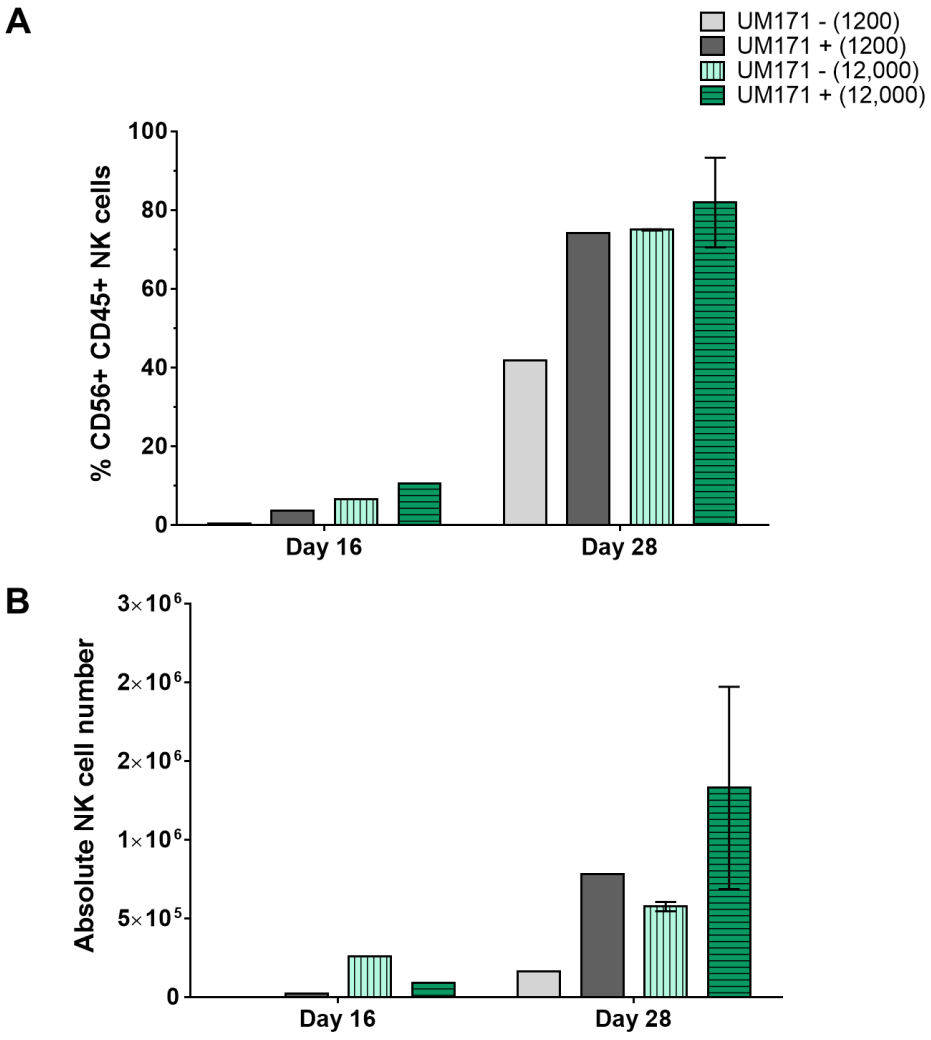



Figure 5.5: UM171 treatment enhances NK cell production and absolute number of differentiating $CD34^+$ HPCs.

*Untransduced $CD34^+$ HPCs were cultured without UM171 (UM171-) and with UM171 (UM171+) for 4 days prior to seeding at 1200 cells/well (solid light grey and dark grey bars, respectively) or 12,000 cells/well (lined light green or dark green bars, respectively). After 16 and 28 days of differentiation, (A) the percentage of NK cells and (B) the absolute number of NK cells were analysed. NK cells were determined as $CD3^-$ $CD45^+$ $CD56^+$. Results were from a single experiment; bars represent average values plus standard deviation. All conditions were N=1 except for the day 28 wells seeded at 12,000 cells which were N=2.*

UM171 treated (UM171+) $CD34^+$ HPCs seeded at the lower density (1200 cells/well) had comparable NK cell percentages to non-UM171 (UM171-) treated cells seeded at a higher density (12,000 cells/well), for both day 16 and 28 (Figure 5.5A). The UM171+ low density well had 3.6% NK cells on day 16 and 72% on day 28, while the UM171- high density wells had 6.6% on day 16 and 75% on day 28. Although the UM171+ low density well was found to have 10-fold lower NK cells ($2.4x10^4$ cells) than the UM171- high density well ($2.6x10^5$ cells) at day 16, by day 28, the UM171+ low density well resulted in higher NK cell production ($7.8x10^5$ cells) than the UM171- high density wells ($5.7x10^5$ NK cells), (Figure 5.5B).

Furthermore, cells seeded at lower density produced more NK cells when UM171 was included than without. On day 16, UM171- low density wells contained 914 NK cells, 26-fold lower than the UM171+ low density well (Figure 5.5B). By day 28, the number of NK cells increased in the UM171- low density well to $1.6x10^5$ cells but was still 4.7-fold lower than the UM171+ low density well. The higher density wells had a similar response on day 28, but with a 2.3-fold increase with UM171 addition ($5.7x10^5$ UM171- NK cells versus $1.3x10^6$ cells UM171+ NK cells).

Upon identification of the viral titres produced post concentration, the increase in transduced cell populations and survival when using Retronectin and CsH, as well as the higher production of NK cells when using UM171, led us to incorporate these changes to improve NKG2A gene targeting efficiency in $CD34^+$ HPC's.

## 5.4. Designing the NKG2A-Cas9-eGFP vector.

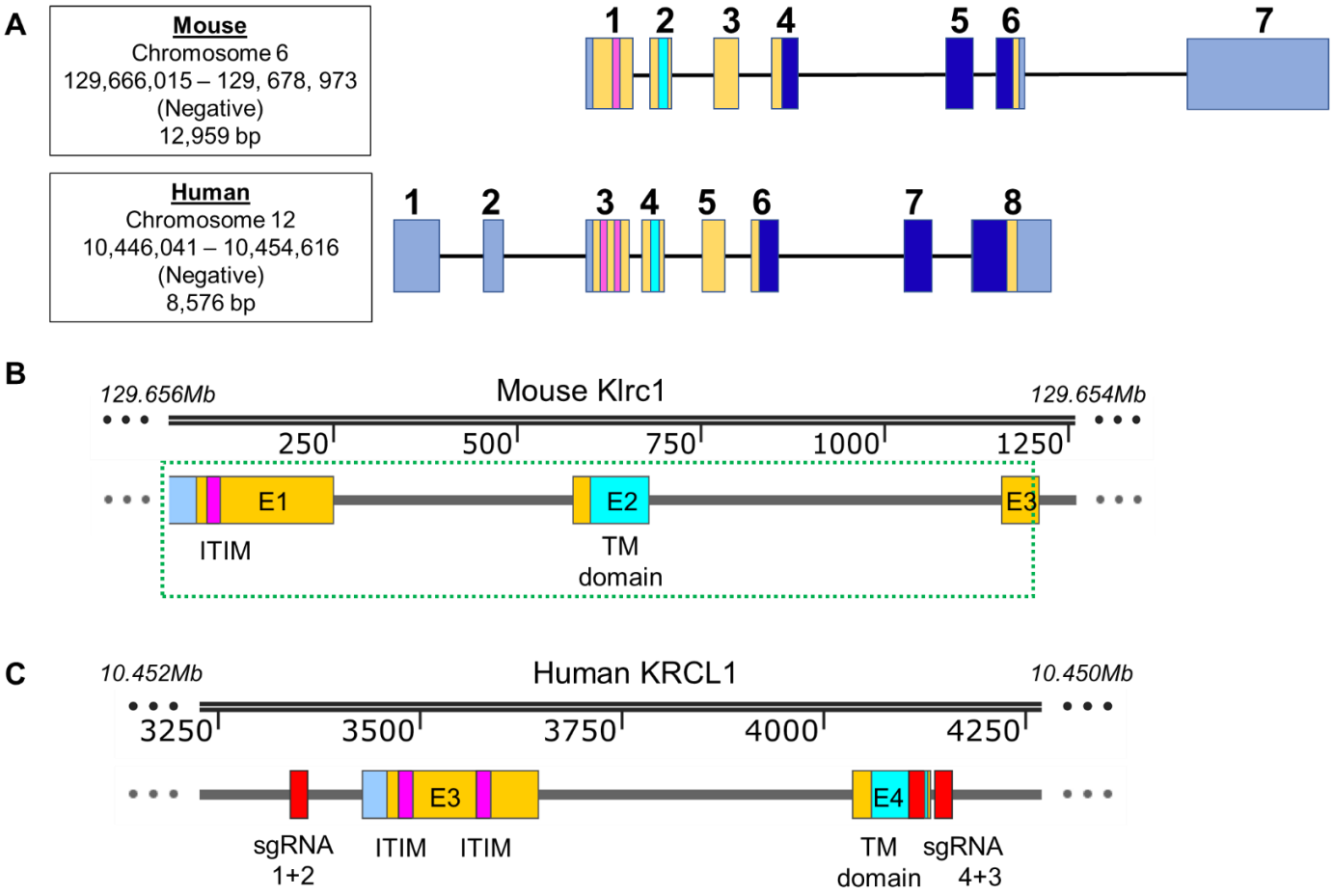



Figure 5.6: Schematic of the KLRC1 (NKG2A) gene in mouse and human

*(A) Chromosomal location, size and regions for functional domains are shown for both the mouse and human NKG2A gene. Exons are numbered and shown as boxes: yellow representing the coding region, blue the non-coding region. The immunoreceptor tyrosine based inhibitory motif (ITIM, pink), the transmembrane domain (TM, cyan) and the extracellular C-type lectin domain (dark blue) is labelled. (B) Enlarged view of the mouse Klrc1 gene, highlighting the ITIM and TM domain. Exon 1, 2 and part of exon 3 were targeted to generate a NKG2A$^{-/-}$ mice model (dotted green box), (Ely et al., 2014). (C) Enlarged view of the human KLRC1 gene, highlighting the ITIM and TM domain. sgRNA 1 and 2 is located on the intron upstream of Exon 3 while sgRNA 4 and 3 is located on Exon 4 or on the intron downstream of Exon 4, respectively (red boxes). E: Exon.*

The mouse and human KLRC1 gene, encoding for NKG2A, were compared when designing sgRNA to target human NKG2A expression. Both species encode one (mouse) or two (human) intracellular ITIM domains, a transmembrane (TM) domain an extracellular C-type lectin domain (Figure 5.6A). Generation of an NKG2A$^{-/-}$ mouse model was achieved by replacing Exon 1 to 3 with an antibiotic resistance cassette, encompassing the ITIM and TM domain (Figure 5.6B), (Ely et al., 2014). Similarly, sgRNA were designed to target these functional domains in human NKG2A, located upstream Exon 3 and at the end or downstream Exon 4 (Figure 5.6C).

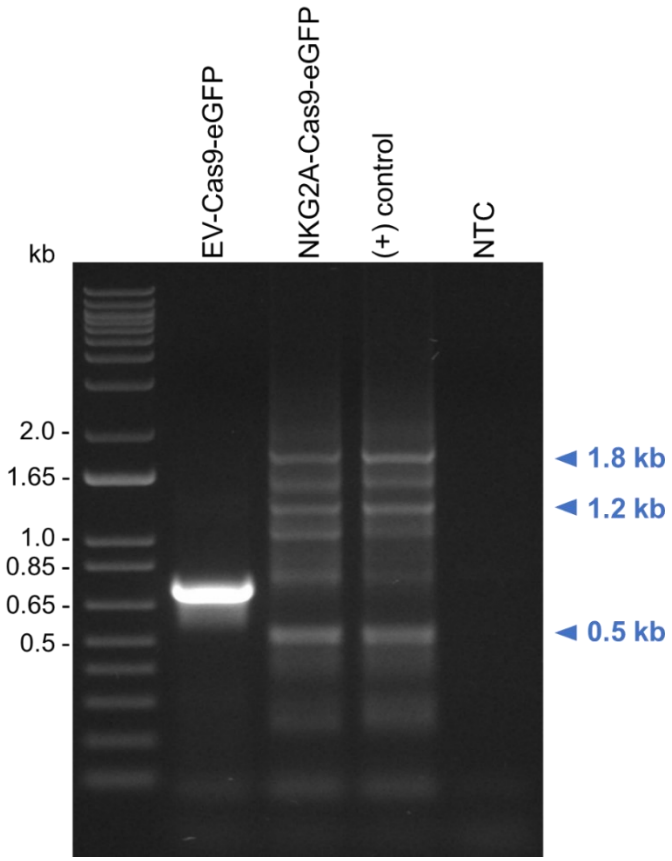



Figure 5.7: PCR gel of the NKG2A-Cas9-eGFP vector.

*PCR was performed on the final NKG2A-Cas9-eGFP lentiviral vector with primers to amplify the clone site. Presence of the original template produced a 0.7kb band while presence of all four promoter-sgRNA-scaffold regions produced a distinct band pattern of 1.8kb, 1.2kb and 0.5kb (Kabadi et al., 2014). EV: Empty vector, (+) control: positive final Cas9-eGFP vector control, NTC: Non template control*.

PCR amplifying the sgRNA insertion site of the NKG2A-Cas9-eGFP vector revealed the expected 1.8kb, 1.2kb and 0.5kb band pattern, matching the positive control (Figure 5.7). Additional loss of the 0.7kb band (seen in the EV-Cas9-eGFP) and sequencing of the clone region confirmed insertion and correct orientation of the sgRNA.

## 5.5. Validation of the NKG2A-Cas9-eGFP vector.

The NKG2A-Cas9-eGFP vector was tested on its ability to transduce the MRC5 cell line, determined by eGFP expression (Figure 5.8), and result in NKG2A gene deletion at the specified region (Figure 5.9).

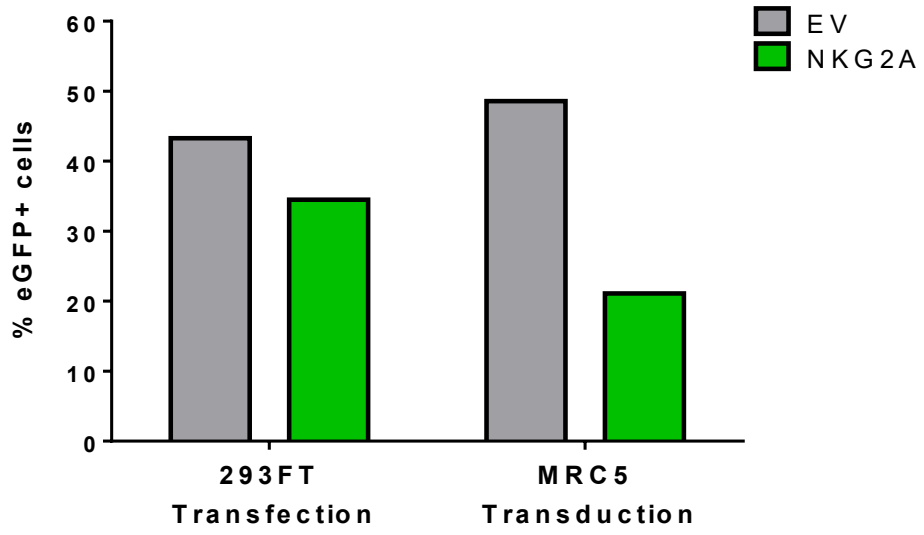



Figure 5.8: Transfection and transduction efficiency of the NKG2A-Cas9-eGFP vector on 293FT and MRC5 cells.

*Percentage of eGFP$^+$ cells is shown for transfected 293FT cells and transduced MRC5 with the EV-Cas9-eGFP vector (grey) and the NKG2A-Cas9-eGFP vector (green). Transfected and transduced cells were analysed for eGFP expression after 48h using flow cytometry. Results were from a single experiment, N=1.*

293FT transfection using the NKG2A-Cas9-eGFP vector resulted in 35% eGFP$^+$ cells, slightly lower than EV-Cas9-eGFP which produced 43.3% eGFP$^+$ cells (Figure 5.8). After transduction, MRC5 cells transduced with NKG2A-Cas9-eGFP were 21% eGFP$^+$, just over 2-fold lower than EV-Cas9-eGFP transduced cells, where 48.6% of MRC5 cells were eGFP$^+$.

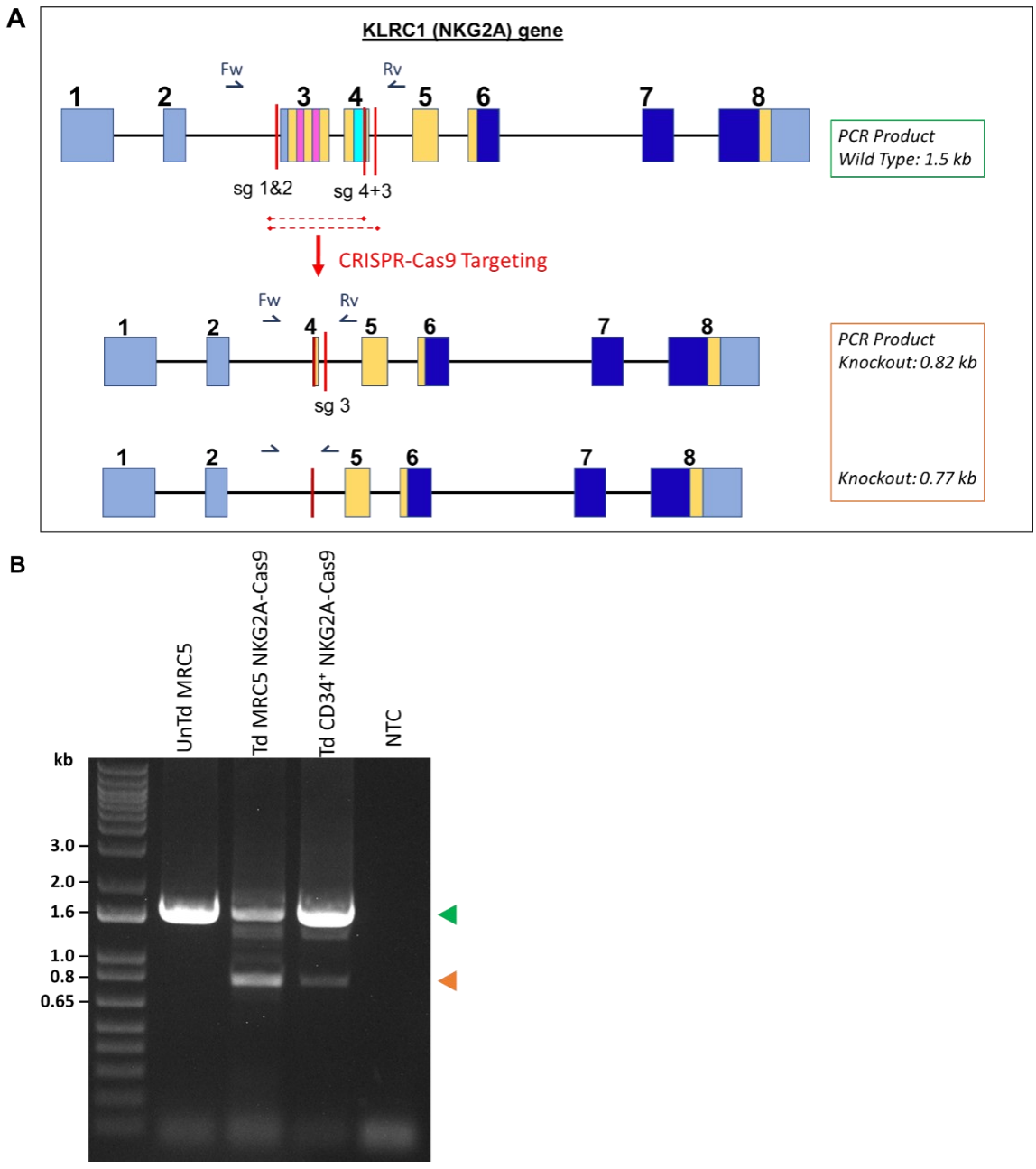



Figure 5.9: Genotyping strategy for NKG2A.

*(Legend on next page).*

Figure 5.9: Genotyping strategy for NKG2A.

*(A) Schematic of the human NKG2A gene in Figure 5.6 indicating the forward (Fw) and reverse (Rv) primers outside the target sgRNA target site. Prior to Cas9 targeting, the PCR produces a 1.5kb WT band. Upon Cas9 mediated deletion at sgRNA 1+2 and sgRNA 4, or sgRNA 1+2 and sgRNA 3, the bands produced are 0.82kb and 0.77kb respectively. ITIMs (pink), TM domain (cyan), C-type lectin domain (dark blue) and the sgRNA (red lines) are indicated. The Indel site after sgRNA deletion and recombination is presented by a marron line. (B) Genotyping gel showing untransduced (UnTd) MRC5 cells or NKG2A-Cas9-eGFP transduced MRC5 cells and CD34⁺ HPCs. The 1.5kb WT band and the 0.77kb KO band is indicated by the green and orange arrowhead respectively. NTC: Non-template control.*

A genotyping PCR was designed to produce a 1.5kb NKG2A WT band if the gene remains intact (Figure 5.9A), as shown in the untransduced MRC5 cell control (Figure 5.9B). After Cas9 mediated gene targeting, depending on whether sgRNA 4 or 3 is cut, two KO bands can be amplified at 0.82kb and 0.77kb, respectively. When MRC5 cells or CD34⁺ HPCs cells were transduced with NKG2A-Cas9-eGFP, the 0.77kb KO band and the 1.5kb WT band is shown.

## 5.6. NKG2A gene deletion in CD34⁺ derived NK cells.

The optimised protocol changes (detailed in Chapter 5.3) was used to target NKG2A within CD34⁺ HPCs. These cells were pre-treated with UM171 and transduced with the NKG2A-Cas9-eGFP lentivirus using Retronectin, in the presence of CsH. After 96h, the HPCs were analysed for eGFP expression (Figure 5.10).

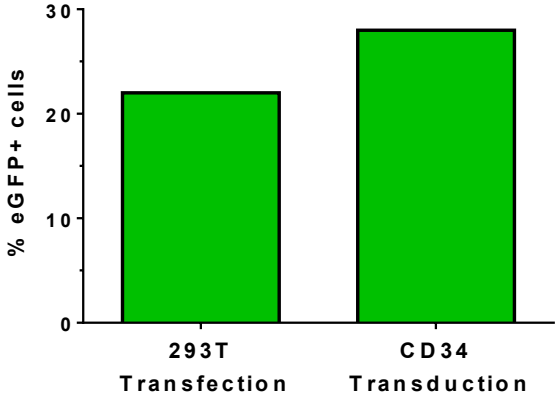



Figure 5.10: Transfection and transduction efficiency of the NKG2A-Cas9-eGFP vector on 293T and CD34+ HPCs.

*Percentage of eGFP$^+$ cells is shown for transfected 293T cells and transduced CD34$^+$ HPCs using the NKG2A-Cas9-eGFP vector. Lentiviral supernatant was concentrated using a sucrose cushion and ultracentrifugation. The HPC's, pre-treated with UM171 for 16-18h, were transduced using Retronectin and CsH. Transfected and transduced cells were analysed after 48h or 96h, respectively. Results were from a single experiment, N=1.*

The percentage of eGFP$^+$ 293T transfected with NKG2A-Cas9-eGFP was 22% (Figure 5.10). After viral concentration and transduction, 28% of transduced CD34$^+$ HPCs expressed eGFP.

Transduced, sorted cells were seeded in NK differentiation conditions at densities from 10 cells/well and lower. Growth of the cells, determined by their circular, reflective appearance, was measured within the well over the early (days 6-15), mid (days 16-27) and late (>27 days) culture stages (Figure 5.11).

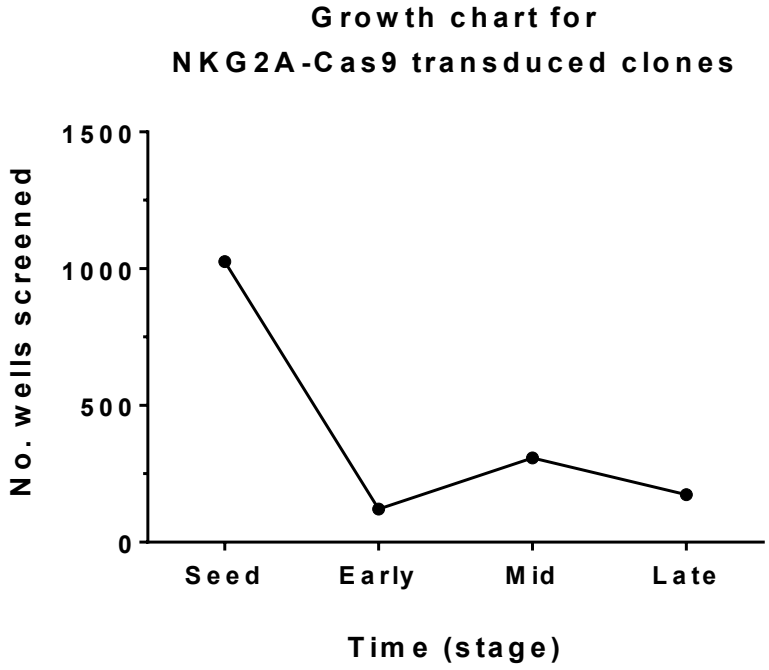



Figure 5.11: Summary of the number of wells containing CD34$^+$ derived cell populations after NKG2A gene targeting.

*1026 wells were seeded with sorted NKG2A-Cas9-eGFP transduced cells, at a seeding density below 10 cells/well. The number of wells with CD34$^+$ derived cells in them were measured during the early (days 6-15), mid (days 16-27) and late stage (days >27). Results were from four separate experiments, N=1026 wells.*

Of the 1026 wells that were seeded, 12% (121/1026) had a population of CD34$^+$ derived cells at the early stage (Figure 5.11). The number of wells increased to 30% (308/1026) at the mid-stage, after which there was another decrease to 17% (17/1026) by the late stage.

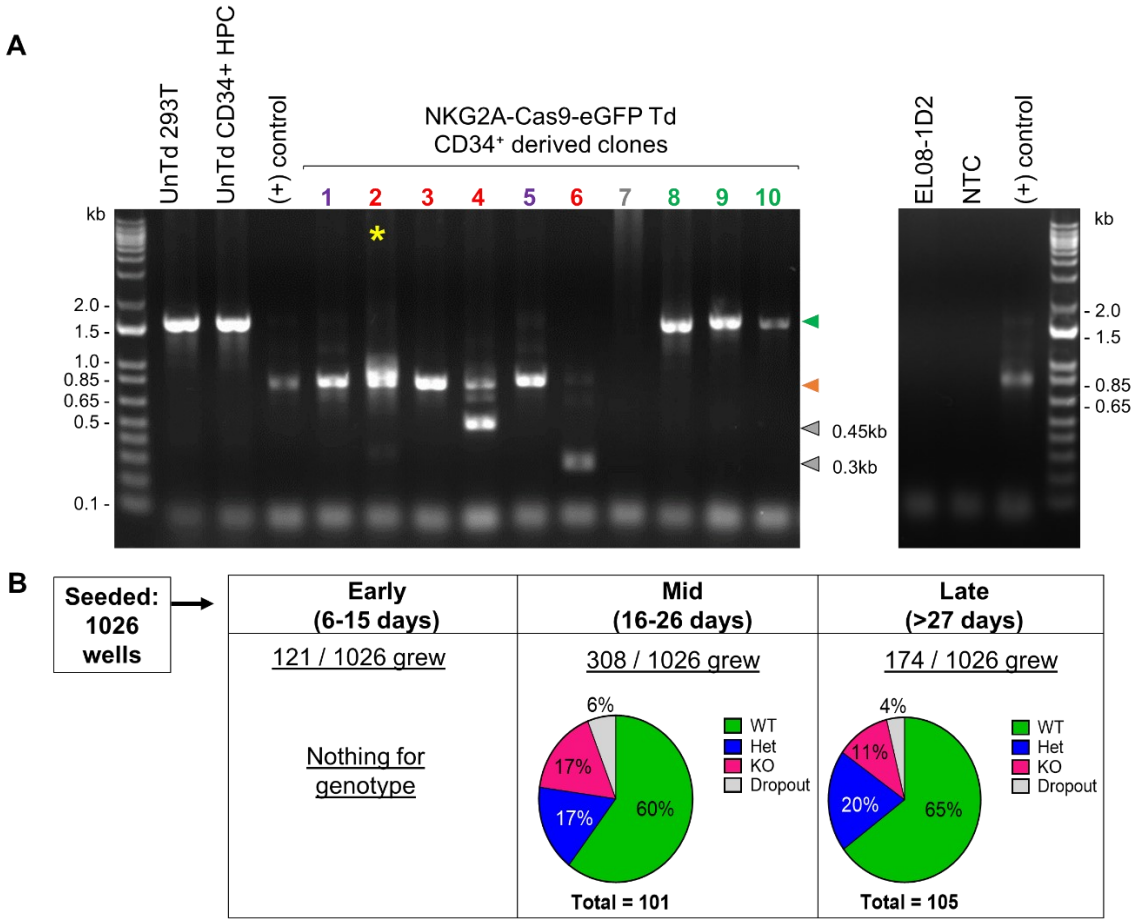



Figure 5.12: Summary of genotyping results from NKG2A-Cas9-eGFP transduced CD34⁺ derived cell clones.

*(A) Representative gel image showing genotyping results of NKG2A-Cas9-eGFP transduced HPC clones after 40/41 days of differentiation. The 1.5kb WT band and the 0.77-0.82 KO band is highlighted by the green and orange arrowhead respectively. NKG2A targeted clones (1-10) are colour labelled based on their determined genotype: WT (green), Het (purple), KO (red) and dropout (grey), with a yellow star highlighting NKG2A KO clone 2. Unexpected band sizes indicated by grey arrowheads (0.45kb and 0.3kb). Positive (+) control consisted of transfected 293T with NKG2A-Cas9-eGFP. (B) Summary of genotypes from NKG2A-Cas9-eGFP transduced cell clones during the early, mid and late stages of NK cell differentiation. Within each stage the number of clones with presence of CD34⁺ derived cells are indicated above the pie chart and the total number of clones that could be genotyped (above 40% cell confluency) are indicated below the pie chart. UnTd: Untransduced, Td: transduced, NTC: Non-template control.*

Clones above 40% cell confluency were genotyped using PCR during NK cell differentiation. A representative gel image (Figure 5.12A) shows that clones with presence of only the 1.5kb WT band (clones 8-10, labelled green) were classified as WT and clones with only the 0.77-0.82kb bands (clones 2-4 and 6, labelled red) were classified as KO. Clones with presence of both WT and KO bands, irrespective of intensity (clones 1 and 5, labelled purple), were classified as Het. On occasion, unexpected bands around 0.45kb (clone 4) or 0.3kb (clone 6 and clone 2) were amplified. Sequencing of these bands, in addition to the expected KO bands, is ongoing so as to confirm if they correspond to expected or bigger deletions at the target site.

There were no clones that met the 40% cell confluency criteria at the early stage, therefore they were not genotyped (Figure 5.12B). By the mid-stage, 33% (101/308) of the clones that had $CD34^+$ cell presence was genotyped, which almost doubled to 60% (105/174) clones by the late stage. The ratio of the genotypes between the mid and late stage also did not differ drastically, with both stages comprising above 60% WT NKG2A clones and between 10-20% Het and KO clones.

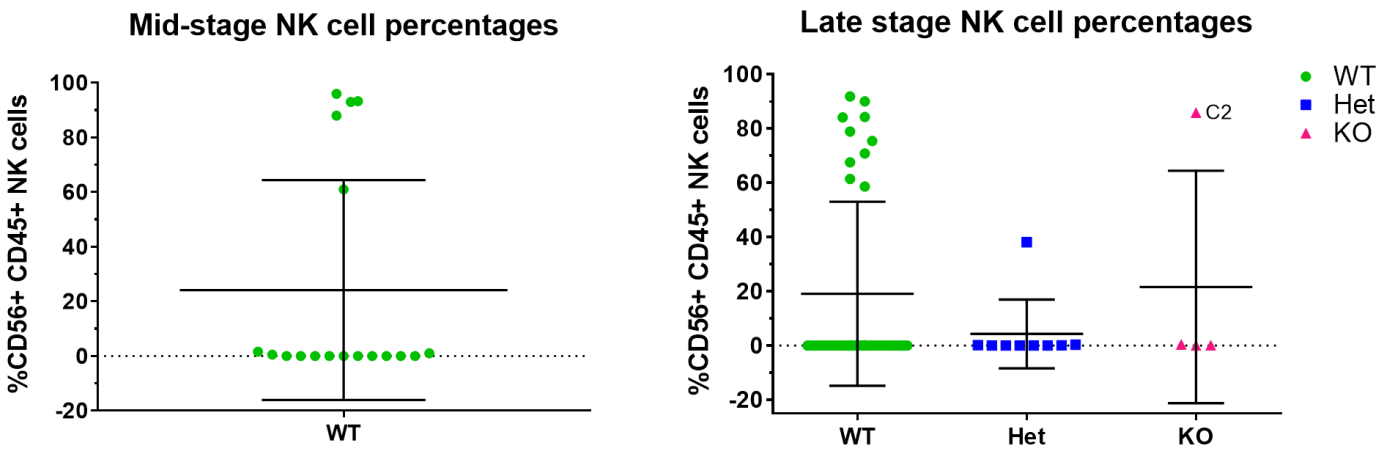



Figure 5.13: NK cell percentages in NKG2A-Cas9-eGFP targeted CD34$^+$ derived clones during NK cell differentiation.

*The percentage of NK cells from clones above 40% confluency in a 48 well or larger is presented, determined by presence of CD3$^-$ CD45$^+$ CD56$^+$ surface markers. Only WT clones were analysed at the mid-stage. Clone 2 (C2), from Figure 5.12, is indicated. Results were from 2 separate experiments; bars represent average values plus standard deviation. Replicates for mid-stage WT N=18 and late stage WT: N=40 Het: N=9, KO: 4. No significant comparisons were observed using a one-way ANOVA.*

Results from 2 separate experiments in which of the total number of clones analysed above 40% cell confluency were examined for NK cell presence by CD3$^-$ CD45$^+$ CD56$^+$ surface marker expression using flow cytometry (Figure 5.13). Of the clones analysed in experiment 1 (43 in total), 90% were detected as WT and the remainder as Het. Within experiment 2, 10% of clones analysed were determined as WT, 50% as Het and 40% as KO for NKG2A.

At the mid-stage of culture, only WT clones were detected while by the late stage, WT, Het and KO clones were detected. Only a single KO clone, clone 2 or C2 (genotype highlighted in Figure 5.12A), was able to produce a population containing 86% NK cells. Similarly, a single Het clone was able to produce a population containing 38% NK cells. Of the WT clones at the late stage, 25% (10/40) produced NK cells, similar to the frequency seen at the mid-stage (27%, 5/18).

To assess whether NKG2A KO clones as determined by genotyping PCR corresponded to phenotypic NKG2A deficient NK cells, NKG2A expression was assessed on the NK cells from the NKG2A KO clone 2 and a representative WT clone (Figure 5.14).

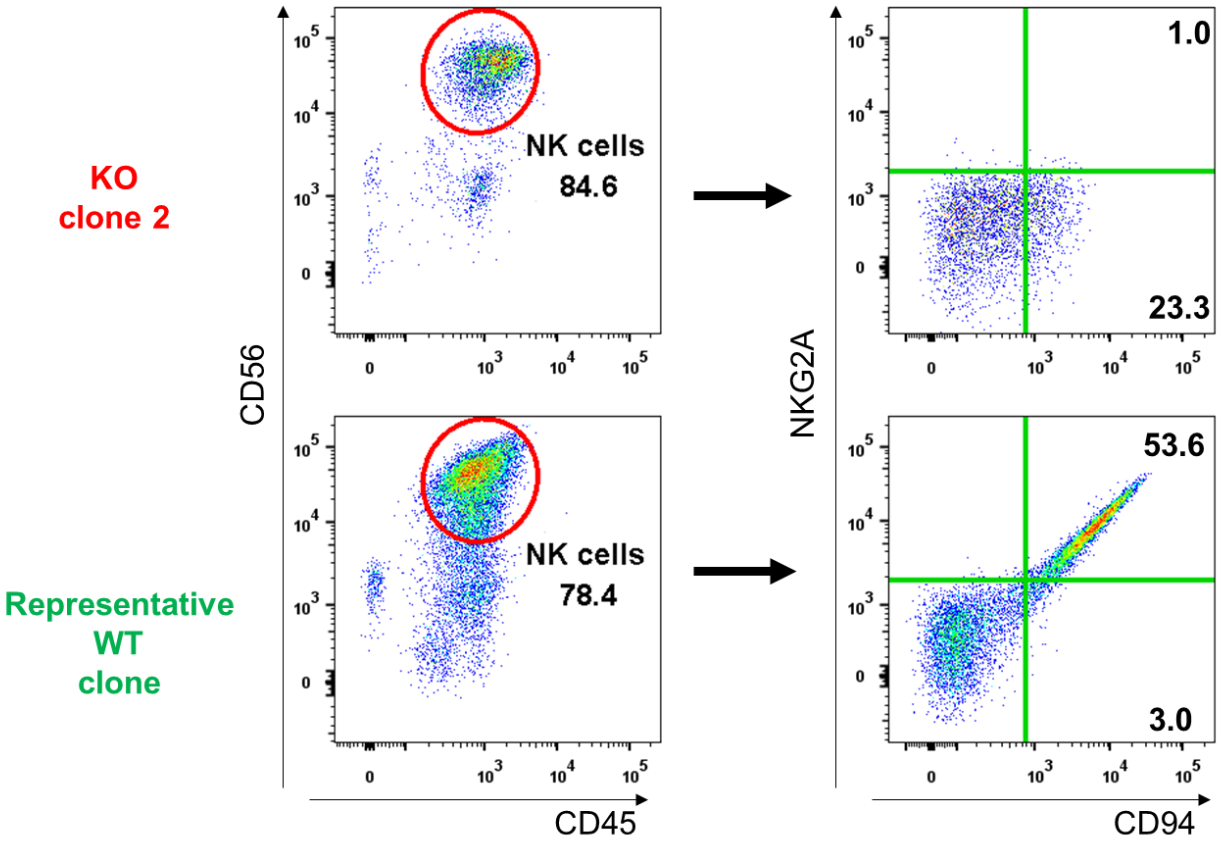



Figure 5.14: NKG2A expression on NK cells from the C2 KO clone.

*Flow cytometry plots show CD34⁺ HPC derived (CD3⁻) CD45⁺ CD56⁺ NK cells, transduced with the NKG2A-Cas9-eGFP vector, for the KO clone 2 (top) and a representative WT clone (bottom). Cells were analysed after 40 days of NK cell differentiation.*

While both the KO and representative WT clones had a high percentage of CD45⁺ CD56⁺ NK cells (84.6% and 78.4% respectively), there was a loss of double positive NKG2A⁺ CD94⁺ expression on the KO clone (1%), (Figure 5.14). This KO clone did retain some single positive CD94 expression, at 23.3%. The WT clone, on the other hand, had 53.6% of its NK cells expressing both NKG2A⁺ CD94⁺ and only 3% expressing CD94⁺ alone.

## 5.7. Killing assessment of NKG2A targeted CD34$^+$ derived NK cells.

NKG2A targeted CD34$^+$ derived NK cells were assessed on their ability to kill the acute myelogenous leukemia HLA-E negative K562 cell line or the ovarian HLA-E positive PEO1 and PEO4 cell lines. As seeding densities below 50 cell/well was previously shown to produce insufficient cell numbers for co-culture assays, sorted NKG2A-Cas9-eGFP or EV-Cas9-eGFP transduced CD34$^+$ HPCs were seeded at 50-cell and 100-cell for NK differentiation. Following the procedure outlined in Figure 3.7A, with the exception of extending the NK cell and cancer cell co-culture to 18-24h, the CD34$^+$ derived NK cell clones (labelled as 50_x or 100_x) were harvested on day 37 for assessment of CFSE$^+$ K562 killing, as well as day 45 for the assessment of CFSE$^+$ PEO1 and PEO4 killing.

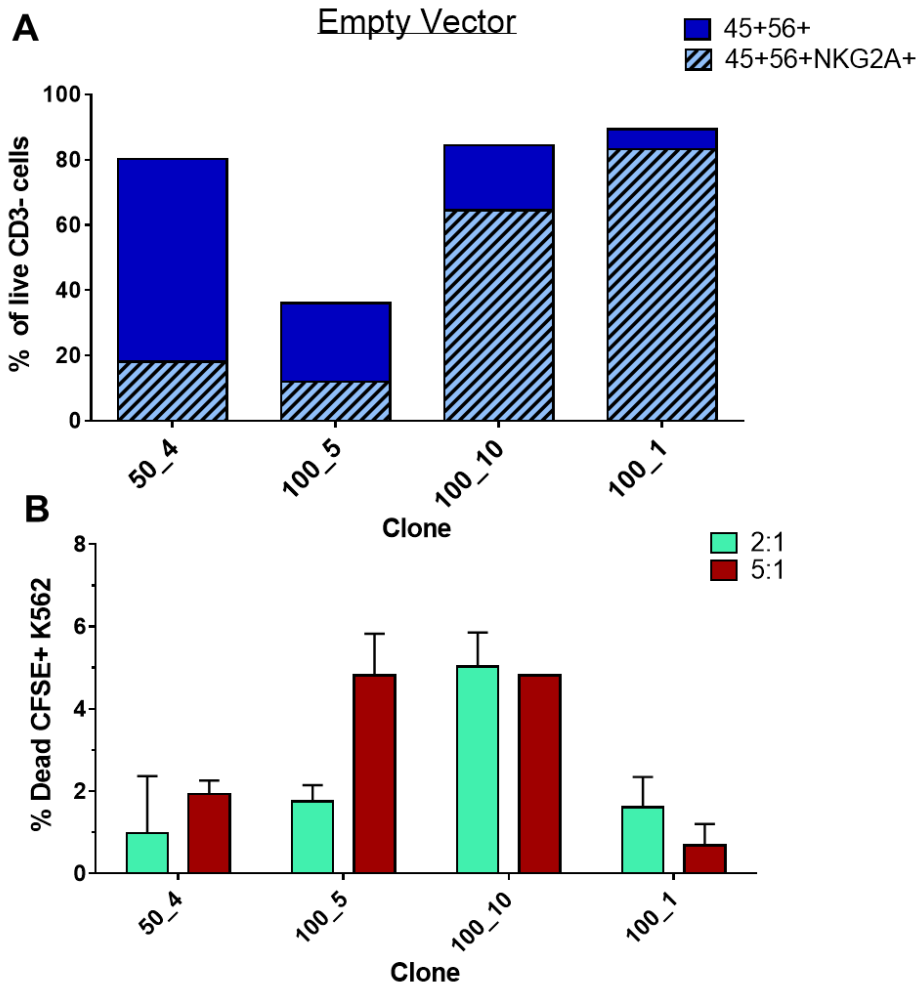



Figure 5.15: K562 killing assay with EV-Cas9-eGFP transduced CD34$^+$ derived NK cells.

*CD34$^+$ HPCs transduced with EV-Cas9-eGFP was seeded at 50-cell and 100-cell/well at the start of differentiation, with clones identified as 50_x or 100_x respectively. After 37 days the clones were harvested for assessment of K562 killing. (A) The percentage of live CD3$^-$ cells expressing CD45$^+$ CD56$^+$ (45$^+$56$^+$, solid dark blue bar) and CD45$^+$ CD56$^+$ NKG2A$^+$ (45$^+$56$^+$NKG2A$^+$, lined light blue bar) are shown. (B) The percentage of dead CFSE$^+$ K562 cells after 18h co-culture with the NK cell clones at E:T ratios of 2:1 (cyan) and 5:1 (maroon). The percentage of dead CFSE$^+$ target cells was normalised to the target cell alone control (1.17%). Results were from a single experiment; bars represent average values plus standard deviation. E:T conditions were all N=2 except for the 100_10 5:1 ratio, which was N=1.*

NK2GA surface expression varied among the EV-Cas9-eGFP transduced NK cells used to set up K562 co-culture (Figure 5.15A). While all but clone 100_5 had a population of $CD56^+$ NK cells above 80%, the percentage of these NK cells expressing NKG2A was lower for the 50_4 and 100_5 clones (18% and 11% respectively) than the 100_10 and 100_1 clones (64% and 83% respectively).

Co-culture with K562 at E:T ratios of 2:1 and 5:1 revealed clone 100_10 resulted in the highest percentage death for both ratios (5%), (Figure 5.15B). Conversely, clone 100_5 also resulted in the same percentage death at the 5:1 ratio, even though NKG2A expression on this clone was lower than the 100_10 clone. Both clone 100_1 and 50_4 killed less than 2% of K562 at either E:T ratio, irrespective of the NKG2A expression on their NK cells.

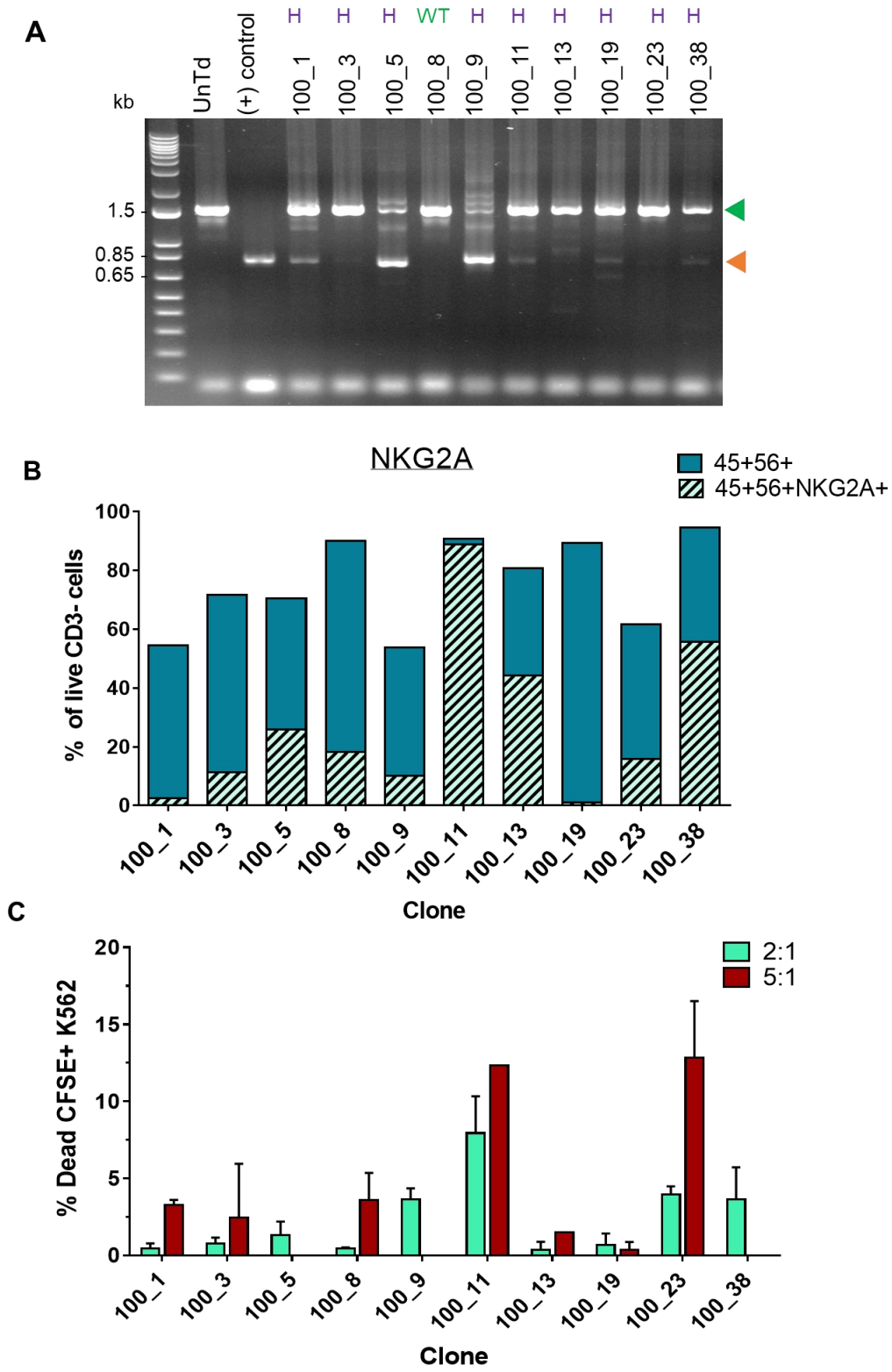



Figure 5.16: K562 killing assay with NKG2A-Cas9-eGFP transduced CD34$^{+}$ derived NK cells.

*(Legend on next page).*

Figure 5.16: K562 killing assay with NKG2A-Cas9-eGFP transduced CD34$^+$ derived NK cells.

*CD34$^+$ HPCs transduced with NK2GA-Cas9-eGFP was seeded at 50-cell and 100-cell/well at the start of differentiation. After 37 days the wells were harvested for assessment of K562 killing. Only the 100 cell seeded clones, identified as 100_x, had enough cells to set up a cytotoxicity assay. (A) Genotyping gel of the NKG2A-Cas9-eGFP transduced NK cell clones, highlighting the determined genotype as WT (green label) or Het (H, purple label) above the clone ID. The 1.5kb WT band and the 0.77-0.82kb KO bands are indicated by the green and orange arrowhead, respectively. UnTd: Untransduced CD34$^+$ HPC control, (+) control: positive control of transfected 293FT with NKG2A-Cas9-eGFP vector. Gel image was adjusting using in microsoft powerpoint for +40% brightness and -20% contrast. (B) The percentage of live CD3$^-$ cells expressing CD45$^+$ CD56$^+$ (45$^+$56$^+$, solid dark blue bar) and CD45$^+$ CD56$^+$ NKG2A$^+$ (45$^+$56$^+$NKG2A$^+$, lined light blue bar) are shown for NKG2A-Cas9-eGFP transduced CD34$^+$ derived NK cell clones. (C) The percentage of dead CFSE$^+$ K562 cells after an 18h co-culture with the NK cells at E:T ratios of 2:1 (cyan) and 5:1 (maroon), normalised to the target cell alone control (1.17%). Results were from a single experiment; bars represent average values plus standard deviation. E:T conditions were all N=2 except for the 100_11 and 100_13 5:1 ratio, which was N=1 and for the 100_5, 100_9 and 100_38 5:1 ratio, which was absent.*

NKG2A targeted NK cells were assessed on their surface NKG2A expression and the ability to kill K562 cells after an 18h co-culture (Figure 5.16). These clones were classified as either Het (purple label) or WT (green label) for NKG2A (Figure 5.16A). While the percentage of CD56$^+$ NK cells within these clones ranged from 53% (100_9) to 94% (100_38), NKG2A expression was highly variable on these NK cells and showed no correlation to the clones' genotype (Figure 5.16B). For example, Het clone 100_11 had the highest percentage of NKG2A$^+$ NK cells (89%) and revealed presence of a strong WT band and faint KO band intensity. Het Clone 100_19, on the other hand, had the lowest percentage of NKG2A$^+$ NK cells (1%) but also revealed presence

of a strong WT band and faint KO band. Conversely, Het clones with stronger KO band intensity, such as clones 100_1, 100_5 and 100_9, produced a range of NKG2A$^+$ NK cells from 2.5% to 25% that also encompassed the 18% of NKG2A$^+$ NK cells produced by the WT 100_8 clone.

There was no correlation between the percentage of NKG2A$^+$ NK cells and the percentage of dead K562 cell during co-culture. Het clone 100_11, with the highest NKG2A$^+$ NK cell percentage (89%), killed 12.3% of K562 cells at the 5:1 E:T ratio. This was similar to Het clone 100_23, which killed 12.8% of K562 yet consisted of only 16% NKG2A$^+$ NK cells (Figure 5.16C). Clones which killed in less than 2% of K562 cells at either E:T ratio also had variable percentages of NKG2A$^+$ NK cells, such as Het clone 100_19 (1%) and 100_13 (44%). Likewise, WT clone 100_8 resulted in an average of 3.6% dead K562 cells yet had a similar NKG2A$^+$ NK cell percentage (at 16%) to Het clone 100_23, which killed 12.8% K562 cells.

EV-Cas9-eGFP and NK2GA-Cas9-eGFP transduced NK cell clones were also harvested after 45 days of NK cell differentiation to assess killing of the HLA-E positive PEO1 and PEO4 target cell line.

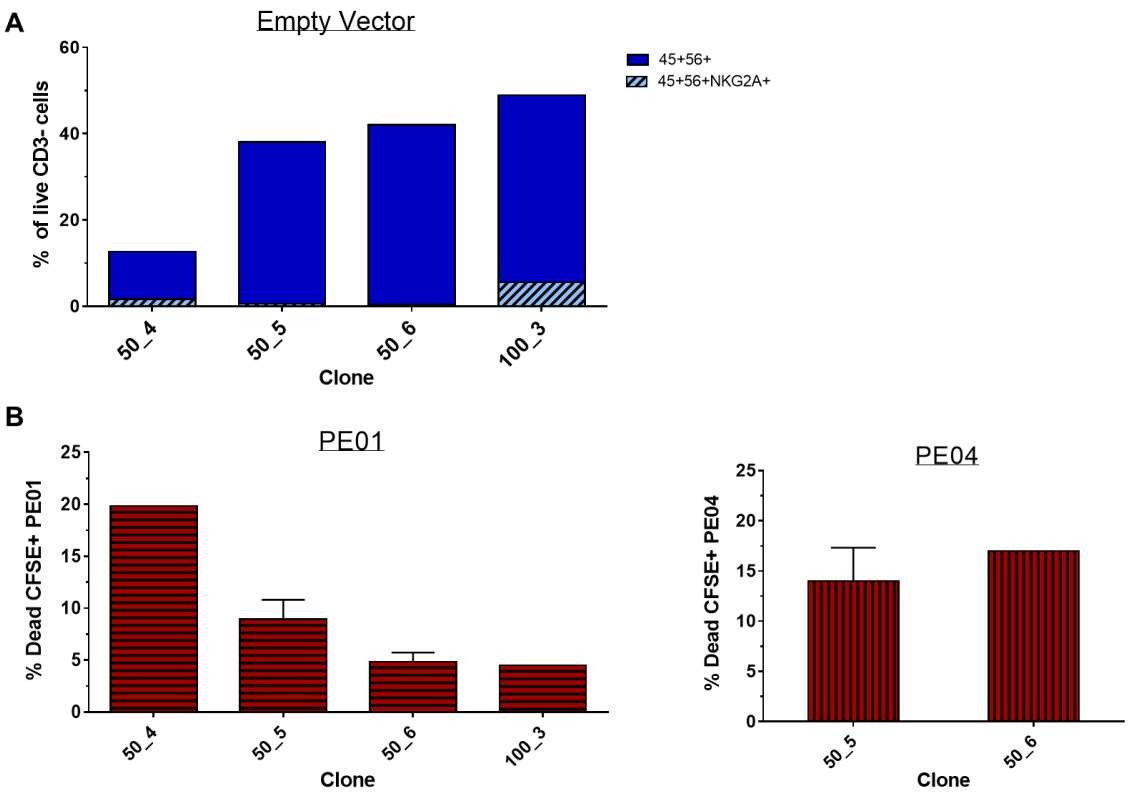



Figure 5.17: PEO1 and PEO4 killing assay with EV-Cas9-eGFP transduced CD34$^+$ derived NK cells.

*CD34$^+$ HPCs transduced with EV-Cas9-eGFP was seeded at 50-cell and 100-cell/well at the start of differentiation, with clones identified as 50_x or 100_x respectively. After 45 days the wells were harvested for assessment of PEO1 and PEO4 killing. (A) The percentage of live CD3$^-$ cells expressing CD45$^+$ CD56$^+$ (45$^+$56$^+$, solid dark blue bar) and CD45$^+$ CD56$^+$ NKG2A$^+$ (45$^+$56$^+$NKG2A$^+$, lined light blue bar) are shown for EV-Cas9-eGFP transduced CD34$^+$ derived NK cell clones. (B) The percentage of dead CFSE$^+$ PEO1 cells (left) and PEO4 cells (right) after an 18h co-culture with the NK cells at a 5:1 E:T ratio. The percentage of dead CFSE$^+$ target cells was normalised to the target cell alone control: 2.58% for the PEO1 and 7.71% for the PEO4. Results were from a single experiment; bars represent average values plus standard deviation. The number of well replicates for the PEO1 assay were N=1 for 50_4 and 100_3, N=2 for 50_6 and N=3 for 50_5. Replicates for the PEO4 assay were N=1 for 50_6 and N=3 for 50_5.*

The percentage of all the EV-Cas9-eGFP transduced CD56$^+$ NK cell clones was below 50%, with the highest percentage of NKG2A$^+$ NK cells from clone 100_3 at 6% (Figure 5.17A). Clones 50_4 had 2% NKG2A$^+$ NK cells while clones 50_5 and 50_6 had negligible NKG2A$^+$ NK cell percentages.

NK cells from clone 50_4 killed the most PEO1 target cells, at 20%, while clones 50_5, 50_6 and 100_3 killed within a range between 5-9% (Figure 5.17B). Interestingly, both clones 50_5 and 50_6 were able to kill more of the PEO4 cell variant than the PEO1 cell variant, showing a 1.5-fold increase in PEO4 killing using clone 50_5 (9% PEO1 to 14% PEO4) and a 3.4-fold increase using clone 50_6 (5% PEO1 to 17% PEO4). As NK cells from clone 50_4 where positive for NKG2A expression at a percentage in-between the other clones, and clones 50_5 and 50_6 had negligible percentages of NKG2A$^+$ NK cells, no correlation could be identified regarding NKG2A$^+$ NK cell percentages and the NK cell cytotoxicity towards either HLA-E positive target cell line.

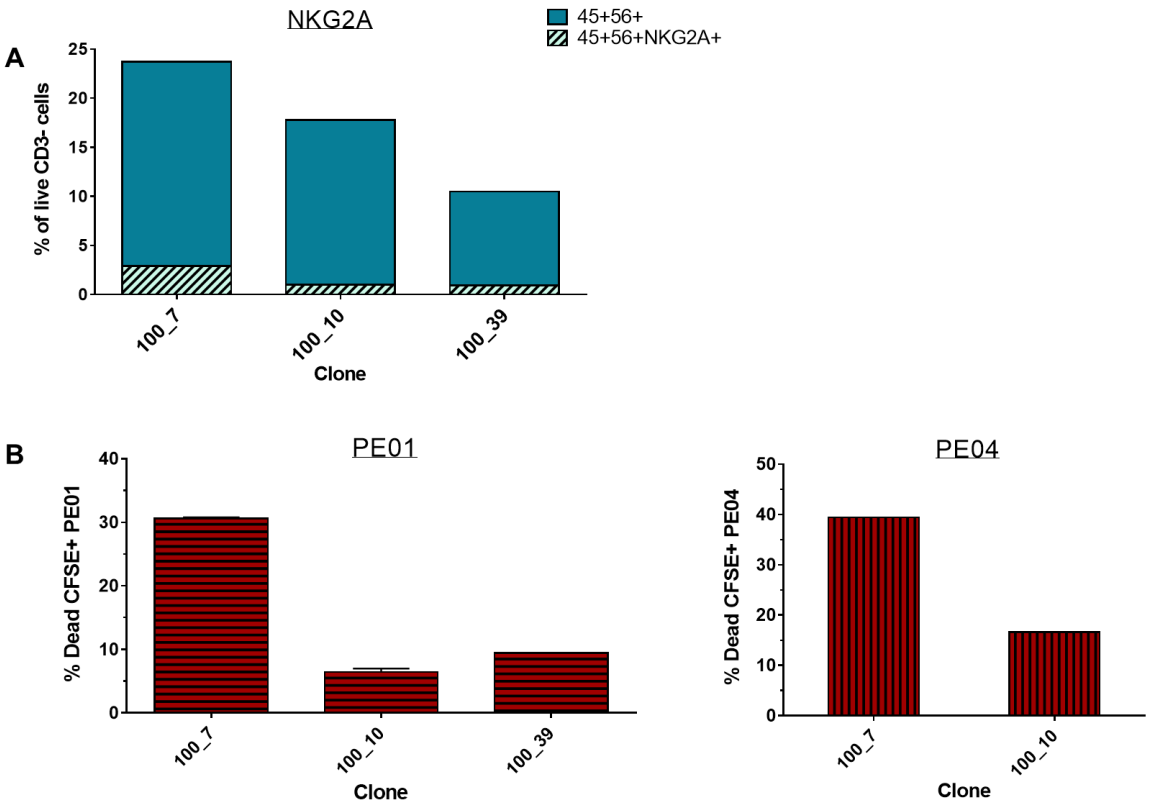



Figure 5.18: PEO1 and PEO4 killing assay with NKG2A-Cas9-eGFP transduced CD34$^+$ derived NK cells.

*CD34$^+$ HPCs transduced with NK2GA-Cas9-eGFP was seeded at 50-cell and 100-cell/well at the start of differentiation. After 45 days the wells were harvested for assessment of PEO1 and PEO4 killing. Only the 100 cell seeded clones, identified as 100_x, had enough cell numbers to set up a cytotoxicity assay. (A) The percentage of live CD3$^-$ cells expressing CD45$^+$ CD56$^+$ (45$^+$56$^+$, solid dark blue bar) and CD45$^+$ CD56$^+$ NKG2A$^+$ (45$^+$56$^+$NKG2A$^+$, lined light blue bar) are shown for NKG2A-Cas9-eGFP transduced CD34$^+$ derived NK cell clones. All clones were previously genotyped as WT for NKG2A. (B) The percentage of dead PEO1 cells (left) and PEO4 cells (right) after an 18h co-culture with the NK cells at a 5:1 E:T ratio. The percentage of dead CFSE+ target cells was normalised to the target cell alone control: 2.58% for the PEO1 and 7.71% for the PEO4. Results were from a single experiment; bars represent average values plus standard deviation. The number of well replicates for the PEO1 assay were N=1 for 100_39 and N=2 for 100_7 and 100_10. The PEO4 assay consisted of only N=1.*

NKG2A-Cas9-eGFP transduced NK cell clones used for PEO1/PEO4 target cell killing were genotyped as WT for NKG2A expression (data not shown). Clone 100_7 had the highest $CD56^+$ NK cell percentage, at 24%, and the highest NKG2A percentage, at 3% (Figure 5.18A). Clones 100_10 and 100_39 had below 20% $CD56^+$ NK cells with 1% NKG2A expression for both.

Clone 100_7 also resulted in the highest percentage of dead PEO1, at 31%, compared to clone 100_10 and 100_39, which did not kill more than 10% of PEO1 cells (Figure 5.18B). NK cell clones were also able to kill more PEO4 cells than PEO1 cells, revealing a 1.3-fold increase using clone 100_7 (31% PEO1 to 40% PEO4) and a 2.4-fold increase using clone 100_10 (9.4% PEO1 to 17% PEO4).

## 5.8. Discussion.

Downregulation or blockade of NKG2A/CD94 receptor signalling within NK cells has been shown to enhance NK cell cytotoxicity against HLA-E overexpressing cancers and is being investigated as an immunotherapeutic strategy to improve NK cell-based cancer therapy. Current strategies targeting NKG2A include anti-NKG2A antibodies, such as Monalizumab (McWilliams et al., 2016, Tinker et al., 2019), or NKG2A knockdown using short interfering RNA or intracellular binding proteins (Figueiredo et al., 2009, Kamiya et al., 2019). Although these approaches have shown beneficial outcomes such as stabilisation of disease progression in clinical trials (McWilliams et al., 2016), internalisation and recycling of the NKG2A/CD94 receptor is believed to reduce therapeutic efficacy (Borrego et al., 2002). Additionally, non-specific effects such as activation of the interferon pathway can be induced by presence of short interfering RNA (Judge et al., 2005). Several papers targeting NKG2A use mature NK cells, therefore the mechanistic role of NK2GA during human NK cell development has yet to be clarified. By targeting NKG2A within $CD34^+$ HPCs prior to NK cell development *in vitro*, it allows us to investigate the importance of NKG2A expression during NK cell differentiation into mature effector cells as well as overcome any complications due to receptor recycling.

When designing sgRNA for human NKG2A, encoded by the KLRC1 gene, mouse models had previously shown efficient KO of protein expression by targeting the gene's single ITIM and TM domains (Figure 5.6B), (Ely et al., 2014). Therefore, a

similar approach was taken to ablate human NKG2A surface expression, with sgRNA designed on either end of Exon 3 and 4 encompassing both ITIM domains and the TM domain (Figure 5.6C).

Confirmation of successful cloning of the NK2GA-Cas9-eGFP vector and validation of the transduction and gene targeting ability was done the same way as the E4BP4-Cas9-hCD2/eGFP and the EOMES-Cas9-eGFP vectors. PCR and sequencing confirmed successful insertion of all four guides (Figure 5.7). Transduction of MRC5 also matched that of the E4BP4-Cas9-eGFP efficiency (Figure 5.8) and the resulting genotype revealed successful NK2GA gene deletion at the target site (Figure 5.9).

We succeeded in obtaining an NKG2A KO NK cell clone that was phenotypically NKG2A deficient (Figure 5.14). This clone (C2) showed complete absence of double positive NKG2A$^+$ CD94$^+$ co-receptor expression yet maintained some single positive CD94$^+$ expression. Since CD94 also heterodimerises with the NKG2C activating receptor (Borrego et al., 2002), this could explain the population of CD94$^+$ single positive NK cells as we have not yet classified NKG2C expression on these cells. As only a single clone was identified with phenotypic NKG2A deficient NK cells, more clones must be generated and expanded to the point where functional assays can be conducted. This would also allow for transcriptomic profiling of NKG2A targeted cells during human NK cell differentiation to assess and widen our current understanding of the downstream signalling mechanisms associated with the receptor. Nevertheless, these results provide us with confidence that our system has the potential to effectively target gene expression within CD34$^+$ HPCs and that biallelic NKG2A KO NK cells is attainable.

NKG2A-Cas9-eGFP transduced CD34$^+$ HPCs were seeded at higher cell densities for NK differentiation, enabling us to investigate the effector response of NKG2A targeted NK cells towards the HLA-E negative K562 cancer cell line. With the absence of HLA-E expression on the target cell, there should be no significant difference in cytotoxicity between NKG2A null and NKG2A$^+$ NK cells. This is seen after K562 co-culture with either EV-Cas9-eGFP or NKG2A-Cas9-eGFP transduced NK cell clones (Figure 5.15 and 5.16 respectively), where no observable correlation can be identified comparing NKG2A expression and killing efficiency. Clones that had higher percentages of NKG2A$^+$ NK cells (above 80%) killed K562 similarly as clones with lower percentages

(below 20%), as shown between EV clones 100_1 and 50_4 (both killing less than 2% of K562 cells) as well as NKG2A Het clones 100_11 and 100_23 (both killing 12% of K562 cells). This supports previous findings where no significant difference of K562 cytotoxicity could be observed between NKG2A deficient NK cells, targeted using protein blockers, and NKG2A$^+$ NK cells (Kamiya et al., 2019).

The cytotoxicity of the NKG2A-Cas9-eGFP transduced NK cells were also measured against known HLA-E positive target cell lines PEO1 and PEO4 (Langdon et al., 1990, Andersson et al., 2016). In the case where HLA-E ligand is present or overexpressed, previous reports showed NKG2A targeted NK cells exhibited enhanced target cell killing compared to NKG2A$^+$ NK cells, due to an absence of inhibitory signalling from the receptor (Kamiya et al., 2019). When co-culture was set up using NKG2A-Cas9-eGFP transduced NK cell clones with the PEO1 or PEO4 cell line, only NKG2A WT clones had continued expansion by day 45 and showed minimal percentages of NKG2A$^+$ NK cells (Figure 5.18). Since the low percentages of NKG2A$^+$ NK was also seen with the EV-Cas9-eGFP transduced NK cell clones (Figure 5.17), this downregulation of NKG2A expression over time is likely a result of NK cell maturation after 45 days of culture, similar to what was observed in reconstituted NK cells after allogenic HSCT in patients (Bjorkstrom et al., 2010). Due to these factors, it was difficult to identify a correlation between NK2GA expression and the killing of the HLA-E positive ovarian cancer cell lines. Nevertheless, these target cells were still sensitive to NK cell killing, irrespective of NKG2A expression, and revealed that the PEO4 cell line was more susceptible to both EV or NKG2A transduced NK cell clones than the PEO1 cell line. Since there is not much work comparing NK cell cytotoxicity towards these two variants, it would be interesting to see what cytotoxic responses would occur if the NK cells retained NKG2A expression compared to NK cells with NKG2A KO.

As NKG2A expression was not consistent across the NK cells that were WT for NKG2A, such as the EV-Cas9-eGFP transduced clones (ranging from 11% to 83%, Figure 5.15), it was difficult to establish correlation between NKG2A expression and genotype between NKG2A targeted clones (Figure 5.16). For example, NK cells within the NKG2A WT clone 100_8 had similar or close NKG2A+ NK cell percentages to the Het clones 100_23, 100_3 and 100_9. This is believed to be a result of NKG2A receptor internalisation and recycling, leading to a non-homogenous population of NK cells with different levels of NKG2A surface expression. Previous papers have shown

that pre-stimulation of NK cells with IL-12 cytokine encourages NKG2A expression, resulting in a homogenous cell population (Figueiredo et al., 2009). This approach will be incorporated into future experiments to ascertain the true NKG2A expression potential of NKG2A targeted clones, permitting me to accurately measure trends between WT, Het and KO genotypes. In addition to this, pushing NK2GA surface expression for Het clones that differ in NKG2A KO band intensity, such as clone 100_9 and 100_23 (Figure 5.16A), would clarify whether a reduction in NKG2A surface expression can be seen with clones that present stronger KO band intensity. If this is the case, it would allow us to use genotyping PCR as a predictor for targeting efficiency during future optimisation work.

Optimisation of the transduction process led to the generation of a successfully targeted NKG2A KO NK cell clone. As viral titres produced for our GOI-Cas9-eGFP vector was calculated at $3.5x10^6$ TU/ml (Figure 5.2C), it was on the lower range of previously reported titres used to transduce $CD34^+$ HPCs, ranging from $3x10^6$ TU/ml (Case et al., 1999) to $8x10^7$ – $2x10^8$ TU/ml (Guenechea et al., 2000, Adair et al., 2016). Because of this, we sought strategies to increase transduction efficiencies using the titre we obtained as well as improve the survival of transduced cells during the transduction and differentiation steps. Increased transduction efficiency and cell viability was observed with the use of Retronectin (Figure 5.3), which co-localises the cells and virus using its VLA5/VLA4 and Heparin-binding domains, respectively, encouraging physical interaction during transduction (Pay et al., 2018). Increased survival of transduced cells, determined by higher frequencies of Het or KO $CD34^+$ derived cell clones, was seen when CsH was included during the transduction step (Figure 5.4). CsH is known to block the interferon-induced transmembrane protein 3 (IFITM3) in HPCs and therefore improve viral gene transfer and editing efficiency (Petrillo et al., 2018). Improved NK cell differentiation from lower seeded numbers of $CD34^+$ HPCs was seen when the HPCs were treated with UM171 prior to differentiation (Figure 5.5). UM171 acts as a proliferative agent that was shown to selectively expand lymphoid progenitors with NK potential (Mesquitta et al., 2019), as well as improve survival and efficiency of lentiviral transduced HPCs (Ngom et al., 2018). When these changes were implemented, improvements to survival and growth of successful NKG2A targeted cells was observed, permitting for the flow cytometry analysis of Het and KO clones (Figure 5.13). Altogether, the combined use of

Retronectin, CsH and UM171 led to the generation of a phenotypic NKG2A KO NK cell clone.

In summary, I have shown that it is possible to obtain biallelic KO of the human NKG2A receptor within $CD34^+$ HPCs, leading to ablation of NK2GA surface expression upon NK cell differentiation. Optimisation of the targeting procedure using Retronectin, CsH and UM171 was shown to improve transduction efficiency, survival and proliferation of targeted, differentiating cells, yet we still face limitations regarding the overall proliferative capacity from small numbers of $CD34^+$ HPCs. This consequently restricts downstream assessment of biallelic KO NK cell's functional capacity. Increasing seeding densities to 50-cell or 100-cell/well enabled sufficient NK cell production to assess killing of a range of cancer cell lines, revealing higher cytotoxicity toward the HLA-E positive ovarian cancer PEO4 line than the PEO1 variant. Having successfully generated a phenotypic NKG2A KO NK cell population, the next steps involve the generation of sufficient KO cells and homogenising NKG2A surface expression through the use of cytokines in order to investigate the functionality of our NKG2A deficient NK cells.

# 6. Final discussion and future work

The versatile functions of NK cells give them several advantages when considered as the cell of choice for cancer immunotherapy. Unlike T cells, NK cells can specifically target cancer cells without prior sensitisation, including cancers with downregulated MHC surface expression, whilst maintaining tolerance towards normal HLA expressing cells (Bi and Tian, 2017). The challenges of NK cell therapy, however, include meeting the high demand for functional cells due to the limited proliferative capacity of mature NK cells. Additionally, these NK cells can exhibit an exhaustive phenotype with reduced effector responses as a result of extensive expansion and activation prior transplantation (Chabannon et al., 2016). To tackle these issues, I investigated the generation of larger quantities of NK cells or NK cells with enhanced cytotoxic responses by using a lentiviral CRISPR/Cas9 system to target single genes associated with early or late NK cell development, defined by the onset of CD56 expression, within $CD34^+$ HPCs. I assessed the effect on growth and NK cell production from these transduced progenitors as they differentiated into NK cells *in vitro*. I show that the system I use can generate genetically modified $CD34^+$ derived cells with biallelic gene KO, and when targeting genes associated in late NK cell development, these cells are able to differentiate into a phenotypically deficient NK cell population. This method does allow investigation into the role of certain genes during NK cell development for the purposes of improving NK cell production or cytotoxicity, however, there is room for improvement to ensure the robustness of this approach.

## 6.1. Genes involved in early NK cell development.

The transcription factor E4BP4 was found to be crucial for the development of NK cells from mouse hematopoietic progenitors (Gascoyne et al., 2009, Male et al., 2014), and was therefore considered as a potential gene target to enhance human NK cell production. It was uncertain, however, whether E4BP4 played a similar role in human NK cell development and what its mechanism of action was within these cells. Using our protocol, I found that expression of E4BP4 was required for human NK cell differentiation from $CD34^+$ HPCs, indicated by the inability for biallelic KO $CD34^+$ derived cell clones to produce any NK cells by the mid-stage (days 16-26) of culture

(Figure 4.8). Some Het clones were able to differentiate into NK cells but at lower percentages, supporting the notion that the decrease in NK cell production was due to a loss of E4BP4.

Similarly, transcription factor EOMES was considered as another potential gene target to investigate the production of mature and functional NK cells. Eomes deletion in murine mature NK cells showed phenotypic and functional reversion towards the immature state. As there is limited information regarding the role of EOMES expression during human NK cell development, along with the identification of $Eomes^{-/low}$ NK cells in both mouse and human (Gordon et al., 2012, Marquardt et al., 2015), it raised the question as to whether functional NK cells can develop in the absence of EOMES (Daussy et al., 2014, Marquardt et al., 2015) or if these cells are an intermediary progenitor population for $Eomes^{+}$ NK cells (Cuff et al., 2016, Gordon et al., 2012). Surprisingly, I found that deletion of at least a single EOMES allele led to an abrupt cell arrest between the early and mid-stage of culture (past day 16), since the only KO clone and the majority of Het clones were identified within the failed growth populations at endpoint (Figure 4.16). Because Eomes was found to be regulated by E4bp4 in mice (Male et al., 2014), it was interesting to see cell arrest with EOMES KO clones earlier than the E4BP4 KO clones, suggesting EOMES may play an important role for cell survival during early NK cell development. Transcriptional analysis of $CD34^{+}$ derived NK cells by Luevano et al., (2014) supports this notion, as the authors saw a large increase in EOMES expression between days 7 to 21 and an increase in E4BP4 expression between days 21 to 28, corresponding to the time periods where I also observed a reduction in cell growth of my Het or KO clones.

Given I categorised the NK cell culture stages as early, mid and late depending on the day of culture, I have yet to characterise the differentiation stages of the NK cells during this time period and evaluate which NK cell stage (precursor, immature or mature) is impacted by loss of E4BP4 or EOMES. Inclusion of markers such as CD34, CD117 and CD94 has previously been used to characterise the 5 stages of NK cell development (Luevano et al., 2014), with stages 4 and 5 distinguished by mature NK markers CD56 and CD16. While these markers need to be assessed to characterise the NK cell differentiation stages during our differentiation protocol, Luevano et al., (2014) used the same method to differentiate NK cells from UCB $CD34^{+}$ HPCs,

permitting us to predict what the differentiation stages may be relative to the early/mid/late culture stages described during gene targeting (Figure 6.1).

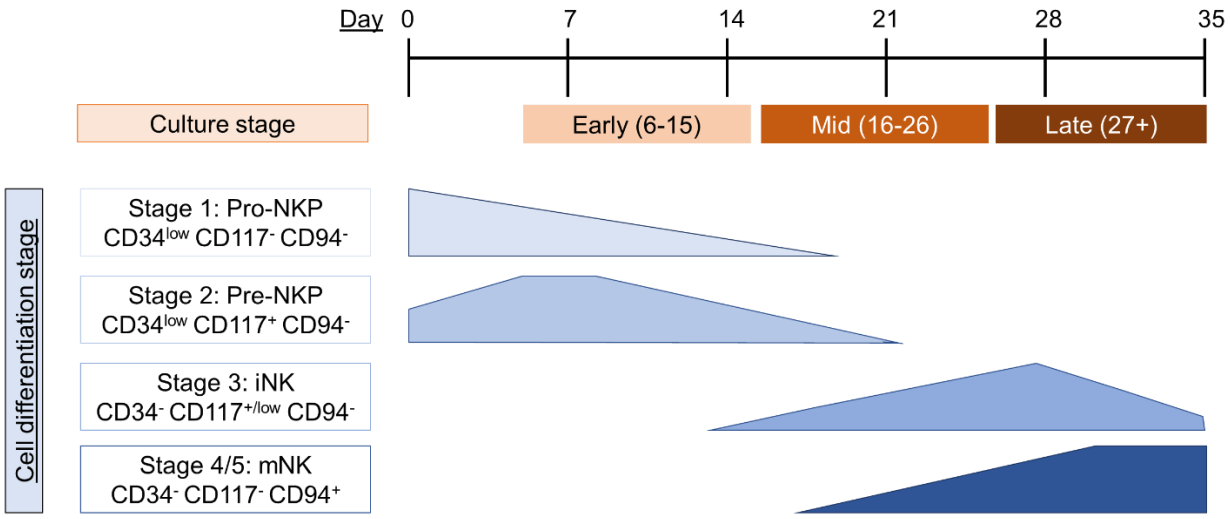



Figure 6.1: Predicted NK cell differentiation stages relative to my culture stages

*Stages of the NK cell differentiation culture, classified as early (days 6-15), mid (days 16-26) and late (days 27+), are presented relative to the NK cell differentiation populations found during the same day, adapted from Luevano et al., (2014). The NK cell differentiation populations are classified as: CD34$^{low}$ CD117$^{-}$ CD94$^{-}$ Stage 1 Pro-NK precursor (NKP) cells, CD34$^{low}$ CD117$^{+}$ CD94$^{-}$ Stage 2 Pre-NKP cells, CD34$^{-}$ CD117$^{+/low}$ CD94$^{-}$ Stage 3 immature NK cells, CD34$^{-}$ CD117$^{-}$ CD94$^{+}$ Stage 4/5 mature NK cells. Mature NK stage 4 and 5 cells are distinguished by markers CD56$^{bri}$ CD16$^{-}$ and CD56$^{dim}$ CD16$^{+}$, respectively. Abundance of the cell populations during the different days of culture are represented by the blue arrows.*

As E4BP4 KO CD34$^{+}$ derived cell clones survived until the mid-stage but were unable to differentiate into CD56$^{+}$ NK cells, this loss of gene effect may correspond with cells transitioning from NKPs into iNK cells (Figure 6.1). Similarly, as EOMES targeted CD34$^{+}$ derived cell clones did not expand past the early stage of culture, this loss of gene effect may correspond with cells at the NKP stages (stage 1 and 2) or with cells

transitioning from NKPs into iNK cells. Future work to characterise the NK cell differentiation stages will include markers described in Figure 6.1, as well as intracellular antibodies for E4BP4 and EOMES. By doing this, it is possible to verify when these genes are upregulated during normal, WT NK cell development and if this corresponds to the expectations presented in Figure 6.1. This will permit me to detect phenotypic loss of E4BP4 or EOMES expression within KO cells at these specific stages. Using flow cytometry, targeted progenitors seeded at higher cell numbers can be isolated at the specified differentiation stages for further NK cell culture. This would allow me to prove that only the WT populations, or possibly E4BP4 Het populations, transition into the next differentiation stage, further validating my previous findings. Quantitative PCR (qPCR) on isolated gene KO cell types will allow transcriptional profiling of these cells, confirming KO on a transcriptional level as well as detection of which potential downstream pathways are affected. For example, as E4bp4 was found to upregulate Eomes in mice (Male et al., 2014), the transcription level of either gene can be detected in KO cells to explore whether this is the case in human, or, as our data suggests, if EOMES plays a role during early NK cell development. Elucidation of these pathways provide insight into how genes like E4BP4 and EOMES regulate NK cell development, permitting me to investigate what methods can be used during normal NK cell differentiation to drive gene expression and increase NK cell production for therapy.

## 6.2. Optimising CRISPR-Cas9 gene targeting with genes involved in late NK cell development.

When targeting genes associated with early NK cell development, I encountered low transduction efficiencies of the Cas9 vectors, forcing me to seed low numbers of transduced cells for NK cell differentiation in order to generate clonal, homogenous populations. Seeding small numbers of transduced $CD34^+$ HPCs resulted in lower frequencies of KO NK cell clones as well as fewer numbers of KO NK cells to assess downstream applications, such as phenotypic characterisation or transcriptional profiling. The relationship between seeding density and NK cell production was also seen with untransduced HPCs differentiating into NK cells (Figure 3.4), (Grzywacz et al., 2011), indicating this effect is not restricted to transduced cells. However,

increasing the seeding density of HPCs without improving the transduction efficiencies would potentially reduce the chances of generating a biallelic KO NK cell clone. Therefore, we included methods to increase transduction efficiency through improving viral entry (Retronectin, Figure 5.3, and CsH, Figure 5.4) as well as cell survival (UM171, Figure 5.5).

The generation of an NKG2A KO NK cell clone was successful using the optimised protocol, however the frequency of KO clones obtained was still restricted due to the low seeding densities required for clonal differentiation. Unlike E4BP4 and EOMES, NKG2A is expressed after CD56 upregulation, allowing me to investigate the effects of gene loss on $CD56^+$ NK cells. Furthermore, NKG2A was selected as the generation of stable NKG2A deficient NK cells for the treatment of HLA-E overexpressing cancers overcomes the issues with antibody-based therapy (Borrego et al., 2002, Luevano et al., 2014). As NKG2A KO has only been achieved in mature NK cells, this approach enables the study of NKG2A gene loss effects during NK cell differentiation, as well as the generation of KO NK cells with NKG2A deficiency for immunotherapy. Nevertheless, due to the low transduction efficiency, transduced $CD34^+$ HPCs were still required to be seeded at low cell densities, resulting in the production of fewer absolute NK cell numbers to examine the functional profile of NK2GA KO NK cells.

Given that 50 to 100 cell seeding densities produced enough NK cell numbers to set up cytotoxicity assays with target cancer cells (Figure 3.4), the seeding density for NKG2A targeted $CD34^+$ HPCs was also increased to assess downstream NK cell function (Figure 5.16 and 5.18). Increasing the starting seeding density, however, resulted in the inability to detect biallelic NKG2A KO NK cell clones (Figure 5.16A). Therefore, while optimisation of the transduction process allowed for the successful generation of a phenotypic NKG2A KO NK cell clone, it was not enough to overcome the limits observed with seeding densities and the resulting heterogeneity of genotype at the start of differentiation. Thus, we sought ways to improve the targeting efficiency and generate a homogenous population of targeted $CD34^+$ HPCs for the start of NK cell differentiation, allowing for higher density seeds and the generation of enough NKG2A KO NK cells for functional assessments.

Alternative strategies to viral mediated CRISPR/Cas9 gene deletion, such as nucleofection, were considered to overcome the low transduction efficiencies seen

with our CRISPR/Cas9 vector. Previous publications have shown successful results of gene editing in human HPCs using electroporation of chemically synthesised sgRNA with Cas9 mRNA or as a protein complex, assessed by successful gene target deletion, high frequencies of indel mutations at the target site or through targeted insertion of a donor gene template via homology domain repair (Bak et al., 2017, Dever et al., 2016, Gundry et al., 2016, Hendel et al., 2015). Preliminary experiments were conducted targeting NKG2A using nucleofection (an electroporation-based transfection method) as the alternative method to introduce the Cas9 and guides. Since nucleofection with protein complexes of Cas9 and sgRNA, called ribonucleoproteins or RNP, have also shown successful gene editing within NK92 cells (Huang et al., 2020), trials were performed using NK92 cells as these cells have approximately 100% NKG2A surface expression and a doubling rate around 2-3 days, thus allowing for a fast assessment of CRISPR/Cas9 mediated deletion. Using NK92 enabled enough cells to be obtained for detection of successful gene deletion via PCR and phenotypic knockout of NKG2A using flow cytometry (Figure 6.2). Nucleofection trials were also conducted using the intended target cells, $CD34^+$ HPCs, and evaluated by genotyping PCR to assess the efficacy of nucleofection on gene targeting compared to the previously described lentiviral based approach.

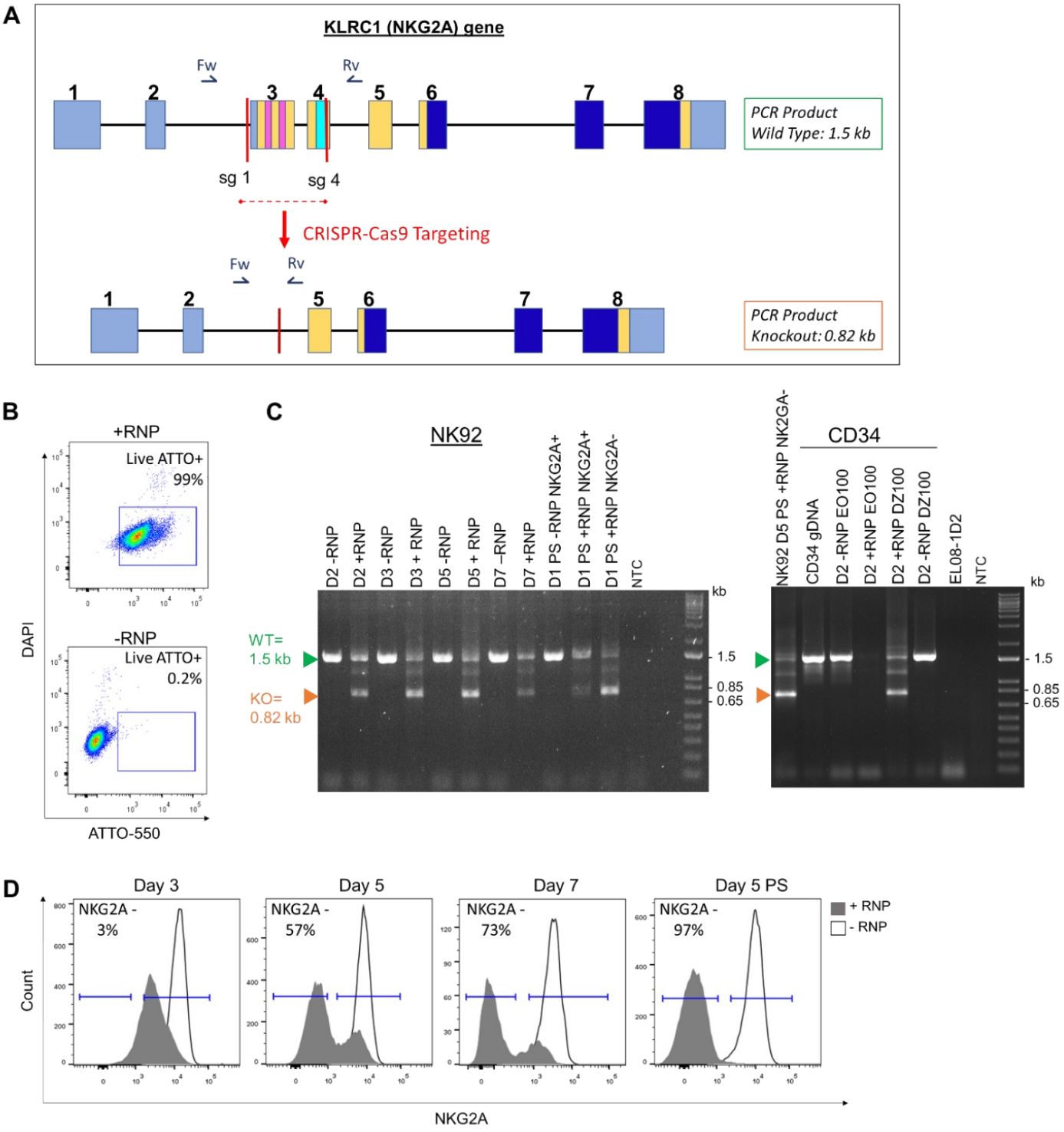



Figure 6.2: Nucleofection of NK92 cells using NKG2A RNP.

*(Legend on next page).*

Figure 6.2: Nucleofection of NK92 cells using NKG2A RNP.

*NK92 cells were nucleofected with and without the NKG2A RNP complex (+RNP and -RNP, respectively) fused to a fluorescent ATTO-550 reporter. After 7 days in culture, NKG2A$^-$ and NKG2A$^+$ +RNP NK92 cells were sorted as well as the NKG2A$^+$ -RNP NK92 cells. Cells were expanded for genotyping and flow cytometry, except for the NKG2A$^+$ +RNP NK92 population, which failed to proliferate 2/3 days post sort. (A) Genotyping strategy of the KLRC1 (NKG2A) target region, where RNP were designed to target sgRNA 1 and 4 encompassing the ITIMS (pink) and TM domain (cyan). Forward and reverse primers produce a 1.5kb WT band prior deletion and a 0.82kb KO band after gene targeting. (B) Percentage of live ATTO-550+ NK92 cells 3 days after nucleofection +RNP or -RNP. (C) NKG2A genotyping gels of the +RNP and -RNP NK92 cell populations on different days post nucleofection. After the NK92 cells were sorted based on NKG2A expression on day 7 (D7) and expanded, genotyping results are indicated as days post sort, e.g. D1 PS: day 1 post sort. NKG2A$^-$ +RNP NK92 cells 5 days post sort (D5 PS) is shown on the right gel image. CD34$^+$ HPCs were nucleofected +RNP and -RNP using two different programmes on the 4D Nucleofector (DZ100 or EO100). After 2 days, these cells were genotyped. NKG2A WT bands (1.5kb) and KO bands (0.82kb) are indicated with green and orange arrowheads respectively. gDNA: genomic DNA from unedited CD34$^+$ HPCs, NTC: Non template control. (D) NKG2A expression is shown for both -RNP NK92 cells (open black graph) and +RNP NK92 cells (solid grey graph) on day 3, 5 and 7 post nucleofection. NKG2A expression is also shown for the NKG2A$^-$ +RNP NK92 cells and the NKG2A$^+$ -RNP NK92 cells 5 days after sort on day 7 (Day 5 PS). Results were obtained from a single experiment and were acquired in collaboration with PhD candidate Ines Ullmo, Hugh Brady group, Imperial College London.*

NKG2A RNP's were designed to target the same sgRNA 1 and sgRNA 4 sites used previously for the lentiviral vector (Figure 6.2A), with a fluorescent reporter, ATTO-550, conjugated to the sgRNA. Three days after nucleofection, approximately all (99%) of the NK92 cells nucleofected with NKG2A RNP (+RNP) were positive for ATTO-550 (Figure 6.2B). While the genotyping PCR of NK92 +RNP cells showed that they were heterozygous, the intensity of the KO band relative to the WT band did not change even after 7 days of culture (Figure 6.1C) and corresponded with a gradual decline in NKG2A surface expression within these cells (Figure 6.1D). After sorting NKG2A$^-$ NK92 +RNP cells on day 7, the populations showed even stronger KO band intensities relative to the WT band, while NKG2A$^+$ NK92 +RNP cells showed the opposite effect. Even after 5 days post sort, the NKG2A$^-$ NK92 +RNP cells remained negative for NKG2A (Figure 6.1D), indicating that the NKG2A gene targeting within these cells was stable and the presence of the WT band did not lead to de novo NKG2A expression.

CD34$^+$ HPCs nucleofected +RNP revealed presence of an intense NKG2A KO band relative to the WT band 2 days after nucleofection (Figure 6.2C). This KO band intensity is observably stronger than what was seen when CD34$^+$ HPCs were transduced with the NKG2A-Cas9-eGFP vector (Figure 5.9B), indicating that nucleofection is a suitable approach to target genes within the CD34$^+$ HPCs. Transfection and transduction efficiencies are dependent on viral titres, influenced by vector size (Cante-Barrett et al., 2016). This is demonstrated by the higher viral titres (Figure 5.2) and transfection/transduction efficiencies (Figure 4.5, 4.13 and 5.8) obtained with the smaller 14.7kb EV-Cas9-eGFP vector compared to the larger 15.8kb GOI-Cas9-eGFP vector. Nucleofection with pre-formed Cas9-guide complexes overcomes the size-titre limitation. Using nucleofection, viral titre is no longer an issue and there is no expected discrepancy between the targeting efficiency of EV- and GOI-Cas9-eGFP vectors. Furthermore, as nucleofection can lead to the successful targeting of NKG2A within NK92 cells (Figure 6.2), resulting in complete ablation of NKG2A expression, this preliminary data gives us confidence that nucleofection provides an efficient and consistent gene targeting alternative to viral mediated systems.

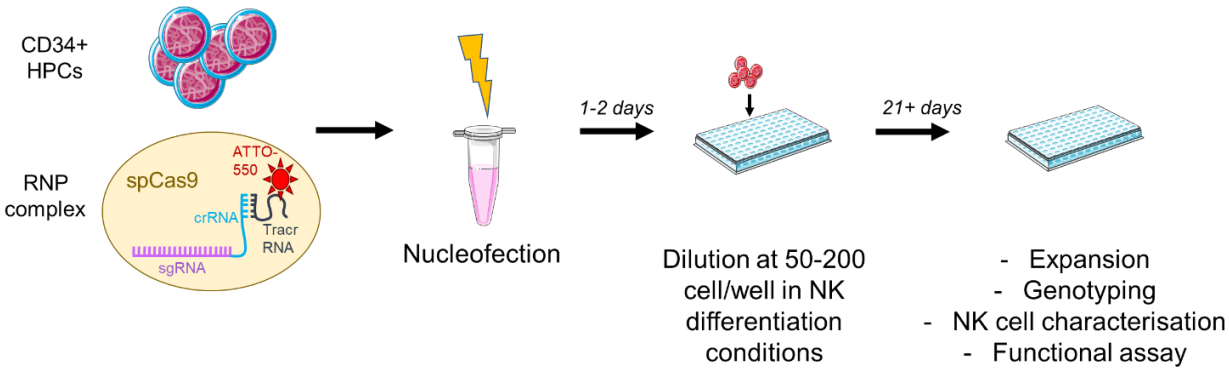



Figure 6.3: Procedure to target genes in CD34⁺ HPCs using CRISPR-Cas9 RNPs and nucleofection to assess NK cell development.

*CD34⁺ HPCs will be combined with the gene specific RNP complex, consisting of the SpCas9 protein (yellow), crRNA (blue, with the sgRNA sequence in pink) and tracrRNA (black) tagged to a fluorescent reporter ATTO-550 (red star). 1-2 days after nucleofection, cells will be serially diluted between 50-200 cells/well for NK cell differentiation. During the 21+ days of differentiation and expansion, CD34⁺ derived cells will be analysed for genotyping, NK cell characterisation and functional testing.*

A new protocol was designed utilising nucleofection to target of CD34⁺ HPCs, in order to assess the effect of gene loss during NK cell development (Figure 6.3). Sorting at this stage is no longer useful as we see approximately 100% of nucleofected cells express ATTO-550 (Figure 6.2B). Since NK92 cells also show high NKG2A targeting efficiency, I expect the gene targeting efficiencies will also be relatively high for the CD34⁺ HPCs. This expected efficiency would permit seeding of targeted HPCs at higher cell densities for NK cell differentiation, increasing the frequency of KO clones as well as the number of KO cells per clone for further functional assessment. Characterisation and transcriptional profiling of targeted cells can be conducted earlier, enabling the observation of progenitors differentiating into iNK and mNK cells for assessment of genes involved in early NK cell development (e.g. E4BP4 and EOMES). Additionally, being able to reliably generate KO clones enable me to identify which potential signalling pathways rescue NK cell development when these genes are targeted. For example, inclusion of recombinant Notch ligands DLL1 and DLL4 during differentiation rescued *in vitro* NK cell development in E4bp4$^{-/-}$ mice

(Kostrzewski et al., 2018) and is a method that could potentially rescue E4BP4 KO human NK cell development. Notch receptor stimulation could therefore be applied to unmodified CD34$^+$ HPCs to see if this improves NK cell development or maturation, providing a novel approach to boost human NK cell production for immunotherapy.

## 6.3. Functional analysis of CD34$^+$ derived NK cells

CD34$^+$ derived NK cells generated using our differentiation system exhibit effector responses when stimulated with cytokines or when co-cultured with cancer lines. Moreover, production of IFNγ and cytotoxicity towards cancer cell lines K562 and PEO1 was greater with the CD34$^+$ derived NK cells than NK92 cells, an activated NK cell line commonly used for immunotherapy (Figure 3.6 and 3.7, respectively). While the CD34$^+$ derived NK cells outperform NK92 in terms of cytotoxicity towards certain cancer types, previous papers have shown that CD34$^+$ derived NK cells differentiated in this same manner have 2-4 fold higher levels of cytotoxicity than our CD34$^+$ derived NK cells (Domogala et al., 2016, Grzywacz et al., 2006, Luevano et al., 2014). Cytotoxic responses also remained low when EV-Cas9-eGFP transduced cells were co-cultured with these cancer cell lines for 18-24h (Figure 5.15 and 5.17). Therefore, possible reasons for the reduced cytotoxicity could be that the differentiating cells received insufficient education signals to become functionally competent, or that the NK cells were not fully mature, requiring additional signals for maturation and activation into to effector cells.

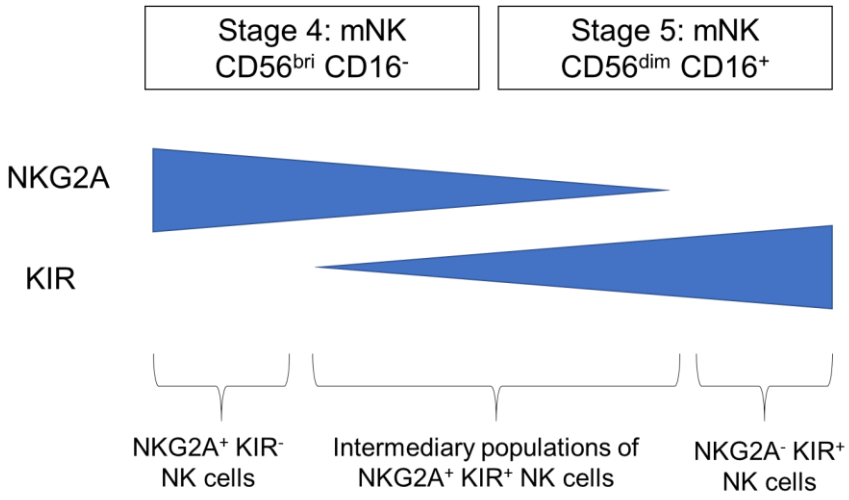



Figure 6.4: NKG2A and KIR expression in mature human NK cells.

*In mature NK cells, NKG2A and KIR exhibit an inverse expression profile during NK cell maturation. Since receptor expression is a dynamic process, intermediary populations of NKG2A$^+$ KIR$^+$ NK cells can be found. In addition to this, both KIR expression levels and the number of KIR subtypes on the NK cell surface can increase during maturation (Freud and Caligiuri, 2006, Ivarsson et al., 2013).*

Education of NK cells, via their inhibitory NKG2A or KIR receptors, ensure that only the NK cells able to interact with self-MHC peptides become functionally competent, preventing the generation of auto-reactive NK cells (Bjorkstrom et al., 2010). It has been reported that CD34$^+$ derived NK cells, differentiated using the same culture method, express low to negligible levels of KIRs and require additional signals to drive KIR expression for education (Luevano et al., 2014). To determine if our CD34$^+$ derived NK cells show low level KIR expression, and thus the reduced cytotoxicity, future work involves characterising KIR expression, such as KIR2DL1/3 and KIR3DL1/2 receptors (Bjorkstrom et al., 2010). Characterisation of KIR expression will also allow me to investigate whether targeting NKG2A has an impact on KIR mediated education. Due to the inverse relationship between NKG2A and KIR expression during NK cell maturation, different NK cell subgroups with varying NKG2A and KIR expression profiles can be found (Figure 6.4). These subgroups of NK cells receive different education signals and therefore vary in their functional capacity, with NKG2A

mediated education eliciting the strongest functional response, as measured by degranulation against K562 cells (Sim et al., 2016). Therefore, NKG2A and KIR expression will be monitored during differentiation of our CD34$^+$ derived NKG2A WT and KO NK cells. Functional assessment of the subgroups that arise will elucidate if NKG2A mediated education is essential for a functional response, or, if the potential KIR expression on NKG2A KO NK cells ensures sufficient education signals for functional maturation.

It is also possible that the low cytotoxic responses observed with our CD34$^+$ derived NK cells were due to these cells being immature, requiring maturation and activation to become effector cells capable of producing a strong cytotoxic response against cancer cells. Luevano et al., (2014) revealed their CD34$^+$ derived NK cells had low to moderate levels of CD16 and were negative for the terminal maturation marker CD57, indicating an immature phenotype. CD16 is upregulated in stage 5 NK cells and are highly cytotoxic, while upon terminal maturation and CD57 upregulation, the proliferative potential of these cells is reduced and they exhibit signs of senescence (Abel et al., 2018, Bjorkstrom et al., 2010). Conversely, it has been reported that *in vitro* UCB CD34$^+$ derived NK cells, low in CD16 expression, underwent maturation and acquisition of CD16, as well as KIRs, 6-8 days post transplantation in AML patients (Dolstra et al., 2017, trial ID NL31699.00020). This suggests there are possible *in vivo* pathways that are not being replicated *in vitro*. Dezell et al., (2012), have found that using Heparin, an anticoagulant drug, to differentiate NK cells supported higher production of a mature CD16 phenotype when compared to co-culture with EL08-1D2 cells. Additionally, inclusion of low doses of IL-12 during culture also encouraged CD16, KIR and NKG2A upregulation on CD34$^+$ derived NK cells (Lehmann et al., 2014). Future assays will therefore include CD16 and CD57 markers to determine the maturation stage of our CD34$^+$ derived NK cells, while incorporation of Heparin and low doses of IL-12 into the differentiation culture will encourage stage 5 differentiation and maturation. These changes ensure the cells reach functional maturity prior to testing effector responses.

Alongside maturation, activation of the CD34$^+$ derived NK cells may be required to produce a functional response. Increased cytotoxic responses have been reported when CD34$^+$ derived NK cells are stimulated with IL-12 or IL-2 prior to co-culture with K562 (Domogala et al., 2016, Luevano et al., 2014). Moreover, activation of NK cells

can be measured by detecting an increase in activation markers such as CD69, CD25 and NKp44 (Skak et al., 2008, Veluchamy et al., 2017). To assess activation of our $CD34^+$ derived NK cells, future work will include pre-stimulation with IL-12 and IL-2, as well as other known NK stimulatory cytokines like IL-18 and IL-21 (Perez et al., 2006, Senju et al., 2018). Measuring the upregulation of activation markers, like CD69, CD25 and NKp44, will allow me to optimise the best combination of stimulatory cytokines that induces cellular activation and see whether this corresponds to an enhancement of the $CD34^+$ derived NK cells cytotoxic response.

Application of the modified functional assay and cell characterisation to NKG2A deficient KO NK cells will allow me to investigate whether these cells exhibit increased cytotoxic responses relative to $NKG2A^+$ WT cells, supporting the use of our approach to generate NKG2A KO NK cells for cell-based immunotherapy. The ability to administer NKG2A deficient NK cells with enhanced cytotoxic function into cancer patients could provide a significant improvement during NK cell immunotherapy against particular tumour microenvironments.

### 6.4. Applications of CRISPR/Cas9 gene editing in human NK cell development.

One of the advantages of utilising CRISPR/Cas9 to target genes at the progenitor cell stage is the flexibility of studying a broad range of genes associated with NK cell development and function. For example, both $Id2^{-/-}$ (Boos et al., 2007) and $T\text{-}bet^{-/-}$ (Townsend et al., 2004) mice have shown to impact NK cell maturation from the NKP stage, and like E4BP4 and EOMES, our targeting protocol can be easily adapted to investigate the roles these genes have during human NK cell differentiation. Also, similar to NKG2A, other inhibitory receptors have been shown to improve NK cytotoxic function through use of antibody blockade, such as CTLA-4, TIGIT and PD-1 (Larkin et al., 2015, Zhang et al., 2018). These receptors can be targeted to generate stably deficient NK cells to assess for potentially improved cytotoxicity. Since the generation of specific CRISPR/Cas9 targeting complexes require only a change in the sgRNA oligonucleotide, it is easy to generate multiple gene targeting complexes in a short period of time. This also includes the ability to target two genes simultaneously, which can be useful when targeting receptors like CTLA-4 and PD-1, as blocking signalling from both receptors during antibody therapy has resulted in greater cytotoxic NK cell

responses than when blocked individually (Larkin et al., 2015). Therefore, our system cannot only be applied to investigate the role of a range of individual genes, but also the relationships between genes during NK cell differentiation.

Using CRISPR/Cas9, there is always risk of potential off-target effects which occur when the Cas9-gRNA complex recognises non-specific DNA sites and induces an unwanted cleavage event. Off-target disruption of genes can be lethal or induce oncogenic effects, but more importantly, these mutations can be silent and difficult to assess during NK cell development, potentially influencing the results (Fu et al., 2013, Wang et al., 2017). A targeted approach I plan to implement in order to assess off-target effects is to use prediction tools to identify off-target sequences similar to the sgRNA. In CRISPR/Cas9 targeted cells, these genomic regions can be amplified using PCR and sequenced to check whether a cleavage event occurred. A global, genome wide approach we could also implement is assays like SITE-seq (selective enrichment and identification of tagged genomic DNA ends by sequencing), which uses next generation sequencing to identify all the possible Cas9 cleavage sites after combining Cas9 RNP complexes with purified human DNA (Cameron et al., 2017). These techniques can be applied to ensure specificity with the gene targeting approach and low risk of off-target effects, improving the safety of using these genetically modified NK cells in a clinical setting.

In conclusion, I have set out to find potential targets to improve NK cell production or enhance NK cell cytotoxicity for use in cancer immunotherapy. Using a lentiviral CRISPR/Cas9 system, I targeted genes associated in early and late NK cell development within $CD34^+$ HPC progenitors, and successfully generated clonal populations of biallelic KO cells. My findings suggest E4BP4 and EOMES play important roles during human NK cell differentiation, supporting previous mice KO studies. Meanwhile, the effect of NKG2A loss is seen after the generation of NK cells, and a biallelic NKG2A KO NK cell clone was successfully generated. I have shown that nucleofection can be used in human $CD34^+$ cells to improve targeting efficiency and thus increase the generation of biallelic KO clones. Improving the occurrence of KO clones will allow us to functionally assess NKG2A KO NK cells and investigate the relationship between NKG2A expression and functional response. When investigating genes believed to play an important role during differentiation, characterising the different NK cell development stages will allow us to investigate the effects of the loss

of those genes in greater detail. In the case of E4BP4 and EOMES targeting, defining the stage of NK cell development at which they are crucial will allow me to fine tune our differentiation method to produce NK cells more efficiently. The ability to manipulate NK cells opens the possibility to customise NK cells for unique tumour microenvironments. This work allows us to examine genes associated with human NK cell development and function, in addition, these studies can provide the basis for more effective human cell immunotherapy.

## References


Abel, A. M., Yang, C., Thakar, M. S. & Malarkannan, S. 2018. Natural Killer Cells: Development, Maturation, and Clinical Utilization. *Front Immunol,* 9**,** 1869.

Adair, J. E., Waters, T., Haworth, K. G., Kubek, S. P., Trobridge, G. D., Hocum, J. D., Heimfeld, S. & Kiem, H. P. 2016. Semi-automated closed system manufacturing of lentivirus gene-modified haematopoietic stem cells for gene therapy. *Nat Commun,* 7**,** 13173.

Afolabi, L. O., Adeshakin, A. O., Sani, M. M., Bi, J. & Wan, X. 2019. Genetic reprogramming for NK cell cancer immunotherapy with CRISPR/Cas9. *Immunology,* 158**,** 63-69.

Allan, D. S. J., Cerdeira, A. S., Ranjan, A., Kirkham, C. L., Aguilar, O. A., Tanaka, M., Childs, R. W., Dunbar, C. E., Strominger, J. L., Kopcow, H. D. & Carlyle, J. R. 2017. Transcriptome analysis reveals similarities between human blood CD3(-) CD56(bright) cells and mouse CD127(+) innate lymphoid cells. *Sci Rep,* 7**,** 3501.

Andersson, E., Poschke, I., Villabona, L., Carlson, J. W., Lundqvist, A., Kiessling, R., Seliger, B. & Masucci, G. V. 2016. Non-classical HLA-class I expression in serous ovarian carcinoma: Correlation with the HLA-genotype, tumor infiltrating immune cells and prognosis. *Oncoimmunology,* 5**,** e1052213.

Andre, P., Denis, C., Soulas, C., Bourbon-Caillet, C., Lopez, J., Arnoux, T., Blery, M., Bonnafous, C., Gauthier, L., Morel, A., Rossi, B., Remark, R., Breso, V., Bonnet, E., Habif, G., Guia, S., Lalanne, A. I., Hoffmann, C., Lantz, O., Fayette, J., Boyer-Chammard, A., Zerbib, R., Dodion, P., Ghadially, H., Jure-Kunkel, M., Morel, Y., Herbst, R., Narni-Mancinelli, E., Cohen, R. B. & Vivier, E. 2018. Anti-NKG2A mAb Is a Checkpoint Inhibitor that Promotes Anti-tumor Immunity by Unleashing Both T and NK Cells. *Cell,* 175**,** 1731-1743 e13.

Arai, S., Meagher, R., Swearingen, M., Myint, H., Rich, E., Martinson, J. & Klingemann, H. 2008. Infusion of the allogeneic cell line NK-92 in patients with advanced renal cell cancer or melanoma: a phase I trial. *Cytotherapy,* 10**,** 625-32.

Bak, R. O., Dever, D. P., Reinisch, A., Cruz Hernandez, D., Majeti, R. & Porteus, M. H. 2017. Multiplexed genetic engineering of human hematopoietic stem and progenitor cells using CRISPR/Cas9 and AAV6. *eLife,* 6.

Banerjea, A., Li, M. J., Remling, L., Rossi, J. & Akkina, R. 2004. Lentiviral transduction of Tar Decoy and CCR5 ribozyme into CD34+ progenitor cells and derivation of HIV-1 resistant T cells and macrophages. *AIDS Res Ther,* 1**,** 2.

Beldi-Ferchiou, A. & Caillat-Zucman, S. 2017. Control of NK Cell Activation by Immune Checkpoint Molecules. *Int J Mol Sci,* 18.

Beziat, V., Descours, B., Parizot, C., Debre, P. & Vieillard, V. 2010. NK cell terminal differentiation: correlated stepwise decrease of NKG2A and acquisition of KIRs. *PLoS One,* 5**,** e11966.

Bi, J. & Tian, Z. 2017. NK Cell Exhaustion. *Front Immunol,* 8**,** 760.

Billadeau, D. D., Brumbaugh, K. M., Dick, C. J., Schoon, R. A., Bustelo, X. R. & Leibson, P. J. 1998. The Vav–Rac1 Pathway in Cytotoxic Lymphocytes Regulates the Generation of Cell-mediated Killing. *J Exp Med,* 188**,** 549-59.

Bjorklund, A. T., Carlsten, M., Sohlberg, E., Liu, L. L., Clancy, T., Karimi, M., Cooley, S., Miller, J. S., Klimkowska, M., Schaffer, M., Watz, E., Wikstrom, K., Blomberg, P., Wahlin, B. E., Palma, M., Hansson, L., Ljungman, P., Hellstrom-Lindberg, E., Ljunggren, H. G. & Malmberg, K. J. 2018. Complete Remission with Reduction of High-Risk Clones following Haploidentical NK-Cell Therapy against MDS and AML. *Clin Cancer Res,* 24**,** 1834-1844.

Bjorkstrom, N. K., Riese, P., Heuts, F., Andersson, S., Fauriat, C., Ivarsson, M. A., Bjorklund, A. T., Flodstrom-Tullberg, M., Michaelsson, J., Rottenberg, M. E., Guzman, C. A., Ljunggren, H. G. & Malmberg, K. J. 2010. Expression patterns of NKG2A, KIR, and CD57 define a process of CD56dim NK-cell differentiation uncoupled from NK-cell education. *Blood,* 116**,** 3853-64.

Boos, M. D., Yokota, Y., Eberl, G. & Kee, B. L. 2007. Mature natural killer cell and lymphoid tissue–inducing cell development requires Id2-mediated suppression of E protein activity. *Journal of Experimental Medicine,* 204**,** 1119-1130.

Borrego, F., Kabat, J., Sanni, T. B. & Coligan, J. E. 2002. NK cell CD94/NKG2A inhibitory receptors are internalized and recycle independently of inhibitory signaling processes. *J Immunol,* 169**,** 6102-11.

Cameron, P., Fuller, C. K., Donohoue, P. D., Jones, B. N., Thompson, M. S., Carter, M. M., Gradia, S., Vidal, B., Garner, E., Slorach, E. M., Lau, E., Banh, L. M., Lied, A. M., Edwards, L. S., Settle, A. H., Capurso, D., Llaca, V., Deschamps, S., Cigan, M., Young, J. K. & May, A. P. 2017. Mapping the genomic landscape of CRISPR-Cas9 cleavage. *Nat Methods,* 14**,** 600-606.

Cante-Barrett, K., Mendes, R. D., Smits, W. K., van Helsdingen-van Wijk, Y. M., Pieters, R. & Meijerink, J. P. 2016. Lentiviral gene transfer into human and murine hematopoietic stem cells: size matters. *BMC Res Notes,* 9**,** 312.

Carrega, P. & Ferlazzo, G. 2012. Natural killer cell distribution and trafficking in human tissues. *Front Immunol,* 3**,** 347.

Case, S. S., Price, M. A., Jordan, C. T., Yu, X. J., Wang, L., Bauer, G., Haas, D. L., Xu, D., Stripecke, R., Naldini, L., Kohn, D. B. & Crooks, G. M. 1999. Stable transduction of quiescent CD34(+)CD38(-) human hematopoietic cells by HIV-1-based lentiviral vectors. . *Proc Natl Acad Sci U S A,* 96**,** 2988-93.

Chabannon, C., Mfarrej, B., Guia, S., Ugolini, S., Devillier, R., Blaise, D., Vivier, E. & Calmels, B. 2016. Manufacturing Natural Killer Cells as Medicinal Products. *Front Immunol,* 7**,** 504.

Chaix, J., Tessmer, M. S., Hoebe, K., Fuseri, N., Ryffel, B., Dalod, M., Alexopoulou, L., Beutler, B., Brossay, L., Vivier, E. & Walzer, T. 2008. Cutting edge: Priming of NK cells by IL-18. *J Immunol,* 181**,** 1627-31.

Chan, A., Hong, D. L., Atzberger, A., Kollnberger, S., Filer, A. D., Buckley, C. D., McMichael, A., Enver, T. & Bowness, P. 2007. CD56bright human NK cells differentiate into CD56dim cells: role of contact with peripheral fibroblasts. *J Immunol,* 179**,** 89-94.

Chan, L. L.-Y., Wucherpfennig, K. W. & de Andrade, L. F. 2019. Visualization and quantification of NK cell-mediated cytotoxicity over extended time periods by image cytometry. *Journal of Immunological Methods,* 469**,** 47-51.

Cheng, M., Chen, Y., Xiao, W., Sun, R. & Tian, Z. 2013. NK cell-based immunotherapy for malignant diseases. *Cell Mol Immunol,* 10**,** 230-52.

Cichocki, F., Bjordahl, R., Gaidarova, S., Mahmood, S., Abujarour, R., Wang, H., Tuininga, K., Felices, M., Davis, Z. B., Bendzick, L., Clarke, R., Stokely, L., Rogers, P., Ge, M., Robinson, M., Rezner, B., Robbins, D. L., Lee, T. T., Kaufman, D. S., Blazar, B. R., Valamehr, B. & Miller, J. S. 2020. iPSC-derived NK cells maintain high cytotoxicity and enhance in vivo tumor control in concert with T cells and anti-PD-1 therapy. *Sci Transl Med,* 12**,** eaaz5618.

Cichocki, F., Grzywacz, B. & Miller, J. S. 2019. Human NK Cell Development: One Road or Many? *Front Immunol,* 10**,** 2078.

Cong, L., Ran, F. A., Cox, D., Lin, S., Barretto, R., Habib, N., Hsu, P. D., Wu, X., Jiang, W., Marraffini, L. A. & Zhang, F. 2013. Multiplex genome engineering using CRISPR/Cas systems. *Science,* 339**,** 819-23.

Cowell, I. G., Skinner, A. & Hurst, H. C. 1992. Transcriptional repression by a novel member of the bZIP family of transcription factors. *Mol Cell Biol.,* 12**,** 3070-77.

Crotta, S., Gkioka, A., Male, V., Duarte, J. H., Davidson, S., Nisoli, I., Brady, H. J. & Wack, A. 2014. The transcription factor E4BP4 is not required for extramedullary pathways of NK cell development. *J Immunol,* 192**,** 2677-88.

Cuff, A. O., Robertson, F. P., Stegmann, K. A., Pallett, L. J., Maini, M. K., Davidson, B. R. & Male, V. 2016. Eomeshi NK Cells in Human Liver Are Long-Lived and Do Not Recirculate but Can Be Replenished from the Circulation. *J Immunol,* 197**,** 4283-4291.

Curti, A., Ruggeri, L., Parisi, S., Bontadini, A., Dan, E., Motta, M. R., Rizzi, S., Trabanelli, S., Ocadlikova, D., Lecciso, M., Giudice, V., Fruet, F., Urbani, E., Papayannidis, C., Martinelli, G., Bandini, G., Bonifazi, F., Lewis, R. E., Cavo, M., Velardi, A. & Lemoli, R. M. 2016. Larger Size of Donor Alloreactive NK Cell Repertoire Correlates with Better Response to NK Cell Immunotherapy in Elderly Acute Myeloid Leukemia Patients. *Clin Cancer Res,* 22**,** 1914-21.

Daussy, C., Faure, F., Mayol, K., Viel, S., Gasteiger, G., Charrier, E., Bienvenu, J., Henry, T., Debien, E., Hasan, U. A., Marvel, J., Yoh, K., Takahashi, S., Prinz, I., de Bernard, S., Buffat, L. & Walzer, T. 2014. T-bet and Eomes instruct the development of two distinct natural killer cell lineages in the liver and in the bone marrow. *J Exp Med,* 211**,** 563-77.

Denman, C. J., Senyukov, V. V., Somanchi, S. S., Phatarpekar, P. V., Kopp, L. M., Johnson, J. L., Singh, H., Hurton, L., Maiti, S. N., Huls, M. H., Champlin, R. E., Cooper, L. J. & Lee, D. A. 2012. Membrane-bound IL-21 promotes sustained ex vivo proliferation of human natural killer cells. *PLoS One,* 7**,** e30264.

Dever, D. P., Bak, R. O., Reinisch, A., Camarena, J., Washington, G., Nicolas, C. E., Pavel-Dinu, M., Saxena, N., Wilkens, A. B., Mantri, S., Uchida, N., Hendel, A., Narla, A., Majeti, R., Weinberg, K. I. & Porteus, M. H. 2016. CRISPR/Cas9 beta-globin gene targeting in human haematopoietic stem cells. *Nature,* 539**,** 384-389.

DiGiusto, D. L., Krishnan, A., Li, L., Li, H., Li, S., Rao, A., Mi, S., Yam, P., Stinson, S., Kalos, M., Alvarnas, J., Lacey, S. F., Yee, J. K., Li, M., Couture, L., Hsu, D.,

Forman, S. J., Rossi, J. J. & Zaia, J. A. 2010. RNA-based gene therapy for HIV with lentiviral vector-modified CD34(+) cells in patients undergoing transplantation for AIDS-related lymphoma. *Sci Transl Med,* 2**,** 36ra43.

Doench, J. G., Hartenian, E., Graham, D. B., Tothova, Z., Hegde, M., Smith, I., Sullender, M., Ebert, B. L., Xavier, R. J. & Root, D. E. 2014. Rational design of highly active sgRNAs for CRISPR-Cas9-mediated gene inactivation. *Nat Biotechnol,* 32**,** 1262-7.

Domogala, A., Blundell, M., Thrasher, A., Lowdell, M. W., Madrigal, J. A. & Saudemont, A. 2017. Natural killer cells differentiated in vitro from cord blood CD34(+) cells are more advantageous for use as an immunotherapy than peripheral blood and cord blood natural killer cells. *Cytotherapy,* 19**,** 710-720.

Domogala, A., Madrigal, J. A. & Saudemont, A. 2016. Cryopreservation has no effect on function of natural killer cells differentiated in vitro from umbilical cord blood CD34(+) cells. *Cytotherapy,* 18**,** 754-9.

Ely, K. H., Matsuoka, M., DeBerge, M. P., Ruby, J. A., Liu, J., Schneider, M. J., Wang, Y., Hahn, Y. S. & Enelow, R. I. 2014. Tissue-protective effects of NKG2A in immune-mediated clearance of virus infection. *PLoS One,* 9**,** e108385.

Fehniger, T. A., Shah, M. H., Turner, M. J., VanDeusen, J. B., Whitman, S. P., Goodsaid, F. & Caligiuri, M. A. 1999. Differential cytokine and chemokine gene expression by human NK cells following activation with IL-18 or IL-15 in combination with IL-12: implications for the innate immune response. *J immunol,* 162**,** 4511-20.

Figueiredo, C., Seltsam, A. & Blasczyk, R. 2009. Permanent silencing of NKG2A expression for cell-based therapeutics. *J Mol Med (Berl),* 87**,** 199-210.

Freud, A. G. & Caligiuri, M. A. 2006. Human natural killer cell development. *Immunological Reviews,* 214**,** 56-72.

Frias, A. M., Porada, C., Crapnell, K. B., Cabral, J. M. S., Zanjani, E. D. & Almeidia-Porada, G. 2008. Generation of Functional Natural Killer and Dendritic Cells in a Human Stromal-based Serum-free Culture System Designed for Cord Blood Expansion. *Exp Hematol,* 36**,** 61-8.

Fu, Y., Foden, J. A., Khayter, C., Maeder, M. L., Reyon, D., Joung, J. K. & Sander, J. D. 2013. High-frequency off-target mutagenesis induced by CRISPR-Cas nucleases in human cells. *Nat Biotechnol,* 31**,** 822-6.

Gascoyne, D. M., Long, E., Veiga-Fernandes, H., de Boer, J., Williams, O., Seddon, B., Coles, M., Kioussis, D. & Brady, H. J. 2009. The basic leucine zipper transcription factor E4BP4 is essential for natural killer cell development. *Nat Immunol,* 10**,** 1118-24.

Gill, S., Vasey, A. E., De Souza, A., Baker, J., Smith, A. T., Kohrt, H. E., Florek, M., Gibbs, K. D., Jr., Tate, K., Ritchie, D. S. & Negrin, R. S. 2012. Rapid development of exhaustion and down-regulation of eomesodermin limit the antitumor activity of adoptively transferred murine natural killer cells. *Blood,* 119**,** 5758-68.

Goh, W. & Huntington, N. D. 2017. Regulation of Murine Natural Killer Cell Development. *Front Immunol,* 8**,** 130.

Goodridge, J. P., Jacobs, B., Saetersmoen, M. L., Clement, D., Hammer, Q., Clancy, T., Skarpen, E., Brech, A., Landskron, J., Grimm, C., Pfefferle, A., Meza-Zepeda, L., Lorenz, S., Wiiger, M. T., Louch, W. E., Ask, E. H., Liu, L. L., Oei, V. Y. S., Kjallquist, U., Linnarsson, S., Patel, S., Tasken, K., Stenmark, H. & Malmberg, K. J. 2019. Remodeling of secretory lysosomes during education tunes functional potential in NK cells. *Nat Commun,* 10**,** 514.

Gordon, S. M., Chaix, J., Rupp, L. J., Wu, J., Madera, S., Sun, J. C., Lindsten, T. & Reiner, S. L. 2012. The transcription factors T-bet and Eomes control key checkpoints of natural killer cell maturation. *Immunity,* 36**,** 55-67.

Gotthardt, D., Trifinopoulos, J., Sexl, V. & Putz, E. M. 2019. JAK/STAT Cytokine Signaling at the Crossroad of NK Cell Development and Maturation. *Front Immunol,* 10**,** 2590.

Grzywacz, B., Kataria, N., Kataria, N., Blazar, B. R., Miller, J. S. & Verneris, M. R. 2011. Natural killer-cell differentiation by myeloid progenitors. *Blood,* 117**,** 3548-58.

Grzywacz, B., Kataria, N., Sikora, M., Oostendorp, R. A., Dzierzak, E. A., Blazar, B. R., Miller, J. S. & Verneris, M. R. 2006. Coordinated acquisition of inhibitory and activating receptors and functional properties by developing human natural killer cells. *Blood,* 108**,** 3824-33.

Guenechea, G., Gan, O. I., Inamitsu, T., Dorrell, C., Pereira, D. S., Kelly, M., Naldini, L. & Dick, J. E. 2000. Transduction of human CD34+ CD38- bone marrow and cord blood-derived SCID-repopulating cells with third-generation lentiviral vectors. *Mol Ther,* 1**,** 566-73.

Guillerey, C., Huntington, N. D. & Smyth, M. J. 2016. Targeting natural killer cells in cancer immunotherapy. *Nat Immunol,* 17**,** 1025-36.

Gundry, Michael C., Brunetti, L., Lin, A., Mayle, Allison E., Kitano, A., Wagner, D., Hsu, Joanne I., Hoegenauer, Kevin A., Rooney, Cliona M., Goodell, Margaret A. & Nakada, D. 2016. Highly Efficient Genome Editing of Murine and Human Hematopoietic Progenitor Cells by CRISPR/Cas9. *Cell Reports,* 17**,** 1453-1461.

Haddad, R., Guardiola, P., Izac, B., Thibault, C., Radich, J., Delezoide, A. L., Baillou, C., Lemoine, F. M., Gluckman, J. C., Pflumio, F. & Canque, B. 2004. Molecular characterization of early human T/NK and B-lymphoid progenitor cells in umbilical cord blood. *Blood,* 104**,** 3918-26.

He, Y. & Tian, Z. 2017. NK cell education via nonclassical MHC and non-MHC ligands. *Cell Mol Immunol,* 14**,** 321-330.

Hendel, A., Bak, R. O., Clark, J. T., Kennedy, A. B., Ryan, D. E., Roy, S., Steinfeld, I., Lunstad, B. D., Kaiser, R. J., Wilkens, A. B., Bacchetta, R., Tsalenko, A., Dellinger, D., Bruhn, L. & Porteus, M. H. 2015. Chemically modified guide RNAs enhance CRISPR-Cas genome editing in human primary cells. *Nat Biotechnol,* 33**,** 985-989.

Herberman, R. B., Nunn, M. E., Holden, H. T. & Lavrin, D. H. 1975a. Nautral cytotoxic reactivity of mouse lymphoid cells against syngeneic and allogeneic tumours. II. Characterization of effector cells. *Int. J. Cancer,* 16**,** 230-9.

Herberman, R. B., Nunn, M. E. & Lavrin, D. H. 1975b. Natural cytotoxic reactivity of mouse lymphoid cells against syngeneic and allogeneic tumors. I. Distribution of reactivity and specificity. *Int. J. Cancer,* 16**,** 216-29.

Herrera, L., Salcedo, J. M., Santos, S., Vesga, M. A., Borrego, F. & Eguizabal, C. 2017. OP9 Feeder Cells Are Superior to M2-10B4 Cells for the Generation of Mature and Functional Natural Killer Cells from Umbilical Cord Hematopoietic Progenitors. *Front Immunol,* 8**,** 755.

Ho, J. W., Hershkovitz, O., Peiris, M., Zilka, A., Bar-Ilan, A., Nal, B., Chu, K., Kudelko, M., Kam, Y. W., Achdout, H., Mandelboim, M., Altmeyer, R., Mandelboim, O., Bruzzone, R. & Porgador, A. 2008. H5-type influenza virus hemagglutinin is functionally recognized by the natural killer-activating receptor NKp44. *J Virol,* 82**,** 2028-32.

Hoogstad-van Evert, J. S., Cany, J., van den Brand, D., Oudenampsen, M., Brock, R., Torensma, R., Bekkers, R. L., Jansen, J. H., Massuger, L. F. & Dolstra, H. 2017.

Umbilical cord blood CD34(+) progenitor-derived NK cells efficiently kill ovarian cancer spheroids and intraperitoneal tumors in NOD/SCID/IL2Rg(null) mice. *Oncoimmunology,* 6**,** e1320630.

Hordyjewska, A., Popiolek, L. & Horecka, A. 2015. Characteristics of hematopoietic stem cells of umbilical cord blood. *Cytotechnology,* 67**,** 387-96.

Horowitz, A., Stegmann, K. A. & Riley, E. M. 2011. Activation of natural killer cells during microbial infections. *Front Immunol,* 2**,** 88.

Hsu, P. D., Scott, D. A., Weinstein, J. A., Ran, F. A., Konermann, S., Agarwala, V., Li, Y., Fine, E. J., Wu, X., Shalem, O., Cradick, T. J., Marraffini, L. A., Bao, G. & Zhang, F. 2013. DNA targeting specificity of RNA-guided Cas9 nucleases. *Nat Biotechnol,* 31**,** 827-32.

Huang, R.-S., Shih, H.-A., Lai, M.-C., Chang, Y.-J. & Lin, S. 2020. Enhanced NK-92 Cytotoxicity by CRISPR Genome Engineering Using Cas9 Ribonucleoproteins. *Frontiers in Immunology,* 11.

Intlekofer, A. M., Takemoto, N., Wherry, E. J., Longworth, S. A., Northrup, J. T., Palanivel, V. R., Mullen, A. C., Gasink, C. R., Kaech, S. M., Miller, J. D., Gapin, L., Ryan, K., Russ, A. P., Lindsten, T., Orange, J. S., Goldrath, A. W., Ahmed, R. & Reiner, S. L. 2005. Effector and memory CD8+ T cell fate coupled by T-bet and eomesodermin. *Nat Immunol,* 6**,** 1236-44.

Ivarsson, M. A., Loh, L., Marquardt, N., Kekalainen, E., Berglin, L., Bjorkstrom, N. K., Westgren, M., Nixon, D. F. & Michaelsson, J. 2013. Differentiation and functional regulation of human fetal NK cells. *J Clin Invest,* 123**,** 3889-901.

Jacobs, R., Hintzen, G., Kemper, A., Beul, K., Kempf, S., Behrens, G., Sykora, K.-W. & Schmidt, R. 2001. CD56bright cells differ in their KIR repertoire and cytotoxic features from CD56dim NK cells. *Eur. J. Immunol,* 31.

Jenne, C. N., Enders, A., Rivera, R., Watson, S. R., Bankovich, A. J., Pereira, J. P., Xu, Y., Roots, C. M., Beilke, J. N., Banerjee, A., Reiner, S. L., Miller, S. A., Weinmann, A. S., Goodnow, C. C., Lanier, L. L., Cyster, J. G. & Chun, J. 2009. T-bet-dependent S1P5 expression in NK cells promotes egress from lymph nodes and bone marrow. *J Exp Med,* 206**,** 2469-81.

Jinek, M., Chylinski, K., Fonfara, I., Hauer, M., Doudna, J. A. & Charpentier, E. 2012. A programmable dual-RNA-guided DNA endonuclease in adaptive bacterial immunity. *Science,* 337**,** 816-21.

Joncker, N. T., Fernandez, N. C., Treiner, E., Vivier, E. & Raulet, D. H. 2009. NK cell responsiveness is tuned commensurate with the number of inhibitory receptors for self-MHC class I: the rheostat model. *J Immunol,* 182**,** 4572-80.

Joncker, N. T., Shifrin, N., Delebecque, F. & Raulet, D. H. 2010. Mature natural killer cells reset their responsiveness when exposed to an altered MHC environment. *J Exp Med,* 207**,** 2065-72.

Joyce, M. G. & Sun, P. D. 2011. The structural basis of ligand recognition by natural killer cell receptors. *J Biomed Biotechnol,* 2011**,** 203628.

Judge, A. D., Sood, V., Shaw, J. R., Fang, D., McClintock, K. & MacLachlan, I. 2005. Sequence-dependent stimulation of the mammalian innate immune response by synthetic siRNA. *Nat Biotechnol,* 23**,** 457-62.

Kabadi, A. M., Ousterout, D. G., Hilton, I. B. & Gersbach, C. A. 2014. Multiplex CRISPR/Cas9-based genome engineering from a single lentiviral vector. *Nucleic Acids Res,* 42**,** e147.

Kabat, J., Borrego, F., Brooks, A. & Coligan, J. E. 2002. Role that each NKG2A immunoreceptor tyrosine-based inhibitory motif plays in mediating the human CD94/NKG2A inhibitory signal. *J Immunol,* 169**,** 1948-58.

Kallies, A., Carotta, S., Huntington, N. D., Bernard, N. J., Tarlinton, D. M., Smyth, M. J. & Nutt, S. L. 2011. A role for Blimp1 in the transcriptional network controlling natural killer cell maturation. *Blood,* 117**,** 1869-79.

Kamiya, T., Seow, S. V., Wong, D., Robinson, M. & Campana, D. 2019. Blocking expression of inhibitory receptor NKG2A overcomes tumor resistance to NK cells. *J Clin Invest,* 129**,** 2094-2106.

Kamizono, S., Duncan, G. S., Seidel, M. G., Morimoto, A., Hamada, K., Grosveld, G., Akashi, K., Lind, E. F., Haight, J. P., Ohashi, P. S., Look, A. T. & Mak, T. W. 2009. Nfil3/E4bp4 is required for the development and maturation of NK cells in vivo. *J Exp Med,* 206**,** 2977-86.

Kashiwada, M., Levy, D. M., McKeag, L., Murray, K., Schroder, A. J., Canfield, S. M., Traver, G. & Rothman, P. B. 2010. IL-4-induced transcription factor NFIL3/E4BP4 controls IgE class switching. *Proc Natl Acad Sci U S A,* 107**,** 821-6.

Kashiwada, M., Pham, N. L., Pewe, L. L., Harty, J. T. & Rothman, P. B. 2011. NFIL3/E4BP4 is a key transcription factor for CD8alpha(+) dendritic cell development. *Blood,* 117**,** 6193-7.

Kee, B. L., Morman, R. E. & Sun, M. 2020. Transcriptional regulation of natural killer cell development and maturation. *Adv Immunol,* 146**,** 1-28.

Khan, M., Arooj, S. & Wang, H. 2020. NK Cell-Based Immune Checkpoint Inhibition. *Front Immunol,* 11**,** 167.

Kiessling, R., Klein, E., Pross, H. & Wigzell, H. 1975. "Natural" killer cells in the mouse. II. Cytotoxic cells with specificity for mouse Moloney leukemia cells. Characteristics of the killer cell. *Eur J Immunol,* 5.

Klingemann, H., Boissel, L. & Toneguzzo, F. 2016. Natural Killer Cells for Immunotherapy – Advantages of the NK-92 Cell Line over Blood NK Cells. *Frontiers in Immunology,* 7.

Knox, J. J., Cosma, G. L., Betts, M. R. & McLane, L. M. 2014. Characterization of T-bet and eomes in peripheral human immune cells. *Front Immunol,* 5**,** 217.

Kobayashi, T., Matsuoka, K., Sheikh, S. Z., Elloumi, H. Z., Kamada, N., Hisamatsu, T., Hansen, J. J., Doty, K. R., Pope, S. D., Smale, S. T., Hibi, T., Rothman, P. B., Kashiwada, M. & Plevy, S. E. 2011. NFIL3 is a regulator of IL-12 p40 in macrophages and mucosal immunity. *J Immunol,* 186**,** 4649-55.

Kostrzewski, T., Borg, A. J., Meng, Y., Filipovic, I., Male, V., Wack, A., DiMaggio, P. A. & Brady, H. J. M. 2018. Multiple Levels of Control Determine How E4bp4/Nfil3 Regulates NK Cell Development. *J Immunol,* 200**,** 1370-1381.

Kutner, R. H., Zhang, X. Y. & Reiser, J. 2009. Production, concentration and titration of pseudotyped HIV-1-based lentiviral vectors. *Nat Protoc,* 4**,** 495-505.

Labun, K., Montague, T. G., Gagnon, J. A., Thyme, S. B. & Valen, E. 2016. CHOPCHOP v2: a web tool for the next generation of CRISPR genome engineering. *Nucleic Acids Res,* 44**,** W272-6.

Langdon, S. P., Hawkes, M. M., Lawrie, S. S., Hawkins, R. A., Tesdale, A. L., Crew, A. J., Miller, W. R. & Smyth, J. F. 1990. Oestrogen receptor expression and the effects of oestrogen and tamoxifen on the growth of human ovarian carcinoma cell lines. *British Journal of Cancer,* 62**,** 213-216.

Lanier, L. L., Ruitenberg, J. J. & Philips, J. H. 1988. Functional and biochemical analysis of CD16 antigen on natural killer cells and granulocytes. *J Immunol,* 141**,** 3478-85.

Lanuza, P. M., Pesini, C., Arias, M. A., Calvo, C., Ramirez-Labrada, A. & Pardo, J. 2019. Recalling the Biological Significance of Immune Checkpoints on NK

Cells: A Chance to Overcome LAG3, PD1, and CTLA4 Inhibitory Pathways by Adoptive NK Cell Transfer? *Front Immunol,* 10**,** 3010.

Larkin, J., Chiarion-Sileni, V., Gonzalez, R., Grob, J. J., Cowey, C. L., Lao, C. D., Schadendorf, D., Dummer, R., Smylie, M., Rutkowski, P., Ferrucci, P. F., Hill, A., Wagstaff, J., Carlino, M. S., Haanen, J. B., Maio, M., Marquez-Rodas, I., McArthur, G. A., Ascierto, P. A., Long, G. V., Callahan, M. K., Postow, M. A., Grossmann, K., Sznol, M., Dreno, B., Bastholt, L., Yang, A., Rollin, L. M., Horak, C., Hodi, F. S. & Wolchok, J. D. 2015. Combined Nivolumab and Ipilimumab or Monotherapy in Untreated Melanoma. *N Engl J Med,* 373**,** 23-34.

Lee, N., Llano, M., Carretero, M., Ishitani, A., Navarro, F., López-Botet, M. & Geraghty, D. E. 1998. HLA-E is a major ligand for the natural killer inhibitory receptor CD94/NKG2A. *Proc Natl Acad Sci U S A,* 95**,** 5199-204.

Lehmann, D., Spanholtz, J., Sturtzel, C., Tordoir, M., Schlechta, B., Groenewegen, D. & Hofer, E. 2014. IL-12 directs further maturation of ex vivo differentiated NK cells with improved therapeutic potential. *PLoS One,* 9**,** e87131.

Leibson, P. J. 1998. Cytotoxic Lymphocyte Recognition of HLA-E: Utilizing a Nonclassical Window to Peer into Classical MHC. *Immunity,* 9**,** 289-294.

Li, Y., Hermanson, D. L., Moriarity, B. S. & Kaufman, D. S. 2018. Human iPSC-Derived Natural Killer Cells Engineered with Chimeric Antigen Receptors Enhance Anti-tumor Activity. *Cell Stem Cell,* 23**,** 181-192 e5.

Lieber, M. R., Ma, Y., Pannicke, U. & Schwarz, K. 2003. Mechanism and regulation of human non-homologous DNA end-joining. *Nat Rev Mol Cell Biol,* 4**,** 712-20.

Liu, E., Marin, D., Banerjee, P., Macapinlac, H. A., Thompson, P., Basar, R., Nassif Kerbauy, L., Overman, B., Thall, P., Kaplan, M., Nandivada, V., Kaur, I., Nunez Cortes, A., Cao, K., Daher, M., Hosing, C., Cohen, E. N., Kebriaei, P., Mehta, R., Neelapu, S., Nieto, Y., Wang, M., Wierda, W., Keating, M., Champlin, R., Shpall, E. J. & Rezvani, K. 2020. Use of CAR-Transduced Natural Killer Cells in CD19-Positive Lymphoid Tumors. *N Engl J Med,* 382**,** 545-553.

Liu, Y., Hangoc, G., Campbell, T. B., Goodman, M., Tao, W., Pollok, K., Srour, E. F. & Broxmeyer, H. E. 2008. Identification of parameters required for efficient lentiviral vector transduction and engraftment of human cord blood CD34(+) NOD/SCID-repopulating cells. *Exp Hematol,* 36**,** 947-56.

Long, E. O., Kim, H. S., Liu, D., Peterson, M. E. & Rajagopalan, S. 2013. Controlling natural killer cell responses: integration of signals for activation and inhibition. *Annu Rev Immunol,* 31**,** 227-58.

Luevano, M., Domogala, A., Blundell, M., Jackson, N., Pedroza-Pacheco, I., Derniame, S., Escobedo-Cousin, M., Querol, S., Thrasher, A., Madrigal, A. & Saudemont, A. 2014. Frozen cord blood hematopoietic stem cells differentiate into higher numbers of functional natural killer cells in vitro than mobilized hematopoietic stem cells or freshly isolated cord blood hematopoietic stem cells. *PLoS One,* 9**,** e87086.

Lundqvist, A., Berg, M., Smith, A. & Childs, R. W. 2011. Bortezomib Treatment to Potentiate the Anti-tumor Immunity of Ex-vivo Expanded Adoptively Infused Autologous Natural Killer Cells. *J Cancer,* 2**,** 383-5.

Male, V., Nisoli, I., Kostrzewski, T., Allan, D. S., Carlyle, J. R., Lord, G. M., Wack, A. & Brady, H. J. 2014. The transcription factor E4bp4/Nfil3 controls commitment to the NK lineage and directly regulates Eomes and Id2 expression. *J Exp Med,* 211**,** 635-42.

Mandelboim, O., Lieberman, N., Lev, M., Paul, L., Arnon, T. I., Bushkin, Y., Davis, D. M., Strominger, J. L., Yewdell, J. W. & Porgador, A. 2001. Recognition of haemagglutinins on virus-infected cells by NKp46 activates lysis by human NK cells. *Nature,* 409**,** 1055-1060.

Marquardt, N., Beziat, V., Nystrom, S., Hengst, J., Ivarsson, M. A., Kekalainen, E., Johansson, H., Mjosberg, J., Westgren, M., Lankisch, T. O., Wedemeyer, H., Ellis, E. C., Ljunggren, H. G., Michaelsson, J. & Bjorkstrom, N. K. 2015. Cutting edge: identification and characterization of human intrahepatic CD49a+ NK cells. *J Immunol,* 194**,** 2467-71.

McCullar, V., Oostendorp, R. A., Panoskaltsis-Mortari, A., Yung, G., Lutz, C. T., Wagner, J. E. & Miller, J. S. 2009. Mouse fetal and embryonic liver cells differentiate human umbilical cord blood (UCB) progenitors into CD56 negative NK cell precursors in the absence of IL-15. *Exp Hematol,* 36**,** 598-608.

McWilliams, E. M., Mele, J. M., Cheney, C., Timmerman, E. A., Fiazuddin, F., Strattan, E. J., Mo, X., Byrd, J. C., Muthusamy, N. & Awan, F. T. 2016. Therapeutic CD94/NKG2A blockade improves natural killer cell dysfunction in chronic lymphocytic leukemia. *Oncoimmunology,* 5**,** e1226720.

Meade, J. L., Wilson, E. B., Holmes, T. D., de Wynter, E. A., Brett, P., Straszynski, L., Ballard, P. A., Trapani, J. A., McDermott, M. F. & Cook, G. P. 2009. Proteolytic activation of the cytotoxic phenotype during human NK cell development. *J Immunol,* 183**,** 803-13.

Mesquitta, W.-T., Wandsnider, M., Kang, H., Thomson, J., Moskvin, O., Suknuntha, K. & Slukvin, I. I. 2019. UM171 expands distinct types of myeloid and NK progenitors from human pluripotent stem cells. *Scientific Reports,* 9.

Miller, J. S., Soignier, Y., Panoskaltsis-Mortari, A., McNearney, S. A., Yun, G. H., Fautsch, S. K., McKenna, D., Le, C., Defor, T. E., Burns, L. J., Orchard, P. J., Blazar, B. R., Wagner, J. E., Slungaard, A., Weisdorf, D. J., Okazaki, I. J. & McGlave, P. B. 2005. Successful adoptive transfer and in vivo expansion of human haploidentical NK cells in patients with cancer. *Blood,* 105**,** 3051-7.

Mitsui, S., Yamaguchi, S., Matsuo, T., Ishida, Y. & Okamura, H. 2001. Antagonistic role of E4BP4 and PAR proteins in the circadian oscillatory mechanism. *Genes Dev,* 15**,** 995-1006.

Montaldo, E., Del Zotto, G., Della Chiesa, M., Mingari, M. C., Moretta, A., De Maria, A. & Moretta, L. 2013. Human NK cell receptors/markers: a tool to analyze NK cell development, subsets and function. *Cytometry A,* 83**,** 702-13.

Moreno-Mateos, M. A., Vejnar, C. E., Beaudoin, J. D., Fernandez, J. P., Mis, E. K., Khokha, M. K. & Giraldez, A. J. 2015. CRISPRscan: designing highly efficient sgRNAs for CRISPR-Cas9 targeting in vivo. *Nat Methods,* 12**,** 982-8.

Moretta, A., Bottino, C., Vitale, M., Pende, D., Cantoni, C., Mingari, M. C., Biassoni, R. & Moretta, L. 2001. Activating receptors and coreceptors involved in human natural killer cell-mediated cytolysis. *Annu Rev Immunol,* 19**,** 197-223.

Morgan, R. A., Gray, D., Lomova, A. & Kohn, D. B. 2017. Hematopoietic Stem Cell Gene Therapy: Progress and Lessons Learned. *Cell Stem Cell,* 21**,** 574-590.

Muntasell, A., Ochoa, M. C., Cordeiro, L., Berraondo, P., Lopez-Diaz de Cerio, A., Cabo, M., Lopez-Botet, M. & Melero, I. 2017. Targeting NK-cell checkpoints for cancer immunotherapy. *Curr Opin Immunol,* 45**,** 73-81.

Nagler, A., Lanier, L. L. & Philips, J. H. 1990. Constitutive expression of high affinity interleukin 2 receptors on human CD16-natural killer cells in vivo. *J Exp Med,* 171**,** 1527-33.

Naiyer, M. M., Cassidy, S. A., Magri, A., Cowton, V., Chen, K., Mansour, S., Kranidioti, H., Mbiribindi, B., Rettman, P., Harris, S., Fanning, L. J., Mulder, A., Claas, F.

H. J., Davidson, A. D., Patel, A. H., Purbhoo, M. A. & Khakoo, S. I. 2017. KIR2DS2 recognizes conserved peptides derived from viral helicases in the context of HLA-C. *Science Immunology,* 2**,** eaal5296.

Naldini, L., Blomer, U., Gallay, P., Ory, D., Mulligan, R., Gage, F. H., Verma, I. M. & Trono, D. 1996. In Vivo Gene Delivery and Stable Transduction of Nondividing Cells by a Lentiviral Vector. *Science,* 272**,** 263-7.

Nash, W. T., Teoh, J., Wei, H., Gamache, A. & Brown, M. G. 2014. Know Thyself: NK-Cell Inhibitory Receptors Prompt Self-Tolerance, Education, and Viral Control. *Front Immunol,* 5**,** 175.

Ngom, M., Imren, S., Maetzig, T., Adair, J. E., Knapp, D. J. H. F., Chagraoui, J., Fares, I., Bordeleau, M.-E., Sauvageau, G., Leboulch, P., Eaves, C. & Humphries, R. K. 2018. UM171 Enhances Lentiviral Gene Transfer and Recovery of Primitive Human Hematopoietic Cells. *Molecular Therapy - Methods & Clinical Development,* 10**,** 156-164.

Papaioannou, V. E. 2014. The T-box gene family: emerging roles in development, stem cells and cancer. *Development,* 141**,** 3819-33.

Parkhurst, M. R., Riley, J. P., Dudley, M. E. & Rosenberg, S. A. 2011. Adoptive transfer of autologous natural killer cells leads to high levels of circulating natural killer cells but does not mediate tumor regression. *Clin Cancer Res,* 17**,** 6287-97.

Pay, S. L., Qi, X., Willard, J. F., Godoy, J., Sankhavaram, K., Horton, R., Mitter, S. K., Quigley, J. L., Chang, L. J., Grant, M. B. & Boulton, M. E. 2018. Improving the Transduction of Bone Marrow-Derived Cells with an Integrase-Defective Lentiviral Vector. *Hum Gene Ther Methods,* 29**,** 44-59.

Perez, S. A., Mahaira, L. G., Demirtzoglou, F. J., Sotiropoulou, P. A., Ioannidis, P., Iliopoulou, E. G., Gritzapis, A. D., Sotiriadou, N. N., Baxevanis, C. N. & Papamichail, M. 2005. A potential role for hydrocortisone in the positive regulation of IL-15-activated NK-cell proliferation and survival. *Blood,* 106**,** 158-66.

Perez, S. A., Mahaira, L. G., Sotiropoulou, P. A., Gritzapis, A. D., Iliopoulou, E. G., Niarchos, D. K., Cacoullos, N. T., Kavalakis, Y. G., Antsaklis, A. I., Sotiriadou, N. N., Baxevanis, C. N. & Papamichail, M. 2006. Effect of IL-21 on NK cells derived from different umbilical cord blood populations. *Int Immunol,* 18**,** 49-58.

Pesce, S., Greppi, M., Tabellini, G., Rampinelli, F., Parolini, S., Olive, D., Moretta, L., Moretta, A. & Marcenaro, E. 2017. Identification of a subset of human natural

killer cells expressing high levels of programmed death 1: A phenotypic and functional characterization. *J Allergy Clin Immunol,* 139**,** 335-346 e3.

Petrillo, C., Thorne, L. G., Unali, G., Schiroli, G., Giordano, A. M. S., Piras, F., Cuccovillo, I., Petit, S. J., Ahsan, F., Noursadeghi, M., Clare, S., Genovese, P., Gentner, B., Naldini, L., Towers, G. J. & Kajaste-Rudnitski, A. 2018. Cyclosporine H Overcomes Innate Immune Restrictions to Improve Lentiviral Transduction and Gene Editing In Human Hematopoietic Stem Cells. *Cell Stem Cell,* 23**,** 820-832 e9.

Pfefferle, A. & Huntington, N. D. 2020. You Have Got a Fast CAR: Chimeric Antigen Receptor NK Cells in Cancer Therapy. *Cancers (Basel),* 12.

Pupuleku, A., Costa-Garcia, M., Farre, D., Hengel, H., Angulo, A., Muntasell, A. & Lopez-Botet, M. 2017. Elusive Role of the CD94/NKG2C NK Cell Receptor in the Response to Cytomegalovirus: Novel Experimental Observations in a Reporter Cell System. *Front Immunol,* 8**,** 1317.

Ramirez, K., Chandler, K. J., Spaulding, C., Zandi, S., Sigvardsson, M., Graves, B. J. & Kee, B. L. 2012. Gene deregulation and chronic activation in natural killer cells deficient in the transcription factor ETS1. *Immunity,* 36**,** 921-32.

Rezvani, K. 2019. Adoptive cell therapy using engineered natural killer cells. *Bone Marrow Transplant,* 54**,** 785-788.

Roeven, M. W., Thordardottir, S., Kohela, A., Maas, F., Preijers, F., Jansen, J. H., Blijlevens, N. M., Cany, J., Schaap, N. & Dolstra, H. 2015. The Aryl Hydrocarbon Receptor Antagonist StemRegenin1 Improves In Vitro Generation of Highly Functional Natural Killer Cells from CD34(+) Hematopoietic Stem and Progenitor Cells. *Stem Cells Dev,* 24**,** 2886-98.

Rolle, A., Meyer, M., Calderazzo, S., Jager, D. & Momburg, F. 2018. Distinct HLA-E Peptide Complexes Modify Antibody-Driven Effector Functions of Adaptive NK Cells. *Cell Rep,* 24**,** 1967-1976 e4.

Romagnani, C., Juelke, K., Falco, M., Morandi, B., D'Agostino, A., Costa, R., Ratto, G., Forte, G., Carrega, P., Lui, G., Conte, R., Strowig, T., Moretta, A., Munz, C., Thiel, A., Moretta, L. & Ferlazzo, G. 2007. CD56brightCD16- killer Ig-like receptor- NK cells display longer telomeres and acquire features of CD56dim NK cells upon activation. *J Immunol,* 178**,** 4947-55.

Russ, A. P., Wattler, S., Colledge, W. H., Aparicio, S. A., Carlton, M. B., Pearce, J. J., Barton, S. C., Surani, M. A., Ryan, K., Nehls, M. C., Wilson, V. & Evans, M. J.

2000. Eomesodermin is required for mouse trophoblast development and mesoderm formation. *Nature,* 404**,** 95-9.

Ryu, S.-M., Hur, J. W. & Kim, K. 2019. Evolution of CRISPR towards accurate and efficient mammal genome engineering. *BMB Reports,* 52**,** 475-481.

Salcedo, T. W., Azzoni, L., Wolf, S. F. & Perussia, B. 1993. Modulation of perforin and granzyme messenger RNA expression in human natural killer cells. *J Immunol,* 151**,** 2511-2520.

Sander, J. D. & Joung, J. K. 2014. CRISPR-Cas systems for editing, regulating and targeting genomes. *Nat Biotechnol,* 32**,** 347-55.

Sarvaria, A., Jawdat, D., Madrigal, J. A. & Saudemont, A. 2017. Umbilical Cord Blood Natural Killer Cells, Their Characteristics, and Potential Clinical Applications. *Front Immunol,* 8**,** 329.

Schlecker, E., Fiegler, N., Arnold, A., Altevogt, P., Rose-John, S., Moldenhauer, G., Sucker, A., Paschen, A., von Strandmann, E. P., Textor, S. & Cerwenka, A. 2014. Metalloprotease-mediated tumor cell shedding of B7-H6, the ligand of the natural killer cell-activating receptor NKp30. *Cancer Res,* 74**,** 3429-40.

Scoville, S. D., Freud, A. G. & Caligiuri, M. A. 2017. Modeling Human Natural Killer Cell Development in the Era of Innate Lymphoid Cells. *Front Immunol,* 8**,** 360.

Seita, J. & Weissman, I. L. 2010. Hematopoietic stem cell: self-renewal versus differentiation. *Wiley Interdiscip Rev Syst Biol Med,* 2**,** 640-53.

Senju, H., Kumagai, A., Nakamura, Y., Yamaguchi, H., Nakatomi, K., Fukami, S., Shiraishi, K., Harada, Y., Nakamura, M., Okamura, H., Tanaka, Y. & Mukae, H. 2018. Effect of IL-18 on the Expansion and Phenotype of Human Natural Killer Cells: Application to Cancer Immunotherapy. *Int J Biol Sci,* 14**,** 331-340.

Shi, F. D., Ljunggren, H. G., La Cava, A. & Van Kaer, L. 2011. Organ-specific features of natural killer cells. *Nat Rev Immunol,* 11**,** 658-71.

Shin, M. H., Kim, J., Lim, S. A., Kim, J., Kim, S. J. & Lee, K. M. 2020. NK Cell-Based Immunotherapies in Cancer. *Immune Netw,* 20**,** e14.

Sim, M. J., Stowell, J., Sergeant, R., Altmann, D. M., Long, E. O. & Boyton, R. J. 2016. KIR2DL3 and KIR2DL1 show similar impact on licensing of human NK cells. *Eur J Immunol,* 46**,** 185-91.

Sim, M. J. W., Rajagopalan, S., Altmann, D. M., Boyton, R. J., Sun, P. D. & Long, E. O. 2019. Human NK cell receptor KIR2DS4 detects a conserved bacterial epitope presented by HLA-C. *Proc Natl Acad Sci U S A,* 116**,** 12964-12973.

Simonetta, F., Pradier, A. & Roosnek, E. 2016. T-bet and Eomesodermin in NK Cell Development, Maturation, and Function. *Front Immunol,* 7**,** 241.

Skak, K., Frederiksen, K. S. & Lundsgaard, D. 2008. Interleukin-21 activates human natural killer cells and modulates their surface receptor expression. *Immunology,* 123**,** 575-83.

Sordo-Bahamonde, C., Lorenzo-Herrero, S., Payer, A. R., Gonzalez, S. & Lopez-Soto, A. 2020. Mechanisms of Apoptosis Resistance to NK Cell-Mediated Cytotoxicity in Cancer. *Int J Mol Sci,* 21.

Spanholtz, J., Preijers, F., Tordoir, M., Trilsbeek, C., Paardekooper, J., de Witte, T., Schaap, N. & Dolstra, H. 2011. Clinical-grade generation of active NK cells from cord blood hematopoietic progenitor cells for immunotherapy using a closed-system culture process. *PLoS One,* 6**,** e20740.

Spits, H. & Di Santo, J. P. 2011. The expanding family of innate lymphoid cells: regulators and effectors of immunity and tissue remodeling. *Nat Immunol,* 12**,** 21-7.

Takahashi, K., Tanabe, K., Ohnuki, M., Narita, M., Ichisaka, T., Tomoda, K. & Yamanaka, S. 2007. Induction of pluripotent stem cells from adult human fibroblasts by defined factors. *Cell,* 131**,** 861-72.

Tanaka, J., Sugita, J., Shiratori, S., Shigematu, A., Asanuma, S., Fujimoto, K., Nishio, M., Kondo, T. & Imamura, M. 2012. Expansion of NK cells from cord blood with antileukemic activity using GMP-compliant substances without feeder cells. *Leukemia,* 26**,** 1149-52.

Thielens, A., Vivier, E. & Romagne, F. 2012. NK cell MHC class I specific receptors (KIR): from biology to clinical intervention. *Curr Opin Immunol,* 24**,** 239-45.

Tinker, A. V., Hirte, H. W., Provencher, D., Butler, M., Ritter, H., Tu, D., Azim, H. A., Jr., Paralejas, P., Grenier, N., Hahn, S. A., Ramsahai, J. & Seymour, L. 2019. Dose-Ranging and Cohort-Expansion Study of Monalizumab (IPH2201) in Patients with Advanced Gynecologic Malignancies: A Trial of the Canadian Cancer Trials Group (CCTG): IND221. *Clin Cancer Res,* 25**,** 6052-6060.

Tonn, T., Schwabe, D., Klingemann, H. G., Becker, S., Esser, R., Koehl, U., Suttorp, M., Seifried, E., Ottmann, O. G. & Bug, G. 2013. Treatment of patients with advanced cancer with the natural killer cell line NK-92. *Cytotherapy,* 15**,** 1563-70.

Townsend, M. J., Weinmann, A. S., Matsuda, J. L., Salomon, R., Farnham, P. J., Biron, C. A., Gapin, L. & Glimcher, L. H. 2004. T-bet regulates the terminal maturation and homeostasis of NK and Valpha14i NKT cells. *Immunity,* 20**,** 477-94.

Vacca, P., Vitale, C., Montaldo, E., Conte, R., Cantoni, C., Fulcheri, E., Darretta, V., Moretta, L. & Mingari, M. C. 2011. CD34+ hematopoietic precursors are present in human decidua and differentiate into natural killer cells upon interaction with stromal cells. *Proc Natl Acad Sci U S A,* 108**,** 2402-7.

van Helden, M. J., Goossens, S., Daussy, C., Mathieu, A. L., Faure, F., Marcais, A., Vandamme, N., Farla, N., Mayol, K., Viel, S., Degouve, S., Debien, E., Seuntjens, E., Conidi, A., Chaix, J., Mangeot, P., de Bernard, S., Buffat, L., Haigh, J. J., Huylebroeck, D., Lambrecht, B. N., Berx, G. & Walzer, T. 2015. Terminal NK cell maturation is controlled by concerted actions of T-bet and Zeb2 and is essential for melanoma rejection. *J Exp Med,* 212**,** 2015-25.

Veluchamy, J. P., Delso-Vallejo, M., Kok, N., Bohme, F., Seggewiss-Bernhardt, R., van der Vliet, H. J., de Gruijl, T. D., Huppert, V. & Spanholtz, J. 2017. Standardized and flexible eight colour flow cytometry panels harmonized between different laboratories to study human NK cell phenotype and function. *Sci Rep,* 7**,** 43873.

Vivier, E., Raulet, D. H., Moretta, A., Caligiuri, M. A., Zitvogel, L., Lanier, L. L., Yokoyama, W. M. & Ugolini, S. 2011. Innate or Adaptive Immunity? The Example of Natural Killer Cells. *Science,* 331**,** 44-9.

Vivier, E., Tomasello, E., Baratin, M., Walzer, T. & Ugolini, S. 2008. Functions of natural killer cells. *Nat Immunol,* 9**,** 503-10.

Wang, D. & Malarkannan, S. 2020. Transcriptional Regulation of Natural Killer Cell Development and Functions. *Cancers (Basel),* 12.

Wang, H. X., Li, M., Lee, C. M., Chakraborty, S., Kim, H. W., Bao, G. & Leong, K. W. 2017. CRISPR/Cas9-Based Genome Editing for Disease Modeling and Therapy: Challenges and Opportunities for Nonviral Delivery. *Chem Rev,* 117**,** 9874-9906.

WareJoncas, Z., Campbell, J. M., Martinez-Galvez, G., Gendron, W. A. C., Barry, M. A., Harris, P. C., Sussman, C. R. & Ekker, S. C. 2018. Precision gene editing technology and applications in nephrology. *Nat Rev Nephrol,* 14**,** 663-677.

Wu, Y., Tian, Z. & Wei, H. 2017. Developmental and Functional Control of Natural Killer Cells by Cytokines. *Front Immunol,* 8**,** 930.

Xie, G., Dong, H., Liang, Y., Ham, J. D., Rizwan, R. & Chen, J. 2020. CAR-NK cells: A promising cellular immunotherapy for cancer. *EBioMedicine,* 59**,** 102975.

Xu, W., Domingues, R. G., Fonseca-Pereira, D., Ferreira, M., Ribeiro, H., Lopez-Lastra, S., Motomura, Y., Moreira-Santos, L., Bihl, F., Braud, V., Kee, B., Brady, H., Coles, M. C., Vosshenrich, C., Kubo, M., Di Santo, J. P. & Veiga-Fernandes, H. 2015. NFIL3 orchestrates the emergence of common helper innate lymphoid cell precursors. *Cell Rep,* 10**,** 2043-54.

Yam, P., Jensen, M., Akkina, R., Anderson, J., Villacres, M. C., Wu, J., Zaia, J. A. & Yee, J. K. 2006. Ex vivo selection and expansion of cells based on expression of a mutated inosine monophosphate dehydrogenase 2 after HIV vector transduction: effects on lymphocytes, monocytes, and CD34+ stem cells. *Mol Ther,* 14**,** 236-44.

Yan, Y., Steinherz, P., Klingemann, H. G., Denning, D., Childs, B. H., McGuirk, J. & O'Reilly, R. J. 1998. Antileukemia activity of a natural killer cell line against human leukemias. *Clin Cancer Res,* 4**,** 2859-68.

Yang, M., Li, D., Chang, Z., Yang, Z., Tian, Z. & Dong, Z. 2015. PDK1 orchestrates early NK cell development through induction of E4BP4 expression and maintenance of IL-15 responsiveness. *J Exp Med,* 212**,** 253-65.

Yu, X., Rollins, D., Ruhn, K. A., Stubblefield, J. J., Green, C. B., Kashiwada, M., Rothman, P. B., Takahashi, J. S. & Hooper, L. V. 2013. TH17 cell differentiation is regulated by the circadian clock. *Science,* 342**,** 727-30.

Zamai, L., Ahmad, M., Bennett, I. M., Azzoni, L., Alnemri, E. S. & Perussia, B. 1998. Natural Killer (NK) Cell–mediated Cytotoxicity: Differential Use of TRAIL and Fas Ligand by Immature and Mature Primary Human NK Cells. *J Exp Med,* 188**,** 2375-80.

Zhang, J., Zheng, H. & Diao, Y. 2019. Natural Killer Cells and Current Applications of Chimeric Antigen Receptor-Modified NK-92 Cells in Tumor Immunotherapy. *Int J Mol Sci,* 20.

Zhang, Q., Bi, J., Zheng, X., Chen, Y., Wang, H., Wu, W., Wang, Z., Wu, Q., Peng, H., Wei, H., Sun, R. & Tian, Z. 2018. Blockade of the checkpoint receptor TIGIT prevents NK cell exhaustion and elicits potent anti-tumor immunity. *Nat Immunol,* 19**,** 723-732.

Zhang, W., Zhang, J., Kornuc, M., Kwan, K., Frank, R. & Nimer, S. D. 1995. Molecular cloning and characterization of NF-IL3A, a transcriptional activator of the human interleukin-3 promoter. *Mol Cell Biol.,* 15**,** 6055-63.

Zielske, S. P. & Gerson, S. L. 2002. Lentiviral transduction of P140K MGMT into human CD34(+) hematopoietic progenitors at low multiplicity of infection confers significant resistance to BG/BCNU and allows selection in vitro. *Mol Ther,* 5**,** 381-7.

Zook, E. C., Li, Z. Y., Xu, Y., de Pooter, R. F., Verykokakis, M., Beaulieu, A., Lasorella, A., Maienschein-Cline, M., Sun, J. C., Sigvardsson, M. & Kee, B. L. 2018. Transcription factor ID2 prevents E proteins from enforcing a naive T lymphocyte gene program during NK cell development. *Sci Immunol,* 3.